THESIS
5
2009
V. 1

LIBRARY
Michigan State
University

This is to certify that the
dissertation entitled

IDENTIFICATION OF GENES INVOLVED IN TUMORIGENESIS THAT ARE DEREGULATED, WITH AN EMPHASIS ON ALTERED DNA METHYLATION

presented by

JENNIFER MARIE PHILLIPS

has been accepted towards fulfillment
of the requirements for the

DOCTORAL degree in BIOCHEMISTRY AND MOLECULAR BIOLOGY

Major Professor's Signature

3/23/09

Date

MSU is an Affirmative Action/Equal Opportunity Institution

PLACE IN RETURN BOX to remove this checkout from your record.
TO AVOID FINES return on or before date due.
MAY BE RECALLED with earlier due date if requested.

DATE DUE	DATE DUE	DATE DUE

5/08 K:/Proj/Acc&Pres/CIRC/DateDue.indd

IDENTIFICATION OF GENES INVOLVED IN TUMORIGENESIS THAT ARE DEREGULATED, WITH AN EMPHASIS ON ALTERED DNA METHYLATION

VOLUME I

By

Jennifer Marie Phillips

A DISSERTATION

Submitted to
Michigan State University
In partial fulfillment of the requirements
for the degree of

DOCTOR OF PHILOSOPHY

Biochemistry and Molecular Biology

2009

ABSTRACT

IDENTIFICATION OF GENES INVOLVED IN TUMORIGENESIS THAT ARE DEREGULATED, WITH AN EMPHASIS ON ALTERED DNA METHYLATION

By

Jennifer Marie Phillips

Epigenetic modifications, including DNA methylation, cause heritable alterations in gene expression via mechanisms that do not affect the base sequence of DNA. Variations in levels of methylation (i.e. 5-methylcytosine) are responsible for transcriptional changes that occur during normal development, as well as disease states, including cancer.

Tumorigenesis is a multistep process that is comprised of 3 experimentally-defined stages: initiation, promotion, and progression. Epigenetic mechanisms such as DNA methylation, plus mutations, can be key contributors to each phase. These changes facilitate the progressive clonal expansion of aberrant subpopulations that possess growth advantages, which ultimately results in the development of frank tumors.

The overall goal of this dissertation research was to elucidate progressive changes, in expression and DNA methylation status, of genes which play key roles in liver tumorigenesis induced by the nongenotoxic hepatocarcinogen phenobarbital (PB), with an emphasis on their potential to affect signaling through critical pathways involved in the regulation of cell growth and differentiation. My hypothesis states that genes which are deregulated uniquely in liver tumor-susceptible, as compared to resistant mice, are among those that are mechanistically important for tumorigenesis.

Two distinct model systems, representing a continuum of treatment, were utilized

in combination to evaluate PB-elicited alterations that arose uniquely in the susceptible mice. Genes were identified that exhibited unique altered methylation and/or expression statuses in 1) B6C3F1 mice, as compared to the relatively resistant C57BL/6, at 2 and/or 4 weeks of PB treatment, and 2) precancerous liver and/or liver tumor tissue from constitutive active/androstane receptor (CAR) wildtype (WT) mice, as compared to liver tissue from PB-treated resistant CAR knockout (KO) mice. Notably, many of the genes are involved in pathways and processes that can control malignant growth (e.g., cell cycle, apoptosis, angiogenesis, invasion/metastasis, epithelial-mesenchymal cell transition, plus transforming growth factor-β and Wnt signaling). The progressive nature of carcinogenesis is demonstrated by the observation that genes whose expression or methylation statuses were disrupted at 2 and/or 4 weeks remained deregulated in precancerous liver and/or liver tumor tissue.

Unique expression changes of DNA methyltransferase (Dnmt) genes in tumor-prone B6C3F1 and CAR WT mice, plus the observation that they harbor CAR response elements (CAREs), suggest a potential direct link between PB and altered DNA methylation. CAREs within numerous additional genes whose expression and/or methylation statuses were altered uniquely, is evidence of the possible functions of CAR during tumor development. Significantly, candidate genes for "fingerprints" of early and late times of PB treatment, including tumors, are proposed. My dissertation research culminated in the identification of genes that, by virtue of their unique deregulation in tumor-prone, as compared to resistant mice, could contribute to tumorigenesis. Collectively, these data provide novel insight into a detailed picture of DNA methylation and gene expression changes that facilitate PB-induced hepatocarcinogenesis.

This thesis is dedicated to my adorable husband Mark Anthony Wasil

ACKNOWLEDGEMENTS

First and foremost, I thank God, because everything that I accomplish in my life is attributable to Him. "When someone has been given much, much will be required in return" (Luke 12:48). My family has been a continuous source of strength and motivation. I thank my mother, Beth Krosse, and my father, Kenneth Phillips, who instilled in me the belief that I can achieve anything that I dream of, and who have continually guided me with their wise advice; my brothers, Douglas and Geoffrey Phillips, who, by following their dreams, have inspired me to pursue mine, and who have constantly reminded me that I stole livers from mice that were once alive ☺; and, of course, my amazing husband (aka Puns) for believing in me, for giving me hope, confidence, and counsel when all seemed lost, and most importantly, for helping me to keep life in perspective. I could not have finished this dissertation without them, and other family members and friends who have supported me during my time here.

I thank the following people, who have collectively taught me that "no graduate student is an island": my professors at Ohio Wesleyan University, Drs. Goldstein and Tuhela-Reuning, plus Mrs. Ichida, for fostering my interest in science; Dr. Ammie Bachman, for being a great professional role model and an even better friend; Emily Flynn, for giving me a chance in G102; Dima Alkawwas, for her visits to B-423; Lauren Michalski, for keeping things fun; Emily Eckenrode, for her assistance in the lab; Emily McClure, for her indulgence during RT-PCR; RTSF (Annette Thelen), for technical assistance; CIT/EITS, for stipend and travel support; Drs. David J. Doolittle and Geoffrey M. Curtin, for the opportunity to collaborate with RJRT Co.; Dr. David Foran, for the chance to dabble in Forensic Science; my committee members, Drs. Arnosti, DeWitt, Kuo, and LaPres, for their scientific insight and advice; and finally, Dr. Jay Goodman, for the opportunity to work in his laboratory.

GO SPARTY!

TABLE OF CONTENTS

PAGE

LIST OF TABLES.....ix

LIST OF FIGURES.....xii

INTRODUCTION.....1
- Liver Cancer.....1
- Multistage Carcinogenesis.....2
- The Origin of the Cancer Stem Cell.....4
- Fundamental Characteristics of a Cancer Cell.....6
- Cell-Cell Interactions in Cancer.....12
- 5-Methylcytosine Distribution and Abundance.....12
- Regulation of DNA Methylation Patterns.....14
  - DNA Methyltransferase Enzymes.....18
  - DNA Demethylation.....20
- Transcriptional Regulation.....22
  - DNA Methylation.....22
  - DNA Methylation and Chromatin Alterations.....24
- Roles of DNA Methylation in Normal Physiology.....26
- Roles of Altered DNA Methylation in Cancer.....29
  - Hypomethylation.....31
  - Hypermethylation.....33
  - Early DNA Methylation Changes Facilitate Tumorigenesis.....35
- Rodent Models of Liver Tumorigenesis.....35
  - B6C3F1 and C57BL/6 Mice.....37
  - CAR Wildtype and Knockout Mice.....40
- Hypothesis and Objectives.....45
- Specific Aims.....49
- References for the Introduction, Summary, and Discussion.....373

CHAPTER 1 – Identification of Genes that May Play Critical Roles in Phenobarbital (PB)-induced Liver Tumorigenesis Due to Altered DNA Methylation.....52
- Abstract.....53
- Introduction.....54
- Materials and Methods.....58
- Results.....65
- Discussion.....79
- Acknowledgement.....87
- References.....87
- APPENDIX I.....93
  - Results.....94
  - References 1.....101
  - References 2.....107

CHAPTER 2 – Phenobarbital (PB) Elicits Unique, Early Changes in the Expression of Hepatic Genes that Affect Critical Pathways in Tumor-Prone B6C3F1 Mice.....110
Abstract.....111
Introduction.....113
Materials and Methods.....116
Results.....126
Discussion.....143
Acknowledgement.....153
References.....153
APPENDIX II: Results.....159

CHAPTER 3 – Orphan Nuclear Receptor Constitutive Active/Androstane Receptor (CAR)-Mediated Alterations in DNA Methylation During Phenobarbital (PB) Promotion of Liver Tumorigenesis.....177
Abstract.....178
Introduction.....179
Materials and Methods.....183
Results.....190
Discussion.....203
Acknowledgements.....209
References.....209
APPENDIX III: Results.....213

CHAPTER 4 – Multiple Genes Exhibit Phenobarbital (PB)-induced Constitutive Active/Androstane Receptor (CAR)-Mediated DNA Methylation Changes During Liver Tumorigenesis and in Liver Tumors.....220
Abstract.....221
Introduction.....223
Materials and Methods.....227
Results.....235
Discussion.....257
Acknowledgement.....265
References.....265
APPENDIX IV: Results.....270

CHAPTER 5 – The Constitutive Active/Androstane Receptor (CAR) Facilitates Unique Phenobarbital (PB)-Induced Expression Changes of Genes Involved in Key Pathways in Precancerous Liver and Liver Tumors.....281
Abstract.....282
Introduction.....283
Materials and Methods.....287
Results.....300

Discussion.....321
Acknowledgement.....330
References.....330
APPENDIX V: Results.....335

SUMMARY: Specific Aims Addressed.....348

DISCUSSION.....359
Significance of Research
1. The use of two model systems (each consisting of a group of liver tumor-prone and tumor-resistant mice) to elucidate unique molecular alterations in tumor-susceptible mice, across a continuum of PB treatment, is an extremely effective approach for assessing changes which are critical for tumor development.....359
2. Both increases and decreases in methylation represent key events that occur during tumor development.....361
3. Uniquely altered genes, and cancer-related pathways/processes in which they are involved, were discerned in PB-treated liver tumor-susceptible mice.....363
4. Altered expression of DNA methyltransferases, in addition to genes involved in 1-carbon metabolism, could represent mechanisms by which unique PB-induced RAMs formed in liver-tumor susceptible mice.....367
5. Evidence supports the role of CAR in mediating gene expression changes that occur in response to PB treatment, at both early and later time points, which might contribute to the carcinogenesis process.....368
Conclusions.....371

LIST OF REFERENCES USED IN INTRODUCTION AND DISCUSSION.....373

LIST OF TABLES

Table 1.1 PCR Products Representing Unique Phenobarbital (PB)-induced RAMs in Liver Tumor-Sensitive B6C3F1, as Compared to Relatively Resistant C57BL/6, Mice were Cloned and Subjected to BLAST-like Alignment Tool (BLAT) Searches.....67

Table 2.1 Quantitative Real-time PCR (qRT-PCR) Analysis of Expression of 3 DNA Methyltransferase (Dnmt) Genes.....139

Table 2.2 Expression of Genes that Contain Putative Constitutive Active/Androstane Receptor Response Elements (CAREs).....141

Table 2.3 Genes Encoding Drug-Metabolizing Enzymes that were Identified as Uniquely Active in B6C3F1 and C57BL/6 Mice.....163

Table 2.4: Quantitative Real-time PCR (qRT-PCR) Analysis of the Expression of 18 Genes that were Uniquely Active in Livers of B6C3F1 Mice at 2 Weeks of Phenobarbital (PB) Treatment.....164

Table 2.5 Quantitative Real-time PCR (qRT-PCR) Analysis of the Expression of 11 Genes that were Uniquely Active in Livers of B6C3F1 Mice at 4 Weeks of Phenobarbital (PB) Treatment.....166

Table 2.6 Connections Between 5 Cancer-related Processes and Genes, Including those which Carried Forward, that were Uniquely Active in B6C3F1 Mice Following Treatment with Phenobarbital (PB) for 2 Weeks.....168

Table 2.7 Connections Between 5 Cancer-related Processes and Genes, Including those which Carried Forward, that were Uniquely Active in B6C3F1 Mice Following Treatment with Phenobarbital (PB) for 4 Weeks.....170

Table 2.8 Kinase, Phosphatase, Phosphatase Activator (Regulatory Subunit), and Phosphatase Regulatory (Inhibitor) Genes Identified as Uniquely Active in Liver Tumor-Susceptible B6C3F1 Mice.....172

Table 2.9 Quantitative Real-time PCR (qRT-PCR) Analysis of Genes which Exhibited Unique Phenobarbital (PB)-induced Regions of Altered DNA methylation (RAMs) in Liver Tumor-Susceptible B6C3F1 Mice.....173

Table 3.1 GC-rich Regions of Altered Methylation (RAMs) in the Livers of C3H/He CAR WT and KO Mice Treated with 0.05% Phenobarbital for 23 or 32 Weeks.....191

Table 4.1 Genes and Genomic Regions Identified from Unique Phenobarbital (PB)-induced RAMs in C3H/He Constitutive Active/Androstane Receptor (CAR) Wildtype

(Precancerous Liver and/or Liver Tumor), as Compared to Resistant PB-Treated Knockout Mice, were Cloned and Subjected to BLAST-like Alignment Tool (BLAT) Searches.....236

Table 4.2 Genes Identified from Unique Phenobarbital (PB)-induced RAMs in C3H/He Constitutive Active/Androstane Receptor (CAR) Wildtype (Precancerous Liver and/or Liver Tumor), as Compared to Resistant CAR Knockout Mice, and their Potential Functional Significance in Tumorigenesis.....251

Table 4.3 Genes Identified from Identical, Unique Phenobarbital (PB)-induced RAMs that Formed in Both CAR Wildtype (Precancerous Liver and/or Liver Tumor) and B6C3F1 (2 and/or 4 Week Treated) Mice.....253

Table 4.4 Identical Uncharacterized Genomic Regions Identified from Identical, Unique Phenobarbital (PB)-induced RAMs that Formed in Both C3H/He CAR Wildtype (Precancerous Liver and/or Liver Tumors) and B6C3F1 (2 and/or 4 Week Treated Liver Tissue) Mice.....279

Table 5.1 Quantitative Real-time PCR (qRT-PCR) Analysis of the Expression of 3 DNA Methyltransferase (Dnmt) Genes.....314

Table 5.2 Expression of Genes that Contain Putative Constitutive Active/Androstane Receptor Response Elements (CAREs).....316

Table 5.3 Quantitative Real-Time PCR (qRT-PCR) Analysis of Expression of 3 DNA Methyltransferase (Dnmt) Genes in 2 Types of Liver Tumor-Susceptible Mice.....319

Table 5.4 Quantitative Real-time PCR (qRT-PCR) Analysis of the Expression of 22 Genes that were Uniquely Active in Precancerous Liver Tissue and/or Individual Liver Tumors.....339

Table 5.5 Kinase, Phosphatase, and Phosphatase Regulatory (Inhibitor) Subunit Genes Identified as Uniquely Active in Precancerous Liver Tissue and/or Individual Liver Tumors.....341

Table 5.6 Quantitative Real-time PCR (qRT-PCR) Analysis of Expression of Genes That Exhibited Unique Phenobarbital (PB)-induced Regions of Altered DNA Methylation (RAMs).....343

Table 5.7 Quantitative Real-Time PCR Analysis (qRT-PCR) of Expression of Genes Identified from Identical, Unique Phenobarbital (PB)-induced Regions of Altered DNA Methylation (RAMs) in 2 Types of Liver Tumor-Prone Mice.....346

Table 6.1 Expression of Genes Identified from Identical Phenobarbital (PB)-induced Regions of Altered DNA Methylation (RAMs) in 2 Types of Liver Tumor-Prone Mice.....356

Table 6.2 Genes Exhibiting Altered Expression at Early and Late Times of Phenobarbital (PB) Treatment.....357

Table 6.3 Common Signaling Pathways and Cellular Processes Involving Genes that Exhibited Methylation and/or Expression Changes in 2 Types of Liver-Tumor Prone Mice.....358

LIST OF FIGURES

Figure 1.1 Multistage Carcinogenesis.....3

Figure 1.2 DNA Methylation, a Heritable Epigenetic Alteration.....15

Figure 1.3 DNA methylation is Affected by Multiple Factors.....16

Figure 1.4 DNA Methylation and 1-Carbon Metabolism.....17

Figure 1.5 The Functions of DNA Methylation.....30

Figure 1.6 Activation of the Constitutive Active/Androstane Receptor (CAR).....43

Figure 1.7 Unique Regions of Altered DNA Methylation (RAMs) that Formed in the Livers of B6C3F1 Mice in Response to 2 or 4 Weeks of Treatment with 0.05% (w/w) Phenobarbital (PB).....66

Figure 1.8 A Scheme to Classify Cloned PCR Products that Represent Unique Phenobarbital (PB)-induced B6C3F1 Regions of Altered DNA Methylation (RAMs) Based on their Locations Within the Mouse Genome as Determined by BLAST-like Sequence Alignment Tool (BLAT) Searches.....73

Figure 1.9 Common Cellular Targets of Genes that Represent Regions of Altered DNA Methylation (RAMs) in Liver Tumor-Susceptible B6C3F1 Mice at 4 Weeks of Phenobarbital (PB) Treatment 78

Figure 1.10 The Possible Functional Significance, Regarding Tumorigenesis, of Selected Genes which Exhibited Altered Methylation Uniquely in the B6C3F1 Mouse Following Treatment with Phenobarbital (PB).....82

Figure 1.11 The Distribution of Genomic Locations to Which the PCR products Representing PB-induced Unique Regions of Altered DNA Methylation (RAMs) in B6C3F1 Mice Aligned 94

Figure 1.12 The Distribution of Chromosomes Within the Mouse Genome to Which the PCR Products Representing PB-induced Unique Regions of Altered DNA Methylation (RAMs) in B6C3F1 Mice Aligned 95

Figure 1.13 Functional Breakdown of the PCR Products that Represent Unique PB-induced Regions of Altered DNA Methylation (RAMs) in B6C3F1 Mice.....96

Figure 1.14 Informatics Analysis of Ral Guanine Nucleotide Dissociation Stimulator (*Ralgds*), a Potential Oncogene that is Uniquely Hypomethylated in B6C3F1 Mice at 4 Weeks of Phenobarbital (PB) Treatment.....97

Figure 1.15 Informatics Analysis of Transforming Growth Factor Beta Receptor II (*Tgfbr2*), a Potential Oncogene that is Uniquely Hypomethylated in B6C3F1 Mice at 4 Weeks of Phenobarbital (PB) Treatment.....98

Figure 1.16 Common Cellular Regulators of Genes that Represent Unique Regions of Altered DNA Methylation (RAMs) in B6C3F1 Mice at 4 Weeks of Phenobarbital (PB) Treatment.....99

Figure 1.17 The Possible Functional Significance, Regarding Tumorigenesis, of Selected Genes Which Exhibited Altered Methylation Uniquely in the B6C3F1 Mouse Following Treatment with Phenobarbital (PB), Including References.....100

Figure 2.1 Identification of Uniquely Active Genes in Tumor-Susceptible B6C3F1 Mice, as Compared to the Relatively Resistant C57BL/6, at 2 or 4 Weeks of Phenobarbital (PB) Treatment 127

Figure 2.2 The Expression and/or Methylation Statuses of Genes Involved in the Cell Cycle, Apoptosis, and Mitogen-Activated Protein Kinase (MAPK) Signaling were Altered by Phenobarbital (PB) at 2 and 4 Weeks.....131

Figure 2.3 The Expression and/or Methylation Statuses of Genes Involved in Angiogenesis and the Epithelial-Mesenchymal Cell Transition (EMT) were Altered by Phenobarbital (PB) at 2 and 4 Weeks.....134

Figure 2.4 The Expression of Genes Involved in Epigenetic-Related Processes, and Those that are Indicative of Nuclear Receptor Activation, was Altered by Phenobarbital (PB) at 2 and 4 Weeks.....136

Figure 2.5 Summary of Pathways and Processes Involving Genes that Exhibited Unique Phenobarbital (PB)-Elicited Expression and/or Methylation Changes at 2 and/or 4 Weeks.....144

Figure 2.6 Principle Component Analysis (PCA) of Gene Expression Patterns of Individual B6C3F1 and C57BL/6 Mice within Control and Phenobarbital (PB)-treated Groups at 2 and 4 Weeks 160

Figure 2.7 Distribution of Gene Expression Data Generated from Individual B6C3F1 and C57BL/6 Mice within Control and Phenobarbital (PB)-treated Groups at 2 and 4 Weeks.....161

Figure 2.8 A Scheme to Classify Cloned PCR Products that Represent Unique Phenobarbital (PB)-induced B6C3F1 Regions of Altered DNA Methylation (RAMs) Based on their Locations Within the Mouse Genome as Determined by BLAST-like Sequence Alignment Tool (BLAT) Searches.....162

Figure 3.1 Identification of PB-Induced Unique Regions of Altered Methylation (RAMs) in the Precancerous as Compared to the CAR KO, 23 wk PB-Treated Tissue.....192

Figure 3.2 Progressive Changes in Methylation: PB-Induced Regions of Altered Methylation (RAMs) which Carry Forward from Precancerous to Tumor Tissue in C3H/He CAR WT Mice.....195

Figure 3.3 Total Unique Regions of Altered Methylation (RAMs) That Occurred as a Result of PB Treatment in the Tumor as Compared to the Precancerous Tissue.....197

Figure 3.4 A Summary of Regions of Altered Methylation (RAMs) that Carry Forward from the Precancerous to the Tumor Tissue and Total Unique RAMs in the Tumor Tissue.....200

Figure 3.5 Determination of Percent Dissimilarity Between Precancerous vs. CAR WT, 23wk Control, Tumor vs. CAR WT, 23 wk Control, and CAR KO, 23 wk PB vs. CAR KO, 23 wk Control Tissue.....202

Figure 3.6 GC-Rich Regions of Altered DNA Methylation: Comparison of Diethylnitrosamine (DEN)-Initiated, 0.05% Phenobarbital (PB)-promoted Precancerous Tissue (CAR Wildtype, 23 wk DEN/PB) to Control (CAR Wildtype,

23 wk DEN).....214

Figure 3.7 GC-Rich Regions of Altered DNA Methylation: Comparison of Diethylnitrosamine (DEN)-Initiated, 0.05% Phenobarbital (PB)-promoted Tumor Tissue (CAR Wildtype, 32 wk DEN/PB) to Control (CAR Wildtype, 23 wk DEN).....216

Figure 3.8 GC-Rich Regions of Altered DNA Methylation: Comparison of Diethylnitrosamine (DEN)-Initiated, 0.05% Phenobarbital (PB)-promoted CAR Knockout (KO) Tissue (CAR KO, 23 wk DEN/PB) to Control (CAR KO, 23 wk DEN).....218

Figure 4.1 Common Targets of Genes Identified from Unique Regions of Altered DNA Methylation (RAMs) in Phenobarbital (PB)-induced Precancerous Liver Tissue from C3H/He Constitutive Active/Androstane Receptor (CAR) Wildtype Mice.....243

Figure 4.2 Common Targets of Genes Identified from Unique Regions of Altered DNA Methylation (RAMs) in Phenobarbital (PB)-induced Liver Tumor Tissue from C3H/He Constitutive Active/Androstane Receptor (CAR) Wildtype Mice.....244

Figure 4.3 Genes which Exhibited Altered Methylation Uniquely in Phenobarbital (PB)-induced Precancerous and Liver Tumor Tissue and which are Potentially Involved in the Regulation of Angiogenesis.....246

Figure 4.4 Genes which Exhibited Altered Methylation Uniquely in Phenobarbital (PB)-induced Precancerous and Liver Tumor Tissue and which are Potentially Involved in the Regulation of Apoptosis.....247

Figure 4.5 Genes which Exhibited Altered Methylation Uniquely in Phenobarbital (PB)-induced Precancerous and Liver Tumor Tissue and which are Potentially Involved in the Regulation of Epithelial-Mesenchymal Cell Transition (EMT).....248

Figure 4.6 Genes which Exhibited Altered Methylation Uniquely in Phenobarbital (PB)-induced Precancerous and Liver Tumor Tissue and which are Potentially Involved in the Regulation of Migration, Invasion and/or Metastasis.....249

Figure 4.7 Genes which Exhibited Altered Methylation Uniquely in Phenobarbital (PB)-induced Precancerous and Liver Tumor Tissue and which are Potentially Involved in the Regulation of Growth/Survival.....250

Figure 4.8 The Distribution of Genomic Locations of the Annotated (Including Uncharacterized Regions) Phenobarbital (PB)-induced Unique Regions of Altered DNA Methylation (RAMs) in C3H/He Constitutive Active/Androstane Receptor (CAR) Precancerous and Liver Tumor Tissue.....271

Figure 4.9 The Chromosomal Distribution of the Annotated (Including Uncharacterized Regions) Phenobarbital (PB)-induced Unique Regions of Altered DNA Methylation (RAMs) in C3H/He Constitutive Active/Androstane Receptor (CAR) Precancerous and Liver Tumor Tissue.....272

Figure 4.10 Functional Breakdown of the Genes Identified from Unique Phenobarbital (PB)-induced Regions of Altered DNA Methylation (RAMs) in C3H/He Constitutive Active/Androstane Receptor (CAR) Precancerous and Liver Tumor Tissue.....273

Figure 4.11 Informatic Analysis of c-Abl Oncogene 1, Receptor Tyrosine Kinase (*Abl1*) Which Represents a Unique Carry Forward Hypomethylated RAM in Both the Precancerous and Liver Tumor Tissue.....274

Figure 4.12 Common Regulators of Genes that were identified from Unique Phenobarbital (PB)-induced Regions of Altered DNA Methylation (RAMs) in C3H/He Constitutive Active/Androstane Receptor (CAR) Wildtype Precancerous and Liver Tumor Tissue.....275

Figure 4.13 Informatic Analysis of Ephrin B2 (*Efnb2*), a Gene Identified from Identical, Unique Phenobarbital (PB)-induced RAMs that Formed in Both C3H/He CAR Wildtype (Precancerous Liver and/or Liver Tumors) and B6C3F1 (2 and/or 4 Weeks) Mice.....276

Figure 4.14 Common Targets of Genes Identified from Identical, Unique Phenobarbital (PB)-induced RAMs that Formed in Both C3H/He CAR Wildtype (Precancerous Liver and/or Liver Tumors) and B6C3F1 (2 and/or 4 Weeks) Mice.....277

Figure 4.15 Common Regulator of Genes Identified from Identical, Unique Phenobarbital (PB)-induced RAMs that Formed in Both C3H/He CAR Wildtype (Precancerous Liver and/or Liver Tumors) and B6C3F1 (2 and/or 4 Weeks) Mice.....278

Figure 5.1 Identification of Uniquely Active Genes in Precancerous Liver Tissue and/or Individual Liver Tumors, as Compared to Liver Tissue from Tumor-Resistant Constitutive Active/Androstane Receptor (CAR) Knockout (KO) Mice.....301

Figure 5.2 The Expression and/or Methylation Statuses of Genes Involved in the Cell Cycle, Apoptosis, and Mitogen-activated Protein Kinase (MAPK) Signaling were Altered in Precancerous and Tumor Tissue.....307

Figure 5.3 The Expression and/or Methylation Statuses of Genes Involved in Angiogenesis, Cytoskeleton Organization/Dynamics, and Adhesion were Altered in Precancerous and Tumor Tissue 309

Figure 5.4 The Expression and/or Methylation Statuses of Genes Involved in Pathways Associated with Development and Differentiation were Altered in Precancerous and Tumor Tissue.....312

Figure 5.5 Summary of Signaling Pathways and Processes Involving Genes that Exhibited Unique Expression and/or Methylation Changes in Precancerous and Tumor Tissue.....323

Figure 5.6 Principle Component Analysis (PCA) of Gene Expression Patterns Exhibited in Tissue Samples from Constitutive Active/Androstane Receptor (CAR) Wildtype (WT) and Knockout (KO) Mice.....336

Figure 5.7 Distribution of Microarray Data that were Generated using RNA Isolated from Constitutive Active/Androstane Receptor (CAR) Wildtype (WT) and Knockout (KO) Mouse Tissues.....337

Figure 5.8 Identification of Uniquely Active Genes in Precancerous Liver and/or Individual Liver Tumors.....338

INTRODUCTION

Liver Cancer

Liver cancer represents a group of histopathologically diverse neoplasms, including bile duct cystadenocarcinoma, epitheliod haemangioendothelioma, haemangiosarcoma, hepatoblastoma, hepatocellular carcinoma (HCC), and intrahepatic bile duct carcinoma (cholangiocarcinoma) (Anthony 2002). HCC is the most common type of liver cancer, accounting for 83% of all cases (American Cancer Society, 2005), and globally, is the 5th most common malignancy (Bruix *et al.*, 2004). In humans, risk factors for HCC development include agents that cause chronic liver injury and cirrhosis, including those that are viral (chronic infection by hepatitis B and C), toxic (alcohol consumption and Aflatoxin B1 ingestion), and metabolic (diabetes, non-alcoholic fatty liver disease), among others (Bruix *et al.*, 2004; Parikh, 2007). It is critical, for effective cancer diagnosis, prognosis, and therapy, to develop a more comprehensive understanding of the complex mechanisms, including signaling networks, which contribute to the pathology of the disease.

Genetic and epigenetic alterations of oncogenes and tumor suppressors, plus the perturbation of numerous signaling pathways, have been implicated in human HCC. Specific events that are thought to play a role in its pathogenesis include loss-of-function mutations in the p53 tumor suppressor, mutation and overexpression of β-catenin, overexpression of ErbB receptors, and overexpression of hepatocyte growth factor (*HGF)* and its receptor (Farazi and DePinho, 2006). Additional genes, typically involved in growth and survival, exhibit mutations and/or expression changes in HCC: *p73, Rb, Mdm2, APC,* E-cadherin, $p16^{INK4a}$, Gankyrin, the Ras inhibitors *RASSF1A* and *NORE1A*,

c-myc and cyclin D1, among others (Berasain *et al.*, 2007). Increased levels of DNA methylation (i.e. 5-methylcytosine) in multiple genes, including but not limited to $p16^{INK4a}$, E-cadherin, *COX2*, *ASC*, and *DLC1* highlight the importance of epigenetic changes in HCC (Farazi and DePinho, 2006). Several growth factors, receptors, and signaling pathways which are normally involved in the regenerative and protective responses of the liver to acute injury (epidermal growth factor (EGF) family of growth factors; HGF; insulin-like growth factor, IGF; transforming growth factor-β, TGF-β; and Wnt) appear to be deregulated during hepatocarcinogenesis, resulting in development and maintenance of the transformed phenotype (Berasain *et al.*, 2007).

Multistage Carcinogenesis

Carcinogenesis is a complex, multistep/multistage process, involving the accumulation of both genetic and epigenetic changes that ultimately result in the development of a frank tumor from a single, initiated cell (Feinberg *et al.*, 2006; Nowell, 1976). There are 3 distinct, experimentally-defined stages of tumorigenesis: initiation, promotion, and progression (Pitot and Dragan, 1991) (Figure 1.1). While this classical view is conceptually important, it is an oversimplification of our increasing understanding of the plethora of biological processes that are altered during the transformation process (Loeb and Harris, 2008).

The first stage, initiation, is a permanent change that occurs spontaneously, or in response to carcinogen treatment (Pitot and Dragan, 1991). The first critical, heritable event that results in the formation of an initiated cell can be either a mutation (Loeb and Harris, 2008) or an epigenetic alteration, e.g. change in DNA methylation (Esteller,

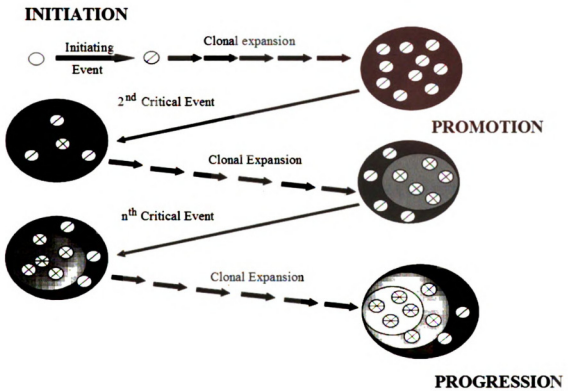


Figure 1.1 Multistage Carcinogenesis. The 3 experimentally-defined stages of carcinogenesis are initiation, promotion, and progression. Initiation occurs when a cell (O) acquires a critical, heritable change (e.g., mutation or altered DNA methylation), represented by a line through the circles. A promoting agent facilitates the selective clonal expansion of the initiated cell by conferring a growth advantage upon it, relative to neighboring cells. Aberrant clonal expansions continue until the progression stage is reached, whereby cells can proliferate autonomously. (Adapted from Goodman and Watson, 2002)

2007a; Goodman and Watson, 2002), either of which can result in the acquisition of a proliferative advantage. Treatment with the potent alkylating mutagen diethylnitrosamine (DEN) causes the development of putatively initiated hepatocytes, some of which can develop into altered hepatic foci (AHF), the presumed precursors of liver tumors (Pitot and Dragan, 1994).

The second stage of carcinogenesis is promotion, during which a reversible, selective clonal expansion of the initiated cell occurs, resulting in the generation of exceedingly aberrant subclone populations that have accumulated critical, heritable changes (i.e. mutation and epigenetic alterations) that provide them with growth advantages over neighboring cells (Feinberg *et al.*, 2006; Pitot and Dragan, 1991). The reversible nature of promotion is illustrated by cessation of treatment with a promoting stimulus, which causes a decrease in the number of hyperplastic foci. This can occur via cell death/apoptosis or architectural "remodeling" (Pitot and Dragan, 1994). Additionally, promoting agents (e.g. phenobarbital, dieldrin) are threshold-exhibiting, i.e. there exists a dose below which there are no effects (Pitot and Dragan, 1991).

The final irreversible stage is progression, in which malignant lesions appear (Pitot and Dragan, 1994). During progression, cells grow autonomously, foci-in-foci develop, and genetic alterations (e.g. elevated chromosomal damage, karyotypic instability, and alterations in ploidy) are evident (Pitot and Dragan, 1994; Pitot *et al.*, 1991).

The Origin of the Cancer Stem Cell

The origin of the cancer cell is highly debated. There are 3 possibilities, which are not mutually exclusive, with regard to which type of cell(s) might receive the first

genetic or epigenetic "hit", and become the initiated cell (i.e. "cancer stem cell"): stem cells, progenitor cells, and/or differentiated cells (Bjerkvig *et al.,* 2005).

A niche of tissue-specific stem cells might exist, and presumably, changes in genes involved in the regulation of self-renewal would be important for the development of the initiated cell (Bjerkvig *et al.,* 2005). Adult stem cells are capable of both self-renewal and multi-lineage differentiation, and there is evidence that mutations within haematopoetic stem cells cause transformation, resulting in multiple types of leukemia (Reya *et al.*, 2001). However, adult liver stem cells have not yet been isolated (Dabeva and Shafritz, 2003).

The initiated cancer cell might also be derived from progenitor cells. In this case, the transformation event must confer the same extensive self-renewal properties to the progenitor cell as the stem cell; if not, the progenitor cell would differentiate. In support of this, mouse models have been created in which restricted, haematopoietic progenitor cells give rise to myeloid leukemia (Reya *et al.*, 2001). Several laboratories have provided evidence of various groups of intrahepatic progenitor cells (Dabeva and Shafritz, 2003; Dan *et al.*, 2006; Wang *et al.*, 2003), including, but not limited to, "oval" cells. Interestingly, it is possible that extrahepatic progenitors are derived from bone marrow (Theise *et al.*, 2000).

Moreover, mature cells might de-differentiate and become capable of serving as the initiated cancer cell. Mature hepatocytes can proliferate in a compensatory fashion, e.g. following partial hepatectomy (Steer, 1995), or in response to treatment with mitogens such as phenobarbital (Counts *et al.*, 1996; Kolaja *et al.*, 1996a). Indeed, mature hepatocytes can divide up to 12 times (Rhim *et al.*, 1994). Furthermore, upon

addition of certain genes, cells can be generated which possess stem-like properties (i.e. induced pluripotent, iPS, cells). Introduction of 4 transcription factors (*Oct3/4*, *Sox2*, *c-Myc*, and *Klf4*) into mouse embryonic or adult fibroblasts (Takahashi *et al.*, 2007; Wernig *et al.*, 2007) resulted in the formation of iPS cells. Importantly, adult mouse liver cells have also been reprogrammed to a stem-like state (Aoi *et al.*, 2008). Taken together, these 3 studies imply that it is possible for mature, differentiated cells to revert into a de-differentiated state. Combined with the fact that mature hepatocytes can replicate, it appears possible that alterations within mature, differentiated cells in the liver (e.g. hepatocytes) could ultimately lead to tumor formation.

Fundamental Characteristics of a Cancer Cell

Cancer cells acquire 6 major features that facilitate their optimal growth, and subsequently, tumor development: self-sufficiency in growth signals, insensitivity to anti-growth signals, evading apoptosis, limitless replicative potential, sustained angiogenesis, and tissue invasion and metastasis (Hanahan and Weinberg, 2000). These characteristics are central to the tumorigenesis process, and so a brief overview of each of them is provided.

Neoplastic cells possess numerous tools that enable them to become independent from exogenous growth signals, and these contribute, in part, to the uncontrolled growth universally exhibited by tumors. Several mechanisms are responsible for this phenomenon. Growth factors (e.g. EGF and IGF), cause quiescent cells to enter the cell cycle, and these, in addition to their cognate receptors, are overexpressed in tumor cells (Aaronson, 1991). Furthermore, production of growth factors by cancer cells can result

in their own proliferation, as in the case of platelet-derived growth factor in glioblastoma multiforme (Lokker *et al.*, 2002). Growth factor receptors, which transduce growth signals from the extracellular to the intracellular environment, are also altered in cancer cells, as well as tumor-associated stromal cells. In particular, EGF receptors are commonly overexpressed or exhibit activating mutations in cancer, resulting in their constitutive activation and consequently, cellular proliferation and survival (Zhang *et al.*, 2007). Extracellular matrix receptors (i.e. integrins) mediate signals, derived from matrix components, that govern intracellular events and contribute to growth. For example, cues from Shc-related integrins help activate the Ras-mitogen-activated protein kinase (MAPK) pathway, an important signaling cascade that regulates crucial responses such as growth and survival (Giancotti and Ruoslahti, 1999). Indeed, activating Ras mutations are observed in approximately 30% of human cancers, leading to deregulation of downstream effectors and aberrant proliferation and survival (Schubbert *et al.*, 2007).

Cancer cells can avoid signals that impede their growth by blocking cell cycle progression or circumventing differentiation. A chief pathway involved in suppressing cellular growth involves the retinoblasoma (Rb) protein, and its activator p16, both of which are deregulated in a wide range of human cancers. Inhibition of the pRB pathway leads to cellular proliferation due to the activation of relevant transcription factors (Kaye, 2002). In tumors, this can be achieved in a variety of ways, including loss of function of pRB, p16, and a number of proteins that act as anti-mitogenic agents to, directly or indirectly, enhance pRB signaling, such as TGF-β, Smad4, and p15 (reviewed in Hanahan and Weinbeg, 2000). Cells can also avoid terminal differentiation, and by doing such, escape growth suppression. During development, the c-myc functions in

conjunction with its heterodimeric binding partner Max to stimulate transcription and growth, while Max binds another protein (Mad), resulting in anti-proliferative effects, including differentiation (Foley and Eisenman, 1999). Furthermore, since c-myc overexpression can impede differentiation and facilitate growth, it is significant that this protein is overexpressed in a variety of cancers.

Tumor cells can escape death in another manner, that is, they are able to evade apoptosis. This is crucial, since programmed cell death is a way to eliminate mutated, transformed, or otherwise aberrant cells. In the context of tumorigenesis, cells can avoid apoptosis in several ways. Caspases are the central players in the induction of the apoptotic program, and thus, it is not unexpected that their reduced expression constitutes a survival mechanism (Philchenkov *et al.*, 2004; Shivapurkar *et al.*, 2003). Functional defects are also apparent in positive (e.g. FADD, Bcl2) or negative (e.g. Survivin) regulators of caspase activity (Philchenkov *et al.*, 2004). The p53 protein, which is activated in response to cellular stress or DNA damage, is capable of stimulating a transcriptional program that induces apoptosis (Vogelstein *et al.*, 2000). Inactivation of p53 occurs in approximately 50% of human cancers, and since p53-dependent apoptosis can inhibit tumor growth, this represents a tactic that cancer cells use to resist programmed cell death, thus potentially facilitating clonal expansion during carcinogenesis.

Survival factors also contribute to the capability of cells to elude apoptotic cell death. Various receptors, including those for cytokines (e.g. IL-3) and growth factors, transmit survival signals via the phosphoinositide 3-OH kinase (PI3-kinase) pathway. In particular, IGF-1 is an extracellular survival signal that can inhibit apoptosis which is

stimulated by from multiple signals (Kurmasheva and Houghton, 2006). The survival effects are generally mediated by activation of v-akt murine thymoma viral oncogene homolog 1 (AKT) plus its downstream effector PI3-kinase (Downward, 1998), and are largely dependent on the suppression of apoptosis (Toretsky *et al.*, 1999). Interestingly, elevated AKT activity has been reported in several cancers (Bellacosa *et al.*, 1995). Moreover, loss of the tumor suppressor phosphatase and tensin homolog (PTEN), which can block AKT-mediated survival, has been observed in a vast array of human neoplasms (Cantley and Neel, 1999).

In order to evolve into a macroscopic tumor, cancer cells must not only disrupt growth and death pathways, they must also evade the program that limits the number of times a cell can multiply (i.e. senescence) (Hayflick, 1997). Most tumor cells in culture have achieved this, as they seem to possess an immortalized phenotype (Hayflick, 1997). Excessive telomere maintenance is the primary mechanism by which cells can bypass proliferation limits. Telomeres, regions of repetitive DNA found at the end of chromosomes that serve to protect them from degradation, are lengthened by the telomerase enzyme. Progressive shortening of the telomeres after each round of DNA replication eventually induces senescence, apoptosis, or genomic instability (Bianchi and Shore, 2008). Typically, normal cells do not exhibit telomerase activity, however, cells from 85-90% of human cancer specimens seem to have re-activated the enzyme (Shay and Bacchetti, 1997). The remaining cells utilize a mechanism called "alternative lengthening of telomeres (ALT)" to lengthen and stabilize telomeres (Bryan *et al.*, 1995). Thus, evidence suggests that maintaining telomere length is a means by which cancer cells can achieve an indefinite replicative capacity, permitting the clonal expansion that

eventually results in tumor formation.

Angiogenesis, the sprouting and branching of new blood vessels from preexisting capillaries, is essential for transformation as well as the growth of the tumor mass, since it maintains a sufficient supply of oxygen and metabolites to neoplastic cells, as well as removes waste byproducts (Bergers and Benjamin, 2003). When the balance of pro-angiogenic and anti-angiogenic regulators shifts towards the pro-angiogenic state, the stimulation of tumor vasculature (i.e. the "angiogenic switch") occurs (Bergers and Benjamin, 2003). Positive regulators of the process include growth factors, such as VEGF and FGF (Madriota and Pepper, 1997), as well as integrins and adhesions (Rüegg and Mariotti, 2003; Tei *et al.*, 2002). Pro-angiogenic factors can be produced and secreted by tumor cells or host cells that have migrated to the tumor (e.g. immune cells), in addition to components of the extracellular matrix (Ribatti *et al.*, 2007). Additionally, angiogenesis inhibitors (e.g. thrombospondin-1) are down-regulated (Ribatti *et al.*, 2007). Thus, tumor cells, in conjunction with stromal cells, have developed methods of enhancing vasculature development in order to augment tumor growth.

Lastly, cancer cells are capable of disseminating from the primary tumor, invading the surrounding tissue, and metastasizing to distant sites. Diminished cell-to-cell adhesion and increased cell-to-matrix adhesion is critical for invasion and metastasis (Jiang, 1998). Accordingly, proteins possessing adhesive potential, namely, cell adhesion molecules (cell-cell interactions) and integrins (cell-matrix interactions), are altered during tumorigenesis. It has been established that dysfunction of cadherins, a family of cell adhesion proteins, contributes to tumor cell invasion and metastasis. Indeed, it is well-known that loss of E-cadherin promotes tumor cell progression by facilitating these

processes (Jeanes *et al.*, 2008). Integrins are glycoproteins that bind a wide range of extracellular matrix molecules (e.g. fibronectin), and they can control cell-matrix adhesion, in addition to cell shape and migration, which are all vital events during invasion and metastasis (Hood and Cheresh, 2002). Extracellular proteases can alter biological adhesion, as well as promote the degradation of multiple proteins that influence tumor behavior. For example, cellular invasion and metastasis is facilitated by matrix metalloproteinase-7 (MMP-7) which is capable of degrading basement membrane proteins (DeClerck *et al.*, 2004).

These 6 basic traits that a cell acquires permit its transformation and control its malignant growth. An extensive array of oncogenes and tumor suppressors that contribute to these biological endpoints have been, and continue to be, identified. Specifically, multiple key oncogenic pathways have been discerned, that serve to drive tumorigenesis when associated constituents are deregulated: protein tyrosine kinases and their associated signaling networks (e.g. fibroblast growth factor, FGF), Wnt, Hedgehog, Notch, Ras (including cytoskeleton proteins), mitogen-activated protein kinases (MAPK), PI3-kinase, cytokines, Tgf-β, and nuclear proteins, such as Jun (Hunter, 1997). Significantly, signaling networks involving transcriptional programs that regulate proliferation and differentiation (epithelial-mesenchymal cell transition, EMT, plus the aforementioned Wnt, Tgf-β, and Notch pathways), and which are critical for normal development, often demonstrate aberrant activity in carcinogenesis (Kelleher *et al.*, 2006). These observations emphasize the importance of deregulation of embryological pathways in tumor biology.

Cell-Cell Interactions in Cancer

In addition to focusing on critical signaling pathways within cancer cells, it is imperative to reflect on the notion that multiple cell types cooperate to enhance tumorigenesis. Hepatocytes comprise approximately 60% of the liver cell population, while non-parenchymal cells (e.g. sinusoidal endothelial cells, Kupffer cells, Ito/hepatic stellate cells, intrahepatic lymphocytes) constitute the remaining 40% (Kmieć, 2001). The functions of hepatocytes, in both normal and pathological states, can be modulated by adjacent, nonparenchymal cells. For example, hepatocytes and Ito cells cooperate to deposit an extracellular matrix *in vitro* (Loréal *et al.*, 1993). It is well-established that the complex tumor microenvironment, containing extracellular matrix, growth factors and cytokines, and a variety of non-epithelial cell types (e.g. immune cells, fibroblasts) substantially influences tumor development (Li *et al.*, 2007). Indeed, cytokine production by non-parenchymal liver cells stimulates DNA synthesis preferentially in initiated hepatocytes, likely facilitating tumor promotion (Drucker *et al.*, 2006). Therefore, it is important to consider interactions between various liver cell types when assessing perturbations in key genes and pathways putatively involved in cancer, in order to more thoroughly comprehend the mechanisms underlying the disease.

5-Methylcytosine: Distribution and Abundance

The epigenetic mark 5-methylcytosine forms upon the covalent addition of a methyl group to the 5-position of the cytosine ring. This base is not mutagenic because it still base pairs with guanine. 5-methylcytosine is found at approximately 70% of all genomic CpG dinucleotides (Ehrlich, 1982; Naveh-Many and Cedar, 1981). Furthermore,

the majority of 5-methylcytosine is located within repetitive genomic regions such as satellite DNA and parasitic elements, including long interspersed elements (LINES), short interspersed elements (SINES), and endogenous retroviruses (Yoder *et al.*, 1997). In general, the genome is CpG-poor (intronic and intergenic regions), while most of the intermittent CpG sites remain methylated. Conversely, GC-rich CpG islands are associated with approximately 60% of all promoters and, with few exceptions, are largely unmethylated in humans and mice (Antequera, 2003). Originally, a CpG island was defined as a stretch of DNA greater than 200 bp long, with a G+C content above 50% and a ratio of observed CpG/expected CpG greater than 0.60 (Gardiner-Garden and Frommer, 1987). A revised, more stringent set of criteria identifies a CpG island as a region which is greater than 500 bp long, possesses a G+C content of at least 55%, and has an observed CpG/expected CpG ratio of at least 0.65 (Takai and Jones, 2002). It is estimated that there are 45,000 and 37,000 CpG islands in the human and mouse genomes, respectively (Antequera and Bird, 1993).

It is theorized that CpG islands remain unmethylated for 3 reasons: 1) demethylation processes remove methylation from CpG islands after they have been *de novo* methylated, 2) enzymes responsible for cytosine methylation do not efficiently methylate GC-rich DNA, or 3) genomic footprinting occurs, in which trans factors, such as transcription factors, bind to DNA and inhibit methylation (Cross and Bird, 1995). With regards to the third hypothesis, CpG islands, often associated with increased gene expression, might be "footprints" of early DNA replication intermediates, and thus, act as replicative origins (Cross and Bird, 1995). While gene-associated CpG islands can be located with coding regions, most are found within promoter regions, and methylation of

these can prevent transcription (Jones, 1999).

CpG dinucleotides are the preferred site of DNA methylation, however, non-CpG methylation also exists. Methylation at CpC, CpA, and CpT dinucleotides has been detected in mouse embryonic stem cells, and methylation at the 2 latter sites is likely established by Dnmt3a (Dodge *et al.*, 2002; Ramsahoye *et al.*, 2000). Additionally, CpNpG methylation in mammals has been assessed (Clark *et al.*, 1995). In humans, non-CpG methylation in the promoter region of a schizophrenia-related gene (*syt11*) correlated with decreased expression, demonstrating that non-CpG methylation might be biologically relevant (Inoue and Oishi, 2005). Thus, diverse methylation patterns throughout the genome presumably have complex biological effects.

Regulation of DNA Methylation Patterns

Methylation patterns are primarily established and maintained by DNA methyltransferase (Dnmt) enzymes and putative demethylases (Figure 1.2). Replication of methylated DNA results in an intermediate state of hemi-methylation, which is restored to a full methylation status by the maintenance methylase, Dnmt1. *De novo* methyltransferases can add methyl groups to completely unmethylated DNA. Methylated DNA can become hypomethylated in a passive (replication-dependent) or active (replication-independent) manner. In addition to enzymes, methylation patterns are shaped by alterations in other processes as well (Figure 1.3). The methyl group utilized in 5-methylcytosine synthesis reactions is derived directly from S-adenosylmethionine (SAM), which is generated as a result of 1-carbon metabolic reactions. Thus, levels of SAM, 1-carbon metabolism substrates, or the relevant enzymes might contribute to changes in methylation patterns (Ulrey *et al.*, 2005) (Figure 1.4).

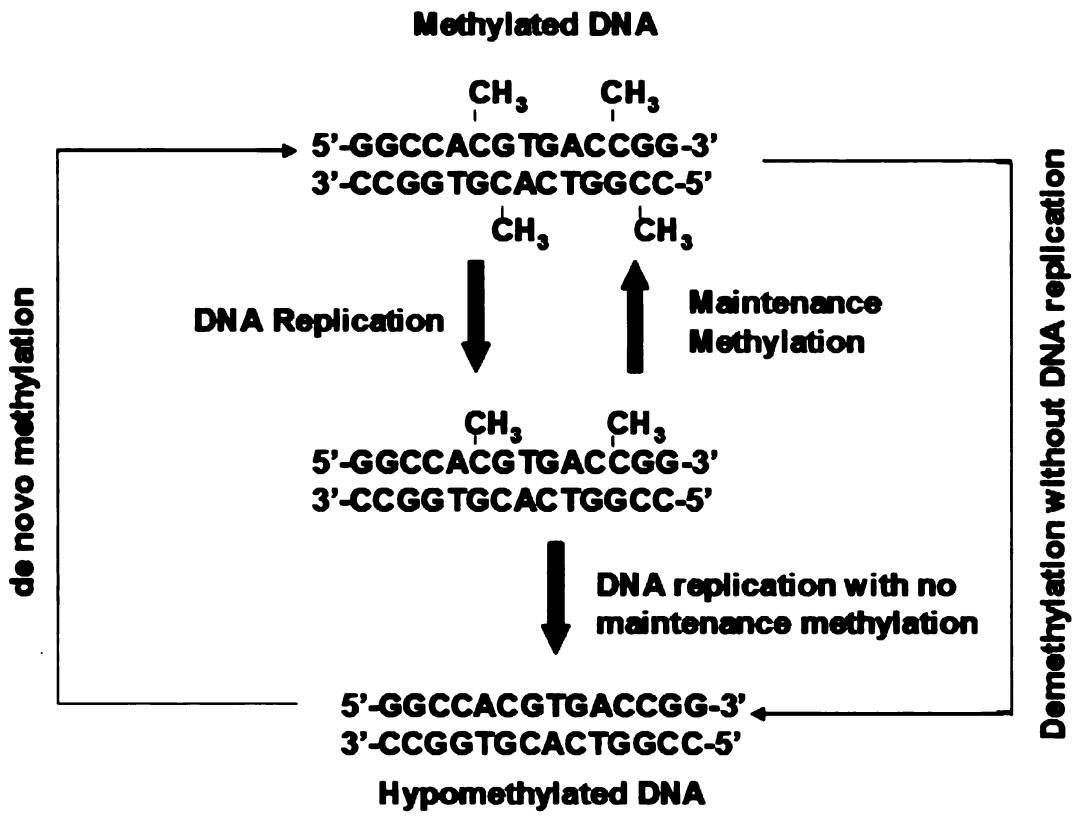


Figure 1.2 DNA Methylation, a Heritable Epigenetic Modification. Immediately after replication, DNA exists in a hemimethylated state, as the newly synthesized strand has not yet been methylated to match the pattern of the parent strand. Following DNA synthesis, the maintenance methyltransferase (DNMT1) adds methyl groups to the appropriate positions of the unmethylated strand. If replication occurs without maintenance methylation, the DNA becomes hypomethylated in a "passive" fashion. DNA can also demethylate by an "active" mechanism (i.e. without DNA replication), however, it is not clear exactly which enzymes are responsible for this process. Alternatively, hypomethylated DNA can become methylated via 2 characterized *de novo* methyltransferases (DNMT3A and DNMT3B). (Adapted from Hergersberg, 1991)

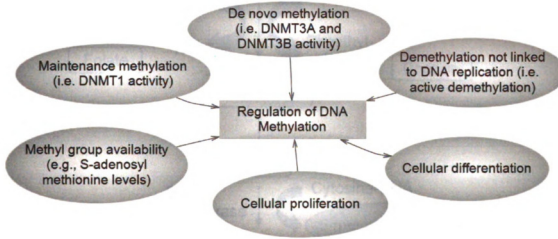


Figure 1.3 DNA Methylation is Affected by Multiple Factors. The process of DNA methylation is dependent upon numerous factors. Variation of any one of these elements can dramatically affect normal DNA methylation patterns. Note that cellular differentiation can be altered by DNA methylation, and DNA methylation patterns can be changed upon cellular differentiation, hence the presence of the double-headed arrow. (Adapted from Goodman and Watson, 2002).

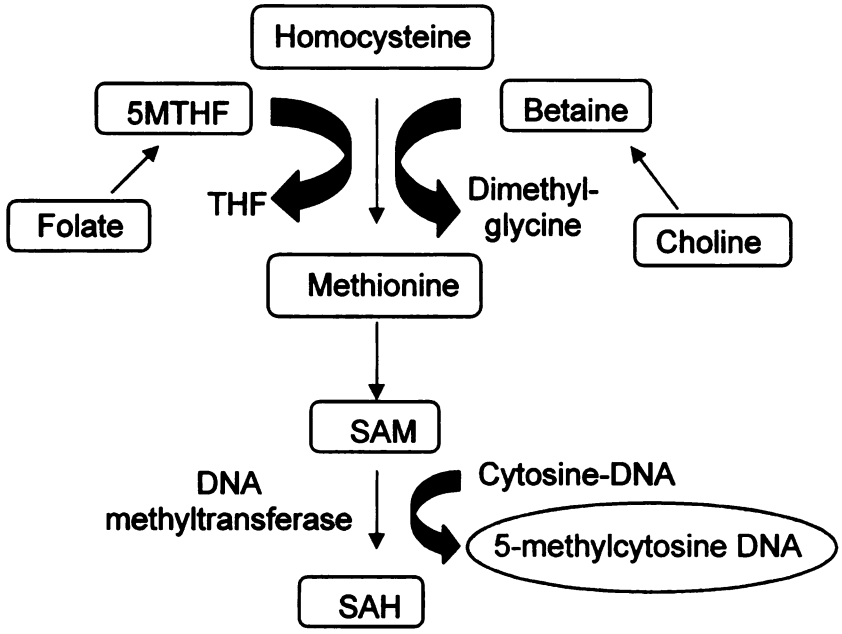


Figure 1.4 DNA Methylation and 1-Carbon Metabolism. The process of DNA methylation is dependent upon multiple factors, including one-carbon metabolic pathways. The methyl groups utilized for DNA methyltransferase reactions originate from a variety of cofactors and methyl donors, such as choline and folate. Ultimately, DNA methyltransferase enzymes transfer a methyl group from S-adenosylmethionine (SAM) to the 5 position of the cytosine ring, resulting in the generation of 5-methylcytosine and S-adenosylhomocysteine (SAH). Abbreviations: 5MTHF, 5-methyltetrahydrofolate; THF, tetrahydrofolate. (Adapted from Dolinoy *et al.*, 2006)

Regulation of DNA Methylation Patterns: DNA Methyltransfase Enzymes

Eukaryotic Dnmt1 prefers hemi-methylated DNA as a substrate, and as such, has been described as the major maintenance methyltransferase that methylates newly replicated DNA. Indeed, Dnmt1 accumulates at replication foci during the S-phase of the cell cycle (Leonhardt *et al.*, 1992). The enzyme exhibits a 5- to 30-fold greater rate of methyl transfer to hemi-methylated, as compared to unmethylated substrates, is highly processive, and shows no sequence specificity (Goyal *et al.*, 2006). DNA replication appears to be coupled to the process of DNA methylation, as Dnmt1 can interact with PCNA (a critical component of the DNA replication machinery) (Schermelleh *et al.*, 2007). While this relationship is not critical for maintenance methylation, it enhances the post-replicative methylation efficiency the enzyme (Schermelleh *et al.*, 2007). Dnmt1 can also be recruited to sites of DNA repair, suggesting a mechanism by which it could more proficiently re-establish epigenetic status after repair of damaged DNA (Mortusewicz, 2005).

A variety of mutant alleles, producing varying degrees of Dnmt1 expression, have been employed to more fully elucidate its biological roles. *Dnmt1*$^{-/-}$ mice die during early embryogenesis and exhibit a substantial loss of DNA methylation (Li *et al.*, 1992). Other effects of decreased/absent *Dnmt1* expression include abnormal imprinting, aberrant X-chromosome inactivation, and demethylation and activation of particular transposable elements (Li *et al.*, 1993; Panning and Jaenisch, 1996; Walsh and Bestor, 1999). Conversely, phenotypes of *Dnmt1* overexpression in embryonic stem cells include lethality, genomic hypermethylation, and loss of imprinting (Biniszkiewicz *et al.*, 2002). Thus, it appears that a delicate balance of Dnmt1 expression and/or activity is necessary

for proper methylation levels and cellular function.

There exist two closely related *de novo* methyltransferases, Dnmt3a and Dnmt3b, which can add methyl groups to unmethylated substrates without discernable sequence specificity (Okano *et al.*, 1998). In mammals, *de novo* methylation is a critical factor in key processes, including transposon suppression, genomic imprinting, and X-chromosome inactivation. While these enzymes are both expressed at low levels in somatic cells, and high levels in embryonic stem cells, early embryos, and developing germ cells, they are together responsible for *de novo* methylation during development (Okano *et al.*, 1999; Chen *et al.*, 2003; Hata *et al.*, 2002). Moreover, Dnmt1 and Dnmt3a/3b have distinct functions, as evidenced by the observation that neither *Dnmt1* overexpression in *Dnmt3a*$^{-/-}$/*3b*$^{-/-}$ embryonic stem cells nor overexpression of *Dnmt3a* in *Dnmt1*$^{-/-}$ cells properly re-established normal methylation patterns (Chen *et al.*, 2003).

Dnmt3a and Dnmt3b appear to methylate different targets and have specialized biological roles. Dnmt3a is associated with heterochromatin (Bachman *et al.*, 2001) and is essential for both paternal and maternal imprinting (Kaneda *et al.*, 2004). Dnmt3a alone can methylate major satellite repeats within the pericentromeric region and a specific CpG site within the *Xist* promoter region (Chen *et al.*, 2003), plus non-CpG sites (Ramsahoye *et al.*, 2000). Conversely, Dnmt3b localizes to both centromeric and pericentromeric heterochromatin and is primarily responsible for methylation at centromeric minor satellite repeats (Okano *et al.*, 1999). In mouse embryonic fibroblasts, inactivation of *Dnmt3b* results in global DNA hypomethylation, chromosomal instability, and spontaneous immortalization or premature senescence (Dodge *et al.*, 2005), whereas inactivation of *Dnmt3a* does not. Inactivating mutations in *Dnmt3b* are responsible for

ICF (immunodeficiency, centromere instability, and facial anomalies) syndrome, which is characterized by severe hypomethylation of classical satellite DNA (Xu *et al.*, 1999).

There is an elevated level of complexity with regard to the functions of Dnmt1, 3a, and 3b, as the *de novo* methyltransferases are involved in maintaining global methylation patterns, which has typically been thought to be the role of Dnmt1. This is evidenced by the observation that inactivation of *Dnmt3a* and *3b* in embryonic stem cells caused demethylation of imprinted genes, nonimprinted genes, and repetitive elements (Chen *et al.*, 2003). After treatment of cells with a DNA demethylating agent, Dnmt3a and Dnmt3b were necessary to restore methylation patterns to distinct genomic sequences that Dnmt1 could not re-methylate alone, further supporting the cooperation of all 3 Dnmt's in preserving normal methylation patterns (Liang *et al.*, 2002).

Dnmt3L is a catalytically inactive paralog that can stimulate the *de novo* methyltransferase activity of Dnmt3a (Chedin *et al.*, 2002). In oocytes, Dnmt3L is essential for the methylation of differentially methylated regions in maternally imprinted genes in oocytes (Bourc'his *et al.*, 2001). In early germ cells, ablation of the *Dnmt3L* gene caused demethylation of long terminal repeat (LTR) and non-LTR retrotransposons, resulting in the transcription of these sequences in spermatogonia and spermatocytes (Bourc'his and Bestor, 2004). Finally, Dnmt2 has weak DNA methyltransferase activity, and primarily methylates aspartic acid transfer RNA, indicating a limited functional role in the DNA methylation process (Jeltsch *et al.*, 2006).

Regulation of DNA Methylation Patterns: DNA Demethylation

DNA can become demethylated in two ways. Passive demethylation is the result

of a lack of maintenance methylation following DNA synthesis (Howlett and Reik, 1991). Indeed, most of the genome-wide demethylation that occurs during early development is passive in nature (Rougier *et al.*, 1998). Alternatively, active demethylation (i.e. independent of DNA replication) also results in hypomethylated DNA. After fertilization, the paternal genome becomes globally hypomethylated by an active mechanism (Oswald *et al.*, 2000). Furthermore, the promoter regions of the *Il2* (Bruniquel *et al.*, 2003) and *pS2/TFF1* (Métivier *et al.*, 2008) genes are also actively demethylated.

Evidence of the existence of bona fide demethylases in mammals is controversial. Initially, demethylase activity was documented in two different model systems (Gjerset and Martin 1982; Weiss *et al.*, 1996), but no potential demethylase proteins were described. An RNA-dependent 5meC glycosylase in the chick embryo lysates (Jost, 1993) was later revealed as thymine DNA glycosylase. However, this enzyme is quite inefficient at removing 5-methylcytosine, and thus it an unlikely demethylase candidate (Cortázar *et al.*, 2007). Additionally, human MBD4 possesses 5-methylcytosine DNA glycosylase activity (Zhu *et al.*, 2000). Another group discovered MBD2, a demethylase that could remove methyl groups using only water as a cofactor (Bhattacharya *et al.*, 1999), however, their findings could not be reproduced. MBD3 appears to induce active demethylation and transcriptional activation of specific genomic targets (Brown *et al.*, 2008). Most recently, conflicting reports have emerged regarding the ability of GADD45a to participate in active demethylation (Ooi and Bestor, 2008).

Another pathway that can result in demethylation involves oxidative deamination. *In vitro* studies have ascertained that Dnmt3a and 3b mediate deamination of 5-methylcytosine, resulting in the generation of thymine, which produces a

thymine:guanine mismatch pair (Métivier *et al.*, 2008). It was then proposed that base excision repair machinery is recruited and converts the base pair back to guanine:unmethylated cytosine (Métivier *et al.*, 2008). In summary, the existence of a bona fide active demethylase enzyme remains controversial.

Transcriptional Regulation: DNA Methylation

Transcriptional repression, due to DNA hypermethylation, can be accomplished in multiple ways. Steric blocking by the methyl groups of trans factors can prevent them from binding their cognate cis elements. Methylation at a cAMP-responsive element impedes transcription factor binding and blocks transcription *in vitro* and *in vivo* (Iguchi-Ariga and Schaffner, 1989). Additionally, methylation of specific CpG dinucleotides abrogates the binding of a key transcription factor (MLTF) and prevents gene transcription from the adenovirus major late promoter (Watt and Molloy, 1988). The transcription factor CTCF, involved in the imprinting process at the *H19/Igf2* locus, can bind to a DNA sequence on the maternal allele, between the *Igf2* promoter and its downstream enhancer, effectively repressing *Igf2* transcription. On the paternal allele, however, CTCF binding is inhibited by methylation of its binding site, allowing the enhancer element to activate *Igf2* transcription (Bell and Felsenfeld, 2000).

DNA methylation can also contribute to transcriptional control by interacting with methyl-binding proteins that are attracted to 5-methylcytosine. These proteins interpret the information encoded by the methylation marks and participate in the recruitment of enzymes and additional transcriptional repressors, which culminate in gene silencing. The two classes of methyl-binding proteins are those of the MBD family (MeCP2, MBD1,

MBD2, MBD3 and MBD4) (Hendrich and Bird, 1998), and those that possess Kaiso-like zinc fingers (Kaiso, ZBTB4 and ZBTB38) (Filion *et al.*, 2006). Four of the MBD proteins (excluding MBD4) recruit and physically interact with slightly different combinations of enzymes and transcriptional repressors, including chromatin-modifying enzymes and nucleosome remodeling proteins (HDAC1, HDAC2, Suv39h1, SETDB1, Mi-2, Sin3A) (Lopez-Serra and Esteller, 2008). In this fashion, the chromatin is restructured into a repressive form, thus abrogating transcription. In human cancer, hypermethylated promoters of tumor suppressor genes contained diverse groups of MBDs, which were dependent upon both the gene and the tumor type (Lopez-Serra *et al.*, 2006). All of the aforementioned zinc finger proteins can also participate in methylation-dependent transcriptional repression (Filion *et al.*, 2006; Yoon *et al.*, 2003). Nonetheless, it is still elusive as to whether, and how, methyl-binding proteins are targeted to specific genomic regions to exert their effects.

Although DNA methylation changes have been discussed in the context of the paradigm "increases in methylation lead to decreases in gene expression" and vice versa, it is crucial that one considers unconventional situations as well. Aberrant hypermethylation of imprinting control regions (ICR) at an imprinted locus can cause increased *Igf2* expression that is associated with cancer (Ehrlich, 2002; Feinberg, 2001; Steenman *et al.*, 1994). Additionally, the growth suppressor gene *Igfr2* is imprinted in mice, and methylation within a DMR on the maternal allele is responsible for maternal expression of the gene (Wutz *et al.*, 1997). Thus, in these examples, DNA hypermethylation contributes to transcriptional activation, indicating that it is entirely possible for elevated methylation levels to facilitate gene expression. This concept has

implications in my research, as gene expression did not always inversely correlate with methylation status (assuming DNA methylation controls transcription), and therefore, one must consider alternatives to the paradigmatic way of thinking.

Transcriptional Regulation: DNA Methylation and Chromatin Alterations

Two types of epigenetic modifications, DNA methylation and chromatin alterations, are closely intertwined, and the latter must be considered when elucidating the mechanisms by which changes in DNA methylation exert transcriptional effects. Chromatin structure controls the spatial and temporal changes in gene expression necessary at different stages of life, and adding to the dynamic nature of this organization are enzyme-catalyzed posttranslational modifications (e.g. acetylation, methylation) to the N-terminal tails of histone proteins (Kouzarides, 2007). These heritable modifications, and combinations of them, are collectively referred to as the "histone code" (Strahl and Allis, 2000), which plays key roles in 2 distinct processes: 1) alterations in nucleosome structure, and 2) recruitment of nonhistone proteins (e.g. HP-1), that modulate gene expression, plus other chromatin functions (Kouzarides, 2007).

A complex and variable relationship exists between DNA methylation and histone modifications, with regard to transcriptional control. For example, Dnmt1 and Dnmt3a directly associate with histone methyltransferases, suggesting the importance of interplay between these 2 epigenetic mechanisms for the enhancement of gene silencing (Fuks *et al.*, 2003). Furthermore, DNA methyltransferase enzymes have been shown to associate with histone deacetylases (Burgers *et al.*, 2002). Indeed, histone modifications and DNA

methylation not only cooperate to silence genes, but also participate in feedback loops that further augment transcriptional repression (Fuks, 2005).

The hierarchical timing of these events, however, remains controversial. In other words, DNA might initiate histone modifications, histone modifications might influence DNA methylation, and/or nucleosome remodeling might facilitate DNA methylation. In fact, there is evidence to support each of these possibilities. In some instances, DNA methylation is the initial change that stimulates alterations in gene expression, and chromatin modifications occur subsequent to this. As described previously, methyl-binding proteins can recruit chromatin-modifying and nucleosome-remodeling enzymes, including histone deacetylases, which have the capacity to affect gene expression. Within the context of cancer, gene silencing has been assessed using DNA methylation and histone deacetylase inhibitors, and results indicate that DNA methylation plays the dominant role in gene expression (Cameron *et al.*, 1999).

In some situations, modifications in DNA methylation are secondary to histone modifications, and the former provides an additional repressive layer that "locks in" gene silencing, e.g. during X-chromosome inactivation, hypermethylation stabilizes silencing, but does not instigate it (Heard, 2004). Trimethylation of lysine 9 on histone H3 can guide Dnmt3b to satellite repeat elements in pericentric heterochromatin, thus dictating DNA methylation patterns (Lehnertz *et al.*, 2003). Also, gene silencing can occur in conjunction with histone modifications, without relevant DNA methylation changes (Bachman *et al.*, 2003).

ATP-dependent chromatin remodeling involves events which alter nucleosome structure. Nucleosome remodeling complexes belong to 4 major families: SWI/SNF,

ISWI, NURD/Mi-2/CHD, and INO80 (Wang *et al.*, 2007). Further demonstrating the complexity of the integration of DNA methylation changes with other epigenetic processes, lack of *Lsh*, a member of the SNF2 family of chromatin remodeling proteins, results in aberrant global methylation levels, implying that chromatin remodeling is critical for the establishment of proper DNA methylation patterns (Dennis *et al.*, 2001). Moreover, the chromatin-remodeling factors *Brm* and *Brg1*, which can modulate transcription themselves, trigger DNA methylation changes that ultimately affect gene expression (Banine *et al.*, 2005). Thus, the processes of DNA methylation, histone modification, and nucleosome remodeling concertedly regulate gene transcription, as well as the actions of one another.

Roles of DNA Methylation in Normal Physiology

In normal physiological situations, DNA methylation plays a variety of roles in cells. For example, dynamic changes in methylation patterns during development are especially significant. The genomes of primordial germ cells are globally demethylated by embryonic day 13 to 14, and although it is not known if this process is active or passive in nature, it is crucial for the resetting of imprinting marks (Reik *et al.*, 2001). Several days later, remethylation of single-copy genes and imprinted loci occurs within the genomes of both male and female primordial germ cells. Post-fertilization, a second broad wave of demethylation takes place in early embryos: the paternal genome is demethylated in an active manner, and the maternal in a passive manner. Simultaneously, certain imprinted genes and repeat sequences are protected, such that their methylation statuses persist, however, the mechanism(s) responsible for this are unclear. Finally,

postzygotic paternal and maternal genomes are remethylated to varying degrees (Reik *et al.*, 2001).

There is limited evidence that methylation regulates cell-type specific genes during development, and the purposes of any known changes remain largely undetermined. Expression of the *maspin* gene is controlled by DNA methylation, and was unmethylated and expressed in cells of epithelial origin, but methylated and repressed in mesenchymal and haematopoetic cells (Futscher *et al.*, 2002). Additional studies have revealed genes whose expression is modulated by differentiation-associated methylation changes during normal development, such as TFIIα/β-like factor (*Alf*), interferon-gamma (*Ifnγ*), and testis-specific genes (of the MAGE-LAGE-GAGE-BAGE superfamily) (Ehrlich, 2003).

Two key developmental processes, each non-mendelian forms of inheritance whereby one allele is silenced during embryogenesis, involve alterations in DNA methylation. X-chromosome inactivation is required for dosage compensation of X-linked genes in female cells, and results in the silencing of the redundant X chromosome. The initiation of silencing is mainly regulated by a noncoding RNA (*Xist*), followed by distinct chromatin alterations, including histone methylation, which cooperate to form repressive heterochromatin (Heard, 2004). Then, increased DNA methylation levels "lock in" stable silencing of the inactive X chromosome, but do not contribute to the initiation of it (Heard, 2004; Sado *et al.*, 2004).

At certain loci, DNA methylation changes also control imprinting, a process by which monoallelic expression is maintained in the cell via silencing of either the paternal or maternal allele. An example of an imprinted locus at which methylation plays a vital

role is the *Igf2/H19* region. The growth factor *Igf2* is paternally expressed and the noncoding RNA *H19* is maternally expressed (Reik and Murrell, 2000). The maternal imprinting control region (ICR) of *H19* remains unmethylated, allowing the binding of the *CTCF* protein, thus inhibiting *Igf2* transcription by blocking the actions of downstream enhancer elements, and facilitating *H19* transcription. Conversely, the methylated ICR of the paternal allele prevents CTCF binding and *H19* transcription, concurrently driving transcription of *Igf2*, whose promoter can be influenced by the enhancers (Reik and Murrell, 2000).

It is hypothesized that DNA methylation maintains genomic integrity via 3 main mechanisms. One role of intergenic methylation might be the inhibition of cryptic transcriptional initiation. While data supporting this idea is sparse in mammals, it has been shown that 5-methylcytosine can block transcriptional elongation in plants (Zilberman *et al.*, 2007). Secondly, methylation might silence transposable elements, as most repeat elements in mammals are methylated (Yoder *et al.*, 1997). Moreover, *Dnmt1*$^{-/-}$ mouse embryos exhibit increased transcriptional activation of IAP retrotransposons (Walsh *et al.*, 1998), and similarly, in germ cells which lack 2 cofactors (Lsh and, separately, Dnmt3L) which are essential for the maintenance of methylation patterns, IAP and/or LINE-1 elements become reactivated (Bourc'his and Bestor, 2004; De La Fuente *et al.*, 2006). Thirdly, genomic instability is associated with global hypomethylation (Chen *et al.*, 1998). Mouse embryonic fibroblasts lacking *Dnmt3b* exhibit not only demethylation, but chromosomal abnormalities and alterations in ploidy, as well (Dodge *et al.*, 2005). Furthermore, deletion of *Dnmt1* and *Dnmt3b* in a human cell line results in chromosomal abnormalities (Karpf and Matsui, 2005). It has been

observed that telomeric regions in *DNMT1*$^{-/-}$ and *DNMT3a,3b*$^{-/-}$ mouse embryonic stem cells become hypomethylated and exhibit an increased frequency of recombination (Gonzalo *et al.*, 2006). Taken together, these data implicate DNA methylation in a variety of cellular processes that are essential for normal growth and viability.

Roles of Altered DNA Methylation in Cancer

Due to the pleiotropic biological effects of DNA methylation changes, it is not surprising that aberrant methylation plays a role in numerous diseases, including multiple imprinting disorders, Fragile X syndrome, immunodeficiency, centromeric instability, and facial anomalies (ICF) syndrome, and systemic lupus erythematosus (Robertson, 2005). The focus of my dissertation research is carcinogenesis, however, and so the diverse roles that DNA methylation plays within the context of tumor development (Figure 1.5) will be discussed. Tumorigenesis results from the accumulation of heritable changes that confer growth advantages upon particular cells, which eventually acquire the 6 fundamental features of a cancer cell (Hanahan and Weinberg, 2000). Epigenetic changes (e.g. DNA methylation, histone modifications, and microRNAs) are central to the carcinogenesis process. DNA hypomethylation, as well as mutation, can elevate gene expression while hypermethylation, as well as mutation, can silence it (Esteller, 2007a; Goodman and Watson, 2002). Additionally, the interplay between epigenetic changes and mutation in a single pathway has been demonstrated, and must be taken into account in order to more comprehensively understand cancer. For example, in colon cancer cells, genes involved in Wnt signaling are both hypermethylated (*SFRP1, SFRP2, SFRP4, SFRP5*) and mutated (*CTNNB1*, gene that encodes β-catenin), and these alterations

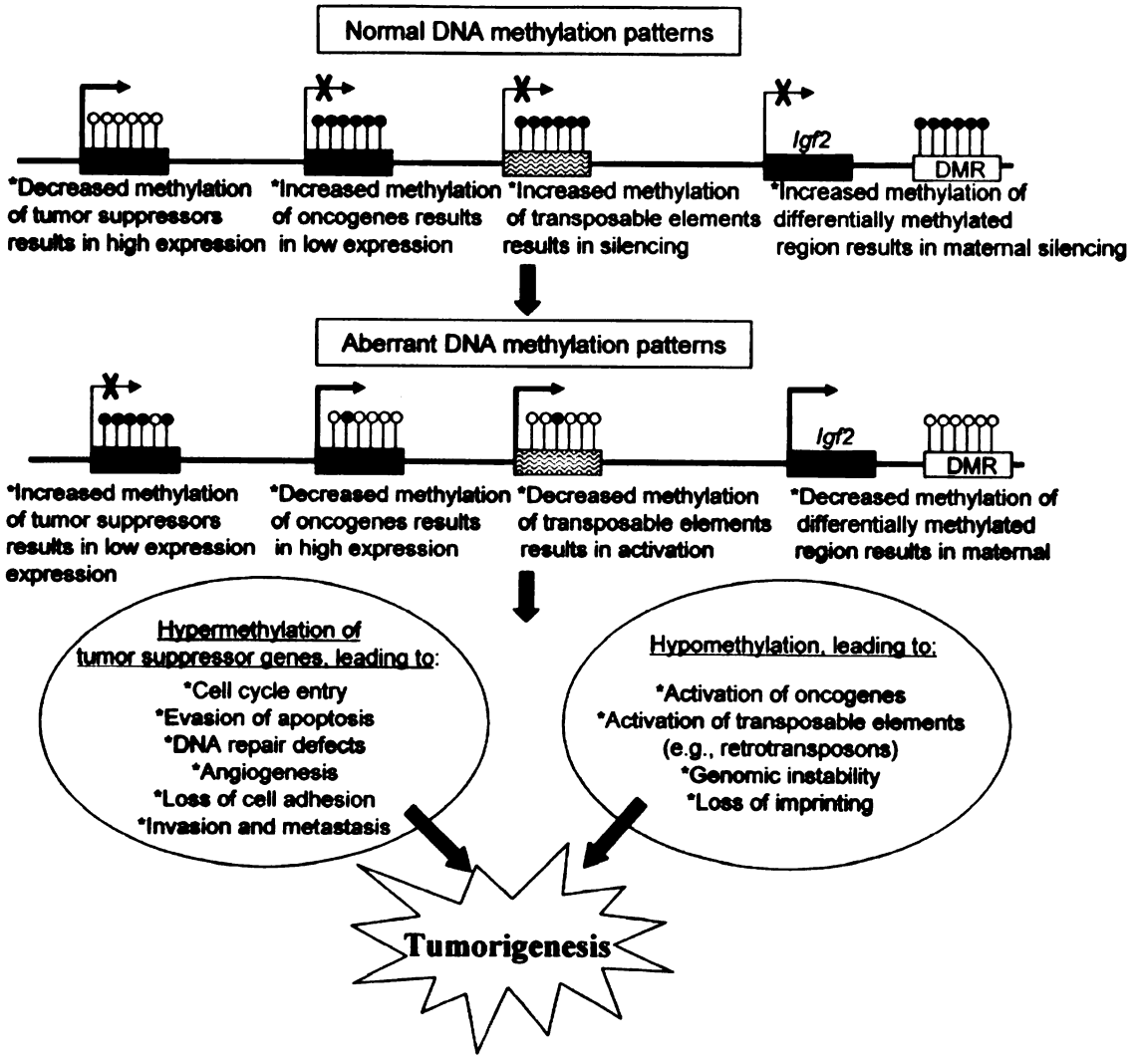


Figure 1.5 The functions of DNA methylation Aberrant alterations in DNA methylation can lead to a variety of cellular changes that can facilitate tumor development. Both hypomethylation and hypermethylation play critical roles during carcinogenesis. CpG sites are depicted (|), and these are unmethylated (white circles) or methylated (gray circles). Genomic regions are promoter regions (▬), transposable elements (▬), or differentially methylated regions, DMRs (▭). (Adapted from Esteller, 2007 and Goodman and Watson, 2002)

complement one another, culminating in the constitutive activation of Wnt signaling (Baylin and Ohm, 2006).

Roles of Altered DNA Methylation in Cancer: Hypomethylation

Hypomethylation of CpG dinucleotides was the first epigenetic aberration to be linked to cancer: human cancer genomes were hypomethylated, as compared to their normal counterparts (Feinberg and Vogelstein, 1983a). This observation was confirmed in subsequent studies, as global methylation levels were decreased in a variety of human tumors (Gama-Sosa *et al.*, 1983). It is presumed that hypomethylation can contribute to cancer by several mechanisms: transcriptional activation of oncogenes, chromosomal instability, activation of transposable elements, and loss of imprinting (Esteller, 2008; Feinberg and Tycko, 2004).

There are multiple examples in which hypomethylation of oncogene promoters can result in increased gene expression. Hypomethylation and increased expression of Ha-*ras* in liver tumor-susceptible mice, but not in those that are relatively resistant, occurred in response to treatment with the nongenotoxic liver tumor promoter phenobarbital (Bachman *et al.*, 2006). Indeed, hypomethylation of Ras oncogenes in carcinogenesis has previously been shown (Feinberg and Vogelstein, 1983b). Other examples of oncogenes that exhibit hypomethylation and increased expression include cyclin D2 in gastric carcinoma (Oshimo *et al.*, 2003), HPV-16 DNA in cervical cancer (Badal *et al.*, 2003), and the S100A4 metastasis-associated gene in colon cancer (Nakamura and Takenaga, 1998).

Genomic instability, in the context of cancer, is associated with hypomethylation. In human hepatocellular carcinoma, hypomethylation of heterochromatic satellite 2 DNA in chromosome 1 correlated with a copy gain of the q-arm (Wong *et al.*, 2001). Moreover, reduced genomic hypomethylation in $Nf1^{+/-}$ $p53^{+/-}$ mice causes cancer and is thought to promote loss of heterozygosity (Eden *et al.*, 2003). Additionally, disruption of the *Dnmt1* gene in murine embryonic stem cells resulted in increased mutation rates due to mitotic recombination or chromosome loss (Chen *et al.*, 1998).

Loss of imprinting is often observed in cancer. Hypomethylation of a differentially methylated region downstream of the first promoter of *Igf2* on the maternal allele results in loss of imprinting and increased *Igf2* expression (Cui *et al.*, 2003; Sullivan *et al.*, 1999). Loss of *Igf2* imprinting occurs in Wilms tumors (Bjornsson *et al.*, 2007; Sullivan *et al.*, 1999), and is associated with an increased risk for colorectal tumorigenesis (Cui *et al.*, 2003).

Finally, hypomethylation of DNA can cause reactivation of transposable elements (Bourc'his and Bestor, 2004). Typically, genomic sequences, including endogenous retroviruses and retrotransposons (e.g. human long interspersed repetitive element 1, LINE-1) become hypomethylated during cancer (Ehrlich, 2002; Schulz *et al.*, 2006). In chronic myelogenous leukemia, promoter hypomethylation of LINE-1 elements was associated with increased levels of transcript (both sense and antisense) and poorer survival (Roman-Gomez *et al.*, 2005). Furthermore, it has also been suggested that transcription of transposable elements can contribute to cancer not only by interfering with endogenous transcription (Whitelaw and Martin, 2001), but also by insertional mutagenesis, genomic rearrangement, and the generation of double-stranded DNA breaks,

leading to genomic instability (Collier and Largaespada, 2007). Therefore, genomic hypomethylation can facilitate oncogene expression and pose significant problems to the integrity of the genome, particularly within the context of tumorigenesis.

Roles of Altered DNA Methylation in Cancer: Hypermethylation

Paradoxically, hypermethylation of the genome occurs in conjunction with hypomethylation, and also influences the carcinogenesis process. As opposed to hypomethylation, an extensive body of literature exists that describes a plethora of genes whose promoters exhibit increased methylation and diminished expression (Esteller, 2007a). Indeed, genes whose expression can be silenced by hypermethylation participate in a variety of biological processes, such as growth suppression, DNA repair, cell adherence, metastasis, angiogenesis, apoptosis and the cell cycle (e.g. the DNA repair gene MLH1, the cell cycle inhibitors $p16^{INK4A}$ and Rb, and APC, an inhibitor of β-catenin) (Esteller, 2007a). Furthermore, recent efforts have resulted in the identification of microRNAs that function as tumor suppressors, and hypermethylation of their promoters is associated with decreased transcriptional activity (Lujambio and Esteller, 2007).

Results from a massive study that analyzed promoter region methylation statuses of 12 tumor suppressor genes in 600 individual tumors, representing 15 tumor types, led to the conclusion that different cancers have particular profiles of hypermethylated genes (Esteller *et al.*, 2001). For instance, p16 exhibited increased methylation across a broad range of tumors, while increased methylation of p15 was more restricted, occurring solely in lymphomas and leukemia (Esteller *et al.*, 2001). Thus, it is instructive to consider the specific hypermethylation profiles of individual tumors in order to gain a more complete

understanding of how hypermethylation influences carcinogenesis, as this has significant implications for diagnosis, prognosis, and treatment.

Silencing of genomic regions by DNA hypermethylation is not always limited to single promoters. In fact, DNA spanning a 4 Mb region across chromosome 2 was subjected to transcriptional repression in colorectal cancer cells, and both DNA hypermethylation and histone H3 lysine 9 methylation were associated with gene silencing (Frigola *et al.*, 2006). This study raises the concept of "seeding," i.e. the ability of methylation changes to spread to nearby unmethylated sites. It is known that methylated foci of CpG sites can cause neighboring unmethylated sites, including promoter regions, to gain this modification (Turker, 1999). Insertion of proviral DNA into a host genome results in methylation of the host's flanking regions (Jähner and Jaenisch, 1985). This might be relevant to my research, as I observed many methylation changes within exons and introns of genes, and a subset of these alterations might be reflective of critical changes that have occurred, or will occur, in regulatory promoter regions.

Compounds that are capable of preventing DNA methylation have been instrumental in cancer therapy development. DNA methyltransferase (Dnmt) inhibitors can be divided into 2 classes (Yoo and Jones, 2006). Nucleosides analogs (e.g. 5-Azacitidine, 5-Aza-2'-deoxycitidine) contain a modified cytosine ring attached to a ribose or deoxyribose sugar, are converted to nucleotides, incorporate into DNA and/or RNA, and subsequently block Dnmt activity. Alternatively, non-nucleoside analogs (e.g. Hydralazine, Procainamide) bind directly to Dnmt enzymes to inhibit them (Yoo and Jones, 2006). There has been some success using such agents in a clinical setting.

Vidaza® (5-azacitidine) and and Decitabine® (5-aza-2'-deoxycitidine) are FDA-approved for treatment of myelodysplastic syndromes, which are characterized by inhibition of hematopoiesis and an increased risk of developing acute myelogenous leukemia. Decitabine® has also been utilized successfully to remedy acute and chronic myelogenous leukemias (de Vos and van Overveld, 2005).

Early DNA Methylation Changes Facilitate Tumorigenesis

There are cited examples of relevant methylation changes that occur early during neoplastic progression, supporting the notion that altered methylation is a driving force of tumorigenesis, as opposed to a consequence of the process. In human colon cancer, gene-specific hypomethylation was detected in both benign and malignant lesions (Goelz *et al.*, 1985). Additionally, hypomethylation was observed in normal-appearing rectal mucosa in colorectal cancer patients, as compared to cancer-free individuals (Cravo *et al.*, 1994). In addition, tumor suppressors are hypermethylated at an early stage, with increasing frequency during tumor progession (Feinberg *et al.*, 2006). Methylation changes in the initial stages of colon cancer ultimately facilitate activation of Wnt signaling, which drives proliferation and survival (Baylin and Ohm, 2006). One main focus of my dissertation research is the identification of genes plus cellular processes and signaling pathways, that might be involved during early stages of tumorigenesis. Such genes ay include those whose regulation might be controlled by aberrant methylation changes.

Rodent Models of Liver Tumorigenesis

Chemical carcinogens were historically considered to be genotoxins, i.e. chemicals which directly, or indirectly via metabolites, cause promutagenic adducts or other types of DNA damage, including chromosomal breakage, fusion, deletion, non-disjuncton, and mis-segregation (Luch, 2005). However, this concept had to be reconciled with the observation that not all mutagenic compounds cause tumors, and additionally, not all carcinogens are mutagens. Nongenotoxic carcinogens (i.e. those that do not cause mutations) affect the balance of proliferation and cell death, and are capable of causing tumorigenesis by mechanisms such as immunosuppression, inflammation, reactive oxygen species generation, receptor activation, and epigenetic alterations (Luch, 2005). Rodent liver models have traditionally been utilized to evaluate the carcinogenicity of both genotoxins and nongenotoxins. While there are differences between the cancer process in mice and humans (Rangarajan and Weinberg, 2003), mouse models have been, and currently are, extremely beneficial for elucidating aspects of the human tumorigenesis process. For example, many genes (e.g. PTEN, MLH1, p53) are disrupted in cancers that develop in both species (Herzig and Christofori, 2002). Therefore, it is likely that that genes which underlie tumorigenesis in humans and rodents are largely the same, and their disparate sensitivities can be attributed, at least in part, to gene regulation.

Both liver tumorigenesis models employed in my dissertation research involve at least 1 group of mice that is susceptible, and 1 group that is resistant, to phenobarbital (PB)-induced carcinogenesis. By evaluating alterations in DNA methylation and gene expression that occur uniquely in the susceptible, as compared to the resistant mice, one can focus upon changes that might be directly related to tumor formation.

B6C3F1 and C57BL/6 Mice

The first model system includes the resistant C57BL/6 strain and the susceptible B6C3F1 stock (cross between the highly susceptible C3H/He paternal strain and the relatively resistant C57BL/6 maternal strain). Genetic background is a contributing factor to liver tumor susceptibility in these mice, as the incidences of spontaneous tumor formation in susceptible C3H/He and B6C3F1 and the relatively resistant C57BL/6 mice are 61% [1-4 tumors/tumor-bearing animal (TBA)], 29% (1-2 tumors/TBA) after 12 months, and 0% after 18 months, respectively (Becker, 1982).

The tumor-sensitive mice are also more prone to chemically-induced carcinogenesis. Specifically, the C3H/He strain is 20-50X more susceptible to liver tumor formation than the C57BL/6, in response to treatment with the mutagens diethylnitrosamine (Drinkwater and Ginsler, 1986) and N-ethyl-N-nitrosourea (Hanigan *et al.*, 1988), and strain-specific differences are also observed upon phenobarbital (PB) treatment. PB, a sedative and anticonvulsant, is a prototypical nongenotoxic rodent liver tumor promoter that induces xenobiotic-metabolizing enzymes, including those of the Phase I (e.g. cytochrome P450s and cytochrome P450 oxidoreductase) and Phase II (e.g. glutathione-S-transferases and UDP-glucuronyltransferase) classes (Whysner *et al.*, 1996). In rodents, PB treatment causes hepatic hypertrophy, hyperplasia, adenomas and hepatocellular carcinomas (Whysner *et al.*, 1996). For example, upon chronic exposure to a promoting dose of PB in drinking water (0.05%, w/w) for 12 months, 100% of the susceptible C3H/He (10+ tumors/TBA) and B6C3F1 (3-8 tumors/TBA) mice develop liver tumors, while conversely, after 18 months, the resistant C57BL/6 mice develop none (Becker, 1982). Additionally, treatment with 0.05% PB induces hepatic DNA

synthesis in B6C3F1 mice, e.g. 1-4 weeks (Counts *et al.*, 1996; Kolaja *et al.*, 1996a), and in C57BL/6 mice, e.g. 1-2 weeks (Counts *et al.*, 1996). Furthermore, the rate of apoptosis decreases in hepatocytes within diethylnitrosamine (DEN)-initiated preneoplastic lesions which are observed following 30 and 60 days of promotion by PB (Kolaja *et al.*, 1996b).

The hepatocarcinogens sensitivity (*Hcs*) locus appears to be responsible for approximately 85% of the aforementioned susceptibility differences (Drinkwater and Ginsler, 1986; Drinkwater *et al.*, 1989). This *Hcs* locus specifically affects the promotion stage of carcinogenesis, as the C3H allele elevates liver tumor yield by increasing the size and growth rate of preneoplastic lesions in the C3H/He as compared to the C57BL/6 group (Hanigan *et al.*, 1988). It should be noted that the alleles of the C3H/He and C57BL/6 mice are semidominant, such that the heterozygous B6C3F1 exhibits intermediate susceptibility (Drinkwater *et al.*, 1989). Three additional regions, located on chromosomes 2, 5 and 19, also exhibit a significant linkage with the development of hepatocellular tumor formation (Manenti *et al.*, 1994). Furthermore, evidence suggests that it is the hepatocytes themselves (versus a component of the cellular microenvironment) which harbor intrinsic differences between the C3H/He and C57BL/6 mice and contribute to the differential susceptibilities (Lee *et al.*, 1991). Variations in proliferation/growth between the groups remain the focus of the disparate sensitivities, particularly since apoptosis does not appear to play a major role (Bursch *et al.*, 2005a; Bursch *et al.*, 2005b).

There are other processes that show strain-related differences among these groups, and it is possible that the aforementioned *Hcs* contains relevant genes. For example, gap

junctional communication (GJIC), which permits intercellular contact, including transport of ions and small molecules, is apparently an integral part of inhibiting tumorigenesis in certain systems. Indeed, most cancer cells exhibit decreased GJIC (Trosko and Chang, 2001). Interestingly, PB inhibits GJIC in hepatocytes from tumor-sensitive B6C3F1 but not the relatively resistant C57BL/6 mice (Warner *et al.*, 2003). In response to PB administration, DNA methylation changes in liver also occur in a strain-specific manner. Data from our laboratory indicate that levels of global hypomethylation decreased to a greater extent in livers of susceptible B6C3F1 mice, as compared to the relatively resistant C57BL/6, after 1, 2, and 4 weeks of 0.05% (w/w) PB in drinking water, while the C57BL/6 group exhibited higher proliferative activity, implying that the B6C3F1 mice are less capable of maintaining normal methylation patterns (Counts *et al.*, 1996). Furthermore, at 2 weeks, PB elicited greater levels of hypermethylation at the internal and external cytosines of 5'-CCGG-3' sites were observed in the susceptible mice, as compared to the relatively resistant group (C3H/He >> B6C3F1 > C57BL/6), further suggesting that altered methylation patterns are more affected in tumor-susceptible mice (Watson and Goodman, 2002). Most recently, unique regions of altered methylation (RAMs) were identified in B6C3F1 mice as compared to their resistant C57BL/6 counterpart, in response to a 0.05% (w/w) promoting dose of PB at 2 and 4 weeks (Bachman *et al.*, 2006). The logical extension of this work, identifying the genes in which these methylation changes occurred, and then determining whether expression levels relate to their altered methylation statuses, was one of the main focal points of my dissertation research.

The mechanisms of PB-induced tumorigenesis remain elusive, although

several details have emerged. Molecular changes within several genes have been ascertained, including mutations in the gene encoding β-catenin (Aydinlik *et al.*, 2001), increased Ha-*ras* expression (Counts *et al.*, 1997), Ha-*ras* hypomethylation (Vorce and Goodman, 1991), Ki-*ras* hypomethylation (Vorce and Goodman, 1991), hypomethylation and increased expression of *raf* (Ray *et al.*, 1994), and amplification of *c-myc* (Vorce and Goodman, 1991). Additionally, connexin32, the major hepatic gap junction-forming protein, is essential for PB-induced liver tumorigenesis (Moennikes *et al.*, 2000). Finally, chronic PB treatment appears to evoke mito-inhibitory effects, and it is thought that tumor progenitor cells escape this growth inhibition. Indeed, after continual exposure, normal hepatocytes exhibited decreased levels of epidermal growth factor receptor (EGFR) and increased levels of transforming growth factor-beta (TGF-β), TGF-β receptors, and mannose 6-phosphate/insulin growth factor II receptor (M6P-IGF2r), which can activate TGF-β (reviewed in Counts *et al.*, 1996). Conversely, PB-associated liver lesions revealed decreased levels of M6P-IGF2r (precancerous lesions) and TGF-β (precancerous lesions and tumors).

Critical data generated from my dissertation research has added to the aforementioned observations and aided in the identification of individual genes (including those whose regulation might be affected by altered DNA methylation), plus key signaling pathways and processes, that might underlie tumor promotion by PB. Importantly, the expression and methylation statuses of the genes discerned are unique in liver tumor-susceptible B6C3F1, as compared to the relatively resistant C57BL/6 mice.

Constitutive Active/Androstane Receptor (CAR) Wildtype and Knockout Mice

Complex signaling networks, involving crosstalk of pathways comprised of

multiple nuclear receptors, are responsible for the metabolism of drugs and xenobiotics. These same receptors regulate homeostatic processes, including metabolism of endogenous substances (e.g. glucose, lipids). Three major nuclear receptors that function as xeno-sensors, modulating gene expression in response to drug treatment or xenobiotic exposure in order to inactivate and/or eliminate these substances, are the aryl hydrocarbon receptor (AhR), constitutive active/androstane receptor (CAR), and pregnane X receptor (PXR) (Pascussi *et al.*, 2008). CAR is predominantly expressed in the liver, and is capable of heterodimerizing with the retinoic acid receptor (RXR) to regulate gene expression (Baes *et al.*, 1994). Particular cis elements within the genome are associated with CAR-mediated transcription (Chen *et al.*, 2003; Gerbal-Chaloin *et al.*, 2002; Goodwin *et al.*, 2002; Honkakoski *et al.*, 1998; Sueyoshi *et al.*, 1999; Sugatani *et al.*, 2001). This receptor constitutively activates transcription in absence of a ligand (Choi *et al.*, 1997), and CAR activity can be suppressed by the binding of 1 of 2 androstane metabolites, androstanol (murine and human CAR) and androstenol (murine CAR only) (Forman *et al.*, 1998; Sueyoshi and Negishi, 2001). CAR participates in biological pathways involving endogenous substances, including thyroid hormone metabolism (Qatanani *et al.*, 2005), bilirubin clearance (Huang *et al.*, 2003), and bile acid detoxification (Saini *et al.*, 2004). However, CAR is most recognized for its mediation of the induction of genes encoding drug-metabolizing enzymes, including cytochrome P450s (e.g. *Cypb10*, *Cyp3a11*) and others (e.g. NADPH-cytochrome P450 reductase, aldehyde dehydrogenase I), plus drug transporters (e.g. *Mrp1-3*), in response to xenobiotic exposure (Maglich *et al.*, 2002; Ueda *et al.*, 2002). PB indirectly activates CAR (i.e. does not bind to the receptor), while other compounds act as direct ligands for

CAR in human and mice (e.g. CITCO and TCPOBOP, respectively) (Swales and Negishi, 2004).

Transcriptional regulation by CAR involves two separate, temporal and spatial activation events that have been investigated but not fully elucidated (Timsit and Negishi, 2007) (Figure 1.6). In normal hepatocytes, CAR is complexed with heat shock protein 90 (HSP90) and cytoplasmic CAR retention protein (CCRP). Upon PB treatment, CAR dissociates from these proteins and translocates to the nucleus. The specific details of this translocation are not entirely clear, but it is known that PB causes the recruitment of protein phosphatase 2A (PP2A) to the CAR:HSP90 cytoplasmic complex (Yoshinari *et al.*, 2003), and that okadaic acid, a phosphatase inhibitor which can inhibit PP2A, blocks the PB-induced nuclear translocation of CAR (Kawamoto *et al.*, 1999). Additionally, this translocation event appears to entail interaction of CAR with a homodimer of the membrane-associated subunit of protein phosphatase 1, PPP1R16A (R16A). The R16A residues dimerize at a region containing protein kinase A phosphorylation sites, and R16A is capable of inhibiting protein phosphatase 1-beta (PP1β), which can block CAR translocation (Sueyoshi *et al.*, 2008). In addition, hepatocyte growth factor treatment can activate MEK1/2, resulting in the phosphorylation and activation of MAPK1/3 and the subsequent inhibition of the nuclear translocation (Koike *et al.*, 2007). The second activation event which is necessary for transcriptional regulation by CAR involves phosphorylation, as evidenced by the observation that CAR-mediated induction of the *Cyp2b10* gene can be blocked by KN-62 (a Ca2+/calmodulin-dependent kinase inhibitor) without affecting nuclear accumulation (Yamamoto *et al.*, 2003). However, the particular kinase(s) involved have not yet been reported.

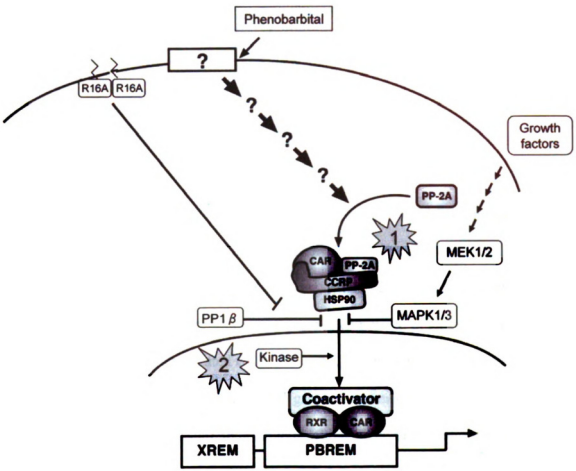


Figure 1.6 Activation of the Constitutive Active/Androstane Receptor (CAR). The activation of CAR by compounds such as phenobarbital (PB), resulting in transcriptional regulation of its target genes, requires 2 distinct steps: 1) translocation from the cytosol to the nucleus, and 2) activation within the nucleus. As of yet, no PB receptor has been characterized, and thus it appears that its activation of CAR occurs through an indirect mechanism, which has not been fully elucidated. The text contains greater detail of the events which are depicted in this schematic representation. Abbreviations: CCRP, cytoplasmic CAR retention protein; HSP, heat shock protein; MAPK, mitogen-activated protein kinase; MEK, mitogen-activated protein kinase kinase; PBREM, PB-responsive enhancer module; PP1β, protein phosphase 1 beta; PP-2A, protein phosphatase 2A; R16A, PPP1R16A, a membrane-associated subunit of protein phosphatase 1; RXR, retinoid X receptor; XREM, xenobiotic-responsive enhancer module. (Adapted from Koike *et al.*, 2007; Sueyoshi *et al.*, 2008; Swales and Negishi, 2004)

CAR is necessary for PB-induced hepatomegaly in mouse liver (Wei *et al.*, 2000), and chronic CAR activation in response to PB or TCPOBOP results in hepatocarcinogenesis (Huang *et al.*, 2005). Additionally, CAR is essential for tumor promotion by PB in diethylnitrosamine (DEN)-initiated C3H/He mice (Yamamoto *et al.*, 2004). Thus, CAR wildtype (WT) mice are considered to be susceptible to liver tumorigenesis, while CAR knockout (KO) mice are tumor-resistant, however the mechanisms of tumor development require elucidation. Microarray data analysis of PB-treated CAR WT and KO mice revealed that of 138 genes (out of 8,736 total genes/ESTs) whose expression was altered, approximately half of these changes were CAR-dependent (Ueda *et al.*, 2002), indicating that PB has effects which are CAR-independent, as well. A major component of my dissertation research was comprised of an extensive analysis of expression changes in PB-treated CAR WT and KO mice, emphasizing those changes that occurred uniquely in the susceptible WT groups (23 weeks PB, precancerous liver and 32 weeks, liver tumor tissue), in order to elucidate potential mechanisms of liver tumorigenesis. Additionally, since PB altered DNA methylation uniquely in tumor-susceptible (i.e. B6C3F1), as compared to relatively resistant (i.e. C57BL/6) mice, I hypothesized that PB might induce unique methylation changes in susceptible CAR WT mice, as compared to the resistant CAR KO, and that at least some of these might be playing critical mechanistic roles during PB-induced tumorigenesis. Therefore, another component of my research involved discerning unique methylation changes in the susceptible CAR WT, as compared to the resistant CAR KO mice. The analysis of both DNA methylation and gene expression alterations was an effective approach to obtain a more comprehensive understanding of how PB promotes liver tumorigenesis.

Hypothesis and Objectives

This dissertation consists of 3 projects that were designed to test the following overall hypothesis: **genes which are disregulated uniquely in liver tumor-susceptible, as compared to tumor-resistant mice, are among those which are mechanistically important for tumorigenesis.** In order to explore this broad concept, my research was comprised of 2 major facets (assessment of DNA methylation changes and gene expression changes) that are complementary, as DNA methylation can regulate gene expression. Three subhypotheses provide compelling support for the overall hypothesis:

1) Regions of altered DNA methylation (RAMs) discerned uniquely in susceptible mice are critical for tumorigenesis and thus, the ability of an animal to maintain normal methylation patterns is related inversely to its susceptibility to tumor development.
2) Changes in gene expression discerned uniquely in liver tumor-susceptible mice are crucial for liver tumorigenesis.
3) Unique RAMs and gene expression changes observed in 2 groups of tumor-susceptible mice, at early and later time points, might be especially important for liver tumorigenesis.

The overall goal of this dissertation research was to elucidate progressive changes, in expression and methylation status, of genes which play key roles in liver tumorigenesis induced by the promoting agent phenobarbital (PB), with an emphasis on their potential to affect signaling through critical pathways involved in the regulation of cell growth and differentiation. To achieve this, 2 murine model systems were utilized:

1) PB-promoted B6C3F1 (liver tumor-susceptible) and C57BL/6 (relatively tumor-resistant) mice.

2) Diethylnitrosamine (DEN)-initiated, PB-promoted C3H/He CAR wildtype (WT) (liver tumor-susceptible) and CAR knockout (KO) (liver tumor-resistant) mice.

Each of these models is characterized by one group of mice that are prone to PB-induced liver tumorigenesis, and one group that are tumor-resistant. Additionally, one model involved early times (B6C3F1, 2 and 4 weeks) of PB treatment, while the second model involved later time points (CAR WT, 23 weeks/precancerous liver and 32 weeks/liver tumors). The combination of these two systems afforded me the opportunity to identify individual genes altered uniquely in livers of tumor-prone mice, and to explore signaling networks that are affected across a continuum of PB-induced liver tumorigenesis. Indeed, any methylation and/or expression changes which occurred at both early and later time points might be especially significant.

As previously discussed, some details of liver tumor promotion by PB have been ascertained, but other mechanisms remain elusive. Historically, our laboratory has focused upon the role of PB-elicited DNA methylation changes as a mechanism that facilitates liver tumor formation. We have demonstrated that liver tumor-susceptible B6C3F1 mice are less capable of maintaining normal methylation patterns than are the relatively resistant C57BL/6 mice (Counts *et al.*, 1996; Watson and Goodman, 2002). Moreover, using a novel, more accurate and sensitive approach (v. Watson and Goodman, 2002), that involves methylation-sensitive restriction digestion, arbitrarily primed PCR, and capillary electrophoresis, unique PB-elicited regions of altered DNA methylation (RAMs) were detected in livers of susceptible B6C3F1 mice, as compared to the relatively resistant C57BL6/, at 2 and 4 weeks of treatment (Bachman *et al.*, 2006).

My research logically extended this work, as I determined which genes/genomic regions harbored these unique methylation changes. Expression levels of a subset of these genes related to their methylation statuses, indicating a potential transcriptional regulatory role for DNA methylation in response to PB. Finally, comprehensive expression analysis of RNA from both PB-treated B6C3F1 and C57BL/6 mice at 2 and 4 weeks resulted in the elucidation of unique expression changes in the susceptible B6C3F1 mice. Together, evaluation of genes whose methylation and/or expression statuses were altered by PB, followed by signaling pathway analysis, provided a more complete picture of how liver tumor promotion might occur, starting at very early treatment time points.

The second model system involves DEN-initiated, PB-promoted C3H/He mice that are susceptible (CAR WT) and resistant (CAR KO) to liver tumorigenesis (Yamamoto *et al.,* 2004). CAR WT mice exposed to PB for 23 weeks developed precancerous liver lesions, while exposure for 32 weeks resulted in liver tumor development. Moreover, KO mice treated with PB for 23 or 32 weeks did not develop liver tumors. In light of the observations that PB elicits 1) CAR-mediated effects in the liver (Huang *et al.*, 2005; Ueda *et al.,* 2002; Wei *et al.*, 2000; Yamamoto *et al.,* 2004), and 2) unique methylation changes in susceptible B6C3F1 mice (Bachman *et al.*, 2006), I explored the possibility that PB could induce methylation changes in CAR WT (23 weeks, precancerous liver and 32 weeks, liver tumors) and KO (23 weeks) mice. I then discerned those which occurred uniquely in the susceptible WT groups. Subsequently, I determined in which genes/genomic regions these RAMs occurred, and investigated whether the methylation statuses of a subset of the genes related to their expression levels. I concluded the work in this model system with an examination of unique

expression changes in the PB-treated susceptible CAR WT groups, as compared to the PB-treated resistant CAR KO mice. Therefore, analogous to the studies performed in the B6C3F1-C57BL/6 model system, an in-depth assessment of DNA methylation and gene expression alterations was undertaken in order to provide a detailed picture of how PB might function at later time points (i.e. 23 and 32 weeks) to promote liver tumors in the susceptible CAR WT mice.

The final component of this dissertation involved the comparison of methylation and gene expression alterations that were discerned in liver tissue at early (B6C3F1, 2 and 4 weeks) and later time points (23 weeks, precancerous liver and 32 weeks, liver tumors) of PB treatment. In this fashion, an extremely thorough analysis of deregulated genes, including those affected by altered DNA methylation, and the signaling pathways and processes in which they participate, was performed across a continuum of PB-induced tumorigenesis. I hypothesized that at least some of the genes which exhibited unique changes in liver-tumor susceptible mice, as compared to their resistant counterparts, are mechanistically critical for tumor development. Ultimately, fingerprints of altered gene expression and DNA methylation, at early and late times (including tumors) of PB exposure, were proposed.

These 3 projects, including the associated specific aims, were designed to comprehensively evaluate the aforementioned hypotheses:

PROJECT 1 (Chapters 1 and 2): Identification of genes that exhibit unique phenobarbital (PB)-induced hepatic methylation and/or expression changes in liver tumor-susceptible B6C3F1 mice, as compared to relatively resistant C57BL/6 mice, at 2 and 4 weeks of treatment.

a) To ascertain key genes that exhibit unique regions of altered DNA methylation (RAMs) in susceptible B6C3F1 mice at 2 and 4 weeks: **Chapter 1**

b) To determine how expression of key genes (identified from unique RAMs in B6C3F1 mice, as discerned in Aim 1a) relates to their methylation statuses, and if transcript levels are altered uniquely in B6C3F1 mice: **Chapter 2**

c) To determine if expression levels of 3 DNA methyltransferase (Dnmt) genes change uniquely in B6C3F1 mice at 2 and 4 weeks of PB treatment: **Chapter 2**

d) To perform microarray analysis and subsequently elucidate unique gene expression changes in B6C3F1 mice, at 2 and 4 weeks: **Chapter 2**

e) To identify putative CAR response cis elements (CAREs) within selected genes, including 3 Dnmt's, whose methylation and/or expression statuses are altered uniquely in B6C3F1 mice due to 2 and/or 4 weeks of PB treatment: **Chapter 2**

PROJECT 2 (Chapters 3, 4, and 5): Identification of genes that exhibit unique PB-induced methylation and/or expression changes in liver tumor-susceptible CAR wildtype (WT) mice at 23 (precancerous liver) and 32 (liver tumors) weeks of treatment, as compared to tumor-resistant CAR knockout (KO) mice at 23 weeks.

a) To compare changes in GC-rich methylation patterns in tumor-susceptible CAR WT and resistant KO mice, and to discern unique RAMs in the CAR WT groups (both precancerous liver and liver tumors): **Chapter 3**

b) To ascertain key genes that exhibit unique RAMs in precancerous liver and/or liver tumors: **Chapter 4**

c) To determine how expression of key genes (identified from unique RAMs in CAR WT mice, as discerned in Aim 2b) relates to their methylation statuses, and if transcript levels are altered uniquely in precancerous liver and/or liver tumors: **Chapter 5**

d) To determine if expression levels of 3 Dnmt genes change uniquely in precancerous liver and/or liver tumors: **Chapter 5**

e) To perform microarray analysis and subsequently elucidate unique gene expression changes in precancerous liver and/or liver tumors: **Chapter 5**

f) To identify putative CAREs within selected genes, including 3 Dnmt's, whose methylation and/or expression statuses are altered uniquely in precancerous liver and/or liver tumors: **Chapter 5**

<u>PROJECT 3 (Chapters 4 and 5)</u>: Comparison of genes that exhibit unique PB-elicited altered methylation and/or gene expression changes in both types of liver tumor-susceptible mice, at early (i.e. 2 and 4 weeks) and late (i.e. 23 weeks, precancerous liver and 32 weeks, liver tumors) time points.

a) To compare genes that exhibit unique RAMs in both the PB-treated susceptible B6C3F1 and CAR WT mice: **Chapter 4**

b) To compare the expression of genes that exhibit unique RAMs, plus 3 Dnmt's, in both PB-treated susceptible B6C3F1 and CAR WT mice: **Chapter 5**

c) To compare genes whose expression is altered uniquely, based on microarray analysis, in both the PB-treated susceptible B6C3F1 and CAR WT mice: **Chapter 5**

REFERENCES FOR THE INTRODUCTION AND DISCUSSION SECTIONS ARE LISTED ON PAGES 373-391.

CHAPTER 1

This chapter represents a manuscript that was published in *Toxicological Sciences* **104**, p. 86-99, 2008. The authors are Jennifer M. Phillips and Jay I. Goodman.

ABSTRACT

Aberrant DNA methylation plays important roles in tumorigenesis and the nongenotoxic rodent tumor promoter phenobarbital (PB) alters methylation patterns to a greater extent in liver tumor-susceptible as compared to resistant mice (Watson and Goodman, 2002). Unique hepatic regions of altered DNA methylation (RAMs) were identified in sensitive B6C3F1, as compared to resistant C57BL/6, mice at 2 or 4 weeks of PB treatment using a novel approach involving methylation-sensitive restriction digestion, arbitrarily primed PCR and capillary electrophoresis (Bachman *et al.*, 2006b). PCR products representing 90 of the 170 (53%) total unique B6C3F1 RAMs at 2 or 4 weeks were cloned and subjected to BLAST-Like Alignment Tool (BLAT) searches which resulted in 51 gene matches; some of these have documented oncogenic or tumor suppressor roles. Importantly, uniquely hypomethylated genes play roles in angiogenesis and invasion and metastasis (e.g., chymase 1, tyrosine kinase nonreceptor 2, and possibly ephrin B2 and triple functional domain, PTPRF interacting), including those involved in the epithelial-mesenchymal transition (transcription factor 4, transforming growth factor beta receptor II and ral guanine nucleotide dissociation stimulator). Common cellular targets and regulators of the genes representing unique B6C3F1 RAMs were uncovered, indicating that they might act in concert to more efficiently promote tumorigenesis. Genes not previously associated with mouse liver tumorigenesis exhibited altered methylation at these very early times following PB treatment. We hypothesize that at least some of the unique PB-induced B6C3F1 RAMs represent key events facilitating transformation, which is consistent with a causative role of altered DNA methylation during early stages of tumorigenesis.

INTRODUCTION

DNA methylation, i.e., 5-methylcytosine, occurs at approximately 70% of CpG dinucleotides (Naveh-Many and Cedar, 1981) and evidence suggests that methylation at non-CpG sites such as CpA and CpT is mediated by DNA methyltransferase 3a (Ramsahoye *et al.*, 2000). DNA methylation silences retrotransposable elements, controls genomic imprinting and regulates tissue-specific gene expression during development (Reik, 2007). Altered DNA methylation is an epigenetic mechanism that plays multiple roles during tumor formation (Counts and Goodman, 1995). Carcinogenesis is a multistep/multistage process involving the progressive clonal expansion of cells which have accumulated critical, heritable alterations within tumor suppressors and oncogenes, providing them with growth advantages over neighboring cells (Feinberg *et al.*, 2006; Hanahan and Weinberg, 2000; Nowell, 1976). The key modifications in genes that contribute to crucial processes can be mutations and/or epigenetic alterations since these might be functionally identical. Mutation as well as DNA hypermethylation can silence tumor suppressor genes, while mutation as well as hypomethylation can activate oncogenes (Goodman and Watson, 2002).

Phenobarbital (PB) is the prototypical nongenotoxic rodent liver tumor promoter that causes hypertrophy, hyperplasia and upregulation of drug metabolizing enzymes, e.g., cytochrome P450s (Whysner *et al.*, 1996). Some details regarding PB-induced tumor promotion have emerged. In N-nitrosodiethylamine (DEN)-initiated B6C3F1 mice, a tumor promoting dose of PB (0.05%, w/w) caused an increase in focal DNA synthesis and a simultaneous decrease in apoptosis, likely facilitating preneoplastic lesion growth in the liver (Kolaja *et al.*, 1996b). DEN-initiated *Connexin32*-null mice develop

liver tumors at a high rate that is not enhanced by PB treatment (Moennikes *et al.*, 2000), indicating that inhibition of gap junctional intracellular communication (GJIC) is key in the mechanism of action of PB; it has been suggested that inhibition and down-regulation of GJIC are involved in tumor promotion and progression (Trosko and Chang, 2001). Additionally, the nuclear constitutive active/androstane receptor (CAR) mediates PB-induced hepatomegaly in mouse liver (Wei *et al.*, 2000) and it is essential for tumor promotion by PB in DEN-initiated C3H/He mice (Yamamoto *et al.*, 2004). Furthermore, DEN-initiated CAR wild-type mice, promoted with PB for 23 (precancerous liver lesions present) or 32 (liver tumors present) weeks, exhibited unique hepatic regions of altered DNA methylation (RAMs) as compared to DEN-initiated CAR knock-out mice promoted for 23 weeks (Phillips *et al.*, 2007).

Importantly, methylation patterns are disrupted to a greater extent in liver tumor-susceptible, as compared to resistant, mice upon treatment with 0.05% (w/w) PB, including higher levels of hypermethylation in the 2 sensitive groups (C3H/He >> B6C3F1 > C57BL/6) (Watson and Goodman, 2002). After 12 months of treatment with 0.05% (w/w) PB in drinking water, 100% of B6C3F1 and no C57BL/6 mice develop liver tumors (Becker, 1982). It is hypothesized that their differential abilities to maintain normal methylation patterns contribute to the disparity in their liver tumor susceptibilities (Watson and Goodman, 2002). An important question to address is, in which genes do changes in methylation play a key role? One approach might have been to look for PB-induced changes in expression (e.g., a microarray study) followed by methylation analysis of those genes whose expression was altered. The problem here lies with the tedious task of evaluating methylation status in, possibly, thousands of genes plus the

likelihood that at early times following treatment with PB some key genes might exhibit modified methylation but not yet to the extent that expression was affected. Therefore, we decided to first look for altered methylation with the understanding that this could be followed-up with expression analysis.

RAMs were detected by a novel approach involving methylation-sensitive restriction digestion, arbitrarily primed PCR, and capillary electrophoresis (Bachman *et al.*, 2006b). Unique RAMs in the sensitive B6C3F1, as compared to the resistant C57BL/6, mice in response to 2 or 4 weeks of 0.05% (w/w) PB treatment were discerned (Bachman *et al.*, 2006b). It is hypothesized that among the PB-induced unique RAMs in the sensitive mice are those that play critical mechanistic roles early during promotion of tumorigenesis.

Only a few genes, including CAR (Yamamoto *et al.*, 2004), have previously been linked to mouse liver tumorigenesis. Promotion by PB (Aydinlik *et al.*, 2001) and 2,2',4,4',5,5'-hexachlorobiphenyl (PCB 153) (Strathmann *et al.*, 2006) lead to tumors with mutations in the β-catenin gene, possibly the result of selective clonal expansion of cells bearing the mutation. *Myc* amplification occurs in liver tumors with no detectable methylation changes (Vorce and Goodman, 1991). Mouse liver tumors display activating Ha-*ras* mutations (Wiseman *et al.*, 1986), in addition to hypomethylation of the 5' region (Vorce and Goodman, 1991) and increased Ha-*ras* expression (Counts *et al.*, 1997). Similarly, Ki-*ras* is hypomethylated in liver tumors and this change might be essential, though not necessarily sufficient, for overexpression (Vorce and Goodman, 1991). PB induces hypomethylation of the *raf* oncogene in B6C3F1 mouse liver, which could lead to increased expression (Ray *et al.*, 1994).

In this study, unique RAMs that formed in hepatic DNA of sensitive B6C3F1, as compared with resistant C57BL/6, mice at an early stage of PB promotion (Bachman *et al.*, 2006b) were annotated. PCR products representing unique RAMs were cloned and the BLAST-Like Alignment Tool (BLAT) was employed to ascertain with which genes, non-protein-coding regions, and "unannotated" regions of the genome these RAMs are associated. Altered DNA methylation was discerned in a number of genes that have not previously been implicated in mouse liver tumorigenesis, though many have been associated with tumorigenesis in other species, including humans. An informatics approach was then utilized to elucidate biological pathways that might be disrupted by PB-induced altered DNA methylation and, therefore, contribute to carcinogenesis.

MATERIALS AND METHODS

Animals, Treatments and Tissue Samples

B6C3F1 (C57BL/6 × C3H/He) and C57BL/6 mice were acquired (Charles River Laboratories, Wilmington, MA) and randomly assigned to control or treatment groups with 6 or 7 animals per group (Bachman *et al.*, 2006b). Phenobarbital was administered in drinking water at a concentration of 0.05% (w/w) for 2 or 4 weeks and liver tissue was harvested as described (Bachman *et al.*, 2006b). Treatment, housing and care were in accordance with the Animal Use and Care Guidelines of Michigan State University.

DNA isolation

Liver tissue was homogenized in 1ml of TRIzol Reagent (Invitrogen, Carlsbad, CA) and DNA was isolated via the manufacturer's protocol (Bachman *et al.*, 2006b).

Evaluation of DNA Methylation Status by Arbitrarily Primed PCR and Capillary Electrophoresis

DNA methylation status was evaluated by an arbitrarily primed PCR, capillary electrophoresis procedure (Bachman *et al.*, 2006a). This technique permits the simultaneous evaluation of treatment-related hypomethylations (less methylation in a region that was methylated in control), hypermethylations (more methylation in a region that was methylated in control) and new methylations (methylation in a region that was not methylated in control) in numerous regions of the genome.

Restriction Digests

Each DNA sample was subjected to three separate double restriction digests that were performed in duplicate with a) a methylation-insensitive enzyme and b) a methylation-sensitive enzyme. Digestion with a methylation-insensitive enzyme, *RsaI* or *BfaI,* ensures complete digestion by the methylation-sensitive enzyme, *MspI, HpaII*, or *BssHII.* Restriction digestion with *RsaI/MspI, RsaI/HpaII* and *BfaI/BssHII* was carried out as described previously (Bachman *et al.*, 2006b). *MspI* and *HpaII* recognize 5' CCGG 3' sites and cut between the internal cytosine and guanine. *MspI* will not restrict DNA if the external cytosine is methylated, while *HpaII* will not restrict DNA if the internal cytosine is methylated. *BssHII* recognizes 5' GCGCGC 3' sites and cuts between the first guanine and cytosine residues and will not restrict DNA if several combinations of cytosines in the sequence are methylated. *BfaI* sites appear less frequently in CpG islands than *RsaI* sites and, thus, CpG islands are more intact following digestion of DNA with the former enzyme as compared to the latter (Shiraishi *et al.*, 1995). Therefore, the use of *BfaI* in combination with *BssHII*, a 6-base rare cutter with a GC-rich recognition sequence, provides an additional, important "window" into our DNA methylation status analysis which complements the data obtained with the *RsaI/MspI* and *RsaI/HpaII* digests.

Arbitrarily Primed PCR (AP-PCR) and Capillary Electrophoretic Separation of Products

AP-PCR and capillary electrophoresis were performed as described previously (Bachman *et al.*, 2006b), however, two corrections were made: the five cycle stage of the AP-PCR reaction was followed by 30 cycles (not 40 cycles as stated originally), starting with a denaturation step of 94° C for 30 s (not 15 s as stated originally). The digested DNA was subjected to AP-PCR using a single arbitrary primer, 5' AAC CCT CAC CCT AAC CCC

GG 3' (Gonzalgo *et al.*, 1997) which was fluorescently labeled at the 5' end with HEX™ (Integrated DNA Technologies, Coralville, IA). This primer binds well to GC-rich regions and the 5' CCGG 3' sequence at its 3' end increases the probability of binding to the *MspI* and *HpaII* restriction sites, permitting the detection of methylation at the site of primer annealing and between sites of primer annealing.

Data Analysis

The resulting PCR products were evaluated with regard to their size, in base pairs, and corresponding peak areas, using the Excel® program. A consensus, average peak area was calculated for each experimental group. This permits the consensus peak area of a control group to be compared with the consensus peak area of a treatment group, in order to determine if there are differences in methylation at a particular PCR product size, and if so, these PCR products are considered to be regions of altered DNA methylation (RAMs). Treatment-related RAMs include: a) hypomethylations, both 100% decreases, and decreases which are statistically significant (Student's *t*-test, $p < 0.05$) when compared to control, b) hypermethylations, which are increases that are statistically significant (Student's *t*-test, $p < 0.05$) when compared to control and c) new methylations, in which PCR product formed following treatment but did not form under control conditions. A detailed description of the data analysis procedure was provided previously (Bachman *et al.*, 2006a; Bachman *et al.*, 2006b) and included the following comparisons: 1) B6C3F1, 2 week 0.05% PB vs. B6C3F1, 2 week control data, 2) C57BL/6, 2 week 0.05% PB vs. C57BL/6, 2 week control data, 3) B6C3F1, 4 week

0.05% PB vs. B6C3F1, 4 week control data and 4) C57BL/6, 4 week 0.05% PB vs. C57BL/6, 4 week control data (Bachman *et al.*, 2006b).

Common and Unique Regions of Altered DNA Methylation (RAMs)

In order to determine if the RAMs that occurred at the same PCR product size in two treatment groups are equivalent (common RAMs) or different (unique RAMs), two-way analysis of variance (ANOVA) tests, $p < 0.05$, were performed (Bachman *et al.*, 2006b). In this way, for example, unique RAMs in the B6C3F1, 4 week 0.05% PB-treated group as compared to the C57BL/6, 4 week 0.05% PB-treated group were identified. In addition, one-way ANOVA, $p < 0.05$, was used to discern unique B6C3F1 0.05% PB-induced RAMs that "carried forward" from the 2 to 4 week timepoint.

Identification of PB-induced Unique B6C3F1 RAMs

Cloning and Sequencing of AP-PCR Products

In order to identify in what regions of the genome the PB-induced unique B6C3F1 RAMs occurred, the AP-PCR products were first cloned using an in-gel approach. The AP-PCR products and a 100 base pair DNA ladder (Invitrogen, Carlsbad, CA) were electrophoresed through a 3% NuSieve® GTG® low melting temperature agarose gel (Lonza Biosciences, Basel, Switzerland). Portions of the gel that contained PCR products within 100 base pair size ranges were excised, melted and used for in-gel cloning reactions prepared with the pGEM®-T Easy Vector Kit (Promega, Madison, WI). Clones that contained PCR product inserts were purified and sequenced at the Research Technology and Support Facility at Michigan State University. Sequencing reactions

were prepared using either SP6 or T7 sequencing primers (as described in the pGEM®-T Easy Vector Technical Manual; Promega, Madison, WI) and subsequently run on an ABI 3730*xl* Genetic Analyzer.

Comparison of the Sizes of Cloned AP-PCR Products to the Sizes of Unique RAMs

After the sequences were obtained, the sizes of the cloned products were compared to the sizes of the unique RAMs in order to determine which cloned products represented unique B6C3F1 RAMs at the 2 or 4 week time points. In many instances, it can be confidently stated that a particular cloned product represents a single RAM and as such, the methylation status of that RAM is unambiguous. However, the raw data analysis performed to establish if a RAM occurred in a treatment as compared to a control group (Bachman *et al.*, 2006a) is based on the understanding that the ABI 3130 Genetic Analyzer capillary electrophoresis instrument does not detect PCR product sizes with 100% accuracy. Therefore, in certain instances during the analysis of the raw data, PCR product sizes are combined. Six or seven animals per experimental group were used and restriction digestions were performed in duplicate, followed by AP-PCR, for a total of 12 or 14 reactions. If multiple PCR product sizes within 2 base pairs of one another displayed product in less than half of the 12 or 14 AP-PCR reactions, these products were considered to be "identical" and were subsequently combined. This procedure has implications for analysis of the cloning data. For example, 2 RAMs occur uniquely in the B6C3F1 mice at 4 weeks as a result of *RsaI/HpaII* digestion: a new methylation at 306 bp and a hypomethylation at 310 bp (Fig. 1.7). A PCR product of 308 bp was cloned and a BLAT search showed that the product spans the transcriptional start site of NK2

transcription factor related, locus 6 (*Nkx6-2*) (Table 1.1). Due to our basic data analysis assumption, we were not able to unambiguously state whether *Nkx6-2* represents the newly methylated RAM at 306 bp or the hypomethylated RAM at 310 bp. The "methylation status" data column in Table 1.1 reflects this limitation, where 16% (14/85) of the genes, and regions of the genome which are greater than 10 kb away from a known gene, are tentatively classified as having multiple methylation statuses at either 2 or 4 weeks (e.g., Hypo/New for a single region at 4 weeks).

Analysis of AP-PCR Product Sequences

The sequences were subjected to BLAT database searches of the mouse genome (UCSC Genome Browser, July 2007 mouse assembly, http://genome.ucsc.edu/cgi-bin/hgBlat) in order to ascertain in which regions of the genome the unique PB-induced B6C3F1 RAMs occurred. The BLAT program allows a nucleotide or amino acid sequence to be aligned to an index of the entire genome of an animal. In the case of DNA sequence queries, BLAT can detect sequence alignments of 95% or greater similarity of regions with lengths of 25 or more base pairs. Additional information about the genomic region/gene is listed, including, but not limited to: gene information, sequence conservation between species, GC percentage and the location of single nucleotide polymorphisms and repeat elements. The unique RAMs were classified according to a scheme that indicates where, in relation to a gene (e.g., within an intron, within an exon, upstream of the transcriptional start site), they are located (Fig. 1.8). Genes that were identified using BLAT searches were subjected to biological pathway analysis via Pathway Studio 5.0 (Ariadne Genomics, Rockville, MD). In this fashion, pathways for the individual genes

were elucidated. In addition, common cellular targets (Fig. 1.9) and regulators (Fig. 1.16) of the unique B6C3F1 genes of interest at 4 weeks were discerned.

RESULTS

Figure 1 depicts the 170 total unique RAMs which were detected following a tumor-promoting dose of phenobarbital for 2 or 4 weeks in the sensitive B6C3F1, as compared to resistant C57BL/6 mice, including 8 carry forward RAMs that were observed at both the 2 and 4 week timepoints (Bachman *et al.*, 2006b). We hypothesized that among the unique RAMs in the B6C3F1 mice, some are playing critical mechanistic roles during liver tumor formation. In this study, PCR products were cloned that represent 90 (53%) of the unique RAMs and these products were annotated via the BLAT sequence alignment tool (Table 1.1). Selected literature references for Table 1.1 are located in the Appendix (References 1). RAMs were also classified based on their location relative to a known gene (Fig. 1.8, Table 1.1 and Fig. 1.11) and chromosomal distribution (Fig. 1.12). All of the annotated genes were subsequently investigated via an informatics approach in order to determine the function of the gene, in addition to any gene products that are common cellular targets and/or regulators of the unique RAMs of interest at 4 weeks. Two representative pathways of individual unique B6C3F1 RAMs in addition to a functional summary of these RAMs can be found in the Appendix (Figs. 1.13-1.15).

As explained in the Methods, some identified RAMs could unambiguously be assigned a specific methylation status (Table 1.1). Hypomethylated RAMs at 2 weeks were coiled-coil domain containing 137 (*Ccdc137*), dead box polypeptide 54 (*Ddx54*), myoferlin (*Fer1l3*), protein phosphatase 4c, catalytic subunit (*Ppp4c*), solute carrier family 9 (sodium/hydrogen exchanger), member 5 (*Slc9a5*) and WSC domain-containing 1 (*Wscd1*). At 4 weeks, hypomethylated RAMs were ADAM metallopeptidase with

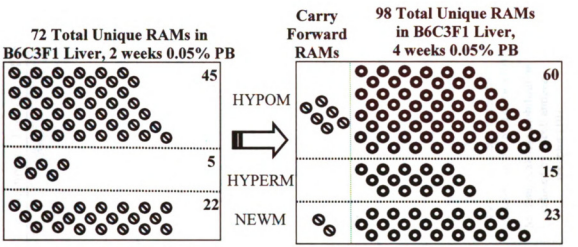


Figure 1.7 Unique Regions of Altered DNA Methylation (RAMs) that Formed in the Livers of B6C3F1 Mice in Response to 2 or 4 Weeks of Treatment with 0.05% (w/w) Phenobarbital (PB). Liver tumor susceptible B6C3F1 and resistant C57BL/6 mice were treated for 2 or 4 weeks with a tumor-promoting dose (0.05%, w/w) of PB. RAMs were detected in both groups by a procedure involving methylation-sensitive restriction digestion, arbitrarily primed PCR and capillary electrophoresis (Bachman *et al.*, 2006b). Unique RAMs in the B6C3F1, as compared to the C57BL/6, mice were identified at 2 (⊘) and 4 (O) weeks. Those that were observed at both the 2 and 4 week time points are referred to as carry forward RAMs (⊘).

Table 1.1 PCR Products Representing Unique Phenobarbital (PB)-induced RAMs in Liver Tumor-Sensitive B6C3F1, as Compared to Relatively Resistant C57BL/6, Mice were Cloned and Subjected to BLAST-like Alignment Tool (BLAT) Searches

Methylation Status		Gene Name	Gene Symbol	Accession Number	Genomic Location[c]	Normal Function	Possible Role in Tumorigenesis
2 wks[a]	4 wks[b]						
Hypo (H)[d]		Protein phosphatase 4c, catalytic subunit	*Ppp4c*	NM_019674	1.A.iii	Serine/threonine phosphatase (1)[e]	Anti-tumor agents inhibit Ppp4c activity (1)
Hypo (H)		Solute carrier family 9, member 5	*Slc9a5*	NM_001081332	1.C.i	Sodium/hydrogen exchanger (2)	--
Hypo (M)		WSC domain containing 1 (120 bp)	*Wscd1*	NM_177618	1.A.iii	Unknown	--
Hypo (H)	Hypo (B,M)[f]	Dead box polypeptide 54	*Ddx54*	NM_028041	1.A.iii	Corepressor of nuclear receptors (3)	--
Hypo (M)	Hypo (M)	Myoferlin	*Fer1l3*	XM_283556	1.A.iii	Membrane fusion (4)	--
Hypo (H)[g]	**Hypo (H)**	Growth-arrest specific 2 like 3	*Gas2l3*	NM_001033331	1.A.iii	Unknown	--
Hypo (H)	**Hypo (H)**	Tyrosine hydroxylase	*Th*	NM_009377	1.A.iii	Physiology of adrenergic neurons (5)	--
Hypo (M)	**Hypo (M)**	Williams-Beuren syndrome chromosome region 17 homolog	*Wbscr17*	NM_145218	1.A.iii	N-acetylgalactosaminyltransferase (6)	--
Hypo (M)	**Hypo (M)**	Potassium channel, subfamily K, member 10	*Kcnk10*	NM_029911	1.C.ii	Mechano-sensitive K+ channel (7)	--
	Hypo (M)	ADAM metallopeptidase with thrombospondin type 1 motif, 17	*Adamts17*	NM_001033877	1.B.ii	Unknown	--
	Hypo (M)	ADP-ribosylation factor interacting protein 1	*Arfip1*	NM_001081093	1.A.iii	Regulates protein secretion/transport from Golgi (8)	--
	Hypo (M)	Anaphase promoting complex subunit 7	*Anapc7*	NM_019805	1.B.i	Part of ubiquitin ligase that regulates mitosis progression (9)	Downregulation linked to breast cancer (9)
	Hypo (M)	B-cell scaffold protein with ankyrin repeats 1	*Bank1*	NM_001033350	1.A.ii	Mediates calcium mobilization induced by B-cell antigen receptor (10)	--

Table 1.1 continued PCR Products Representing Unique Phenobarbital (PB)-induced RAMs in Liver Tumor-Sensitive B6C3F1, as Compared to Relatively Resistant C57BL/6, Mice were Cloned and Subjected to BLAST-like Alignment Tool (BLAT) Searches

	Hypo (M)	CMT1A duplicated region transcript 4	*Cdrt4*	NM_025496	1.C.ii	Unknown	--
	Hypo (M)	Chymase 1	*Cma1*	NM_010780	1.C.ii	Facilitates local production of angiotensin II (11)	Angiogenesis (12)
	Hypo (M)	Cut-like 2	*Cutl2*	NM_007804	1.A.iii	Homeobox gene; potential transcriptional repressor (13)	--
	Hypo (M)	F-box and WD-40 domain protein 7, archipelago homolog	*Fbxw7*	NM_080428	1.A.i	Ubiquitin-mediated degradation (14)	Loss of function mutations in cancer (15)
	Hypo (M)	Meteorin, glial cell differentiation regulator-like	*Metrnl*	NM_144797	1.A.iii	Nervous system development (16)	--
	Hypo (M)	Odd Oz/ten-m homolog 2	*Odz2*	NM_011856	1.A.iii	Transcriptional regulation (17)	--
	Hypo (M)	Ral guanine nucleotide dissociation stimulator	*Ralgds*	NM_009058	1.A.iii	Mediates Ras signals (18)	Invasion and metastasis (18)
	Hypo (M)	Semaphorin 3G	*Sema3g*	NM_001025379	1.A.ii	Repel sympathetic axons (19)	--
	Hypo (M)	Stromal interaction molecule 1	*Stim1*	NM_009287	1.A.iii	Putative Ca2+ sensor in the endoplasmic reticulum (20)	Potential growth suppressor (21)
	Hypo (M)	Transcriptional enhancer factor-1	*Tead1*	NM_009346	1.A.iii	Cardiogenesis (22)	--
	Hypo (M)	Transforming growth factor, beta receptor II	*Tgfbr2*	NM_009371	1.A.iii	Receptor for Tgfb (23)	Oncogene or tumor suppressor (24)
	Hypo (M)	Threonine aldolase	*Tha1*	NM_027919	1.B.ii	Converts L-threonine to glycine and acetaldehyde (25)	--
	Hypo (M)	Tyrosine kinase non-receptor 2	*Tnk2*	NM_016788	1.A.iii	Intracellular kinase that might be involved in cell growth/movement (26)	Invasion and metastasis (27)
	Hypo (M)	Transient receptor potential cation channel, subfamily M, member 3	*Trpm3*	NM_001035239	1.A.iii	Calcium signaling and homeostasis (28)	--
Hypo (M)	Hyper (M)	Coiled-coil domain containing 137	*Ccdc137*	NM_152807	1.A.iii	Unknown	--

Table 1.1 continued PCR Products Representing Unique Phenobarbital (PB)-induced RAMs in Liver Tumor-Sensitive B6C3F1, as Compared to Relatively Resistant C57BL/6, Mice were Cloned and Subjected to BLAST-like Alignment Tool (BLAT) Searches

	Hyper (M)	RNA binding motif protein 10	*Rbm10*	NM_145627	1.A.ii	Unknown	--
	Hyper (M)	THAP domain containing apoptosis associated protein 3	*Thap3*	NM_175152	1.A.ii	Unknown	--
New (H)	**New (H)**	Brain-specific angiogenesis inhibitor 3	*Bai3*	NM_175642	1.A.iii	Ischemia-induced angiogenesis in brain (29)	Might suppress brain tumor progression (29)
New (H)	**New (H)**	C630007B19Rik	*Tafa-1*	NM_182808	1.A.iii	Unknown	Downregulated in breast cancer cell lines (30)
	New (M)	Branched chain aminotransferase 2, mitochondrial	*Bcat2*	NM_009737	1.A.ii	Metabolism of branched chain amino acids (31)	--
	New (H)	Bcl2-like 13	*Bcl2l13*	NM_153516	1.A.iii	Induction of apoptosis (32)	Overexpression associated with childhood ALL (33)
	New (H)	Discs, large homolog-associated protein 4	*Dlgap4*	NM_146128	1.A.iii	Might be involved in clustering at postsynaptic density regions (34)	--
	New (H)	Nuclear receptor corepressor 2	*Ncor2*	NM_011424	1.A.iii	Nuclear receptor corepressor (35)	--
	New (H)	Retinoid X receptor beta	*Rxrb*	NM_011306	1.A.iii	Binding partner of various nuclear receptors (36)	Decreased expression in lung/prostate cancers (37a,b)
	New (H)	ST6 (alpha-N-acetyl-neuraminyl-2,3-beta-galactosyl-1,3)-N-acetylgalactosaminide alpha-2,6-sialyltransferase 3	*Siat7c*	NM_011372	1.A.iii	Glycosyltransferase catalyzes sialic acid transfer (38)	--
	New (H)	Transmembrane protein 104	*Tmem104*	NM_001033393	1.A.iii	Predicted amino acid/polyamine transporter (39)	--
	New (M)	WSC domain containing 1 (153 bp)	*Wscd1*	NM_177618	1.A.iii	Unknown	--

Table 1.1 continued PCR Products Representing Unique Phenobarbital (PB)-induced RAMs in Liver Tumor-Sensitive B6C3F1, as Compared to Relatively Resistant C57BL/6, Mice were Cloned and Subjected to BLAST-like Alignment Tool (BLAT) Searches

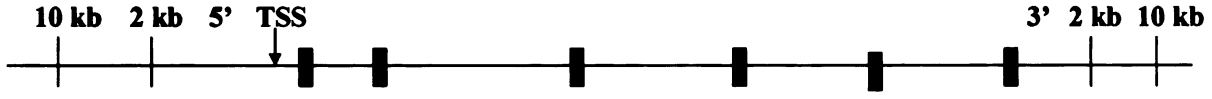
New (H)	Hypo (M)	Pleckstrin homology domain containing, family F, member 1	*Plekhf1*	NM_024413	1.C.ii	Induction of caspase-independent apoptosis (40)	--
Hypo (H) and/or New (B)[f]	Hypo (B,H)[f]	Prickle-like protein 2	*Prickle2*	NM_001081146	1.B.ii	Tissue/planar polarity via the WNT/PCP signaling pathway (41)	Expression detected in gastric and uterine cancers (42)
Hypo (H,M) and/or Hyper (B)[f]	Hypo (B)	Transcription factor 4	*Tcf4*	NM_013685	1.A.iii	Wnt signaling (43)	Expression increased in cancer (44a,b)
Hypo (H) or New (H)[h]	New (M)	Ubiquitin-conjugating enzyme E2D1	*Ube2D1*	NM_145420	1.B.ii	Involved in ubiquitination (45)	Ubiquitination of the tumor suppressor p53 (46)
Hypo (H) or New (H)[h]		Nuclear factor, erythroid derived 2, like 2	*Nfe2l2*	NM_010902	1.B.i	Key regulator of many detoxifying enzymes (47)	--
	Hypo (M) and/or Hyper (B)[f]	WSC domain containing 1 (359-361 bp)	*Wscd1*	NM_177618	1.A.iii	Unknown	--
	Hypo (H) or New (H)[h]	NK2 transcription factor related, locus 6	*Nkx2-6*	NM_183248	1.A.i	Homeodomain protein (48)	--
	Hypo (M) and/or New(H)[f]	Zinc finger and SCAN domain containing 22	*Zscan22*	NM_001001447	1.A.i	Potential transcriptional regulator (49)	--
	Hypo (H) or New (H)[h]	Inositol 1,4,5-trisphosphate (InsP3) 5-phophatase	*Inpp5a*	NM_183144	1.C.i	Hydrolyzes second messenger molecules (50,51)	Decreased expression is associated with cellular transformation (51)

Table 1.1 continued PCR Products Representing Unique Phenobarbital (PB)-induced RAMs in Liver Tumor-Sensitive B6C3F1, as Compared to Relatively Resistant C57BL/6, Mice were Cloned and Subjected to BLAST-like Alignment Tool (BLAT) Searches

Hypo (B,H) and/or New (H)[f,h]	Hypo (B) and/or Hyper (M)[f]	Protein tyrosine phosphatase, receptor type O	*Ptpro*	NM_011216	1.A.iii	Transmembrane protein tyrosine phosphatase (52)	Tumor suppressor (52)
Hypo (M) or New (M)[h]	Hypo (H) or Hyper (H)[h]	Ephrin B2	*Efnb2*	NM_010111	1.A.iii	Vascular development/angiogenesis in adult mice (53a)	Angiogenesis and invasion (53a-c)
Hypo (M) or New (M)[h]	Hypo (H) or Hyper (H)[h]	Triple functional domain (PTPRF interacting)	*Trio*	XM_001474968	1.A.ii	Cytoskeleton remodeling and cell growth (54)	Invasion (55)
Hypo (M) or Hyper (M) and/or New (B)[f, h] at 2 wks		Src-related kinase lacking C- and N-terminal myristylation sites	*Srms*	NM_011481	1.A.i	Unknown	--
Hypo at 2 and/or 4 wks (B/H/M)		Uncharacterized[i]	17 RAMs	--	2	--	--
Hyper at 2 and/or 4 wks (B/H/M)		Uncharacterized[i]	2 RAMs	--	2	--	--
New at 2 and/or 4 wks (B/H/M)		Uncharacterized[i]	3 RAMs	--	2	--	--
Methylation statuses are opposite at 2 and 4 wks		Uncharacterized[i]	3 RAMs	--	2	--	--
2 wk status is ambiguous[f, h]; 4 wk status is unambiguous		Uncharacterized[i]	2 RAMs	--	2	--	--
	Hypo (M)	Multiple gene hits[j]	237 bp	Various	3	Various	Various
	Hypo (M)	Multiple gene hits[j]	260 bp	Various	3	Various	Various
Hypo (H)	**Hypo (H)**	Multiple gene hits[j]	295 bp	Various	3	Various	Various
Hypo (H)	Hypo (M)	Multiple gene hits[j]	442-445 bp	Various	3	Various	Various
	Hypo (M)	Uncharacterized[i,j]	259 bp	--	4	--	--

Table 1.1 continued PCR Products Representing Unique Phenobarbital (PB)-induced RAMs in Liver Tumor-Sensitive B6C3F1, as Compared to Relatively Resistant C57BL/6, Mice were Cloned and Subjected to BLAST-like Alignment Tool (BLAT) Searches

[a]Unique RAM at 2 weeks of PB treatment
[b]Unique RAM at 4 weeks of PB treatment
[c]Genomic location relative to the transcriptional start site
[d]The letter in parentheses indicates which methylation-sensitive restriction enzyme (*BssHII*, *HpaII* or *MspI*) led to the identification of a RAM.
[e]The numbers in parentheses correspond to references which are located in Appendix References 1.
[f]The region of the genome might be represented by more than 1 RAM because different restriction digestions (e.g., *HpaII* and/or *MspI* and/or *BssHII*) led to the identification of multiple RAMs represented by PCR products that aligned to the same region of the genome.
[g]**Carry forward RAMs (i.e. those observed at 2 and 4 weeks) are listed in bold font.**
[h]Indicates that the region of the genome might be represented by 1 of 2 RAMs that formed via the same restriction digestion and the reason for this uncertainty is explained in the Methods.
[i]The uncharacterized genomic regions that these RAMs represent are greater than 10 kb away from an annotated gene.
[j]BLAT showed multiple top hits for the particular PCR product and the sequence associates with a specific repeat element.



1) Associated with a gene
   A. Within a gene
      i. Spans transcriptional start site (TSS) and/or 5' untranslated region
      ii. Exon
      iii. Intron
   B. Upstream from transcriptional start site
   i. $\leq$ 2 kb
   ii. $\leq$ 10 kb and > 2 kb
   C. Downstream from last exon/intron
   i. $\leq$ 2 kb
   ii. $\leq$ 10 kb and > 2 kb

2) > 10 kb away from either the transcriptional start site or the last exon/intron

3) Repeat element: multiple "top" hits and one/several are associated with a gene(s)

4) Repeat element: multiple "top" hits and no hits are associated with a gene(s)

Figure 1.8 A Scheme to Classify Cloned PCR Products that Represent Unique Phenobarbital (PB)-induced B6C3F1 Regions of Altered DNA Methylation (RAMs) Based on their Locations Within the Mouse Genome as Determined by BLAST-like Sequence Alignment Tool (BLAT) Searches (UCSC Genome Browser). PCR products representing unique B6C3F1 RAMs were cloned and subjected to BLAT searches. Depending on where, in relation to a gene, the PCR product aligned, it was assigned a particular genomic classification. For example, any PCR products designated as 1.B.i. are located less than or equal to 2 kilobases upstream from an annotated gene.

thrombospondin type 1 motif, 17 (*Adamts17*), anaphase promoting complex subunit 7 (*Anapc7*), ADP-ribosylation factor interacting protein 1 (*Arfip1*), B-cell scaffold protein with ankyrin repeats 1 (*Bank1*), CMT1A duplicated region transcript 4 (*Cdrt4*), chymase 1 (*Cma1*), cut-like 2 (*Cutl2*), dead box polypeptide 54 (*Ddx54*), myoferlin (*Fer1l3*), F-box and WD-40 domain protein 7, archipelago homolog (Drosophila) (*Fbxw7*), meteorin, glial cell differentiation regulator-like (*Metrnl*), odd Oz/ten-m homolog 2 (*Odz2*), pleckstrin homology domain containing, family F (with FYVE domain) member 1 (*Plekhf1*), prickle-like protein 2 (*Prickle2*), ral guanine nucleotide dissociation stimulator (*Ralgds*), sema domain, immunoglobulin domain (Ig), short basic domain, secreted, (semaphorin) 3G (*Sema3g*), stromal interaction molecule 1 (*Stim1*), transcription factor 4 (*Tcf4*), transcriptional enhancer factor-1 (*Tead1*), transforming growth factor, beta receptor II (*Tgfbr2*), threonine aldolase (*Tha1*), tyrosine kinase non-receptor 2 (*Tnk2*), and transient receptor potential cation channel, subfamily M, member 3 (*Trpm3*). Carry forward hypomethylations were those that were seen at both the 2 and 4 week timepoints: growth-arrest specific 2 like 3 (*Gas2l3*), potassium channel, subfamily K, member 10 (*Kcnk10*), tyrosine hydroxylase (*Th*), Williams-Beuren syndrome chromosome region 17 homolog (*Wbscr17*), a probable repeat element which was linked to multiple chromosomes (295 bp), and a PCR product which aligned to an uncharacterized region (479 bp).

RAMs that were unambiguously assigned a hypermethylated status at 4 weeks of PB treatment were coiled-coiled domain containing 137 (*Ccdc137*), RNA binding motif protein 10 (*Rbm10*) and THAP domain containing and apoptosis associated protein 3 (*Thap3*). Furthermore, unambiguous new methylations at 4 weeks were branched chain

aminotransferase 2, mitochondrial (*Bcat2*), bcl2-like 13 (*Bcl2l13*), Discs, large homolog-associated protein 4 (*Dlgap4*), nuclear receptor corepressor 2 (*Ncor2*), retinoid X receptor beta (*Rxrb*), ST6 (alpha-N-acetyl-neuraminyl-2,3-beta-galactosyl-1,3)-N-acetylgalactosaminide alpha-2,6-sialyltransferase 3 (*Siat7c*), transmembrane protein 104 (*Tmem104*), ubiquitin-conjugating enzyme E2D 1 (*Ube2d1*) and WSC domain-containing 1 (*Wscd1*). Carry forward newly methylated RAMs were brain-specific angiogenesis inhibitor 3 (*Bai3*), RIKEN cDNA C630007B19 gene (*Tafa-1*) and an uncharacterized region (524 bp). With regards to increases in methylation at 2 weeks, pleckstrin homology domain containing, family F (with FYVE domain) member 1 (*Plekhf1*) was newly methylated, and there were no unambiguous examples of hypermethylations.

Since the data analysis procedure sometimes involved the combination of PCR product sizes that are within 2 base pairs of one another, in addition to the fact that 3 different methylation-sensitive enzyme pairs were utilized, situations occurred in which it was not possible to unambiguously assign a specific methylation status to a RAM. For example, in the case of *Nfe2l2*, restriction digestion by *RsaI/HpaII* followed by AP-PCR and CE resulted in the detection of 2 RAMs, each within 2 base pairs of the cloned PCR product, that possessed different methylation statuses (Table 1.1). Because of the $\pm$ 2 base pair combination rule of the data analysis procedure, one cannot be certain whether *Nfe2l2* is hypomethylated or newly methylated at 2 weeks based on digestion with *RsaI/HpaII*. In the case of *Prickle2*, *RsaI/HpaII* digestion revealed a hypomethylated RAM while the *BfaI/BssHII* digest revealed a newly RAM at 2 weeks (Table 1.1). Thus, *Prickle2* could represent one or both of these RAMs since different restriction digestions were utilized, each of which reveals information regarding the methylation patterns of

different cytosines at and within the sites of primer annealing. Therefore, multiple genes were discerned which could not be assigned a specific methylation status. Table 1.1 indicates the methylation statuses and particular treatment periods at which these genes displayed altered methylation. These genes were: ephrin B2 (*Efnb2*), zinc finger and SCAN domain containing 22 (*Zscan22*), inositol polyphosphate-5-phosphatase A (*Inpp5a*), nuclear factor, erythroid derived 2, like 2 (*Nfe2l2*), NK2 transcription factor related, locus 6 (*Nkx2-6*), prickle-like protein 2 (*Prickle2*), protein tyrosine phosphatase, receptor type O (*Ptpro*), src-related kinase lacking C-terminal regulatory tyrosine and N-terminal myristylation sites (*Srms*), transcription factor 4 (*Tcf4*), triple functional domain (PTPRF interacting) (*Trio*), ubiquitin-conjugating enzyme E2D 1 (*Ube2d1*) and WSC domain-containing 1 (*Wscd1*).

There were 5 PCR products which each associated with multiple hits that displayed the highest BLAT scores, indicating that many top hits for each PCR product showed the fewest mismatches as compared to the sequence of interest. As such, any of these top hits might correspond to the PCR product sequence. Furthermore, all of the top hits for a particular PCR product represented regions on various chromosomes, yet the product aligned to the identical repetitive element. Therefore, these 5 RAMs (237, 259, 260, 295 and 442-445 bp) appear to be linked to a different, specific repetitive element, and thus we are unable to determine with certainty which genomic region the unique RAM represents. BLAT searches also revealed that regions of the genome, represented by 27 RAMs, are uncharacterized (i.e. located more than 10 kb away from a known gene). Of these 27 RAMs, the methylation statuses of 22 were unambiguous and therefore could be classified as either hypo- (17 RAMs), hyper- (2 RAMs) or new- (3

RAMs) methylations at a particular time point. Three of the 27 uncharacterized RAMs could be assigned a specific methylation status at both the 2 and 4 week time points, although the changes were opposite in direction (e.g., the RAM was hypomethylated at 2 weeks and newly methylated at 4 weeks). Finally, for 2 out of the 27 uncharacterized RAMs, the methylation statuses at 4 weeks were unambiguous, while the statuses at 2 weeks were not (e.g., at 2 weeks, the RAM is either hypo- or newly methylated).

In order to uncover interconnections between the genes whose methylation statuses changed uniquely in the B6C3F1 mice, an informatics program was utilized to identify their common protein targets and regulators at 4 weeks of PB treatment. Figure 1.9 illustrates the common cellular targets of several of the unique RAMs of interest at 4 weeks; those genes listed in Table 1.1 that do not appear in Figure 1.9 do not possess targets that are in common with any of the other 4 week genes. As examples, interleukin 8 (IL-8) is a common target of Cma1, Ncor2 and Tcf4 and similarly, vascular endothelial growth factor (Vegf) is a common target of Cma1, Tcf4 and Tgfbr2. In this way, potential common targets of multiple RAMs of interest were ascertained in order to determine whether common cellular processes might be affected which might more efficiently facilitate tumorigenesis. Additionally, common cellular regulators of the genes of interest at 4 weeks were identified and this figure is located in the Appendix (Fig. 1.16).

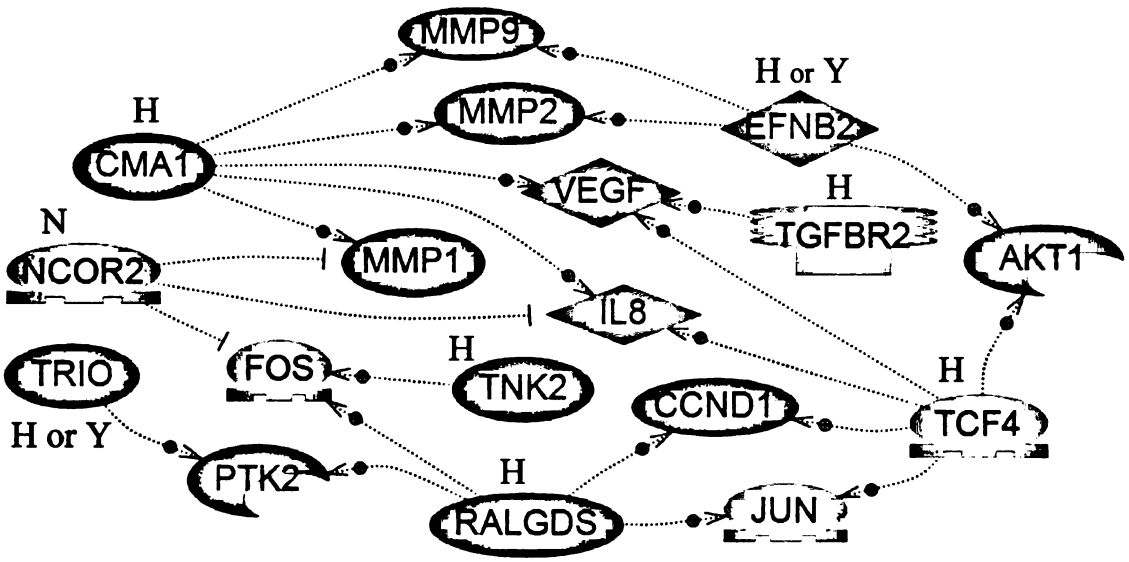


Figure 1.9 Common Cellular Targets of Genes that Represent Regions of Altered DNA Methylation (RAMs) in Liver Tumor-Susceptible B6C3F1 Mice at 4 Weeks of Phenobarbital (PB) Treatment. An informatics approach was utilized to uncover cellular targets that can be affected by 2 or more genes representing unique PB-induced B6C3F1 RAMs at 4 weeks. Entities that lack a H, Y, or N are common targets. The arrows point towards the common target: positive (···⊕➢) and negative (·····|) effects are shown. The methylation status of a unique RAM is indicated by H (hypomethylation), Y (hypermethylation) or N (new methylation). A combination of letters (e.g., H or Y) denotes a RAM with an ambiguous methylation status at 4 weeks. The shapes of the entities represent the specific class of molecules to which each gene belongs: extracellular proteins or nuclear receptors ( ), ligands ( ), kinases ( ), membrane receptors ( ), and transcription factors ( ).

DISCUSSION

Following administration of a liver tumor promoting dose of PB (0.05%, w/w) for 2 or 4 weeks, 170 unique RAMs were identified in livers of B6C3F1 mice, which are sensitive to PB-induced tumorigenesis, as compared to the resistant C57BL/6 (Figure 1.7) (Bachman *et al.*, 2006b). The current study focused upon annotating those unique RAMs via BLAT searches in order to determine in which genomic regions these methylation changes occurred and discerning the processes that these RAMs might affect which could facilitate tumorigenesis. PCR products were cloned that represent 90 of the 170 RAMs, and 51 genes whose methylation statuses changed uniquely in the sensitive mice were ascertained. These genes and their functions are summarized in Table 1.1. PCR products representing 27 RAMs aligned to regions of the mouse genome which are located further than 10 kb away from any known genes.

Prior to this study, only a few specific genes, in addition to CAR (Yamamoto *et al.*, 2004) were associated with mouse liver tumorigenesis, e.g., Ha-*ras, raf, myc* and *Ctnnb1 (*β-Catenin*)* (Aydinlik *et al.*, 2001; Counts *et al.*, 1997; Ray et al., 1994; Vorce and Goodman, 1991; Wiseman *et al.*, 1986); these generally were identified late during tumorigenesis. It is possible that some of the altered methylation observed after carcinoma development might have arisen secondarily, rather than having been causal. Therefore we are interested in understanding the role(s) of methylation changes occurring early during the multi-stage transformation process. The time-dependence of the unique PB-induced B6C3F1 RAMs, as well as the identification of several changes which were observed at both 2 and 4 weeks ("carry forward" RAMs), support the notion that this anomalous methylation plays a causative role in tumor formation (Bachman *et al.*,

2006b). The current data support our hypothesis that this approach can discern "new" genes which might be involved in PB-induced tumorigenesis due to aberrant methylation (Table 1.1). Individually, the genes with altered methylation statuses might be critical; however, importantly, evidence presented here suggests that these genes can influence common cellular processes. In other words, unique RAMs might cooperate to increase/decrease cellular functions, i.e., up-regulation of oncogenes and down-regulation of suppressor genes, which drive tumorigenesis.

For example, PB altered methylation patterns of multiple genes involved in invasion and metastasis. At 4 weeks, *Tgfbr2*, *Tcf4* and *Ralgds* were hypomethylated uniquely and Bachman *et al.* (2006b) demonstrated Ha-*ras* hypomethylation and its increased expression in B6C3F1 mice. These 4 genes are associated with the epithelial-mesenchymal cell transition (EMT), a mechanism of tumor progression ultimately leading to invasion and migration. Several events are linked to EMT, including but not limited to the down-regulation of E-cadherin, which can sequester β-catenin, rendering this protein unavailable for heterodimerizing with Tcf4 and facilitating transcription genes which promote proliferation, plus the initiation of Tgf-β and Ras signal transduction pathways (Thiery, 2002). Additionally, Tnk2 and Ralgds (hypomethylated, 4 weeks), along with Efnb2 and Trio (both possibly hypomethylated, 4 weeks) play crucial roles during invasion and metastasis (Gale *et al.*, 1996; Nakada *et al.*, 2004; van der Horst *et al.*, 2000; Ward *et al.*, 2001; Yoshizuka *et al.*, 2004).

The existence of common cellular targets and regulators of a subset of the unique genes indicate that key signaling processes are potentially affected (Fig. 1.9 and Fig. 1.16). Involved in angiogenesis are Efnb2 (possibly hypomethylated, 4 weeks)

(Maekawa *et al.*, 2003), and Tcf4 and Cma1 (both hypomethylated, 4 weeks), both of which can upregulate Vegf (Katada *et al.*, 2002; Zhang *et al.*, 2001). An increase in Nf-kB activity might result from Ppp4c (hypomethylated, 4 weeks), which activates it (Hu *et al.*, 1998) and Ncor2 (newly methylated, 4 weeks), which inhibits it (Lee *et al.*, 2000). Nf-κB-induced secretion of IL-6 from liver macrophages increases tumor cell survival and growth, promoting carcinogenesis (Lawrence *et al.*, 2007) and a Nf-κB-dependent increase in IL-8 expression contributes to both angiogenesis and metastasis in tumor cells (Karashima *et al.*, 2003). Furthermore, common targets and regulators of IL-6 and IL-8 were demonstrated (Fig. 1.9 and Fig. 1.16). IL-6 might be upregulated via relieving inhibition by Ncor2 (Song *et al.*, 2005); we show that *Ncor2* is newly methylated at 4 weeks and thus possibly silenced. IL-6 can upregulate Ralgds in leukemic cells (Senga *et al.*, 2001) and Efnb2 in Kaposi sarcoma cells (Masood *et al.*, 2005). Ralgds mediates the survival of transformed cells via the JNK/SAPK pathway, and also is essential for skin tumor formation in mice (González-García *et al.*, 2005). Thus, IL-6 might indirectly contribute to survival, angiogenesis, invasion and metastasis. Similarly, IL-8 can be regulated by several genes representing unique RAMs: Tcf4 and Cma1 (hypomethylated, 4 weeks) up-regulate *IL-8* in liver and EoL-1 cells, respectively (Levy *et al.*, 2002; Terakawa *et al.*, 2006), while Ncor2 (newly methylated, 4 weeks) can block IL-8 transcription (Hoberg *et al.*, 2004). Therefore, IL-6 and IL-8, common targets and/or regulators of several key genes, might facilitate the clonal expansion of preneoplastic cells by further contributing to cell growth/survival, angiogenesis, invasion and metastasis. Figure 1.10 summarizes the possible functional significance, regarding tumorigenesis, of selected genes which exhibited altered methylation uniquely in the

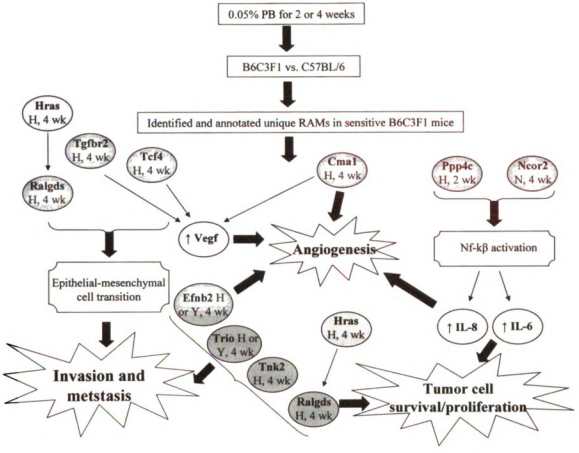


Figure 1.10 The Possible Functional Significance, Regarding Tumorigenesis, of Selected Genes which Exhibited Altered Methylation Uniquely in the B6C3F1 Mouse Following Treatment with Phenobarbital (PB). The current study identified regions of altered DNA methylation (RAMs) at 2 or 4 weeks of 0.05% PB treatment and annotated 51 genes that represent these regions. Several of these genes are well-documented as playing critical roles in tumorigenesis (dark gray ovals). Unique PB-induced hypomethylation and decreased expression of Ha-*ras* (light gray oval) in B6C3F1 mice has been demonstrated (Bachman *et al.*, 2006b). The appropriate time point of PB treatment is denoted (2 or 4 wk), and the methylation statuses of the RAMs are indicated by H (hypomethylation), Y (hypermethylation) or N (new methylation). RAMs with an ambiguous methylation status are indicated by the presence of 2 letters (i.e. H or Y). Interleukin 6 (IL-6) is a common 4 week regulator, and interleukin 8 (IL-8) and vascular endothelial growth factor (VEGF) are common 4 week targets, of multiple genes identified from unique RAMs in the liver tumor-susceptible B6C3F1 mice (white ovals). RALGDS is a key downstream effector of HRAS. Selected literature references for the relationships depicted in this diagram are noted in the Appendix (Fig. 7 and References 2).

B6C3F1 mouse following PB treatment, along with a subset of key common targets/regulators of these genes. Selected literature references for the relationships depicted in this figure are noted in the Appendix (Fig. 1.17 and References 2).

Since our approach for the identification of unique RAMs in the sensitive B6C3F1 mice involved isolation of DNA from homogenized whole liver, it is impossible to determine whether each methylation change occurred in the same cell or in numerous, different cells. Regardless, 1 unique RAM might provide a growth advantage to a single cell; accumulation of multiple RAMs in the same cell could additively or synergistically enhance aberrant proliferation. Moreover, these RAMs might occur in various liver cell types: hepatocytes, Kupffer macrophages, and/or sinusoidal endothelial cells. Hepatocytes are not the only cells that play crucial roles in hepatocarcinogenesis; liver macrophages secrete IL-6 which can increase tumor cell growth and survival (Lawrence *et al.*, 2007). Interactions between different cell types are important during tumor formation, so it is essential to utilize whole animal studies which permit critical interactions between different cell types in the target tissue to be observed, e.g., the innate immune system plays a crucial role in DEN-induced hepatocellular carcinoma in mice (Naugler *et al.*, 2007). Mature mammalian cells can be stimulated to dedifferentiate into an embryonic stem cell-like state (Okita *et al.*, 2007; Wernig *et al.*, 2007). This fact, coupled with the capability of hepatocytes to proliferate either in a compensatory fashion, e.g., following partial hepatectomy (Steer, 1995), or in response to treatment with mitogens such as PB (Counts *et al.*, 1996; Kolaja *et al.*, 1996a), indicates that it is possible that mature hepatocytes are liver tumor cell progenitors. This notion is not incompatible with the suggestion that tumors originate from stem cell transformation

(Reya *et al.*, 2001), as both scenarios might be operative. Thus, it is important to evaluate methylation changes in whole tissue.

Treatment with a tumor-promoting dose of PB for 2 or 4 weeks stimulates hepatocyte proliferation in B6C3F1 male mice (Counts *et al.*, 1996; Kolaja *et al.*, 1996a). Upon further treatment, PB inhibits proliferation in the normal hepatocyte population, while preneoplastic cells may continue to divide (reviewed in Counts *et al.*, 1996). The observed methylation changes might give certain cells the ability to "escape" the inhibition of proliferation by PB, facilitating clonal expansion of preneoplastic cells. Therefore, replication-dependent passive demethylation could produce hypomethylated RAMs. Conversely, active demethylation (Bhattacharya *et al.*, 1999) or cytidine deaminases (Morgan *et al.*, 2004) could also generate hypomethylated RAMs. PB-induced differences in activity and/or localization of demethylases, DNA methyltransferases (DNMT1, DNMT3a and DNMT3b), methyl-binding proteins and/or enzymes involved in 1-carbon metabolism (Ulrey *et al.*, 2005) could be responsible for the detected methylation changes. While the detailed mechanism(s) involved in PB-induced alteration of methylation remain to be discerned, it is important to recognize that the sensitive B6C3F1, as compared to the C57BL/6, mice appear to be "defective" with regard to the ability to preserve normal methylation patterns (Watson and Goodman, 2002).

Methylation changes in 57% (29/51) of the genes representing unique B6C3F1 RAMs occur within introns (Table 1.1). Alterations in methylation within immediate 5' promoter regions might result in gene expression changes (Esteller, 2007). However, current studies indicate that most mammalian genes possess multiple promoters and a

large number of novel intergenic promoters have been discovered, and these might result in the transcription of non-coding RNA products (Sandelin *et al.*, 2007). Additionally, a PB-responsive gene (*Ugt1a1*) contains an important cis regulatory element located 3 kilobases upstream from the transcriptional start site (Sugatani *et al.*, 2001), and regulatory elements can also be found within introns (Fedorova and Fedorov, 2003) and near the 3' region (Cawley *et al.*, 2004). Hence, it is possible that the RAMs associated with genomic regions other than immediate 5' promoter sequences can facilitate changes in gene expression.

The unique B6C3F1 RAMs occurred very early, at 2 and 4 weeks of PB treatment, and a subset of the discerned genes that represent the RAMs of interest can potentially influence processes that are associated with late stages of tumorigenesis, including angiogenesis, invasion and metastasis. These data support the idea that cancer evolves in a stepwise series of clonal expansions, accumulating heritable alterations in their genomes (mutations and/or epigenetic changes) which, in a progressive fashion, provide a growth advantage over neighboring cells (Nowell, 1976). It is our contention that altered methylation plays critical roles during PB-induced liver tumor formation in rodents. We believe that the genes involved in rodent liver tumorigenesis are fundamentally the same as those underlying tumorigenesis in human tissues and hypothesize that there are key differences in the capacity to maintain overall stability of the genome (e.g., DNA methylation status is more stable in human cells as compared to rodent cells) (reviewed in Goodman and Watson, 2002). This could account, in part, for the increased susceptibility to tumorigenesis exhibited by rodents as compared to humans (Rangarajan and Weinberg, 2003). This study has discerned genes that display unique

methylation changes in PB-treated liver tumor-susceptible mice and which can now be linked to liver tumorigenesis based on the processes in which they are involved. We are now turning our attention towards real-time PCR and microarray analysis of the key genes in order to determine the extent to which expression changes are associated with the observed PB-induced altered DNA methylation during early phases of tumorigenesis.

ACKNOWLEDGEMENTS

J.M.P. is a predoctoral fellow supported by National Institutes of Health–National Institute of Environmental Health Sciences training grant No. T32-ES-7255. Research support, in the form of a gift, from the R.J. Reynolds Tobacco Company is acknowledged gratefully.

REFERENCES

Aydinlik, H., Nguyen, T. D., Moennikes, O., Buchmann, A., and Schwarz, M. (2001). Selective pressure during tumor promotion by phenobarbital leads to clonal outgrowth of β-catenin-mutated mouse liver tumors. *Oncogene* **22**, 7812-7816.

Bachman, A. N., Kamendulis, L. M., and Goodman, J. I. (2006a). Diethanolamine and phenobarbital produce an altered pattern of methylation in GC-rich regions of DNA in B6C3F1 mouse hepatocytes similar to that resulting from choline deficiency. *Toxicol. Sci.* **90**, 317-320.

Bachman, A. N., Phillips, J. M, and Goodman J. I. (2006b). Phenobarbital induces progressive patterns of GC-rich and gene-specific altered DNA methylation in the liver of tumor-prone B6C3F1 mice. *Toxicol. Sci.* **91**, 393-405.

Becker, F.F. (1982). Morphological classification of mouse liver tumors based on biological characteristics. *Cancer Res.* **42**, 3918-3923.

Bhattacharya, S. K., Ramchandani, S., Cervoni, N., and Szyf, M. (1999). A mammalian protein with specific demethylase activity for mCpG DNA. *Nature* **397**, 579-583.

Cawley, S., Bekiranov, S., Ng, H. H., Kapranov, P., Sekinger, E. A., Kampa, D., Piccolboni, A., Sementchenko, V., Cheng, J., Williams, A. J., Wheeler, R., Wong, B., Drenkow, J., Yamanaka, M., Patel, S., Brubaker, S., Tammana, H., Helt, G., Struhl, K., Gingeras, T. R. (2004) Unbiased mapping of transcription factor binding sites along human chromosomes 21 and 22 points to widespread regulation of noncoding RNAs. *Cell* **116**, 499-509.

Counts, J. L. and Goodman, J. I. (1995). Alterations in DNA methylation may play a variety of roles in carcinogenesis. *Cell* **83**, 13-15.

Counts, J. L., McClain, R. M., and Goodman, J. I. (1997). Comparison of effect of tumor promoter treatments on DNA methylation status and gene expression in B6C3F1 and C57BL/6 mouse liver and in B6C3F1 mouse liver tumors. *Mol. Carcinog.* **18**, 97-106.

Counts, J. L., Sarmiento, J. I., Harbison, M. L., Downing, J. C., McClain, R. M., and Goodman, J. I. (1996). Cell proliferation and global methylation status changes in mouse

liver after phenobarbital and/or choline-devoid, methionine-deficient diet administration. *Carcinogenesis* **17**, 1251-1257.

Esteller, M. (2007). Cancer epigenomics: DNA methylomes and histone-modification maps. *Nat. Rev. Genet.* **8**, 286-298.

Fedorova, L., and Fedorov, A. (2003). Introns in gene evolution. *Genetica* **118**, 123-31.

Feinberg, A. P., Ohlsson, R., and Henikoff, S. (2006). The epigenetic progenitor origin of human cancer. *Nat. Rev. Genet.* **7**, 21-33.

Gale, N. W., Holland, S. J., Valenzuela, D. M., Flenniken, A., Pan, L., Ryan, T. E., Henkemeyer, M., Strebhardt, K., Hirai, H., Wilkinson, D. G., Pawson, T., Davis, S., and Yancopoulos, G. D. (1996) Eph receptors and ligands comprise two major specificity subclasses and are reciprocally compartmentalized during embryogenesis. *Neuron* **17**, 9-19.

Gonzalgo, M. L., Liang, G., Spruck, C. H., III, Zingg, J. M., Rideout, W. M., III, and Jones, P. A. (1997). Identification and characterization of differentially methylated regions of genomic DNA by methylation-sensitive arbitrarily primed PCR. *Cancer Res.* **57**, 594-599.

González-García, A., Pritchard, C. A., Paterson, H. F., Mavria, G., Stamp, G., and Marshall, C. J. (2005) RalGDS is required for tumor formation in a model of skin carcinogenesis. *Cancer Cell.* **7**, 219-226.

Goodman, J.I. and Watson, R.E. (2002). Altered DNA methylation: A secondary mechanism involved in carcinogenesis. *Annu. Rev. Pharmacol. Toxicol.* **42**, 501-525.

Hanahan D. and Weinberg, G. F. (2000). The hallmarks of cancer. *Cell* **100**, 57-70.

Hoberg, J. E., Yeung, F., and Mayo, M. W. (2004). SMRT derepression by the IκB kinase α: a prerequisite to NF-κB transcription and survival. *Mol. Cell* **16**, 245-255.

Hu, M. C., Tang-Oxley, Q., Qiu, W. R., Wang, Y. P., Mihindukulasuriya, K. A., Afshar, R., and Tan, T. H. (1998). Protein phosphatase X interacts with c-Rel and stimulates c-Rel/nuclear factor κB activity. *J. Biol. Chem.* **50**, 33561-33565.

Karashima, T., Sweeney, P., Kamat, A., Huang, S., Kim, S. J., Bar-Eli, M., McConkey, D. J., and Dinney, C. P. (2003) Nuclear factor-κB mediates angiogenesis and metastasis of human bladder cancer through the regulation of interleukin-8. *Clin. Cancer Res.* **9**, 2786-2797.

Katada, J., Muramatsu, M., Hayashi, I., Tsutsumi, M., Konishi, Y., and Majima, M. (2002). Significance of vascular endothelial cell growth factor up-regulation mediated via

a chymase-angiotensin-dependent pathway during angiogenesis in hamster sponge granulomas. *J. Pharmacol. Exp. Ther.* **302**, 949-956.

Kolaja, K. L., Stevenson, D. E., Johnson J. T., Walborg, Jr., E. F., and Klaunig, J. E. (1996a) Subchronic effects of dieldrin and phenobarbital on hepatic DNA synthesis in mice and rats. *Fundam. Appl. Toxicol.* **29**, 219-228.

Kolaja, K. L., Stevenson, D. E., Walborg Jr., E. F., and Klaunig J. E. (1996b). Dose dependence of phenobarbital promotion of preneoplastic hepatic lesions in F344 rats and B6C3F1 mice: effects on DNA synthesis and apoptosis. *Carcinogenesis* **17**, 947-954.

Lawrence, T., Hageman, T., and Balkwill, F. (2007). Sex, cytokines, and cancer. *Science* **317**, 51-52.

Lee, S. K., Kim, J. H., Lee, Y. C., Cheong, J., and Lee, J. W. (2000). Silencing mediator of retinoic acid and thyroid hormone receptors, as a novel transcriptional corepressor molecule of activating protein-1, nuclear factor-κB, and serum response factor. *J. Biol. Chem.* **275**, 12470-12474.

Lévy, L., Neuveut, C., Renard, C. A., Charneau, P., Branchereau, S., Gauthier, F., Van Nhieu, J. T., Cherqui, D., Petit-Bertron, A. F., Mathieu, D., and Buendia, M. A. (2002). Transcriptional activation of interleukin-8 by β-catenin-Tcf4. *J. Biol. Chem.* **277**, 42386-42393.

Maekawa, H., Oike, Y., Kanda, S., Ito, Y., Yamada, Y., Kurihara, H., Nagai, R., and Suda, T. (2003). Ephrin-B2 induces migration of endothelial cells through the phosphatidylinositol-3 kinase pathway and promotes angiogenesis in adult vasculature. *Arterioscler Thromb. Vasc. Biol.* **23**, 2008-2014.

Masood, R., Xia, G., Smith, D. L., Scalia, P., Still, J. G., Tulpule, A., and Gill, P. S. (2005). Ephrin B2 expression in Kaposi sarcoma is induced by human herpesvirus type 8: phenotype switch from venous to arterial endothelium. *Blood* **105**, 1310-1318.

Moennikes, O., Buchmann, A., Romualdi, A., Ott, T., Werringloer, J., Willecke, K., and Schwarz, M. (2000). Lack of phenobarbital-mediated promotion of hepatocarcinogenesis in connexin32-null mice. *Cancer Res.* **15**, 5087-5091.

Nakada, M., Niska, J. A., Miyamori, H., McDonough, W. S., Wu, J., Sato, H., and Berens, M. E. (2004). The phosphorylation of EphB2 receptor regulates migration and invasion of human glioma cells. *Cancer Res.* **64**, 3179-3185.

Naugler, W. E., Sakurai, T., Kim, S., Maeda, S., Kim, K., Elsharkawy, A. M., and Karin, M. (2007). Gender disparity in liver cancer due to sex differences in MyD88-dependent IL-6 production. *Science* **317**, 121-124.

Naveh-Many, T., and Cedar, H. (1981). Active gene sequences are undermethylated. *Proc. Natl. Acad. Sci. USA,* **78**, 4246-4250.

Nowell, P.C. (1976). The clonal evolution of tumor cell populations. *Science* **194**, 24-28.

Okita, K., Ichisaka, T., and Yamanaka, S. (2007). Generation of germline-competent induced pluripotent stem cells. *Nature* **448**, 313-317.

Phillips, J. M., Yamamoto. Y,, Negishi, M., Maronpot, R. R., and Goodman, J. I. (2007). Orphan nuclear receptor constitutive active/androstane receptor-mediated alterations in DNA methylation during phenobarbital promotion of liver tumorigenesis. *Toxicol. Sci.* **96**, 72-82.

Ramsahoye, B. H., Biniszkiewicz, D., Lyko, F., Clark, V., Bird, A. P., and Jaenisch, R. (2000) Non-CpG methylation is prevalent in embryonic stem cells and may be mediated by DNA methyltransferase 3a. *Cell Biology* **97**, 5237-5242.

Rangarajan, A. and Weinberg, R.A. (2003). Comparative biology of mouse versus human cells: Modeling human cancer in mice. *Nature Rev. Cancer* **3**, 952-959.

Ray, J. S., Harbison, M. L., McClain, R. M., and Goodman, J. I. (1994) Alterations in the methylation status and expression of the *raf* oncogene in phenobarbital-induced and spontaneous B6C3F1 mouse live tumors. *Mol. Carcinog.* **9**, 155-166.

Reik, W. (2007). Stability and flexibility of epigenetic gene regulation in mammalian development. *Nature* **447**, 425-432.

Reya, T., Morrison, S. J., Clarke M. F., and Weissman, I. L. (2001) Stem cells, cancer, and cancer stem cells. *Nature* **414**, 105-111.

Sandelin, A., Carninci, P., Lenhard, B., Ponjavic, J., Hayashizaki, Y., and Hume, D. A. (2007). Mammalian RNA polymerase II core promoters: insights from genome-wide studies. *Nat. Rev. Genet.* **8**, 424-436.

Senga, T., Iwamoto, T., Kitamura, T., Miyake, Y., and Hamaguchi, M. (2001). JAK/STAT3-dependent activation of the RalGDS/Ral pathway in M1 mouse myeloid leukemia cells. *J. Biol. Chem.* **35**, 32678-32681.

Shiraishi, M., Lerman L. S., and Sekiya T. (1995). Preferential isolation of DNA fragments associated with CpG islands. *Proc. Natl. Acad. Sci.* **92**, 4229-4233.

Song, L., Zlobin, A., Ghoshal, P., Zhang, Q., Houde, C., Weijzen, S., Jiang, Q., Nacheva, E., Yagan, D., Davis, E., Galiegue-Zouitina, S., Catovsky, D., Grogan, T., Fisher, R. I., Miele, L., and Coignet, L. J. (2005). Alteration of SMRT tumor suppressor function in transformed non-Hodgkin lymphomas. *Cancer Res.* **65**, 4554-4561.

Steer, C. J. (1995). Liver regeneration. *FASEB J.* **9**, 1396-1400.

Strathmann, J., Schwarz, M., Tharappel, J. C., Glauert, H. P., Spear, B.T., Robertson, L. W., Appel, K. E., and Buchmann, A. (2006). PCB 153, a non-dioxin-like tumor promoter, selects for β-catenin (*Catnb*)-mutated mouse liver tumors. *Toxicol. Sci.* **93**, 34-40.

Sugatani, J., Kojima, H., Ueda, A., Kakizaki, S., Yoshinari, K., Gong, Q. H., Owens, I. S., Negishi, M., and Sueyoshi, T. (2001). The phenobarbital response enhancer module in the human bilirubin UDP-glucuronosyltransferase *UGT1A1* gene and regulation by the nuclear receptor CAR. *Hepatology* **33**, 1232-1238.

Terakawa, M., Tomimori, Y., Goto, M., and Fukuda, Y. (2006). Mast cell chymase induces expression of chemokines for neutrophils in eosinophilic EoL-1 cells and mouse peritonitis eosinophils. *Eur. J. Pharmacol.* **538**, 175-181.

Thiery, J. P. (2002). Epithelial-mesenchymal transitions in tumour progression. *Nat. Rev. Cancer* **2**, 442-454.

Trosko, J. E., and Chang C., C. (2001). Role of stem cells and gap junctional intercellular communication in human carcinogenesis. *Radiat. Res.* **155**, 175-180.

Ulrey, C. L., Liu, L., Andrews, L. G., and Tollefsbol, T. O. (2005) The impact of metabolism on DNA methylation. *Hum. Mol. Genet.* **14** Spec No 1:R139-147.

van der Horst, E. H., Degenhardt, Y. Y., Strelow, A., Slavin, A., Chinn, L., Orf, J., Rong, M., Li, S., See, L. H., Nguyen, K. Q., Hoey, T., Wesche, H., and Powers, S. (2005) Metastatic properties and genomic amplification of the tyrosine kinase gene *ACK1*. *Proc. Natl. Acad. Sci. U S A* **102**, 15901-15906.

Vorce, R. L., and Goodman, J. I. (1991). Hypomethylation of *ras* oncogenes in chemically induced and spontaneous B6C3F1 mouse liver tumors. *Toxicol. Environ. Health.* **34**, 367-384.

Ward,Y., Wang, W., Woodhouse, E., Linnoila, I., Liotta, L., and Kelly, K. (2001) Signal pathways which promote invasion and metastasis: critical and distinct contributions of extracellular signal-regulated kinase and Ral-specific guanine exchange factor pathways. *Mol. Cell Biol.* **21**, 5958-5969.

Watson, R. E., and Goodman, J. I. (2002) Effects of phenobarbital on DNA methylation in GC-rich regions of hepatic DNA from mice that exhibit different levels of susceptibility to liver tumorigenesis. *Toxicol Sci.* **68**, 51-58.

Wei, P., Zhang, J., Egan-Hafley, M., Liang, S., and Moore, D. D. (2000). The nuclear receptor CAR mediates specific xenobiotic induction of drug metabolism. *Nature* **407**, 920-923.

Wernig, M., Meissner, A., Foreman, R., Brambrink, T., Ku, M., Hochedlinger, K., Bernstein, B. E., and Jaenisch, R. (2007). In vitro reprogramming of fibroblasts into a pluripotent ES-cell-like state. *Nature* **448**, 318-324.

Whysner, J., Ross, P. M., and Williams, G. M. (1996). Phenobarbital mechanistic data and risk assessment: enzyme induction, enhanced cell proliferation, and tumor promotion. *Pharmacol. Ther.* **71**, 53-91.

Wiseman, R. W., Stowers, S. J., Miller, E. C., Anderson, M. W., and Miller, J. A. (1986). Activating mutations of the c-Ha-*ras* protooncogene in chemically induced hepatomas of the male B6C3 F1 mouse. *Proc. Natl. Acad. Sci. U S A* **83**, 5825-5829.

Yamamoto, Y., Moore, R., Goldsworthy, T. L., Negishi, M., and Maronpot, R. R. (2004). The orphan nuclear receptor constitutive active/androstane receptor is essential for liver tumor promotion by phenobarbital in mice. *Cancer Res.* **64**, 7197-7200.

Yoshizuka, N., Moriuchi, R., Mori, T., Yamada, K., Hasegawa, S., Maeda, T., Shimada, T., Yamada, Y., Kamihira, S., Tomonaga, M., and Katamine, S. (2004) An alternative transcript derived from the *Trio* locus encodes a guanosine nucleotide exchange factor with mouse cell-transforming potential. *J. Biol. Chem.* **279**, 43998-44004.

Zhang, X., Gaspard, J. P., and Chung, D. C. (2001). Regulation of vascular endothelial growth factor by the Wnt and K-ras pathways in colonic neoplasia. *Cancer Res.* **15**, 6050-6054.

CHAPTER 1 APPENDIX

Data within the appendix consist of: 1) A series of figures which provide a breakdown of the genomic locations (Fig. 1.11), chromosomal alignments (Fig. 1.12) and functions (Fig. 1.13) of all the unique B6C3F1 RAMs plus 2 examples of informatics pathways of unique B6C3F1 RAMs (Figs. 1.14 and 1.15), the common cellular regulators of unique B6C3F1 RAMs at 4 weeks (Fig. 1.16) and appropriate literature references for both Table 1.1 (Appendix References 1) and Figure 1.10 (Fig. 1.17 plus Appendix References 2). Note that these data are a subset of the total Supplementary Information that can be found in the version of this manuscript that was published in *Toxicological Sciences* in 2008.

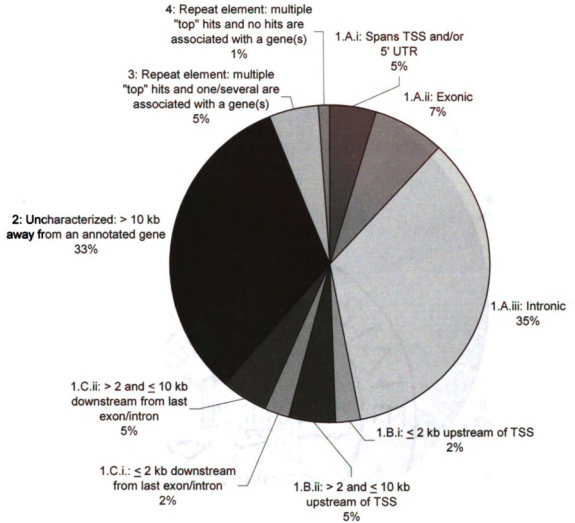


Figure 1.11 The Distribution of Genomic Locations to Which the PCR Products Representing PB-induced Unique Regions of Altered DNA Methylation (RAMs) in B6C3F1 Mice Aligned. PCR products representing unique B6C3F1 RAMs were assigned a genomic location relative to an annotated gene, based on the classification scheme in Figure 1.8. Abbreviations: TSS, transcriptional start site; UTR, untranslated region.

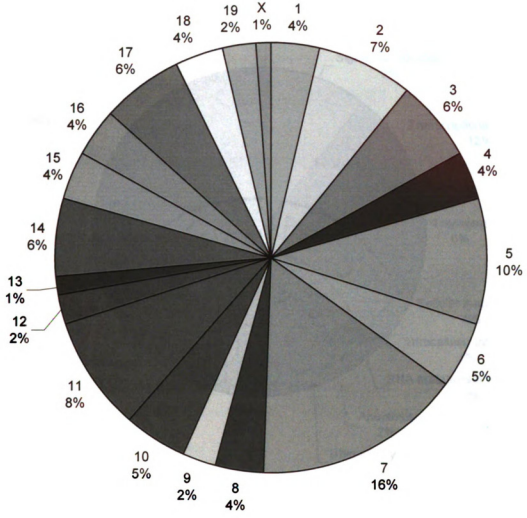


Figure 1.12 The Distribution of Chromosomes Within the Mouse Genome to Which the PCR Products Representing PB-induced Unique Regions of Altered DNA Methylation (RAMs) in B6C3F1 Mice Aligned. The chromosomes proceed from 1 to 19, including X, in a clockwise fashion.

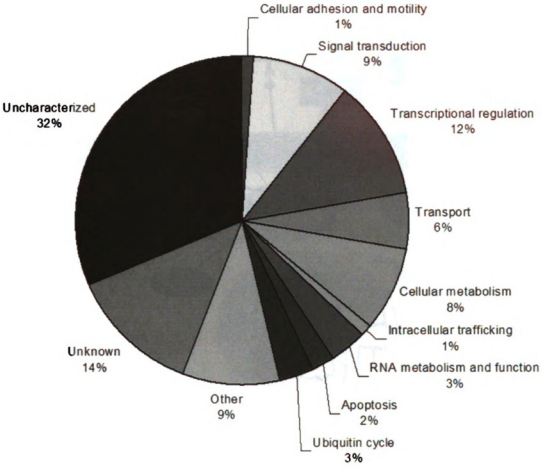


Figure 1.13 Functional Breakdown of the Genomic Regions that Represent Unique PB-induced Regions of Altered DNA Methylation (RAMs) in B6C3F1 Mice. The genomic regions, including genes, representing unique RAMs were broken down into 12 categories, 10 of which are based on Gene Ontology (GO) functional information. For genes in the "unknown" category, no information about them exists in the literature. Regions in the "uncharacterized" category align to the mouse genome greater than 10 kilobases away from an annotated gene.

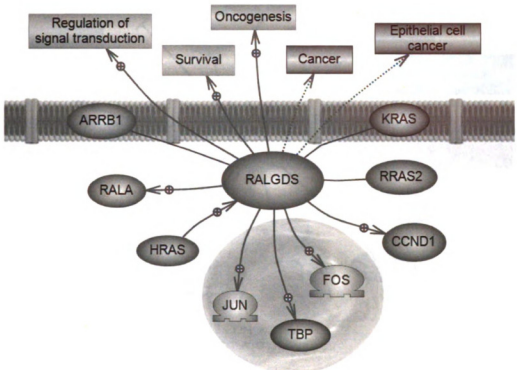


Figure 1.14 Informatic Analysis of Ral Guanine Nucleotide Dissociation Stimulator (*Ralgds*), a Potential Oncogene that is Uniquely Hypomethylated in B6C3F1 Mice at 4 Weeks of Phenobarbital (PB) Treatment. RALGDS plays a critical role in the oncogenic Ras pathway. Solid arrows indicate positive (—➔) or negative (—⊣) interactions. Dotted arrows (·····➔) indicate involvement in disease states, and lines with no arrowheads (——) indicate a direct interaction. The shapes of the entities represent a specific class of molecules to which each gene belongs: extracellular proteins (⬭) and transcription factors (⌒).

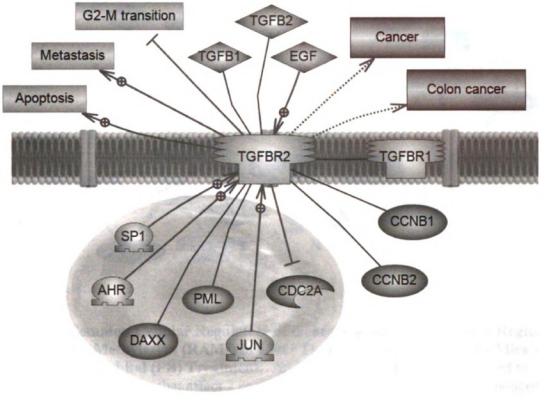


Figure 1.15 Informatic Analysis of Transforming Growth Factor Beta Receptor II (*Tgfbr2*), which is Uniquely Hypomethylated in B6C3F1 Mice at 4 Weeks of Phenobarbital (PB) Treatment. TGFBR2 plays a central role in Tgf-β signaling. Solid arrows indicate positive (—⊕➤) or negative (—⊣). Dotted arrows (.....➤) indicate involvement in disease states. Lined with no arrowheads (——) indicate a direct interaction. The shapes of the entities represent a specific class of molecules to which each gene belongs: extracellular proteins (⬭), kinases (◠), transcription factors (▯), and membrane receptors (▭).

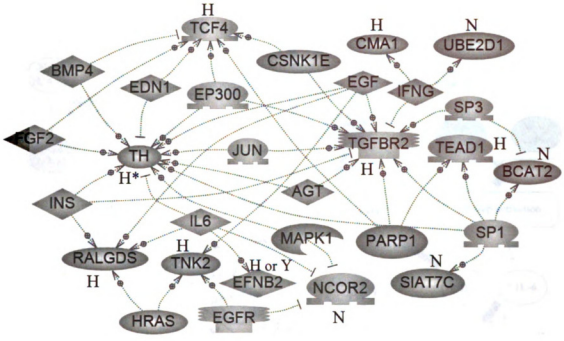


Figure 1.16 Common Cellular Regulators of Genes that Represent Unique Regions of Altered DNA Methylation (RAMs) in Liver Tumor-Susceptible B6C3F1 Mice at 4 Weeks of Phenobarbital (PB) Treatment. An informatics approach was utilized to uncover cellular regulators that affect 2 or more genes representing unique PB-induced B6C3F1 RAMs at 4 weeks. Entities that lack a H, Y, or N are common regulators. The arrows point away from the common regulator: positive (→) and negative (⊣) interactions are shown. The methylation status of a unique RAM is indicated by H (hypomethylation), Y (hypermethylation) or N (new methylation). A combination of letters (e.g., H and Y) denotes a RAM with an ambiguous methylation status at 4 weeks. An asterisk (*) represents a RAM that carried forward (i.e. it was observed at both 2 and 4 weeks). The shapes of the entities represent a specific class of molecules to which each gene belongs: extracellular proteins or nuclear receptors ( ), ligands ( ), kinases ( ), transcription factors ( ), and membrane receptor ( ).

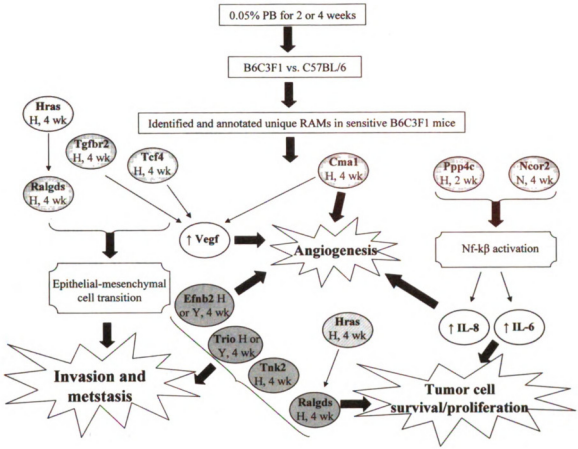


Figure 1.17 The Possible Functional Significance, Regarding Tumorigenesis, of Selected Genes which Exhibited Altered Methylation Uniquely in the B6C3F1 Mouse Following Treatment with Phenobarbital (PB). The current study identified regions of altered DNA methylation (RAMs) at 2 or 4 weeks of 0.05% PB treatment and annotated 51 genes that represent these regions. Several of these genes are well-documented as playing critical roles in tumorigenesis (dark gray ovals). Unique PB-induced hypomethylation and decreased expression of Ha-*ras* (light gray oval) in B6C3F1 mice has been demonstrated (Bachman *et al.*, 2006b). The appropriate time point of PB treatment is denoted (2 or 4 wk), and the methylation statuses of the RAMs are indicated by H (hypomethylation), Y (hypermethylation) or N (new methylation). RAMs with an ambiguous methylation status are indicated by the presence of 2 letters (i.e. H or Y). Interleukin 6 (IL-6) is a common 4 week regulator, and interleukin 8 (IL-8) and vascular endothelial growth factor (VEGF) are common 4 week targets, of multiple genes identified from unique RAMs in the liver tumor-susceptible B6C3F1 mice (white ovals). RALGDS is a key downstream effector of HRAS. The numbers correspond to selected literature references, listed in Appendix References 2, for the relationships depicted in this figure.

REFERENCES 1: Literature References for the Genes Representing Unique B6C3F1 Regions of Altered DNA Methylation (RAMs), for Normal Functions and Possible Roles in Tumorigenesis. The number of the reference corresponds to the number in parentheses proceeding the normal function or possible role in tumorigenesis as noted in Table 1.

1) Cohen, P. T., Philp, A., and Vázquez-Martin, C. (2005) Protein phosphatase 4--from obscurity to vital functions. *FEBS Lett.* **579**, 3278-3286.

2) Szaszi, K., Paulsen, A., Szabo, E. Z., Numata, M., Grinstein, S., and Orlowski, J. (2002) Clathrin-mediated endocytosis and recycling of the neuron-specific Na+/H+ exchanger NHE5 isoform: regulation by phosphatidylinositol 3'-kinase and the actin cytoskeleton. *J. Biol. Chem.* **277**, 42623-42632.

3) Rajendran, R. R., Nye, A. C., Frasor, J., Balsara, R. D., Martini, P. G., and Katzenellenbogen, B. S. (2003) Regulation of nuclear receptor transcriptional activity by a novel DEAD box RNA helicase (DP97). *J. Biol. Chem.* **278**, 4628-4638.

4) Davis, D. B., Doherty, K. R., Delmonte, A. J., and McNally, E. M. (2002) Calcium-sensitive phospholipid binding properties of normal and mutant ferlin C2 domains. *J. Biol. Chem.* **277**, 22883-22888.

5) Swanson, D. J., Zellmer, E., and Lewis, E. J. (1998) AP1 proteins mediate the cAMP response of the dopamine β-hydroxylase gene. *J. Biol. Chem.* **273**, 24065-24074.

6) Nakamura, N., Toba, S., Hirai, M., Morishita, S., Mikami, T., Konishi, M., Itoh, N., and Kurosaka, A. (2005) Cloning and expression of a brain-specific putative UDP-GalNAc: polypeptide N-acetylgalactosaminyltransferase gene. *Biol. Pharm. Bull.* **28**, 429-433.

7) Lesage, F., Terrenoire, C., Romey, G., and Lazdunski, M.J. (2000) Human TREK2, a 2P domain mechano-sensitive K+ channel with multiple regulations by polyunsaturated fatty acids, lysophospholipids, and Gs, Gi, and Gq protein-coupled receptors. *J. Biol. Chem.* **275**, 28398-28405.

8) Williger, B. T., Provost, J. J., Ho, W. T., Milstine, J., and Exton, J. H. (1999) Arfaptin 1 forms a complex with ADP-ribosylation factor and inhibits phospholipase D. *FEBS Lett.* **454**, 85-89.

9) Park KH, Choi SE, Eom M, Kang Y. (2005) Downregulation of the anaphase-promoting complex (APC)7 in invasive ductal carcinomas of the breast and its clinicopathologic relationships. *Breast Cancer Res.* **7**, R238-247.

10) Yokoyama, K., Su, I. H., Tezuka, T., Yasuda, T., Mikoshiba, K., Tarakhovsky, A., and Yamamoto, T. (2002) BANK regulates BCR-induced calcium mobilization by promoting tyrosine phosphorylation of IP_3 receptor. *EMBO J.* **21**, 83-92.

11) Shiota, N., Jin, D., Takai, S., Kawamura, T., Koyama, M., Nakamura, N., and Miyazaki, M. (1997) Chymase is activated in the hamster heart following ventricular fibrosis during the chronic stage of hypertension. *FEBS Lett.* **406**, 301-304.

12) Significance of vascular endothelial cell growth factor up-regulation mediated via a chymase-angiotensin-dependent pathway during angiogenesis in hamster sponge granulomas. *J. Pharmacol. Exp. Ther.* **302**, 949-56.

13) Gingras, H., Cases, O., Krasilnikova, M., Bérubé, G., and Nepveu, A. (2005) Biochemical characterization of the mammalian Cux2 protein. *Gene.* **344**, 273-285.

14) Wu, G., Lyapina, S., Das, I., Li, J., Gurney, M., Pauley, A., Chui, I., Deshaies R. J., and Kitajewski, J. (2001) SEL-10 is an inhibitor of notch signaling that targets notch for ubiquitin-mediated protein degradation. *Mol Cell Biol.* **21**, 7403-7415.

15) Akhoondi, S., Sun, D., von der Lehr, N., Apostolidou, S., Klotz, K., Maljukova, A., Cepeda, D., Fiegl, H., Dofou, D., Marth, C., Mueller-Holzner, E., Corcoran, M., Dagnell, M., Nejad, S. Z., Nayer, B. N., Zali, M. R., Hansson, J., Egyhazi, S., Petersson, F., Sangfelt, P., Nordgren, H., Grander, D., Reed, S. I., Widschwendter, M., Sangfelt, O., and Spruck, C. (2007) *FBXW7/hCDC4* is a general tumor suppressor in human cancer. *Cancer Res.* **67**, 9006-9012.

16) Nishino, J., Yamashita, K., Hashiguchi, H., Fujii, H., Shimazaki, T., and Hamada, H. (2004) Meteorin: a secreted protein that regulates glial cell differentiation and promotes axonal extension. *EMBO J.* **5**, 1998-2008.

17) Bagutti, C., Forro, G., Ferralli, J., Rubin, B., and Chiquet-Ehrismann, R. (2003) The intracellular domain of teneurin-2 has a nuclear function and represses zic-1-mediated transcription. *J. Cell Sci.* **116 (Pt 14)**, 2957-2966.

18) Ward,Y., Wang, W., Woodhouse, E., Linnoila, I., Liotta, L., and Kelly, K. (2001) Signal pathways which promote invasion and metastasis: critical and distinct contributions of extracellular signal-regulated kinase and Ral-specific guanine exchange factor pathways. *Mol. Cell Biol.* 21, 5958-5969.

19) Taniguchi, M., Masuda, T., Fukaya, M., Kataoka, H., Mishina, M., Yaginuma, H., Watanabe, M., and Shimizu, T. (2005) Identification and characterization of a novel member of murine semaphorin family. *Genes Cells.* **10**, 785-792.

20) Huang, G. N., Zeng, W., Kim, J. Y., Yuan, J. P., Han, L., Muallem, S., and Worley, P. F. (2006) STIM1 carboxyl-terminus activates native SOC, I_{crac} and TRPC1 channels. *Nat. Cell Biol.* **8**, 1003-1010.

21) Manji, S. S., Parker, N. J., Williams, R. T., van Stekelenburg, L., Pearson, R. B., Dziadek, M., and Smith, P. J. (2000) STIM1: a novel phosphoprotein located at the cell surface. *Biochim Biophys Acta.* **1481**, 147-155.

22) Chen, Z., Friedrich, G. A., and Soriano, P. (1994) Transcriptional enhancer factor 1 disruption by a retroviral gene trap leads to heart defects and embryonic lethality in mice. *Genes Dev.* **8,** 2293-2301.

23) Mathew, S., Murty, V. V., Cheifetz, S., George, D., Massagué, J., and Chaganti, R. S. (1994) Transforming growth factor receptor gene *TGFBR2* maps to human chromosome band 3p22. *Genomics.* **20,** 114-115.

24) Roberts, A. B., and Lalage, M. Wakefield. (2003). The two faces of transforming growth factor β in carcinogenesis. *PNAS* **100**, 8621-8623

25) Edgar A. J. (2005) Mice have a transcribed L-threonine aldolase/GLY1 gene, but the human GLY1 gene is a non-processed pseudogene. *BMC Genomics.* **6**, 32.

26) Ahmed, I., Calle, Y., Sayed, M. A., Kamal, J. M., Rengaswamy, P., Manser, E., Meiners, S., and Nur-E-Kamal, A. (2004) Cdc42-dependent nuclear translocation of non-receptor tyrosine kinase, ACK. *Biochem. Biophys. Res. Commun.* **314**, 571-9.

27) van der Horst, E. H., Degenhardt, Y. Y., Strelow, A., Slavin, A., Chinn, L., Orf, J., Rong, M., Li, S., See, L. H., Nguyen, K. Q., Hoey, T., Wesche, H., and Powers, S. (2005) Metastatic properties and genomic amplification of the tyrosine kinase gene *ACK1*. *Proc. Natl. Acad. Sci. U S A.* **102**, 15901-15906.

28) Grimm, C., Kraft, R., Sauerbruch, S., Schultz, G., and Harteneck, C. (2003) Molecular and functional characterization of the melastatin-related cation channel TRPM3. *J. Biol. Chem.* **278**, 21493-21501.

29) Kee, H. J., Ahn, K. Y., Choi, K. C., Won Song, J., Heo, T., Jung, S., Kim, J. K., Bae, C. S., and Kim, K. K. (2004) Expression of brain-specific angiogenesis inhibitor 3 (BAI3) in normal brain and implications for BAI3 in ischemia-induced brain angiogenesis and malignant glioma. *FEBS Lett.* **569**, 307-316.

30) Cowell, J. K., LaDuca, J., Rossi, M. R., Burkhardt, T., Nowak, N. J., and Matsui, S. (2005) Molecular characterization of the t(3;9) associated with immortalization in the MCF10A cell line. *Cancer Genet. Cytogenet.* **163**, 23-29.

31) She, P., Reid, T. M., Bronson, S. K., Vary, T. C., Hajnal, A., Lynch, C. J., and Hutson, S. M. (2007) Disruption of BCATm in mice leads to increased energy expenditure associated with the activation of a futile protein turnover cycle. *Cell Metab.* **6**, 181-194.

32) Kataoka, T., Holler, N., Micheau, O., Martinon, F., Tinel, A., Hofmann, K., and Tschopp, J. (2001) Bcl-rambo, a novel Bcl-2 homologue that induces apoptosis via its unique C-terminal extension. *J. Biol. Chem.* **276**, 19548-19554.

33) Holleman, A., den Boer, M. L., de Menezes, R. X., Cheok, M. H., Cheng, C., Kazemier, K. M., Janka-Schaub, G. E., Göbel, U., Graubner, U. B., Evans, W. E., and Pieters, R. (2006) The expression of 70 apoptosis genes in relation to lineage, genetic subtype, cellular drug resistance, and outcome in childhood acute lymphoblastic leukemia. *Blood* **107**, 769-776

34) Takeuchi, M., Hata, Y., Hirao, K., Toyoda, A., Irie, M., and Takai, Y. (1997) SAPAPs: a family of PSD-95/SAP90-associated proteins localized at postsynaptic density. *J. Biol. Chem.* **272,** 11943-11951.

35) Hu, X., and Lazar, M. A. (2000) Transcriptional repression by nuclear hormone receptors. *Trends Endocrinol. Metab.* **11**, 6-10.

36) Mangelsdorf, D. J., and Evans R. M. (1995) The RXR heterodimers and orphan receptors. *Cell* **83**, 841-850.

37a) Alfaro, J. M., Fraile, B., Lobo, M. V., Royuela, M., Paniagua, R., and Arenas, M. I. (2003) Immunohistochemical detection of the retinoid X receptors α, β, and γ in human prostate. *J. Androl.* **24**, 113-119.

37b) Brabender, J., Danenberg, K. D., Metzger, R., Schneider, P. M., Lord, R. V., Groshen, S., Tsao-Wei, D. D., Park, J., Salonga, D., Hölscher, A. H., and Danenberg, P. V. (2002) The role of retinoid X receptor messenger RNA expression in curatively resected non-small cell lung cancer. *Clin. Cancer Res.* **8**, 438-443.

38) Sjoberg, E. R., Kitagawa, H., Glushka, J., van Halbeek, H., and Paulson, J. C. (1996) Molecular cloning of a developmentally regulated N-acetylgalactosamine alpha2,6-sialyltransferase specific for sialylated glycoconjugates. *J. Biol. Chem.* **271**, 7450-7459.

39) Entrez Gene; search term "Tmem104."

40) Chen, W., Li, N., Chen, T., Han, Y., Li, C., Wang, Y., He, W., Zhang, L., Wan, T., and Cao, X. (2005) The lysosome-associated apoptosis-inducing protein containing the pleckstrin homology (PH) and FYVE domains (LAPF), representative of a novel family of PH and FYVE domain-containing proteins, induces caspase-independent apoptosis via the lysosomal-mitochondrial pathway. *J. Biol. Chem.* **280**, 40985-40995.

41) Tissir, F., and Goffinet, A. M. (2006) Expression of planar cell polarity genes during development of the mouse CNS. *Eur. J. Neurosci.* **23**, 597-607.

42) Katoh, M., and Katoh, M. (2003) Identification and characterization of human *PRICKLE1* and *PRICKLE2* genes as well as mouse *Prickle1* and *Prickle2* genes homologous to Drosophila tissue polarity gene prickle. *Int. J. Mol. Med.* **11**, 249-256.

43) Seidensticker, M. J., and Behrens. J. (2000) Biochemical interactions in the wnt pathway. *Biochim. Biophys. Acta.* **1495**, 168-182.

44a) Zhao, D. H., Hong, J. J., Guo, S. Y., Yang, R. L., Yuan, J., Wen, C. Y., Zhou, K. Y., and Li, C. J. (2004) Aberrant expression and function of TCF4 in the proliferation of hepatocellular carcinoma cell line BEL-7402. *Cell Res.* **14**, 74-80.

44b) Li, C. Y., Wang, Y., Cui, Z. S., and Wang, E. H. (2005) Expression of T cell factor-4 in non-small-cell lung cancer. *Chin. Med. J. (Engl).* **118**, 136-140.

45) Scheffner, M., Huibregtse, J. M., and Howley, P. M. (1994) Identification of a human ubiquitin-conjugating enzyme that mediates the E6-AP-dependent ubiquitination of p53. *Proc. Natl. Acad. Sci. U S A.* **91**, 8797-8801.

46) Scheffner, M., Huibregtse, J. M., and Howley, P. M. (1994) Identification of a human ubiquitin-conjugating enzyme that mediates the E6-AP-dependent ubiquitination of p53. *Proc. Natl. Acad. Sci. U S A.* **91**, 8797-8801.

47) Köhle, C., and Bock, K. W. (2007) Coordinate regulation of Phase I and II xenobiotic metabolisms by the Ah receptor and Nrf2. *Biochem Pharmacol.* **73**, 1853-1862.

48) Tanaka, M., Yamasaki, N., and Izumo, S. (2000) Phenotypic characterization of the murine Nkx2.6 homeobox gene by gene targeting. *Mol. Cell Biol.* **20**, 2874-2879.

49) Entrez Gene; search term "Zscan22."

50) Mitchell, C. A., Speed, C. J., Nicholl, J., and Sutherland, G. R. (1996) Chromosomal mapping of the gene (INPP5A) encoding the 43-kDa membrane-associated inositol polyphosphate 5-phosphatase to 10q26.3 by fluorescence *in situ* hybridization. *Genomics* **31**, 139-140.

51) Speed, C. J., Little, P. J., Hayman, J. A., and Mitchell, C. A. (1996) Underexpression of the 43 kDa inositol polyphosphate 5-phosphatase is associated with cellular transformation. *EMBO J.* **15**, 4852-4861.

52) Motiwala, T., Kutay, H., Ghoshal, K., Bai, S., Seimiya, H., Tsuruo, T., Suster, S., Morrison, C., and Jacob, S. T. (2004) Protein tyrosine phosphatase receptor-type O (PTPRO) exhibits characteristics of a candidate tumor suppressor in human lung cancer. *Proc. Natl. Acad. Sci. U S A.* **101**, 13844-13849.

53a) Maekawa, H., Oike, Y., Kanda, S., Ito, Y., Yamada, Y., Kurihara, H., Nagai, R., and Suda, T. (2003) Ephrin-B2 induces migration of endothelial cells through the

phosphatidylinositol-3 kinase pathway and promotes angiogenesis in adult vasculature. *Arterioscler. Thromb. Vasc. Biol.* **23**, 2008-2014.

53b) Gale, N. W., Holland, S. J., Valenzuela, D. M., Flenniken, A., Pan, L., Ryan, T. E., Henkemeyer, M., Strebhardt, K., Hirai, H., Wilkinson, D. G., Pawson, T., Davis, S., and Yancopoulos, G. D. (1996) Eph receptors and ligands comprise two major specificity subclasses and are reciprocally compartmentalized during embryogenesis. *Neuron* **17**, 9-19.

53c) Nakada, M., Niska, J. A., Miyamori, H., McDonough, W. S., Wu, J., Sato, H., and Berens, M. E. (2004) The phosphorylation of EphB2 receptor regulates migration and invasion of human glioma cells. *Cancer Res.* **9**, 3179-3185.

54) Seipel, K., Medley, Q. G., Kedersha, N. L., Zhang, X. A., O'Brien, S. P., Serra-Pages, C., Hemler, M. E., and Streuli, M. (1999) Trio amino-terminal guanine nucleotide exchange factor domain expression promotes actin cytoskeleton reorganization, cell migration and anchorage-independent cell growth. *J. Cell Sci.* **112** (Pt 12):1825-1834.

55) Yoshizuka, N., Moriuchi, R., Mori, T., Yamada, K., Hasegawa, S., Maeda, T., Shimada, T., Yamada, Y., Kamihira, S., Tomonaga, M., and Katamine, S. (2004) An alternative transcript derived from the *Trio* locus encodes a guanosine nucleotide exchange factor with mouse cell-transforming potential. *J. Biol. Chem.* **279**, 43998-44004.

REFERENCES 2: Selected Literature References for the Relationships Depicted in Figure 4. The numbered references correspond to the red numbered relationships noted in Appendix Figure 10.

1) Roberts, A. B., and Wakefield, L. M. (2003) The two faces of transforming growth factor β in carcinogenesis. *Proc. Natl. Acad. Sci U S A* **100**, 8621-8623.

2) Oft, M., Peli, J., Rudaz, C., Schwarz, H., Beug, H., and Reichmann, E. (1996) TGF-beta1 and Ha-Ras collaborate in modulating the phenotypic plasticity and invasiveness of epithelial tumor cells. *Genes Dev.* **10**, 2462-2477.

3) Kang, Y., and Massagué, J. (2004) Epithelial-mesenchymal transitions: Twist in development and metastasis. *Cell* **118**, 277-279.

4) Wolthuis, R. M., and Bos, J. L. (1999) Ras caught in another affair: the exchange factors for Ral. *Curr. Opin. Genet. Dev.* **9**, 112-117.

5) Thiery, J. P. (2002). Epithelial-mesenchymal transitions in tumour progression. *Nat. Rev. Cancer* **2**, 442-454.

6) Gilles, C., Polette, M., Mestdagt, M., Nawrocki-Raby, B., Ruggeri, P., Birembaut, P., and Foidart, J. M. (2003) Transactivation of vimentin by β-catenin in human breast cancer cells. *Cancer Res.* **63**, 2658-2664.

7) Zhang, X., Gaspard, J. P., and Chung, D. C. (2001) Regulation of vascular endothelial growth factor by the Wnt and K-ras pathways in colonic neoplasia. *Cancer Res.* 61, 6050-4.

8) Saadeh, P. B., Mehrara B. J., Steinbrech D. S., Spector J. A., Greenwald, J. A., Chin, G. S., Ueno, H., Gittes, G. K., and Longaker M. T. (2000) Mechanisms of fibroblast growth factor-2 modulation of vascular endothelial growth factor expression by osteoblastic cells. *Endocrinology* **141**, 2075-2083.

9) Katada, J., Muramatsu, M., Hayashi, I., Tsutsumi, M., Konishi, Y., and Majima, M. (2002) Significance of vascular endothelial cell growth factor up-regulation mediated via a chymase-angiotensin-dependent pathway during angiogenesis in hamster sponge granulomas. *J. Pharmacol. Exp. Ther.* **302**, 949-956.

10) Muramatsu, M., Katada, J., Hayashi, I., and Majima, M. (2000) Chymase as a proangiogenic factor: a possible involvement of chymase-angiotensin-dependent pathway in the hamster sponge angiogenesis model. *J. Biol. Chem.* **8**, 5545-5552.

11) Ferrara, N. (2002) VEGF and the quest for tumour angiogenesis factors. *Nat. Rev. Cancer*. **2**, 795-803.

12) Maekawa, H., Oike, Y., Kanda, S., Ito, Y., Yamada, Y., Kurihara, H., Nagai, R., and Suda, T. (2003) Ephrin-B2 induces migration of endothelial cells through the phosphatidylinositol-3 kinase pathway and promotes angiogenesis in adult vasculature. *Arterioscler. Thromb. Vasc. Biol.* **23**, 2008-2014.

13) Gale, N. W., Holland, S. J., Valenzuela, D. M., Flenniken, A., Pan, L., Ryan, T. E., Henkemeyer, M., Strebhardt, K., Hirai, H., Wilkinson, D. G., Pawson, T., Davis, S., and Yancopoulos, G. D. (1996) Eph receptors and ligands comprise two major specificity subclasses and are reciprocally compartmentalized during embryogenesis. *Neuron* **17**, 9-19.

14) Nakada, M., Niska, J. A., Miyamori, H., McDonough, W. S., Wu, J., Sato, H., and Berens, M. E. (2004) The phosphorylation of EphB2 receptor regulates migration and invasion of human glioma cells. *Cancer Res.* **9**, 3179-3185.

15) Yoshizuka, N., Moriuchi, R., Mori, T., Yamada, K., Hasegawa, S., Maeda, T., Shimada, T., Yamada, Y., Kamihira, S., Tomonaga, M., and Katamine, S. (2004) An alternative transcript derived from the *Trio* locus encodes a guanosine nucleotide exchange factor with mouse cell-transforming potential. *J. Biol. Chem.* **279**, 43998-44004.

16) van der Horst, E. H., Degenhardt, Y. Y., Strelow, A., Slavin, A., Chinn, L., Orf, J., Rong, M., Li, S., See, L. H., Nguyen, K. Q., Hoey, T., Wesche, H., and Powers, S. (2005) Metastatic properties and genomic amplification of the tyrosine kinase gene *ACK1*. *Proc. Natl. Acad. Sci. USA.* **102**, 15901-15906.

17) Ward,Y., Wang, W., Woodhouse, E., Linnoila, I., Liotta, L., and Kelly, K. (2001) Signal pathways which promote invasion and metastasis: critical and distinct contributions of extracellular signal-regulated kinase and Ral-specific guanine exchange factor pathways. *Mol. Cell Biol.* 21, 5958-5969.

18) González-García, A., Pritchard, C. A., Paterson, H. F., Mavria, G., Stamp, G., and Marshall, C. J. (2005) RalGDS is required for tumor formation in a model of skin carcinogenesis. *Cancer Cell.* **7**, 219-226.

19) Hu, C.-T. M., Tang-Oxley, Q., Qiu, W. R., Wang, Y.-P., Mihindukulasuriya, K. A., Afshar, R., and Tan, T.-H. (1998) Protein phosphatase X interacts with c-rel and stimulates c-rel/nuclear factor κB activity. *J. Biol. Chem.* **273**, 33561-33565.

20) Lee, S. K., Kim, J. H., Lee, Y. C., Cheong, J., and Lee, J. W. (2000) Silencing mediator of retinoic acid and thyroid hormone receptors, as a novel transcriptional corepressor molecule of activating protein-1, nuclear factor-κB, and serum response factor. *J. Biol. Chem.* **275**, 12470-12474.

21) Karashima, T., Sweeney, P., Kamat, A., Huang, S., Kim, S. J., Bar-Eli, M., McConkey, D. J., and Dinney, C. P. (2003) Nuclear factor-κB mediates angiogenesis

and metastasis of human bladder cancer through the regulation of interleukin-8. *Clin. Cancer Res.* **9**, 2786-2797.

22) Lawrence, T., Hageman, T., and Balkwill, F. (2007) Sex, cytokines, and cancer. *Science* 317, 51-52.

CHAPTER 2

PHENOBARBITAL (PB) ELICITS UNIQUE, EARLY CHANGES IN THE EXPRESSION OF HEPATIC GENES THAT AFFECT CRITICAL PATHWAYS IN TUMOR-PRONE B6C3F1 MICE

This chapter represents a manuscript that is in press for publication (as of March 2009) in *Toxicological Sciences*. The authors are Jennifer M. Phillips, Lyle D. Burgoon, and Jay I. Goodman.

ABSTRACT

At 2 and 4 weeks following treatment with Phenobarbital (PB), the classical nongenotoxic rodent liver carcinogen, we elucidated unique gene expression changes (both induction and repression) in liver tumor-susceptible B6C3F1 mice, as compared to the relatively resistant C57BL/6. Based on their cancer-related roles, we believe that altered expression of at least some of these genes might underlie PB-induced liver tumorigenesis. Putative constitutive active/androstane (CAR) response elements (CAREs), a subset of PB response elements, were present within multiple genes whose expression was uniquely altered in the B6C3F1 mice, suggesting a role for CAR in their regulation. Additionally, 3 DNA methyltransferase genes (*Dnmt1*, *Dnmt3a*, and *Dnmt3b*) were repressed uniquely in the tumor-prone B6C3F1 mice, and all possess putative CAREs, providing a potential direct link between PB and expression of key genes that regulate DNA methylation status.

Previously, we demonstrated that PB elicited unique regions of altered methylation (RAMs) in B6C3F1 mice, as compared to the relatively resistant C57BL/6, at 2 and 4 weeks (Bachman *et al.*, 2006), and annotation of the regions harboring these changes revealed 51 genes (Phillips and Goodman, 2008). This is extended by the current study, which employed RNA isolated from the same liver tissue used in the earlier investigations. Genes elucidated from both the methylation and expression analyses are involved in identical processes/pathways (e.g., cell cycle, apoptosis, angiogenesis, epithelial-mesenchymal cell transition (EMT), invasion/metastasis, and mitogen-activated protein kinase (MAPK), transforming growth factor-beta (TGF-β), and Wnt signaling). Therefore, these changes might represent very early events that directly

contribute to PB-induced tumorigenesis. It is instructive to consider the possibility that, in a hypothesis-driven fashion, these genes are initial candidates that could be utilized to develop a biomarker "fingerprint" of early exposure to PB and PB-like compounds.

INTRODUCTION

The accumulation of key heritable modifications, including epigenetic alterations, e.g., changes in DNA methylation (Esteller, 2007) which can play a variety of roles in carcinogenesis (Counts and Goodman, 1995) and be involved in the initiation as well as promotion stages (Goodman and Watson, 2002), as well as mutations (Loeb and Harris, 2008), drives the progressive clonal expansions of cells during tumorigenesis (Feinberg, 2006; Hanahan and Weinberg, 2000). While genotoxic carcinogens can interact directly with DNA to form promutagenic adducts, nongenotoxic compounds cause tumorigenesis by other mechanisms, including inflammation, immunosuppression, receptor activation, and epigenetic changes (Luch, 2005). Phenobarbital (PB) is the classical nongenotoxic rodent liver carcinogen (Whysner *et al.*, 1996), and upon treatment with a promoting dose in drinking water (0.05%, (w/w)) for 12 months, 100% of susceptible C3H/He and B6C3F1 (C3H/He x C57BL/6) mice develop liver tumors, while the relatively resistant C57BL/6 mice develop none after 18 months (Becker, 1982).

The mechanism(s) of action of PB remain to be completely elucidated; however, some details have emerged. Connexin32, the major hepatic gap junction-forming protein, is essential for PB-induced liver tumorigenesis (Moennikes *et al.*, 2000), and moreover, PB inhibits gap junction intercellular communication in hepatocytes from sensitive B6C3F1 mice but not the relatively resistant C57BL/6 (Warner *et al.*, 2003). Furthermore, multiple events appear to be linked to PB-associated mouse liver tumorigenesis: mutations in β-catenin (Aydinlik *et al.*, 2001), Ha-*ras* hypomethylation (Vorce and Goodman, 1991), increased Ha-*ras* expression (Counts *et al.*, 1997), Ki-*ras* hypomethylation (Vorce and Goodman, 1991), hypomethylation and increased

expression of *raf* (Ray *et al.*, 1994), and amplification of *c-myc* (Vorce and Goodman, 1991).

Changes in DNA methylation have been implicated in the ability of PB to promote tumorigenesis. PB treatment resulted in higher levels of regional hypermethylation in 2 tumor-prone groups (C3H/He >> B6C3F1) v. the relatively resistant C57BL/6 (Watson and Goodman, 2002), as well as a greater decrease in global methylation levels in B6C3F1 v. C57BL/6 mice (Counts *et al.*, 1996). Furthermore, PB-elicited unique regions of altered DNA methylation (RAMs), representing both increases and decreases in methylation levels, were discerned in B6C3F1 v. C57BL/6 mice at 2- and 4-weeks (Bachman *et al.*, 2006). Cloning and annotation of these RAMs resulted in the identification of 51 genes, many of which participate in cancer-related processes, whose methylation statuses were altered uniquely in the susceptible mice (Phillips and Goodman, 2008). These data support the notion that the mechanism of action of PB involves alteration of DNA methylation in key genes which can facilitate tumor formation.

The constitutive active/androstane receptor (CAR) mediates the actions of PB, including induction of xenobiotic-metabolizing enzymes and hepatomegaly (Wei *et al.*, 2000). Microarray analysis of CAR wildtype (WT) and knockout (KO) mice revealed CAR-dependent regulation of approximately half of the 138 gene expression changes (out of 8,736 total genes/ESTs) that PB elicited (Ueda *et al.*, 2002). Therefore, not all of the effects of PB are CAR-dependent. Chronic PB treatment culminates in liver tumor development (Huang *et al.*, 2005) and importantly, CAR is necessary for tumor promotion by PB in diethylnitrosamine (DEN)-initiated C3H/He mice (Yamamoto *et al.*,

2004). Phillips *et al.* (2007) discerned PB-induced unique DNA methylation changes in liver tumor-susceptible CAR WT (both precancerous and liver tumor tissue), as compared to PB-treated resistant CAR KO mice. Annotation of these unique RAMs uncovered multiple genes that conceivably function in cancer-related processes, raising the possibility that at least some of the CAR-mediated alterations in DNA methylation contribute to PB-induced hepatocarcinogenesis (Phillips and Goodman, 2009).

We hypothesized that at least some of the changes in hepatic gene expression that occur uniquely in liver tumor-susceptible B6C3F1 mice v. the relatively resistant C57BL/6, following both 2 and 4 weeks of PB treatment, contribute directly to liver tumorigenesis. In the current study, both microarray and quantitative real-time PCR (qRT-PCR) analyses were utilized to discern the aforementioned unique expression changes, including those of a subset of genes identified from unique PB-induced RAMs in the susceptible B6C3F1 mice (Phillips and Goodman, 2008), plus 3 DNA methyltransferase (Dnmt) genes, at very early time points (i.e. 2 and 4 weeks). Additionally, CAR response elements (CAREs), which are a subset of PB response elements, were located within multiple genes that exhibited unique B6C3F1 expression and/or methylation changes in response to PB. Furthermore, we ascertained signaling pathways and processes that the distinctively affected genes might influence. Overall, these results provide support for the notion that at least some of the genes whose expression was uniquely altered in susceptible B6C3F1 mice, as compared to the relatively resistant C57BL/6, might be mechanistically crucial for tumor development, thus enhancing our understanding of how PB promotes hepatocarcinogenesis.

MATERIALS AND METHODS

Animals, Treatments and Tissue Samples

As described previously, animals were treated, liver tissue was harvested, and RNA was isolated (Bachman *et al.*, 2006). Briefly, B6C3F1 (C57BL/6 x C3H/He) and C57BL/6 mice (ages 29-32 days) were administered PB in drinking water at a concentration of 0.05% (w/w), a dose which will cause liver tumors in 100% of the tumor-prone B6C3F1 mice within 12 months, while no liver tumors are observed in the relatively resistant C57BL/6 mice after 18 months of treatment (Becker, 1982), for 2 or 4 weeks. Liver tissue was harvested from a total of 8 groups (n = 6 per group): B6C3F1, 2- and 4-week, control and PB-treated, and C57BL/6, 2- and 4-week, control and PB-treated. RNA was isolated from samples of the same livers employed in our earlier study aimed at identifying PB-induced RAMs (Bachman *et al.*, 2006), and stored at -80°C until its use in the current study.

RNA Preparation

Upon removal from -80°C, RNA samples were purified with the Qiagen RNeasy Mini Kit (Qiagen, Valencia, CA) according to the manufacturer's protocol. Samples were eluted in diethyl pyrocarbonate (DEPC)-treated water, and RNA integrity was evaluated on the Agilent 2100 Bioanalyzer using 5 ng sample aliquots and the RNA 6000 Pico Lab-on-a-Chip (Agilent Technologies, Santa Clara, CA). The presence of 2 distinct peaks, representing 18S and 28S rRNA levels, were indicative of high quality samples. The purity (A260/A280 ratios) and concentrations of the RNA samples were determined via the NanoDrop™ 8000 spectrophotometer (Thermo Scientific, Wilmington, DE).

Microarray Analysis

All procedures were performed according to standard protocols found within the Affymetrix Genechip® Expression Analysis Technical Manual (Affymetrix, Santa Clara, CA).

RNA Labeling and Fragmentation

The One-Cycle Target Labeling and Control Reagent kit (Affymetrix, Santa Clara, CA) was utilized for first- and second- strand cDNA synthesis plus double-stranded cDNA sample cleanup, and synthesis plus cleanup of biotin-labeled cRNA, of 48 samples (n = 6, for 8 groups). To start, 1 μg of total RNA was used for the generation of double-stranded cDNA, which was then used as a template for the synthesis of biotinylated cRNA. The size distribution and yield of the labeled cRNA products were evaluated on the Agilent 2100 Bioanalyzer using 5 ng sample aliquots and the RNA 6000 Pico Lab-on-a-Chip (Agilent Technologies, Santa Clara, CA). Subsequently, 15 μg of labeled cRNA was fragmented to a range of 35-200 bp in a 40 μl volume reaction (40mM Tris-acetate at pH 8.1, 100mM potassium acetate, and 30mM magnesium acetate) at 94°C for 35 min. The size distribution of the fragmented cRNA was assessed on the Agilent 2100 Bioanalyzer using 5 ng sample aliquots and the RNA 6000 Pico Lab-on-a-Chip (Agilent Technologies, Santa Clara, CA).

Hybridization, Washing, Staining, and Scanning

Fifteen μg of fragmented cRNA was hybridized to a GeneChip® Mouse Genome 430 2.0 Array (Affymetrix, Santa Clara, CA), containing more than 45,000 probe sets representing over 34,000 genes. The instrumentation utilized for the washing and scanning of the chips is operated by the GeneChip® Operating Software (GCOS, Affymetrix, Santa Clara, CA), version 3.1. After hybridization cocktails were removed, arrays were washed and stained on an Affymetrix Fluidics 450 station, and subsequently scanned using the Affymetrix GeneChip® Scanner 3000 7G, in order to detect hybridization signals. From the resulting image files (DAT file), GCOS computes cell intensity data (CEL file), which is further analyzed to determine differential gene expression patterns.

Data Analysis

Data from Affymetrix GeneChip CEL files were normalized using GC Robust Multi-array Average (GCRMA) (Wu *et al.*, 2004). Boxplots and Principal Components Analysis (PCA) were employed to assess data quality. Linear models were built and contrast estimates were performed, comparing treatment to time-matched control samples, using Limma. An empirical Bayes method was used to calculate false discovery rate controlled p-values on the contrast estimates from Limma. A CDF file established by Dai *et al.* (2005), containing more accurate gene/transcript definitions (as compared to those from Affymetrix) based on up-to-date Entrez Gene information, was utilized (Mouse430, version 9.0, from (http://brainarray.mbni.med.umich.edu/Brainarray/Database/CustomCDF/CDF_download_v9.asp). Based upon these new probe set definitions, data was generated for 16,475

genes (as compared to more than 45,000 features representing over 34,000 genes, as indicated by Affymetrix). All statistical analyses were performed in R (v2.6.1) using Bioconductor (2.1).

Identification of Uniquely Active Genes in Liver Tumor-Prone B6C3F1 Mice, as Compared to the Relatively Resistant C57BL/6

Differentially expressed, i.e. active, genes in PB-treated v. control groups were identified based on meeting two criteria: 1) statistical significance, $p < 0.01$, and 2) a $\geq$ 2-fold change in expression (up- or down-regulated). Uniquely active genes in the susceptible B6C3F1 groups, as compared to the C57BL/6, were then discerned. At 2 weeks, and separately, at 4 weeks, active genes in the B6C3F1 and C57BL/6 groups were compared to one another. Common genes observed in both the B6C3F1 and C57BL/6 groups, at 2 or 4 weeks, which exhibited expression changes in the same direction (i.e. induced or repressed in both) were not given further consideration. Thus, uniquely active genes in the B6C3F1 mice, as compared to C57BL/6, at 2 or 4 weeks, included: 1) common active genes whose expression changes were opposite (e.g., induction in the B6C3F1 and repression in the C57BL/6), and 2) genes which were active only in the B6C3F1. In an analogous manner, uniquely active genes in the C57BL/6 mice, as compared to the B6C3F1, at 2 and 4 weeks, were elucidated.

Uniquely active genes in the B6C3F1 mice at 2 and 4 weeks were compared, in order to ascertain genes that were active only at 2 weeks, only at 4 weeks, and those which "carried forward," i.e., expression changed in the same direction at both 2 and 4 weeks.

Quantitative Real-time PCR (qRT-PCR) Analysis

Expression levels of 3 groups of genes were evaluated by qRT-PCR: 1) a subset of genes which were uniquely active, based on microarray analysis, in the susceptible B6C3F1 mice at 2 (all 18 genes listed in Table 2.4) and/or 4 (all 11 genes listed in Table 2.5) weeks of PB treatment; 2) a subset of genes identified from unique PB-induced RAMs in B6C3F1 mice at 2 (2 genes listed in Table 2.9) and/or 4 (17 genes listed in Table 2.9) weeks, as discerned by Phillips and Goodman (2008); and 3) 3 DNA methyltransferase (Dnmt) genes (*Dnmt1, Dnmt3a, Dnmt3b*) at 2 and 4 weeks. The genes in group 1 and 3, above, were chosen for analysis based on their interesting, potentially cancer-related, documented functions, and the possibility that they affect pertinent signaling pathways (e.g., the 3 genes from Group 3 are involved in maintaining DNA methylation patterns). The genes in Group 2 also can influence key pathways, and many were selected because they exhibited unique PB-induced RAMs in both the liver tumor-susceptible B6C3F1 and CAR WT mice (Phillips and Goodman, 2009).

Reverse Transcription of RNA

RNA, from the same samples used for microarray analysis, was treated with amplification grade DNAse I enzyme (Invitrogen, Carlsbad, CA) to eliminate contaminating genomic DNA. Each reaction, containing 1 μg of RNA, 10X DNase I Reaction Buffer, 2 U DNase I, and DEPC-treated water (Ambion Inc., Austin, TX) up to 10 μl, was incubated for 15 min. at room temperature. DNAse I was inactivated by adding 1 μl of 25 mM EDTA solution and subsequently heating the reactions for 10 min.

at 65°C. Reverse transcription reactions containing DNAse I-treated RNA were prepared with reagents from the High Capacity cDNA Reverse Transcription Kit (Applied Biosystems, Foster City, CA). Each reaction contained 1 μg RNA, 10X reverse transcription buffer, 25X dNTP mix (100 mM), 10X random primers, 50 U MultiScribe™ reverse transcriptase, and RNAse-free water, up to 20 total μl. Reactions were incubated at 25°C for 10 min., 37°C for 120 min., and 85°C for 5 s. All samples were stored at 4°C until needed.

Primers for qRT-PCR

Primers were designed using the web-based Primer3 program, v. 0.4.0 (http://frodo.wi.mit.edu/primer3/input.htm) and synthesized by the Macromolecular Structure Facility at Michigan State University. The sizes of the amplicons ranged from 100-140 bp and the primers were 20mers; all other parameters (e.g., melting temperature) remained on the default settings. The majority of primers were designed such that the amplicon spanned an intron-exon junction near the 3' end of the gene of interest. This was confirmed using GenBank sequence information, and also, in most instances, the UCSC In-Silico PCR web-based tool (July 2007 build, http://genome.ucsc.edu/cgi-bin/hgPcr?command=start). This was done so as to preclude the possibility that the expression data could be attributed to contamination with genomic DNA. Furthermore, we are attempting to not simply confirm the microarray data but are extending this to evaluate proper splicing, i.e. this represents a stringent attempt to evaluate changes in expression of functional mRNAs. Names and symbols, accession numbers, and forward and reverse primer sequences of genes chosen for qRT-PCR analysis, plus amplicon

sizes, are listed in Supplementary Tables S1A (selected genes that were uniquely active in B6C3F1 mice, based on microarray analysis) and S1B (selected genes identified from unique RAMs, plus 3 Dnmts) in the accepted manuscript.

qRT-PCR Assays

Reactions were prepared with *Power* SYBR® Green PCR Master Mix (Applied Biosystems, Foster City, CA), according to the manufacturer's protocol, with each reaction containing 1 μl of cDNA from the aforementioned reverse transcription reaction (with the exception of 18S reactions, which contained 1 μl of 1:100 diluted cDNA), 1X *Power* SYBR® Green PCR Master Mix, 0.3 μM of both the forward and reverse primers (with the exception of *Dnmt3b*, 0.1 μM) , and DEPC-treated water (Ambion Inc., Austin, TX) up to 50 μl. PCR amplification of duplicate reactions was conducted in MicroAmp™ 96-well Optical Plates (Applied Biosystems, Foster City, CA) using the Applied Biosystems 7500 Real-Time PCR System, with the following thermal cycling conditions: 50°C for 2 min., 95°C for 10 min., and 40 cycles of 95°C for 15 s plus 60°C for 1 min. A dissociation protocol was run for each primer pair to ensure that a single product formed, and agarose gel electrophoresis of amplified products was performed to verify amplicon size.

Before samples were analyzed, standard curves for each gene were generated from purified amplicons. Standard curve samples (spanning 10^2 to 10^8 copies) for a particular gene were included on the appropriate sample plate so that the absolute quantitation method, which compares the threshold cycle of an unknown sample against a standard curve with known copy numbers, could be used to determine mRNA expression

levels. The copy number of the gene of interest for each sample was standardized to that of the 18S rRNA gene to control for differences in RNA quantity, quality, and reverse transcription efficiency. Finally, fold changes in the treatment groups (v. their time-matched controls) were calculated. Statistical outliers were excluded from the final calculations following their identification by the Grubbs' test ($p < 0.05$, http://www.graphpad.com/quickcalcs/Grubbs1.cfm). Significance was determined by a Student's *t*-test ($p < 0.05$).

Changes in Gene Expression in the B6C3F1 v. C57BL/6

Unique: Based on qRT-PCR analysis, where there is a statistical difference (Student's t-test, $p < 0.05$) or the change is in an opposite direction.

Confirmed: Microarray data which are confirmed based on qRT-PCR, where the change is unique.

Apparently Confirmed: Circumstances, based on qRT-PCR analysis, where data from at least 3 of the 6 samples fell outside the 95% confidence interval (CI) of the control group data were considered an 'indication of a change' and thus, apparently confirming the microarray data.

Functional Analysis of Uniquely Active B6C3F1 Genes at 2 and 4 Weeks of PB Treatment

The Pathway Studio® 5.0 (Ariadne Genomics, Rockville, MD) informatics program was utilized to elucidate functions of uniquely active genes. Additionally, the program discerned connections between multiple genes, and linked them to key cellular

processes and pathways. The Database for Annotation, Visualization and Integrated Discovery (DAVID), version 6 (Dennis *et al.*, 2003; http://david.abcc.ncifcrf.gov/) was utilized to overlay uniquely active genes on pathways from the Kyoto Encyclopedia of Genes and Genomes (KEGG) database.

Identification of Constitutive Active/Androstane Receptor Response Elements (CAREs)

CAREs are a subset of PB-responsive elements (PBREMs) since 1) CAR-independent effects of PB have been observed (Ueda *et al.*, 2002), and thus it is presumed that other classes of cis elements modulate those effects, and 2) there might exist elements which are necessary, but not sufficient, for transcriptional regulation by CAR. Seven *bona fide* CAREs were identified from the literature (Chen *et al.*, 2003; Gerbal-Chaloin *et al.*, 2002; Goodwin *et al.*, 2002; Honkakoski *et al.*, 1998; Sueyoshi *et al.*, 1999; Sugatani *et al.*, 2001) and used to construct a position weight matrix (PWM). The criteria for *bona fide* CAREs are that the elements are functional in a reporter gene assay and have been shown to bind to CAR by either gel shift or chromatin immunoprecipitation assays. Additionally, there had to be a match between the sequences of the elements reported in the literature and the most recent build, i.e. compilation of genome sequence and annotation data at a particular point in time, of the human, mouse, or rat genome. The matrix similarity score threshold used was 0.80, i.e. the identified CAREs were at least 80% similar to the consensus cis element.

The search for putative CAREs was performed on genes from the 3 groups described above, under Quantitative Real-time PCR (qRT-PCR) Analysis.

Potential/possible regulatory regions (-10,000 bp relative to the transcription start site through the 5'-untranslated region), for the genes selected for analysis, were obtained from the UCSC genome database (http://genome.ucsc.edu). These regulatory regions were analyzed using previously described methods (Sun *et al.*, 2004).

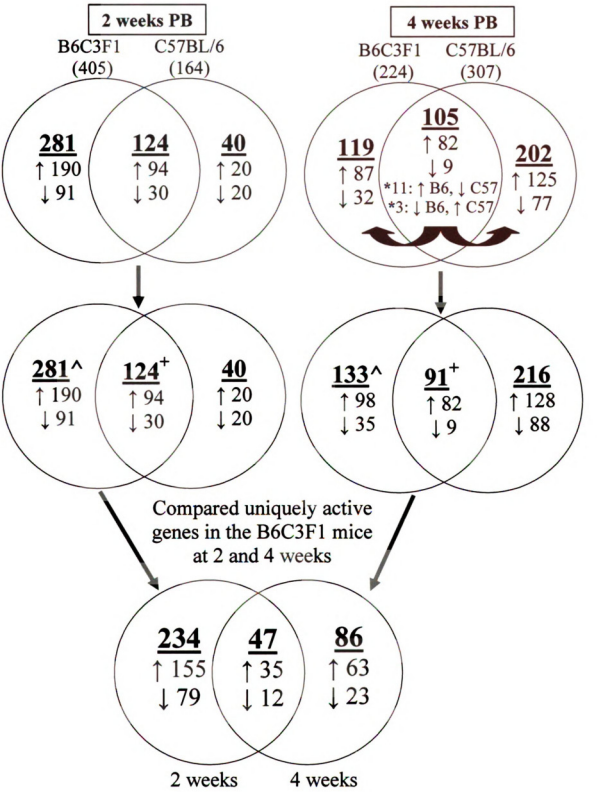
RESULTS

The complete microarray data set is provided as Supplementary Table S2 in the accepted manuscript. PCA revealed distinct differences in gene expression patterns based on treatment and mouse strain (Fig. 2.6). One animal (from the B6C3F1, 4-week PB group) was omitted from subsequent data analysis after it was deemed to be an outlier by PCA (data point not shown). Additionally, animals within a particular group (e.g., C57BL/6, 4-week PB-treated) typically exhibited similar expression patterns (Appendix Fig. 1). The microarrays (with the exception of 1 outlier) showed consistent distributions, based on box plots, which is an indication that the experiments are reproducible, while some outlying data points for each individual mouse were observed (Fig. 2.7). The aforementioned outlier (one B6C3F1, 4-week PB-treated animal) is depicted in Fig. 2.7 but was not utilized for data analysis.

Active genes in the 4 PB-treated groups, as compared to their time-matched controls, were identified (Fig. 1). Lists of the active genes represented in the Venn diagrams (Fig. 1) can be found in Supplementary Tables S3A-I in the accepted manuscript.

At 2 weeks, PB altered the expression of 405 and 164 genes in the B6C3F1 and C57BL/6 mice, respectively (Fig. 1). Comparison of these revealed 124 overlapping active genes and for all of them, the changes occurred in the same direction (i.e. 94 were induced and 30 were repressed) in both groups. These genes were not considered further. Therefore, 281 genes (190 induced and 91 repressed) were uniquely active in the B6C3F1 mice, as compared to the C57BL/6, at 2 weeks of PB treatment. Conversely, 40 genes (20 induced and 20 repressed) were uniquely active in the C57BL/6 mice v. the B6C3F1.

Figure 2.1 Identification of uniquely active genes in susceptible B6C3F1, as compared to relatively resistant C57BL/6 mice, in response to 2 or 4 weeks of phenobarbital (PB) treatment. Microarray analysis was utilized to ascertain genes whose hepatic expression was altered (↑, induced or ↓, repressed) in 4 groups of PB-treated mice, as compared to their time-matched controls. Genes were considered to be differentially expressed (i.e. active) based on meeting two criteria: 1) statistical significance, $p < 0.01$, and 2) a $\geq$ 2-fold change in expression (up- or down-regulated). First, active genes in the B6C3F1 and C57BL/6 groups were compared, at both 2 and 4 weeks. Genes that exhibited opposite changes (e.g., induced in the B6C3F1 and repressed in the C57BL/6) at a particular time point, depicted by asterisks (*), were considered to be uniquely active in each of the groups, and thus, segregated. Uniquely active genes in the B6C3F1 at 2 and 4 weeks (^) were discerned by excluding those genes at each time point which overlapped in the B6C3F1 and C57BL/6 mice (overlapping portions of Venn diagrams), and whose fold changes occurred in the same direction (i.e. induced or repressed in both groups, +). Of the 367 total uniquely active genes elicited by PB in the susceptible B6C3F1 mice, as compared to the relatively resistant C57BL/6, 234 were observed only at 2 weeks, 86 were observed only at 4 weeks, and 47 were observed at both time points of treatment.


2 weeks PB
B6C3F1 (405)
C57BL/6 (164)
281 ↑ 190 ↓ 91
124 ↑ 94 ↓ 30
40 ↑ 20 ↓ 20
4 weeks PB
B6C3F1 (224)
C57BL/6 (307)
105 ↑ 82 ↓ 9
119 ↑ 87 ↓ 32
202 ↑ 125 ↓ 77
*11: ↑ B6, ↓ C57
*3: ↓ B6, ↑ C57
281^ ↑ 190 ↓ 91
124+ ↑ 94 ↓ 30
40 ↑ 20 ↓ 20
133^ ↑ 98 ↓ 35
91+ ↑ 82 ↓ 9
216 ↑ 128 ↓ 88
Compared uniquely active genes in the B6C3F1 mice at 2 and 4 weeks
234 ↑ 155 ↓ 79
47 ↑ 35 ↓ 12
86 ↑ 63 ↓ 23
2 weeks
4 weeks

At 4 weeks, PB altered the expression of 224 and 307 genes in the B6C3F1 and C57BL/6 mice, respectively (Fig. 1). Comparison of these revealed 105 overlapping active genes, of which 91 exhibited fold changes in the same direction (i.e. 82 induced and 9 repressed) in both groups, and thus were not considered further. Additionally, 14 active genes exhibited opposite changes: 11 were induced in the B6C3F1 and repressed in the C57BL/6, while 3 were repressed in the B6C3F1 and induced in the C57BL/6. Due to their opposing expression changes, these 14 genes were considered to be uniquely active in the B6C3F1, as well as in the C57BL/6. In total, 133 genes (98 induced and 35 repressed) were uniquely active in B6C3F1 mice, as compared to the C57BL/6, at 4 weeks of PB treatment. In contrast, 216 genes (128 induced and 88 repressed), including the 14 that exhibited opposite changes, were uniquely active in the C57BL/6 mice, as compared to the B6C3F1.

The validity of the microarray data is supported by the observations that, as expected, induction of classical PB-induced genes (e.g., *Cyp2b9, Cyp2b10, Cyp2b13, Gsta2, Gstt3*) in both the susceptible B6C3F1 and relatively resistant C57BL/6 groups at 2 and 4 weeks was observed (Table 2.3). These genes are included among the 124 common active 2-week genes and 91 active common 4-week genes (Fig. 1; Supplementary Tables S3B and S3E, respectively, in the accepted manuscript).

Next, uniquely active genes in the susceptible B6C3F1 mice at 2 (281 genes) and 4 (133 genes) weeks were compared (Fig. 1; Supplementary Tables S3G-I in the accepted manuscript): 47 were altered in the same direction (35 induced and 12 repressed) at both time points, 234 (155 induced and 79 repressed) were observed only at 2 weeks, and 86 (63 induced and 23 repressed) were observed only at 4 weeks. In total, PB treatment

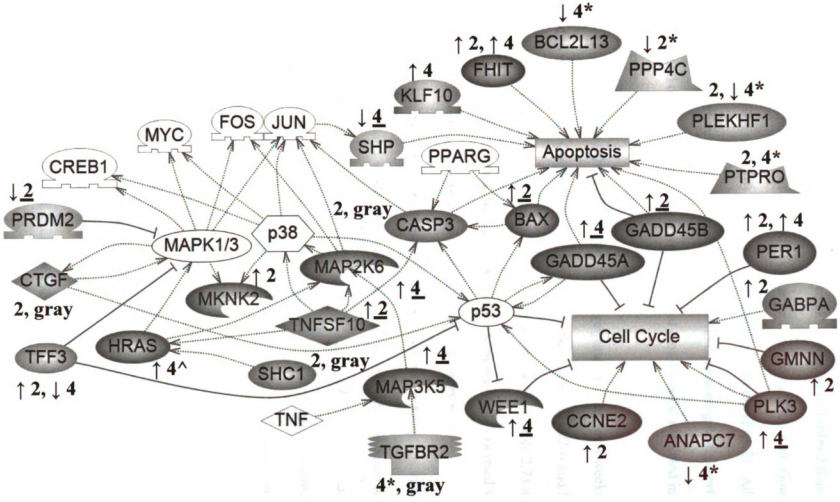
resulted in 367 total uniquely active genes in B6C3F1 mice at 2 and/or 4 weeks. Twenty-eight of these were selected, as described in the Methods, for confirmation of their expression statuses by qRT-PCR analysis. Of the 17 genes chosen that were uniquely active only at 2 weeks, expression changes of 11 were confirmed (Table 2.4). The expression change of the single uniquely active carry forward gene (i.e. its expression was induced at both 2 and 4 weeks) that was tested, *Slco1a4*, was confirmed at 2, but not 4, weeks (Tables 2.4 and 2.5, respectively). Finally, of the 10 genes chosen that were uniquely active only at 4 weeks, expression changes of 8 were confirmed (Table 2.5).

Many of the 367 total uniquely active genes in B6C3F1 mice at 2 and/or 4 weeks were found to be involved in multiple key signaling pathways (Figs. 2-5; Appendix Tables 4-5), and emphasis will be placed on those whose expression changes were confirmed by qRT-PCR, plus those genes that were not selected for confirmation.

Genes which can affect mitogen activated protein kinase (MAPK) signaling were induced (*Map3k5*, *Map2k6*, *Mknk2*, and *Tnfsf10*) or repressed (*Prdm2* and *Tff3*) by PB at 2 or 4 weeks (Fig. 2). MAPK pathways that involve *p38* and *Mapk1/3* can eventually result in the activation of key transcription factors, including *Myc*, *Jun*, and *Fos* (Fig. 2).

PB altered the expression of genes that can influence cell cycle progression (*Ccne2*, *Gabpa*, *Gadd45a*, *Gadd45b*, *Gmnn*, *Per1*, *Plk3*, and *Wee1)* at 2 and/or 4 weeks (Fig. 2). For *Gadd45b*, the B6C3F1 PB-treated animals demonstrated a statistically significant increase in expression over their controls at 2 weeks, as determined by qRT-PCR (Table 2.4). The level of expression in the B6C3F1 appears to be higher than that seen in the C57BL/6; however, this does not reach statistical significance due to a particularly low level of expression in one of the B6C3F1 mice (Table 2.4). A complete

Figure 2.2 The expression and/or methylation statuses of genes involved in the cell cycle, apoptosis, and mitogen-activated protein kinase (MAPK) signaling were altered by phenobarbital (PB) at 2 and 4 weeks. Microarray analysis was used to identify uniquely active genes in livers of tumor-susceptible B6C3F1 mice at 2 and/or 4 weeks, as described in the Methods. Functional annotation of 367 uniquely active genes (Fig. 1; Supplementary Tables S3G-I in the published manuscript) was performed. Expression is denoted as up-regulated (↑) or down-regulated (↓). Regarding qRT-PCR analysis, a change was confirmed if the time point is underlined (data in Appendix Tables 2-3); the word 'gray' indicates either 'not confirmed' (genes identified by microarray analysis) or 'no expression change' (genes identified from regions of altered DNA methylation, RAMs). Genes that lack underlining, symbols, and the word 'gray' were not selected for confirmation. Genes identified from unique PB-induced RAMs in the B6C3F1 mice at 2 and/or 4 weeks (Phillips and Goodman, 2008) are denoted by asterisks (*), and their expression was evaluated at the time point directly preceding the asterisk (Appendix Table 7). Ha-*ras* (^) was hypomethylated and up-regulated uniquely in B6C3F1 mice at 4 weeks (Bachman *et al.*, 2006). White symbols represent "bridging" genes that were not altered in response to PB. Positive (.....➤) or negative (—┤) regulation is illustrated, and the shapes of the entities represent the specific class of molecules to which the gene belongs: extracellular proteins (⬭), ligands (◇), kinases (⬭), transcription factors (⌒), phosphatases (▲), and membrane receptors (⊓).


↓ 4*
↑ 2, ↑ 4
BCL2L13
↓ 2*
PPP4C
FHIT
↑ 4
KLF10
2, ↓ 4*
PLEKHF1
FOS
JUN
MYC
↓ 4
SHP
PPARG
Apoptosis
2, 4*
PTPRO
CREB1
↓ 2
PRDM2
2, gray
CASP3
↑ 2
BAX
↑ 2
↑ 4
GADD45B
↑ 2, ↑ 4
PER1
MAPK1/3
p38
GADD45A
CTGF
2, gray
MAP2K6
↑ 2
MKNK2
↑ 4
↑ 2
GABPA
TNFSF10
↑ 2
p53
Cell Cycle
TFF3
↑ 2, ↓ 4
HRAS
↑ 4^
2, gray
SHC1
↑ 4
MAP3K5
GMNN
↑ 2
TNF
WEE1
↑ 4
CCNE2
↑ 2
PLK3
ANAPC7
↑ 4
↓ 4*
TGFBR2
4*, gray

list of the genes that were uniquely active in the B6C3F1 mice, which have discernable connections to growth/survival, at 2 and/or 4 weeks are listed in Tables 2.6 and 2.7, respectively. The induction of genes that can affect apoptosis (*Bax*, *Fhit*, *Gadd45a*, *Gadd45b*, *Klf10*, *Shp*, *Tnfsf10*) was observed at 2 and/or 4 weeks (Fig. 2). Additional genes that are positively or negatively associated with decreased growth/survival (i.e. apoptosis and cell death), and which were altered at 2 or 4 weeks, are listed in Table 2.6 and 2.7, respectively.

Fig. 3 depicts a subset of the uniquely active genes at 2 and/or 4 weeks which are linked to angiogenesis (*Angptl4*, *Cxcr7*, *Ddah1*, *Map3k5*, *Mme*, *Tnfsf10*) and EMT (*Cldn1*). Complete lists of uniquely active 2- (Table 2.6) and 4- (Table 2.7) week genes, including carry forward genes, which are positively or negatively associated with angiogenesis, invasion, and metastasis are included in the Appendix.

The pregnane X nuclear receptor (PXR), a xenobiotic sensor, was induced at 2 weeks (Fig. 4). At 2 or 4 weeks, PB altered the expression of several genes which are documented downstream targets of CAR and/or PXR (e.g., *Alas1*, *Abcc3*, *Gadd45b*, *Slco1a4: 2 weeks*). Additionally, uniquely active kinase, phosphatase, phosphatase activator (regulatory subunit), and phosphatase regulatory (inhibitor) genes are presented in Appendix 6.

The expression of genes involved in epigenetic processes (DNA methylation: *Dnmt3b*, one-carbon metabolism: *Cbs*, *Mtrr*, *Shmt1*, and histone methylation: *Prdm2*) was affected by PB at 2 or 4 weeks (Fig. 4). Additionally, unique repression of 3 Dnmt genes (*Dnmt1*, *Dnmt3a*, *Dnmt3b*) was demonstrated in the B6C3F1 groups at both 2 and 4 weeks, and these changes were strikingly different from what was observed in the

Figure 2.3 The expression and/or methylation statuses of genes involved in angiogenesis and the epithelial-mesenchymal cell transition (EMT) were altered by phenobarbital (PB) at 2 and 4 weeks. Microarray analysis was used to identify uniquely active genes in livers of tumor-susceptible B6C3F1 mice at 2 and/or 4 weeks, as described in the Methods. Functional annotation of 367 uniquely active genes (Fig. 1; Supplementary Tables S3G-I in the published manuscript) was performed. Expression is denoted as up-regulated (↑) or down-regulated (↓). Regarding qRT-PCR analysis, a change was confirmed if the time point is underlined (data in Appendix Tables 2-3); the word 'gray' indicates either 'not confirmed' (genes identified by microarray analysis) or 'no expression change' (genes identified from regions of altered DNA methylation, RAMs). Genes denoted by an arrow that lacks underlining and symbols were not selected for confirmation. Genes identified from unique PB-induced RAMs in the B6C3F1 mice at 2 and/or 4 weeks (Phillips and Goodman, 2008) are denoted by asterisks (*), and their expression was evaluated at the time point directly preceding the asterisk (Appendix Table 7). Ha-*ras* (^) was hypomethylated and up-regulated uniquely in B6C3F1 mice at 4 weeks (Bachman et al., 2006). White symbols represent "bridging" genes that were not altered in response to PB. Positive (.....➤) or negative (—┤) regulation is illustrated, and the shapes of the entities represent the specific class of molecules to which the gene belongs: extracellular proteins ( ), ligands ( ), kinases ( ), transcription factors ( ), and membrane receptors ( ).

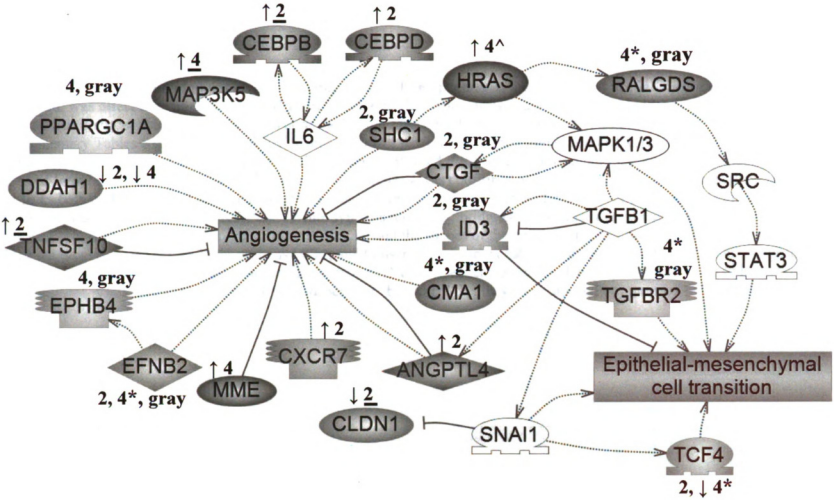

↑2
CEBPB
↑2
CEBPD
↑4^
HRAS
4*, gray
RALGDS
↑4
MAP3K5
4, gray
PPARGC1A
IL6
2, gray
SHC1
2, gray
MAPK1/3
SRC
CTGF
↓2, ↓4
DDAH1
2, gray
ID3
TGFB1
↑2
TNFSF10
Angiogenesis
4*
gray
STAT3
4*, gray
CMA1
TGFBR2
4, gray
EPHB4
↑2
CXCR7
↑2
ANGPTL4
Epithelial-mesenchymal
cell transition
EFNB2
2, 4*, gray
↑4
MME
↓2
CLDN1
SNAI1
TCF4
2, ↓4*

Figure 2.4 The expression of genes involved in epigenetic-related processes, and those that are indicative of nuclear receptor activation, was altered by phenobarbital (PB) at 2 and 4 weeks. Microarray analysis was used to identify uniquely active genes in livers of tumor-susceptible B6C3F1 mice, as described in the Methods. Functional annotation of 367 uniquely active genes (Fig. 1; Supplementary Tables S3G-I in the published manuscript) was performed. Expression is denoted as up-regulated (↑) or down-regulated (↓). Regarding qRT-PCR analysis, a change was confirmed if the time point is underlined (data in Appendix Tables 2-3); the word 'gray' indicates 'not confirmed'. Expression of *Slco1a4* was confirmed at 2, but not 4 (§) weeks. Genes denoted by arrow that lacks both underlining and particular symbols (+ and §) were not selected for confirmation. A plus sign (+) denotes a gene whose expression was evaluated only by qRT-PCR. White symbols represent "bridging" genes that were not altered in response to PB. Positive (.....➢) or negative (—┤) regulation is illustrated, and the shapes of the entities represent the specific class of molecules to which the gene belongs: extracellular proteins (⬭), and transcription factors (⬭). According to Ueda *et al.* (2002), 2 genes (*Krt4* and *Pck1*) exhibited constitutive active/androstane receptor (CAR)-dependent down-regulation in response to PB (while we detected up-regulation), and 3 genes (¥) were under CAR-dependent "blocking", i.e. they were induced or repressed only in CAR knockout mice (v. the wildtype).

2, gray
ABCC2
↑2, 4§
SLCO1A4
↑2
CYP7A1
4, gray
PPARGC1A
↑2
ABCC3
↑4
ALAS1
↑2
AQP1
↑2¥
GNPNAT1
↑2
KRT4
↑2¥
PKLR
↑2
PCK1
↓2¥
CYP4A10
↑2
GADD45B
↓4
SHP
CAR
PXR
PPARG
DNA methylation
DNMT1
↓2+, ↓4+
DNMT3A
↓2+, ↓4+
DNMT3B
↓2, ↓4+
PRDM2
↓2
Histone methylation
↓2
CBS
↑4
MTRR
↑2
SHMT1
1-carbon metabolism

C57BL/6 at the corresponding time points (Table 1). At 2 weeks, expression of *Dnmt3b* decreased to a statistically greater extent (Student's t-test, $p < 0.05$) in the B6C3F1 mice, as compared to the C57BL/6, and thus, the change is considered to be unique in the B6C3F1.

In addition to assessing the effects of PB on global gene expression, we were interested in evaluating the expression of genes that were previously shown to exhibit unique RAMs in DNA isolated from the same livers of these tumor-susceptible B6C3F1 mice, as compared to their relatively resistant C57BL/6 counterparts (Phillips and Goodman, 2008). The expression of a subset of these (19 total: 2 at 2 weeks and 17 at 4 weeks) was initially evaluated in the B6C3F1 mice (Table 2.9). If the methylation and expression statuses appeared to be inversely correlated (as described Table 2.9), expression in the time-matched C57BL/6 group was evaluated. At 4 weeks, 3 genes (*Bcat2, Bcl2l13, Ube2d1*) exhibited unique decreases in expression and unique increases in methylation in the B6C3F1 mice, as compared to the C57BL/6. Two genes exhibited decreases in expression that were not statistically different (Student's t-test, $p < 0.05$) in the B6C3F1 and C57BL/6 mice at 2 (*Srms*) or 4 (*Trio*) weeks, and their methylation statuses were ambiguous (either increased and/or decreased). At 4 weeks, *Ncor2* exhibited increased methylation levels and decreased expression in the B6C3F1 mice, and the extent of the fold change was statistically less (Student's t-test, $p < 0.05$) than that observed in the C57BL/6. The expression of 13 genes was only evaluated in the B6C3F1 mice: 7 were down-regulated and hypomethylated, while expression of the other 6 did not change.

Genes identified from unique RAMs (Phillips and Goodman, 2008) were added to

Table 2.1 Quantitative real-time PCR (qRT-PCR) analysis of expression of 3 DNA methyltransferase (Dnmt) genes.

Gene	Time Point[a]	B6C3F1		C57BL/6	
		Fold Change[b]	No. of Mice that Exhibited a Change Outside 95% CI of Control Group[c]	Fold Change[b]	No. of Mice that Exhibited a Change Outside 95% CI of Control Group[c]
Dnmt1: DNA methyltransferase 1	2 wk	↓ -1.47[d]	--	n.c.	↑ 3
	4 wk	↓ -1.49[d]	--	n.c.	--
Dnmt3a: DNA methyltransferase 3a	2 wk	↓ -1.60[d]	--	↑ 1.33	--
	4 wk	↓ -1.81[d]	--	n.c.	↓ 3
Dnmt3b: DNA methyltransferase 3b	2 wk	↓ -6.60[d,e,f]	--	↓ -4.08[e]	--
	4 wk	↓ -2.00[d]	--	↑ 1.47	--

[a] Phenobarbital (PB) was administered to B6C3F1 and C57BL/6 mice for 2 or 4 weeks.

[b] A fold change of gene expression (↑, up-regulation or ↓, down-regulation) is listed if it was statistically significant (Student's t-test, $p < 0.05$) in a treatment group v. its time-matched control. If it was not significant, no change (n.c.) is listed.

[c] If a fold change was not statistically significant, a gene was considered to show an 'indication of a change' if data from at least 3 of the 6 samples in the PB-treated group fell outside (above, ↑ or below, ↓) the 95% confidence interval (CI) of the control group data. If there was no indication of a change, or if a fold change was statistically significant, these data are not shown (--).

[d] The expression change was considered to be unique in the B6C3F1 mice, as compared to the C57BL/6.

[e] At 2 weeks, expression of *Dnmt3b* decreased to a statistically greater extent (Student's t-test, $p < 0.05$) in the B6C3F1, as compared to the C57BL/6, and thus, the change was considered to be unique in the B6C3F1.

[f] At 2 weeks, *Dnmt3b* was uniquely active, based on microarray analysis, in the B6C3F1 mice.

Figures 2-5 in order to depict complementary data from the gene expression and DNA methylation analyses. Also included in Figures 2 and 3 is Ha-*ras*, which we previously demonstrated to be hypomethylated and induced uniquely in B6C3F1 mice, as compared to the C57BL/6, at 4 weeks of PB treatment (Bachman *et al.*, 2006).

Thirty genes of interest (18 uniquely active genes based on microarray analysis, 3 Dnmts, and 9 genes identified from unique RAMs) harbored at least 1 putative CARE within 10 kb upstream of their transcriptional start sites (Table 2; base sequences of the putative CAREs are listed in Supplementary Table S10 in the accepted manuscript). All 30 genes were subjected to qRT-PCR analysis (Table 1, Tables 2.4, 2.5 and 2.9). Of the 18 which were identified as uniquely active based on microarray analysis, the expression statuses of 13 were confirmed by qRT-PCR (Tables 2.4 and 2.5).

Table 2.2 Expression of Genes that Contain Putative Constitutive Active/Androstane Receptor Response Elements (CAREs)[A,B]

Gene[C]		Time Point (weeks) in B6C3F1	Microarray Analysis[D]	qRT-PCR Analysis	Methylation Change[E]	No. of Putative CAREs
Exhibited Expression Changes Based on Microarray Analysis[F]	***Abcc3***	**2**	↑	C[G]		5
	Bax	**2**	↑	A.C.[H]		6
	Casp3	2	↑	n.c.[I]		2
	Cbs	**2**	↓	C[G]		3
	Cebpb	**2**	↑	C[G]		2
	Gadd45b	**2**	↑	A.C.[H]		4
	Id3	2	↓	n.c.[I]		1
	Lcn2	2	↑	n.c.[I]		1
	Prdm2	**2**	↓	A.C.[H]		1
	Shmt1	**2**	↑	A.C.[H]		2
	Tnfsf10	**2**	↑	C[G]		1
	Ephb4	4	↑	n.c.[I]		5
	Gadd45a	**4**	↑	C[G]		2
	Map3k5	**4**	↑	A.C.[H]		4
	Mtrr	**4**	↑	C[G]		1
	Plk3	**4**	↑	A.C.[H]		1
	Ppargc1a	4	↑	n.c.[I]		1
	Wee1	**4**	↑	C[G]		5
DNA methyltransferases[J]	*Dnmt1*	2	N.D.[K]	↓[L]		3
		4	N.D.[K]	↓[L]		
	Dnmt3a	2	N.D.[K]	↓[L]		2
		4	N.D.[K]	↓[L]		
	Dnmt3b	2	↓	C[G]		1
		4	N.D.[K]	↓[L]		

Table 2.2 continued Expression of Genes that Contain Putative Constitutive Active/Androstane Receptor Response Elements

Exhibited Unique Regions of Altered DNA methylation (RAMs)[M]	*Anapc7*	4	N.D.[K]	↓[L]	HypoM	2
	Bcat2	4	N.D.[K]	↓[L]	NewM	2
	Bcl2l13	4	N.D.[K]	↓[L]	NewM	2
	Ddx54	2	N.D.[K]	n.a.[N]	HypoM	1
		4	N.D.[K]	↓[L]	HypoM	
	Ncor2	4	N.D.[K]	↓[L]	NewM	2
	Plekhf1	2	N.D.[K]	n.a.[N]	NewM	3
		4	N.D.[K]	↓[L]	HypoM	
	Prickle2	2	N.D.[K]	n.a.[N]	HypoM and/or NewM^	1
		4	N.D.[K]	n.s.[O]	HypoM	
	Srms	2	N.D.[K]	↓[L]	HypoM or HyperM, and/or NewM^	4
	Tgfbr2	4	N.D.[K]	n.s.[O]	HypoM	1

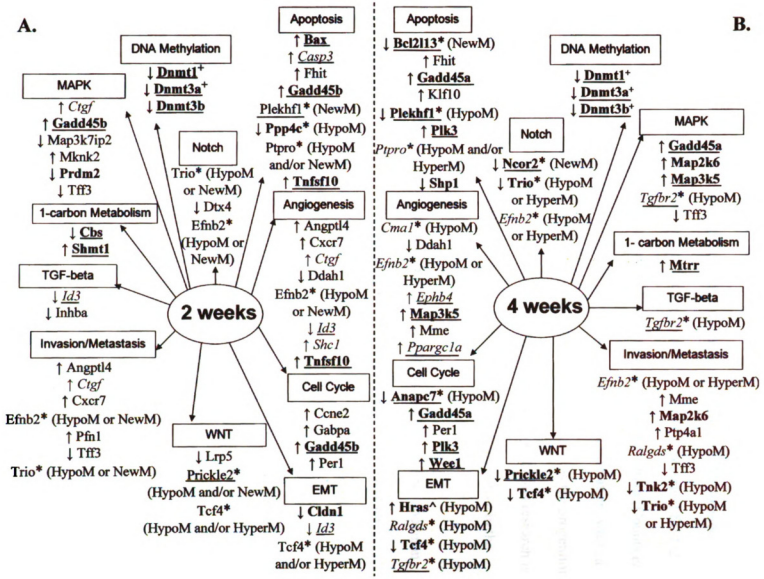
[A]Base sequences of putative CAREs, located 10 kb upstream of the transcriptional start site, are listed in Supplementary Table S10 in the published manuscript; [B]We used the same position weight matrix and 80% stringency cut-off on 25,000 randomly constructed sequences of 10 kb in length and found that, on average, there were only 0.561 CAREs found per sequence (across all 25,000 sequences). The probability of a gene having more than 1 CARE is 10.8%, while the probability of having more than 2, 3, or 4 CAREs is 2.2%, 0.38%, and 0.044%, respectively. The probability of not having any CAREs is 57.4%; [C]Genes that exhibited unique PB-elicited expression changes (Table 1, Supplementary Tables S3G-I in the published manuscript and Appendix Tables 2-3) and/or methylation (Phillips and Goodman, 2008a) in B6C3F1 mice at 2 and/or 4 weeks of phenobarbital (PB) treatment; [D]Expression changes (↑, up-regulation and ↓, down-regulation) of uniquely active genes that were identified based on microarray analysis (as described in the Methods). For genes and time points listed in **bolded font**, the expression change was confirmed, or appeared to be confirmed, by quantitative real-time PCR (qRT-PCR) analysis. The expression of genes listed in normal black font was evaluated but was not confirmed; [E]PB-induced decreases in methylation (Hypomethylation, HypoM) and increases in methylation (Hypermethylation, HyperM and new methylations, NewM), as determined by Phillips and Goodman (2008a). For certain genes (^), the methylation statuses were ambiguous (i.e. not definitively determined); [F]Detailed confirmatory qRT-PCR data are found in Appendix Tables 2 (2 weeks) and 3 (4 weeks); [G]The expression change, based on microarray analysis, was confirmed (C); [H]The expression change, based on microarray analysis, was apparently confirmed (A.C.); [I]The expression change, based on microarray analysis, was not confirmed (n.c.); [J]Detailed qRT-PCR data are found in Table 1; [K]N.D. (not detected) indicates that the gene was not active; [L]Direction (↑, up-regulation and ↓, down-regulation) of the statistically significant (Student's t-test, $p \leq 0.05$) fold change; [M]Detailed qRT-PCR data are found in Appendix Table 7; [N]Expression was not evaluated; [O]Fold change was not significant, n.s. (Student's t-test, $p < 0.05$).

DISCUSSION

Unique hepatic gene expression changes in tumor-prone B6C3F1, as compared to relatively resistant C57BL/6 mice, were discerned at very early time points following PB treatment. We hypothesize that at least some of these contribute directly to the development of liver tumors which are destined to become evident at later time points, e.g., 12 months (Becker, 1982). Strikingly, as early as 2 and 4 weeks, the expression of genes that regulate key cancer-related processes is altered uniquely in tumor-susceptible mice, as compared to their relatively resistant counterparts (Figs. 2-5). These data both complement and extend our previous research, which identified multiple genes that exhibited unique methylation changes in hepatic DNA from the same B6C3F1 mice at 2 and 4 weeks of PB treatment (Phillips and Goodman, 2008). Importantly, genes elucidated from both the methylation and expression analyses participate in several of the same overarching pathways and signaling processes (e.g., cell cycle, apoptosis, angiogenesis, EMT, invasion/metastasis, and MAPK, Tgf-β and Wnt signaling) (Fig. 5). Additionally, several pathways are represented by genes that exhibited changes only in methylation (Notch signaling) or expression (DNA methylation, 1-carbon metabolism) (Fig. 5). Overall, these data illuminate very early events (alterations in DNA methylation and gene expression) which might facilitate selective clonal expansion, and ultimately, tumor formation, in response to PB.

A subset of the uniquely active B6C3F1 genes at 2 and/or 4 weeks are involved in growth (e.g., cell cycle), survival, and apoptosis (Figs. 2 and 5; Appendix Tables 2.6 and 2.7). Multiple genes identified from unique B6C3F1 RAMs (Phillips and Goodman, 2008) participate in these same processes (Fig. 5), and several of them (*Anapc7, Bcl2l13,*

Figure 2.5 Summary of pathways and processes involving genes that exhibited unique phenobarbital (PB)-elicited expression and/or methylation changes at 2 and/or 4 weeks. PB induced unique hepatic regions of altered DNA methylation (RAMs), including hypomethylations (HypoM), hypermethylations (HyperM), and new methylations (NewM) in tumor-susceptible B6C3F1 mice at 2 (in A) and/or 4 (in B) weeks (Bachman *et al.*, 2006). Genes, identified from unique RAMs (Phillips and Goodman, 2008a), are depicted by an asterisk (*). Regarding analysis of their expression in B6C3F1 mice by qRT-PCR (Appendix Table 7): genes that exhibited an expression change (induction, ↑ or repression, ↓) are **bolded**, those that did not are in *italics*, and those that were not evaluated are in normal font. Bachman *et al.* (2006) demonstrated unique hypomethylation and up-regulation of Ha-*ras* (^) in the B6C3F1 mice at 4 weeks. As described in the Methods, microarray analysis was employed to identify uniquely active genes in the B6C3F1 mice at 2 and/or 4 weeks. Expression of uniquely active genes was confirmed (**bolded**), or evaluated and not confirmed (*italics*) by qRT-PCR (Appendix Tables 2-3). Uniquely active genes that were not selected for confirmation are listed in normal font. A plus sign (+) denotes a Dnmt gene whose unique expression change was revealed only by qRT-PCR. A line underneath a gene indicates that at least 1 putative CARE was found within 10 kb of the transcriptional start site. Abbreviations: EMT, epithelial-mesenchymal cell transition; MAPK, mitogen-activated protein kinase; TGFB, transforming growth factor-beta.


A.
2 weeks
Apoptosis
↑ Bax
↑ Casp3
↑ Fhit
↑ Gadd45b
Plekhf1* (NewM)
↓ Ppp4c* (HypoM)
Ptpro* (HypoM and/or NewM)
↑ Tnfsf10
DNA Methylation
↓ Dnmt1+
↓ Dnmt3a+
↓ Dnmt3b
MAPK
↑ Ctgf
↑ Gadd45b
↓ Map3k7ip2
↑ Mknk2
↓ Prdm2
↓ Tff3
Notch
Trio* (HypoM or NewM)
↓ Dtx4
Efnb2* (HypoM or NewM)
Angiogenesis
↑ Angptl4
↑ Cxcr7
↑ Ctgf
↓ Ddah1
Efnb2* (HypoM or NewM)
1-carbon Metabolism
↓ Cbs
↑ Shmt1
TGF-beta
↓ Id3
↓ Inhba
Invasion/Metastasis
↑ Angptl4
↑ Ctgf
↑ Cxcr7
Efnb2* (HypoM or NewM)
↑ Pfn1
↓ Tff3
Trio* (HypoM or NewM)
WNT
↓ Lrp5
Prickle2* (HypoM and/or NewM)
Tcf4* (HypoM and/or HyperM)
↓ Id3
Tcf4* (HypoM and/or HyperM)
Cell Cycle
↑ Ccne2
↑ Gabpa
↑ Gadd45b
↑ Per1
EMT
↓ Cldn1
↓ Id3
Tcf4* (HypoM and/or HyperM)
B.
4 weeks
Apoptosis
↓ Bcl2l13* (NewM)
↑ Fhit
↑ Gadd45a
↑ Klf10
↓ Plekhf1* (HypoM)
↑ Plk3
Ptpro* (HypoM and/or HyperM)
↓ Shp1
DNA Methylation
↓ Dnmt1+
↓ Dnmt3a+
↓ Dnmt3b+
MAPK
↑ Gadd45a
↑ Map2k6
↑ Map3k5
Tgfbr2* (HypoM)
↓ Tff3
Notch
↓ Ncor2* (NewM)
↓ Trio* (HypoM or HyperM)
Efnb2* (HypoM or HyperM)
Angiogenesis
Cma1* (HypoM)
↓ Ddah1
Efnb2* (HypoM or HyperM)
↑ Ephb4
↑ Map3k5
↑ Mme
↑ Ppargc1a
1- carbon Metabolism
↑ Mtrr
TGF-beta
Tgfbr2* (HypoM)
Invasion/Metastasis
Efnb2* (HypoM or HyperM)
↑ Mme
↑ Map2k6
↑ Ptp4a1
Ralgds* (HypoM)
↓ Tff3
↓ Tnk2* (HypoM)
↓ Trio* (HypoM or HyperM)
Cell Cycle
↓ Anapc7* (HypoM)
↑ Gadd45a
↑ Per1
↑ Plk3
↑ Wee1
WNT
↓ Prickle2* (HypoM)
↓ Tcf4* (HypoM)
EMT
↑ Hras^ (HypoM)
Ralgds* (HypoM)
↓ Tcf4* (HypoM)
Tgfbr2* (HypoM)

Ppp4c, Plekhf1) exhibited an expression change (Table 2.9). These observations are consistent with the known ability of PB to enhance hepatocyte proliferation between 1-4 weeks of treatment (Counts *et al.*, 1996; Kolaja *et al.*, 1996a) and decrease apoptosis within focal lesions that become evident after prolonged treatment (i.e. 30-60 days) (Kolaja *et al.*, 1996b). In this context, it is important to note that PB treatment for 1-2 weeks also increases hepatocyte proliferation in the resistant C57BL/6 strain (Counts *et al.*, 1996). Chronic PB administration inhibits normal hepatocyte proliferation, while a subpopulation of cells escapes the mitoinhibitory effects and may serve as the progenitors for tumor formation (reviewed in Counts *et al.*, 1996). A novel aspect of this research is the identification of several growth regulatory genes which are uniquely active in the tumor-susceptible B6C3F1 mice.

Importantly, PB elicited unique changes in methylation (Phillips and Goodman 2008) and expression of angiogenesis-associated genes at 2 and/or 4 weeks in the susceptible B6C3F1 mice (Figs. 3 and 5; Tables 2.6 and 2.7). Angiogenesis is required for both normal development and tumor growth and metastasis (Folkman, 2002; Papetti and Herman, 2002). It is remarkable to see altered expression of genes involved in this process so soon after commencing PB treatment. Furthermore, genes involved in invasion and metastasis, plus EMT, a developmental program which appears to facilitate the two former processes (Thiery, 2002; Yang *et al.*, 2006), were uniquely active in the susceptible B6C3F1 mice at 2 and/or 4 weeks of PB treatment (Figs. 3 and 5; Tables 2.6 and 2.7). Genes in which unique PB-induced B6C3F1 RAMs occurred (Phillips and Goodman, 2008) are also involved in these processes (Fig. 5), and notably, PB altered the expression of *Tcf4* in the B6C3F1 mice (Fig. 3). While invasion and metastasis are

typically regarded as late events in tumorigenesis, untransformed cells can travel through the bloodstream to a secondary site, where additional molecular alterations leading to malignant growth may occur (Podsypanina *et al.*, 2008). The current report is the first to indicate that PB can start to facilitate EMT, invasion and metastasis at a very early stage of tumor development.

The fundamental genes involved in human and mouse tumorigenesis are likely identical, however, mice are more susceptible than humans (Rangarajan and Weinberg, 2003). The regulation of these genes, of which epigenetic control (e.g., altered DNA methylation) is a component, might be a key species-specific difference that contributes to their disparate sensitivities. For instance, methylation patterns are less stable in rodent, as compared to human, cells (reviewed in Goodman and Watson, 2002). In the B6C3F1 mice, PB uniquely altered the expression of genes which influence methylation status. Changes in genes that function in 1-carbon metabolism (*Cbs, Mtrr, and Shmt1*; Fig. 4), which generates the Dnmt methyl donor S-adenosylmethionine, occurred. Remarkably, the expression of 3 Dnmt genes (*1*, *3a*, and *3b*) was uniquely repressed in the B6C3F1 mice at both 2 and 4 weeks (Table 1), thus linking PB to early expression changes of key genes involved in regulating DNA methylation patterns. Interestingly, all 6 of these genes harbor CAREs, indicating that CAR might modulate their transcription.

Additional genes whose expression and/or methylation statuses were altered uniquely at these extremely early time points in the susceptible B6C3F1 mice can participate in multiple signaling pathways of development and differentiation that have previously been linked to tumorigenesis: transforming growth factor-beta (Tgf-β), Wnt, and Notch (Fig. 5). Tgf-β signaling functions in a tumor suppressive manner in normal

cells and in an oncogenic fashion during later stages of tumorigenesis (Massagué, 2008). Aberrant Wnt signaling is known for its prominent role in colorectal cancer (Klaus and Birchmeier, 2008), as epigenetic silencing of Wnt antagonists (e.g., secreted frizzled-related proteins) and activating mutations in β-catenin occur (Baylin and Ohm, 2006). β-catenin mutations are also prevalent in DEN-initiated, PB-promoted mouse liver tumors (Schwarz *et al.*, 2003). Finally, abnormal Notch signaling can contribute to a variety of human malignancies in an oncogenic or tumor suppressive manner (Bolós *et al.*, 2007).

We are interested in developing a pattern of gene expression and DNA methylation that could be used as an early biomarker of PB treatment. The current study takes us a step in that direction by focusing on a subset of the uniquely active B6C3F1 genes at 2 and/or 4 weeks of PB treatment. Candidate genes include those with documented roles in cancer-related processes (*Ccne2, Cxcr7, Gadd45a, Gadd45b, Inhba, Lrp5, Mknk2, Wee1*). Other potential candidates include those genes, possessing tumorigenesis-related functions, that exhibited unique RAMs solely in the B6C3F1 group (*Cma1, Ralgds, Tgfbr2*; from Phillips and Goodman, 2008), and common RAMs with the same methylation status in both liver tumor-prone B6C3F1 and CAR WT mice (*Bcat2, Ddx54, Srms, Wscd1, Zscan22*; from Phillips and Goodman, 2009).

Efforts have been made to identify expression signatures of nongenotoxic rodent hepatocarcinogenesis. Iida *et al.* (2005) evaluated hepatic gene expression in B6C3F1 mice treated for 2 weeks with oxazepam. Two of the 6 genes which were up-regulated, excluding those involved in drug metabolism, (*Gadd45b* and *Maff*), and 1 of the 3 which were down-regulated (*Tsc-22*) matched our results. Fielden *et al.* (2007) reported a 37 gene signature based on expression data from rats (which are not as responsive to PB-

induced tumorigenesis as the susceptible strains/stocks of mice) treated for 5 days with one of a variety of nongenotoxic compounds. Only one of these (*Usp2*) was active in our study. However, the direction of change was opposite and, thus, there were no real matches. Our approach for elucidating PB-induced gene expression changes that might be useful biomarker candidates is more appropriate than what is in the literature currently because we are "subtracting out" those alterations that occurred in the relatively resistant C57BL/6 mice, and thus, are focusing upon changes in the susceptible B6C3F1 that might truly be related directly to tumorigenesis.

The RNA utilized for gene expression analysis was isolated from whole liver. Thus, the expression patterns are presumably derived from multiple cell types (e.g., hepatocytes, sinusoidal epithelial cells, Kupffer cells), which could partially explain changes that do not appear to obviously correlate with overall enhancement or inhibition of a process (e.g., genes that positively regulate angiogenesis are both induced and repressed, Fig. 3 and Tables 2.6 and 2.7). This approach is beneficial for ascertaining early changes that accumulate in multiple cells, including potential tumor progenitors, such as stem cells (Reya *et al.*, 2001), or mature cells (e.g., hepatocytes) that have de-differentiated. Indeed, since hepatocytes can proliferate (Counts *et al.*, 1996; Kolaja *et al.*, 1996a; Michalopolous, 2007) and can be reprogrammed to a stem-like phenotype (Aoi *et al.*, 2008), it is possible that adult liver cells can revert into a de-differentiated state and serve as the tumor progenitor. Importantly, this notion is not incompatible with the aforementioned stem cell theory.

Kinase, phosphatase, phosphatase activator (regulatory subunit), and phosphatase regulatory (inhibitor) genes, which were uniquely active in the tumor-susceptible

B6C3F1 mice at 2 and 4 weeks, are listed in Table 2.8. In this context it is instructive to note that phosphorylation and dephosphorylation events (Kawamoto *et al.*, 1999; Sueyoshi *et al.*, 2008; Yamamoto *et al.*, 2003) are necessary for CAR activation, and we speculate that PB might affect expression levels of genes involved. Induction of known CAR target genes was observed (Fig. 4). Furthermore, in a hypothesis generating fashion, putative CAREs were discerned within a subset of uniquely active genes in the B6C3F1 mice, plus multiple genes that harbored unique PB-elicited B6C3F1 RAMs (Supplementary Table S10 in the accepted manuscript). These data indicate that CAR might regulate gene transcription at 2 and 4 weeks.

Expression analysis of a subset of genes that exhibited unique RAMs in the B6C3F1 mice (Table 2.9) revealed several (*Bcat2, Bcl2l13, Ube2d1*) whose levels were unique as compared to the C57BL/6 group, suggesting that they might be important for tumor formation, particularly the apoptosis-inducer *Bcl2l13*. For others (*Srms* and *Trio*), the expression patterns were not statistically different in the B6C3F1 and C57BL/6 mice, and therefore, in the case of *Trio*, which has been linked to cancer, the expression change might be necessary, but not sufficient, for tumor formation. For numerous genes, decreased methylation was associated with decreased expression. This resembles the situation for the imprinted insulin-like growth factor receptor type-2 (*Igf2r*) gene, in which hypomethylation of an intronic CpG island is associated with paternal silencing, while methylation appears to facilitate maternal expression (Wutz *et al.*, 1997).

There often is not an association between expression and the genomic location of the DNA methylation change (Table 2.9). The approach taken to discern unique B6C3F1 RAMs is unbiased, in the sense that regions to be assayed are not pre-determined

(Bachman *et al.*, 2006). Thus, methylation changes were ascertained in various genomic locations (not only promoters) that could potentially influence expression. It is possible that numerous regulatory elements, including regions in which RAMs occurred, function in concert to control expression. Additionally, multiple methylation changes may be required to affect expression of a gene and not all might have accumulated within 4 weeks. In these instances, an obvious link between expression status and the location of a RAM might not be apparent.

In general, there was good agreement between the microarray and qRT-PCR data (Tables 2.4 and 2.5). However, discrepancies between these 2 techniques are often encountered (Etienne *et al.*, 2004; Morey *et al.*, 2006), and there were a few instances when the expression statuses of genes, identified as uniquely active in the B6C3F1 mice by microarray analysis, were not confirmed by qRT-PCR (Tables 2.4 and 2.5). Nonetheless, the overall validity of the microarray data is supported by the observed induction of typical PB-responsive genes in both the B6C3F1 and C57BL/6 groups at 2 and 4 weeks (Table 2.3). Furthermore, our data reinforce published results that demonstrate PB-elicited induction of *Gadd45β* (Peffer *et al.*, 2007), *Aqp1* and *Alas1* (Ueda *et al.*, 2002), and *Abcc3*, *Dio1*, *Gna14*, *Lcn2*, *Por*, and *Thrsp*, plus repression of *Arntl* (Stahl *et al.*, 2005). All of these were altered in the same directions in the B6C3F1 at 2 or 4 weeks (Supplementary Tables S3G and S3I, in the accepted manuscript). Contrastingly, different expression patterns of several uniquely active B6C3F1 genes (*Cyp4a10, Gnpnat1*, *Krt4*, *Pck1,* and *Pklr)*, as compared to Ueda *et al.* (2002), were reported (Fig. 4). Reasons for these inconsistencies might be differences in our microarray platforms, the number of genes/ESTs on the array plus more recent and

accurate annotation information, mouse strain/stock, and/or the method/duration of PB administration.

In summary, this extensive analysis of PB-elicited expression at very early time points has revealed numerous uniquely active genes in tumor-susceptible B6C3F1, as compared to relatively resistant C57BL/6 mice, many of which are involved in key cancer-related processes (Figs. 2-5; Tables 2.6 and 2.7). Significantly, genes which demonstrated unique RAMs in the B6C3F1 mice (Phillips and Goodman, 2008) also participate in several of these pathways (Figs. 2-5), and for a subset, their expression levels in the B6C3F1 groups were affected by PB treatment. The unique repression of 3 major Dnmt genes in the B6C3F1 mice at both 2 and 4 weeks provides a potential direct link between PB and the expression of key genes that regulate DNA methylation patterns. Furthermore, we located putative CAREs within numerous genes that were altered by PB, including all 3 Dnmts, suggesting that these might be regulated by CAR. We propose that at least some of the genes that exhibited unique changes in expression and/or DNA methylation represent initial key, heritable changes that confer proliferative advantages to cells, resulting in the progressive accumulation of modifications and the perturbation of signaling pathways that facilitate PB-induced tumorigenesis. It is instructive to reflect on the possibility that, in a hypothesis-driven fashion, these genes represent appropriate candidates that could be utilized to develop a biomarker "fingerprint" of early exposure to PB and PB-like compounds.

ACKNOWLEDGEMENTS

Predoctoral fellowship support for J.M.P was received from the National Institutes of Health/National Institute of Environmental Health Sciences training grant No. T32-ES-7255. Research support, in the form of an unrestricted gift, from the R.J. Reynolds Tobacco Company is acknowledged gratefully. We thank the Michigan State University Research Technology and Support Facility for technical assistance with the microarray analyses.

REFERENCES

Aoi, T., Yae, K., Nakagawa, M., Ichisaka, T., Okita, K., Takahashi, K., Chiba, T., and Yamanaka, S. (2008) Generation of pluripotent stem cells from adult mouse liver and stomach cells. *Science* **321**, 699-702.

Aydinlik, H., Nguyen, T. D., Moennikes, O., Buchmann, A., and Schwarz, M. (2001). Selective pressure during tumor promotion by phenobarbital leads to clonal outgrowth of β-catenin-mutated mouse liver tumors. *Oncogene* **22**, 7812-7816.

Bachman, A. N., Phillips, J. M, and Goodman J. I. (2006). Phenobarbital induces progressive patterns of GC-rich and gene-specific altered DNA methylation in the liver of tumor-prone B6C3F1 mice. *Toxicol. Sci.* **91**, 393-405.

Baylin, S. B., Ohm, J. E. (2006) Epigenetic gene silencing in cancer - a mechanism for early oncogenic pathway addiction? *Nat. Rev. Cancer.* **6**, 107-116.

Becker, F.F. (1982). Morphological classification of mouse liver tumors based on biological characteristics. *Cancer Res.* **42**, 3918-3923.

Bolós, V., Grego-Bessa, J., and de la Pompa, J. L. (2007) Notch signaling in development and cancer. *Endocr. Rev.* **28**, 339-363.

Chen, Y., Ferguson, S. S., Negishi, M., and Goldstein, J. A. (2003) Identification of constitutive androstane receptor and glucocorticoid receptor binding sites in the *CYP2C19* promoter. *Mol. Pharmacol.* **64**, 316-324.

Counts, J. L., and Goodman, J. I. (1995) Alterations in DNA methylation may play a variety of roles in carcinogenesis. *Cell* **83**, 13-15.

Counts, J. L., McClain, R. M., and Goodman, J. I. (1997). Comparison of effect of tumor promoter treatments on DNA methylation status and gene expression in B6C3F1 and C57BL/6 mouse liver and in B6C3F1 mouse liver tumors. *Mol. Carcinog.* **18**, 97-106.

Counts, J. L., Sarmiento, J. I., Harbison, M. L., Downing, J. C., McClain, R. M., and Goodman, J. I. (1996). Cell proliferation and global methylation status changes in mouse

liver after phenobarbital and/or choline-devoid, methionine-deficient diet administration. *Carcinogenesis* **17**, 1251-1257.

Dai, M., Wang, P., Boyd, A. D., Kostov, G., Athey, B., Jones, E. G., Bunney, W. E., Myers, R. M., Speed, T. P., Akil, H., Watson, S. J., and Meng, F. (2005) Evolving gene/transcript definitions significantly alter the interpretation of GeneChip data. *Nucleic Acids Res.* **33**, 175.

Dennis, G. Jr., Sherman, B. T., Hosack, D. A., Yang, J., Gao, W., Lane, H. C., Lempicki, R. A. (2003) DAVID: Database for Annotation, Visualization, and Integrated Discovery. *Genome Biol.* **4**, P3.

Esteller, M. (2007) Cancer epigenomics: DNA methylomes and histone-modification maps. *Nat. Rev. Genet.* **8**, 286-298.

Etienne, W., Meyer, M. H., Peppers, J., and Meyer, R. A. Jr. (2004) Comparison of mRNA gene expression by RT-PCR and DNA microarray. *Biotechniques* **36**, 618-20, 622, 624-626.

Feinberg AP, Ohlsson R, Henikoff S. (2006) The epigenetic progenitor origin of human cancer. *Nat. Rev. Genet.* **7**, 21-33.

Fielden, M. R., Brennan, R., and Gollub, J. (2007) A gene expression biomarker provides early prediction and mechanistic assessment of hepatic tumor induction by nongenotoxic chemicals. *Toxicol. Sci.* **99**, 90-100.

Folkman, J. (2002) Role of angiogenesis in tumor growth and metastasis. *Semin. Oncol.* **29**, 15-18.

Gerbal-Chaloin, S., Daujat, M., Pascussi, J. M., Pichard-Garcia, L., Vilarem, M. J., and Maurel, P. (2002) Transcriptional regulation of *CYP2C9* gene. Role of glucocorticoid receptor and constitutive androstane receptor. *J. Biol. Chem.* **277**, 209-217.

Goodman, J.I. and Watson, R.E. (2002). Altered DNA methylation: A secondary mechanism involved in carcinogenesis. *Annu. Rev. Pharmacol. Toxicol.* **42**, 501-525.

Goodwin, B., Hodgson, E., D'Costa, D. J., Robertson, G. R., and Liddle, C. (2002) Transcriptional regulation of the human *CYP3A4* gene by the constitutive androstane receptor.
Mol. Pharmacol. **62**, 359-65.

Hanahan D. and Weinberg, G. F. (2000). The hallmarks of cancer. *Cell* **100**, 57-70.

Honkakoski, P., Zelko, I., Sueyoshi, T., and Negishi, M. (1998) The nuclear orphan receptor CAR-retinoid X receptor heterodimer activates the phenobarbital-responsive enhancer module of the *CYP2B* gene. *Mol. Cell. Biol.* **18**, 5652-5658.

Huang, W., Zhang, J., Washington, M., Liu, J., Parant, J. M., Lozano, G., and Moore, D. D. (2005) Xenobiotic stress induces hepatomegaly and liver tumors via the nuclear receptor constitutive androstane receptor. *Mol. Endocrinol.* **19**, 1646-1653.

Iida, M., Anna, C. H., Holliday, W. M., Collins, J. B., Cunningham, M. L., Sills, R. C., Devereux, T. R. (2005) Unique patterns of gene expression changes in liver after treatment of mice for 2 weeks with different known carcinogens and non-carcinogens. *Carcinogenesis* **26**, 689-99.

Kawamoto, T., Sueyoshi, T., Zelko, I., Moore, R., Washburn, K., and Negishi, M. (1999) Phenobarbital-responsive nuclear translocation of the receptor CAR in induction of the *CYP2B* gene. *Mol. Cell. Biol.* **19**, 6318-6322.

Klaus, A., and Birchmeier, W. (2008) Wnt signalling and its impact on development and cancer. *Nat. Rev. Cancer* **8**, 387-398.

Kolaja, K. L., Stevenson, D. E., Johnson J. T., Walborg, Jr., E. F., and Klaunig, J. E. (1996a) Subchronic effects of dieldrin and phenobarbital on hepatic DNA synthesis in mice and rats. *Fundam. Appl. Toxicol.* **29**, 219-228.

Kolaja, K. L., Stevenson, D. E., Walborg Jr., E. F., and Klaunig J. E. (1996b). Dose dependence of phenobarbital promotion of preneoplastic hepatic lesions in F344 rats and B6C3F1 mice: effects on DNA synthesis and apoptosis. *Carcinogenesis* **17**, 947-954.

Loeb, L. A., and Harris, C. C. (2008) Advances in chemical carcinogenesis: a historical review and prospective. *Cancer Res.* **68**, 6863-6872.

Luch, A. (2005) Nature and nurture - lessons from chemical carcinogenesis. *Nat. Rev. Cancer* **5**, 113-125.

Massagué, J. (2008) TGFβ in Cancer. *Cell* **134**, 215-230.

Michalopoulos, G. K. (2007) Liver regeneration. *J. Cell. Physiol.* **213**, 286-300.

Moennikes, O., Buchmann, A., Romualdi, A., Ott, T., Werringloer, J., Willecke, K., and Schwarz, M. (2000). Lack of phenobarbital-mediated promotion of hepatocarcinogenesis in connexin32-null mice. *Cancer Res.* **15**, 5087-5091.

Morey, J. S., Ryan, J. C., and Van Dolah, F. M. (2006) Microarray validation: factors influencing correlation between oligonucleotide microarrays and real-time PCR. *Biol. Proced. Online.* **8**, 175-193.

Papetti, M., and Herman, I. M. (2002) Mechanisms of normal and tumor-derived angiogenesis. *Am. J. Physiol. Cell. Physiol.* **282**, C947-970.

Peffer, R. C., Moggs, J. G., Pastoor, T., Currie, R. A., Wright, J., Milburn, G., Waechter, F., and Rusyn, I. (2007) Mouse liver effects of cyproconazole, a triazole fungicide: role of the constitutive androstane receptor. *Toxicol. Sci.* **99**, 315-325.

Phillips, J. M., and Goodman, J. I. (2008) Identification of genes that may play critical roles in phenobarbital (PB)-induced liver tumorigenesis due to altered DNA methylation. *Toxicol. Sci.* **104**, 86-99.

Phillips, J. M., and Goodman, J. I. (2009) Multiple genes exhibit phenobarbital (PB)-induced constitutive active/androstane receptor (CAR)-mediated DNA methylation changes during liver tumorigenesis and in liver tumors. *Toxicol. Sci.*, in press.

Phillips, J. M., Yamamoto. Y,, Negishi, M., Maronpot, R. R., and Goodman, J. I. (2007). Orphan nuclear receptor constitutive active/androstane receptor-mediated alterations in DNA methylation during phenobarbital promotion of liver tumorigenesis. *Toxicol. Sci.* **96**, 72-82.

Podsypanina, K., Du, Y. C., Jechlinger, M., Beverly, L. J., Hambardzumyan, D., and Varmus, H. (2008) Seeding and propagation of untransformed mouse mammary cells in the lung. *Science* **26**, 1841-1844.

Rangarajan, A., and Weinberg, R. A. (2003) Opinion: Comparative biology of mouse versus human cells: modelling human cancer in mice. *Nat. Rev. Cancer* **3**, 952-959.

Ray, J. S., Harbison, M. L., McClain, R. M., and Goodman, J. I. (1994) Alterations in the methylation status and expression of the *raf* oncogene in phenobarbital-induced and spontaneous B6C3F1 mouse liver tumors. *Mol. Carcinog.* **9**, 155-166.

Reya, T., Morrison, S. J., Clarke, M. F., and Weissman, I. L. (2001) Stem cells, cancer, and cancer stem cells. *Nature* **414**, 105-111.

Schwarz, M., Wanke, I., Wulbrand, U., Moennikes, O., and Buchmann, A. (2003) Role of connexin32 and β-catenin in tumor promotion in mouse liver. *Toxicol. Pathol.* **31**, 99-102.

Stahl, S., Ittrich, C., Marx-Stoelting, P., Köhle, C., Ott, T., Buchmann, A., and Schwarz, M. (2005) Effect of the tumor promoter phenobarbital on the pattern of global gene expression in liver of connexin32-wild-type and connexin32-deficient mice. *Int. J. Cancer* **115**, 861-869.

Sueyoshi, T., Kawamoto, T., Zelko, I., Honkakoski, P., and Negishi, M. (1999) The repressed nuclear receptor CAR responds to phenobarbital in activating the human *CYP2B6* gene. *J. Biol. Chem.* **274**, 6043-6046.

Sueyoshi, T., Moore, R., Sugatani, J., Matsumura, Y., and Negishi, M. (2008) PPP1R16A, the membrane subunit of protein phosphatase 1β, signals nuclear

translocation of the nuclear receptor constitutive active/androstane receptor. *Mol. Pharmacol.* **73**, 1113-1121.

Sugatani, J., Kojima, H., Ueda, A., Kakizaki, S., Yoshinari, K., Gong, Q. H., Owens, I. S., Negishi, M., and Sueyoshi, T. (2001) The phenobarbital response enhancer module in the human bilirubin UDP-glucuronosyltransferase *UGT1A1* gene and regulation by the nuclear receptor CAR. *Hepatology* **33**, 1232-1238.

Sun, Y. V., Boverhof, D. R., Burgoon, L. D., Fielden, M. R., and Zacharewski, T. R. (2004) Comparative analysis of dioxin response elements in human, mouse and rat genomic sequences. *Nucleic Acids Res.* **32**, 4512-4523.

Thiery, J. P. (2002) Epithelial-mesenchymal transitions in tumour progression. *Nat. Rev. Cancer* **2**, 442-454.

Ueda, A., Hamadeh, H. K., Webb, H. K., Yamamoto, Y., Sueyoshi, T., Afshari, C. A., Lehmann, J. M., and Negishi, M. (2002) Diverse roles of the nuclear orphan receptor CAR in regulating hepatic genes in response to phenobarbital. *Mol. Pharmacol.* **61**, 1-6.

Vorce, R. L., and Goodman, J. I. (1991). Hypomethylation of *ras* oncogenes in chemically induced and spontaneous B6C3F1 mouse liver tumors. *Toxicol. Environ. Health.* **34**, 367-384.

Warner, K. A., Fernstrom, M. J., and Ruch, R. J. (2003) Inhibition of mouse hepatocyte gap junctional intercellular communication by phenobarbital correlates with strain-specific hepatocarcinogenesis. *Toxicol. Sci.* **71**, 190-197.

Watson, R. E., and Goodman, J. I. (2002) Effects of phenobarbital on DNA methylation in GC-rich regions of hepatic DNA from mice that exhibit different levels of susceptibility to liver tumorigenesis. *Toxicol. Sci.* **68**, 51-58.

Wei, P., Zhang, J., Egan-Hafley, M., Liang, S., and Moore, D. D. (2000). The nuclear receptor CAR mediates specific xenobiotic induction of drug metabolism. *Nature* **407**, 920-923.

Whysner, J., Ross, P. M., and Williams, G. M. (1996). Phenobarbital mechanistic data and risk assessment: enzyme induction, enhanced cell proliferation, and tumor promotion. *Pharmacol. Ther.* **71**, 53-91.

Wu, Z., Irizarry, R. A., Gentleman, R., Martinez-Murillo, F., and Spencer, F. (2004) A model based background adjustment for oligonucleotide expression arrays. *J. Am. Stat. Assoc.* **99**, 909-917.

Wutz, A., Smrzka, O. W., Schweifer, N., Schellander, K., Wagner, E. F., Barlow, D. P. (1997) Imprinted expression of the *Igf2r* gene depends on an intronic CpG island. *Nature* **389**, 745-749.

Yamamoto, Y., Kawamoto, T., and Negishi, M. (2003) The role of the nuclear receptor CAR as a coordinate regulator of hepatic gene expression in defense against chemical toxicity. *Arch. Biochem. Biophys.* **409**, 207-211.

Yamamoto, Y., Moore, R., Goldsworthy, T. L., Negishi, M., and Maronpot, R. R. (2004) The orphan nuclear receptor constitutive active/androstane receptor is essential for liver tumor promotion by phenobarbital in mice. *Cancer Res.* **64**, 7197-7200.

Yang, J., Mani, S. A., and Weinberg, R. A. (2006) Exploring a new twist on tumor metastasis. *Cancer Res.* **66**, 4549-4552.

CHAPTER 2 APPENDIX

Data within the appendix consist of: Principal Component Analysis of the microarray data (Fig. 2.6), box plot depicting the distribution of microarray data (Fig. 2.7), microarray data of classical PB-induced genes (Table 2.3), data from qRT-PCR assays of uniquely active B6C3F1 genes (identified by microarray analysis) at 2 (Table 2.3) and 4 (Table 2.4) weeks, uniquely active B6C3F1 genes that show documented connections to 5 cancer-related processes at 2 (Table 2.6) and 4 (Table 2.7) weeks, uniquely active kinase, phosphatase, phosphatase activator (regulatory subunit), and phosphatase regulatory (inhibitor) genes that are candidates for involvement in PB-induced CAR activation (Table 2.8), and qRT-PCR data from genes identified from unique B6C3F1 RAMs at 2 and/or 4 weeks (Table 2.9). A scheme to classify PB-induced RAMs is found in Fig. 2.8. Note that these data are a subset of the total Supplementary Information that can be found in the version of this manuscript that is in press for publication in *Toxicological Sciences* in 2009.

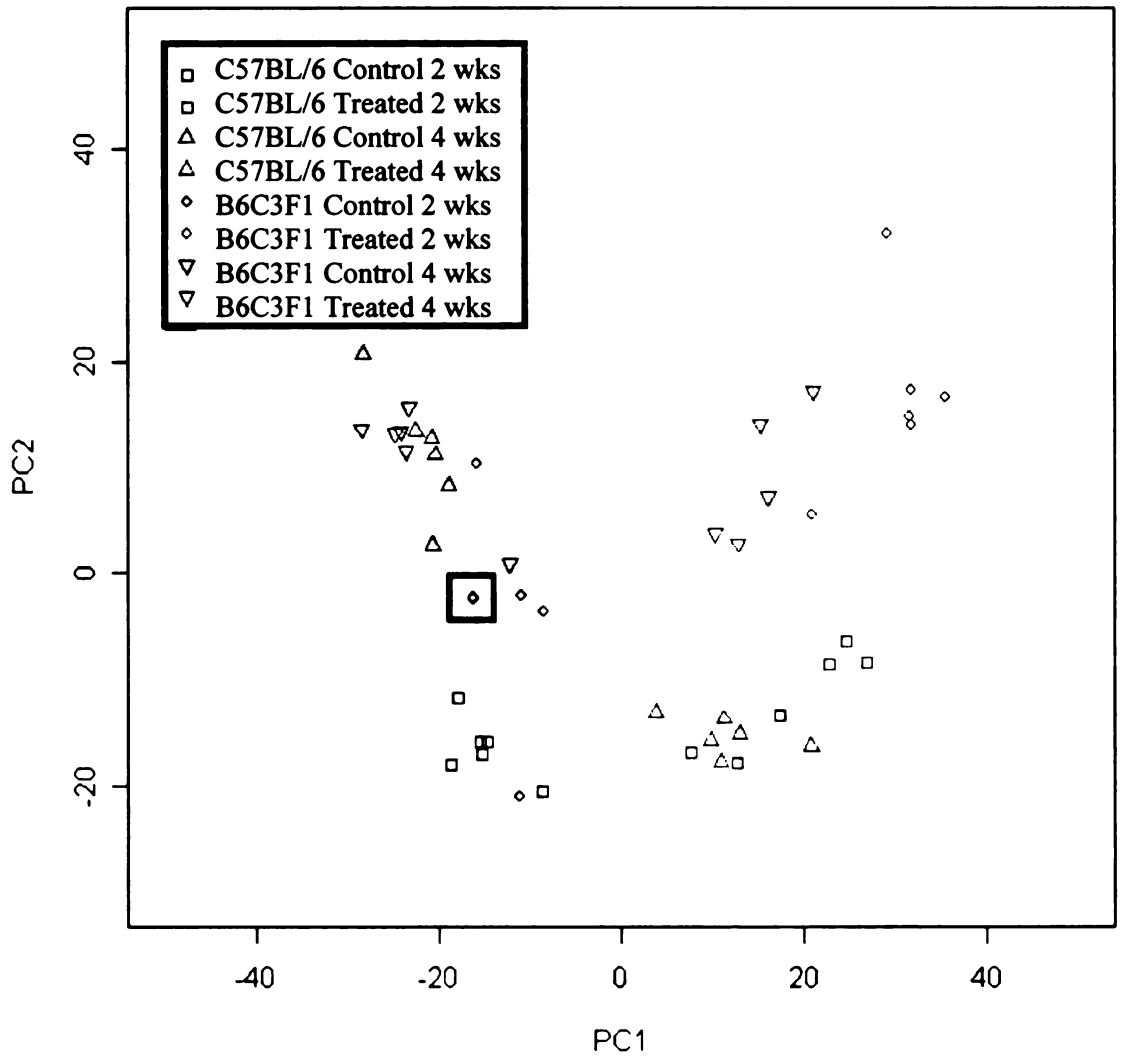


Figure 2.6 Principle Component Analysis (PCA) of Gene Expression Patterns of Individual B6C3F1 and C57BL/6 Mice Within Control and Phenobarbital (PB)-treated Groups at 2 and 4 Weeks. Microarray analysis of RNA isolated from livers of tumor-susceptible B6C3F1 and relatively resistant C57BL/6 mice left untreated (control), or administered 0.05% (w/w) PB in drinking water for 2 or 4 weeks, was performed. PCA of data from individual B6C3F1 and C57BL/6 mice depict similarities and differences of their overall gene expression patterns. PCA is a dimension reduction technique that creates axes through the data (Principal Components; PC) that account for variability within the data set. PC1 accounts for the largest variance, PC2 is orthogonal to PC1 and accounts for the next largest variance, and so forth, until all of the variance is explained. Data from 8 groups of mice (n = 6, with the exception of the B6C3F1, 4-week PB-treated group, n = 5) are shown. Data from 1 mouse in the B6C3F1, 4-week PB group was excluded because it does not fall within the boundaries of this chart, and as such, it was deemed an outlier and not utilized for subsequent analysis. The black box contains data points for 2 separate B6C3F1, 2-week control mice; they fall directly on top of one another. This image is presented in color.

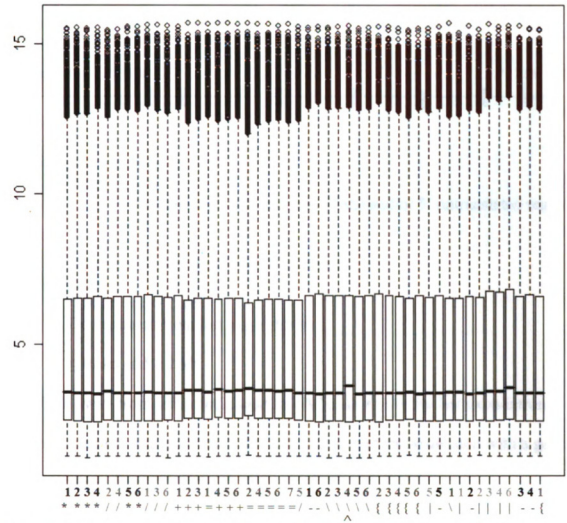
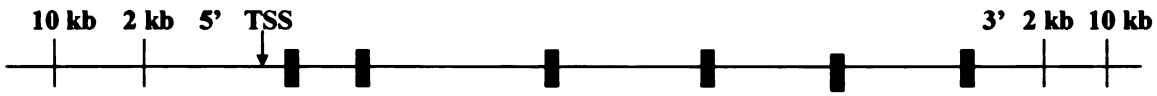


Figure 2.7 Distribution of Gene Expression Data Generated from Individual B6C3F1 and C57BL/6 Mice Within Control and Phenobarbital (PB)-treated Groups at 2 and 4 Weeks. Microarray analysis of RNA isolated from livers of tumor-susceptible B6C3F1 and relatively resistant C57BL/6 mice left untreated (control), or administered 0.05% (w/w) PB in drinking water for 2 or 4 weeks, was performed. A "box-and-whisker" plot was utilized to express the distribution of the data. The individual animals are listed by group, along the bottom of the chart, and the normalized intensity values (in log2 form), from the microarray data, are listed along the left-hand side. The white bars represent the interquartile range (IQR), which extends from the 25th to the 75th percentiles, and the horizontal black bars within the IQR represent the median value. The "whiskers" end at + 1.5 * IQR units. Every dot (o) beyond the "whiskers" reflects an outlying data point. The 8 groups of mice (n = 6) include: B6C3F1 controls at 2 (*) and 4 (+) weeks; B6C3F1 PB-treated at 2 (|) and 4 (\) weeks; C57BL/6 controls at 2 (/) and 4 (=) weeks; and C57BL/6 PB-treated at 2 (-) and 4 ({) weeks. One B6C3F1 4-week PB-treated animal which was deemed an outlier, and omitted from further analysis, because it fell outside the boundaries of the Principle Component Analysis (discussed in the legend to Appendix Figure 2), also appears different in this "box and whisker" plot (^).



1) Associated with a gene
    A. Within a gene
        i. Spans transcriptional start site (TSS) and/or 5' untranslated region
        ii. Exon
        iii. Intron
    B. Upstream from transcriptional start site
    i. $\leq$ 2 kb
    ii. $\leq$ 10 kb and > 2 kb
    C. Downstream from last exon/intron
    i. $\leq$ 2 kb
    ii. $\leq$ 10 kb and > 2 kb

2) > 10 kb away from either the transcriptional start site or the last exon/intron

3) Repeat element: multiple "top" hits and one/several are associated with a gene(s)

4) Repeat element: multiple "top" hits and no hits are associated with a gene(s)

Figure 2.8 A Scheme to Classify Cloned PCR Products that Represent Unique Phenobarbital (PB)-induced B6C3F1 Regions of Altered DNA Methylation (RAMs) Based on their Locations Within the Mouse Genome as Determined by BLAST-like Sequence Alignment Tool (BLAT) Searches (UCSC Genome Browser). PCR products representing unique B6C3F1 RAMs were cloned and subjected to BLAT searches. Depending on where, in relation to a gene, the PCR product aligned, it was assigned a particular genomic classification. For example, any PCR products designated as 1.B.i. are located less than or equal to 2 kilobases upstream from an annotated gene.

Table 2.3 Genes Encoding Drug-Metabolizing Enzymes that were Identified as Uniquely Active in B6C3F1 and C57BL/6 Mice

Gene[a]	Fold Change[b]			
	2 Weeks[c]		4 Weeks[c]	
	B6C3F1	C57BL/6	B6C3F1	C57BL/6
Cyp2b10	↑ 899.1	↑ 462.4	↑ 1076.8	↑ 584.1
Cyp2b9	↑ 27.0	↑ 82.2	↑ 27.4	↑ 103.0
Cyp2b13	↑ 18.3	↑ 47.1	↑ 12.5	↑ 76.6
Gstt3	↑ 13.6	↑ 8.0	↑ 12.0	↑ 10.4
Gsta2	↑ 4.7	↑ 2.8	↑ 3.8	↑ 2.5

[a]Representative genes encoding classical PB-induced drug-metabolizing enzymes that were identified as being uniquely active, based on microarray analysis (as described in the Methods), in liver-tumor susceptible B6C3F1 and relatively resistant C57BL/6 mice at both 2 and 4 weeks.

[b]Fold change of gene expression (↑, induction or ↓, repression) based on microarray analysis.

[c]Time point at which the uniquely active gene was detected.

Table 2.4 Quantitative Real-time PCR (qRT-PCR) Analysis of the Expression of 18 Genes that were Uniquely Active in Livers of B6C3F1 Mice at 2 Weeks of Phenobarbital (PB) Treatment

Uniquely Active Gene at 2 Weeks[a]	Fold Change Based on Microarray Analysis[b]	qRT-PCR Data					
		Mean Fold Change in PB-treated Group[c]		No. of animals above upper limit of 95% CI of control group[d]		No. of animals below lower limit of 95% CI of control group[d]	
		B6	C57	B6	C57	B6	C57
Abcc2[e]	2.01	↑ 1.76	↑ 1.57	6	6	0	0
Abcc3[f]	3.03	↑ 2.51	↑ 1.53	6	6	0	0
Bax[g]	2.77	n.c.	n.c.	3	1	0	2
Casp3	2.28	n.c.	n.c.	4	3	0	2
Cbs[f]	-2.13	↓ -2.28	↓ -1.31	0	0	6	5
Cebpb	3.12	↑ 3.81	n.c.	6	1	0	0
Cldn1[f]	-3.07	↓ -4.45	↓ -2.06	0	0	6	6
Ctgf[e]	2.86	↑ 2.98	↑ 2.26	6	6	0	0
Dnmt3b[f]	-2.56	↓ -6.60	↓ -4.08	0	0	6	6
Gadd45b[h]	2.00	↑ 4.28	↑ 2.60	6	6	0	0
Id3[e]	-2.33	↓ -1.71	↓ -1.56	0	0	5	6
Lcn2	5.91	n.c.	↑ 1.58	2	4	0	0
Prdm2[g]	-2.18	n.c.	n.c.	0	1	4	2
Pxr	2.22	↑ 1.43	n.c.	6	0	0	0
Shc1	2.35	n.c.	n.c.	0	0	3	0
Shmt1[g]	2.03	n.c.	n.c.	3	0	0	1
Slco1a4[f],+	3.52	↑ 2.96	↑ 1.33	6	5	0	0
Tnfsf10	2.56	↑ 1.26	n.c.	6	0	0	0

Table 2.4 continued Quantitative Real-time PCR (qRT-PCR) Analysis of the Expression of 18 Genes that were Uniquely Active in Livers of B6C3F1 Mice at 2 Weeks of Phenobarbital (PB) Treatment

[a]Seventeen uniquely active genes observed in livers of B6C3F1 mice only at 2 weeks, a subset of the 234 identified based on microarray analysis (as described in the Methods), were chosen for confirmation of their expression statuses by qRT-PCR. Additionally, 1 (of the 47 total) uniquely active carry forward genes (i.e. its induction or repression was observed in the B6C3F1 at both 2 and 4 weeks), indicated by the plus sign (+), was assayed at 2 weeks.

[b]Fold changes of gene expression are expressed as a change in a phenobarbital (PB)-treated group v. its time-matched control (up-regulation, ↑ or down-regulation, ↓). Those that are highlighted in gray were confirmed, or apparently confirmed, by qRT-PCR (as described in the Methods). (--) indicates that a gene was not active.

[c]All fold changes listed are statistically significant in a PB-treated group v. its time-matched control (Student's t-test, $p < 0.05$). No change (n.c.) indicates that the fold change was not significant.

[d]The 95% confidence interval (CI) of the control group data was calculated, and the number of samples (out of 6 total) from a PB-treated group that fell outside the 95% CI are listed. Highlighted in gray are those circumstances where data from at least 3 of the samples that fell outside the 95% CI of the control group data were considered an 'indication of a change', thus apparently confirming the microarray data (see footnote 'g').

[e]Expression was not confirmed, since the fold changes in the B6C3F1 and C57BL/6 mice were not statistically different (Student's t-test, $p < 0.05$).

[f]Expression was confirmed, since the fold changes in the B6C3F1 and C57BL/6 mice were statistically different (Student's t-test, $p < 0.05$).

[g]Expression was apparently confirmed.

[h]Expression was apparently confirmed. The level of expression in the B6C3F1 appears to be higher than that seen in the C57BL/6; however, this does not reach statistical significance due to a particularly low level of expression in one of the B6C3F1 mice.

Table 2.5 Quantitative Real-time PCR (qRT-PCR) Analysis of the Expression of 11 Genes that were Uniquely Active in Livers of B6C3F1 Mice at 4 Weeks of Phenobarbital (PB) Treatment

Uniquely Active Gene at 4 Weeks[a]	Fold Change Based on Microarray Analysis[b]	qRT-PCR Data					
		Mean Fold Change in PB-treated Group[c]		No. of animals above upper limit of 95% CI of control group[d]		No. of animals below lower limit of 95% CI of control group[d]	
		B6	C57	B6	C57	B6	C57
Alas1	8.12	↑ 4.57	↓ -3.14	6	0	0	6
Ephb4	2.24	↓ -1.25	n.c.	0	0	4	1
Gadd45a	4.27	↑ 2.32	n.c.	6	0	0	0
Map2k6	2.16	↑ 1.70	n.c.	4	1	0	0
Map3k5[e]	2.79	n.c.	↓ -1.20	4	0	0	4
Mtrr	4.48	↑ 1.43	↓ -1.36	6	0	0	6
Plk3[e]	5.85	n.c.	↓ -4.99	3	0	2	6
Ppargc1a	2.34	n.c.	n.c.	1	1	1	2
Shp	-2.51	↓ -1.94	n.c.	0	2	3	0
Slco1a4[f],+	2.14	↑ 1.64	↑ 1.56	4	5	0	0
Wee1	3.05	↑ 3.72	n.c.	5	0	0	1

Table 2.5 continued Quantitative Real-time PCR (qRT-PCR) Analysis of the Expression of 11 Genes that were Uniquely Active in Livers of B6C3F1 Mice at 4 Weeks of Phenobarbital (PB) Treatment

[a]Ten uniquely active genes observed in livers of B6C3F1 mice only at 4 weeks, a subset of the 86 identified based on microarray analysis (as described in the Methods), were chosen for confirmation of their expression statuses by qRT-PCR. Additionally, 1 (of the 47 total) uniquely active carry forward genes (i.e. its induction or repression was observed in the B6C3F1 at both 2 and 4 weeks), indicated by the plus sign (+), was assayed at 4 weeks.

[b]Fold changes of gene expression are expressed as a change in a phenobarbital (PB)-treated group v. its time-matched control (up-regulation, ↑ or down-regulation, ↓). Those that are highlighted in gray were confirmed, or apparently confirmed, by qRT-PCR. (--) indicates that a gene was not active.

[c]All fold changes listed are statistically significant in a PB-treated group v. its time-matched control (Student's t-test, $p < 0.05$). No change (n.c.) indicates that the fold change was not significant.

[d]The 95% confidence interval (CI) of the control group data was calculated, and the number of samples (out of 6 total) from a PB-treated group that fell outside the 95% CI are listed. Highlighted in gray are those circumstances where data from at least 3 of the samples that fell outside the 95% CI of the control group data were considered an 'indication of a change', thus apparently confirming the microarray data (see footnote 'e').

[e]Expression was apparently confirmed.

[f]Expression was not confirmed, since the fold changes in the B6C3F1 and C57BL/6 mice were not statistically different (Student's t-test, $p < 0.05$).

Table 2.6 Connections Between 5 Cancer-related Processes and Genes, Including those which Carried Forward, that were Uniquely Active in B6C3F1 Mice Following Treatment with Phenobarbital (PB) for 2 Weeks[a]

	Genes that ENHANCE growth, survival, angiogenesis, invasion, metastasis[b]		Genes that SUPPRESS growth, survival, angiogenesis, invasion, metastasis[b]	
	↑[c]	↓[c]	↓[c]	↑[c]
Totals[d] (out of 234 unique B6C3F1, 2-week genes)	**32** g = 23, a = 7, m = 4, s = 18, i = 6	**15** g = 13, a = 1, m = 2, s = 4, i = 3	**12** g = 9, a = 1, m = 0, s = 7, i = 0	**33** g = 21, a = 3, m = 3, s = 22, i = 5
	Ddit4 (s) Blnk (g,s) Kcnk5 (s) Sp3 (g) Gpr182 (g,i) Hmox1 (g,s) Ccne2 (g) **Shc1 (g,s,a)** **Cebpb (g,s)** Pfn1 (g) Tk1 (g) Pscd1 (g) Ngef (g) Cxcr7 (g,s,a,i,m) **Ctgf (g,a,i,m)** Aqp1(g,a,i,m) Slc37a4 (s,i) Gabpa (g) Gnpnat1 (g) **Shmt1 (g)** Hyal1 (g,a) Brap (s) **Tnfsf10 (s,a,i)** Pctp (s) Angptl4 (s,a,m) Fkbp5 (g,s) [e]**Gadd45b (g,s)** Mknk2(g,s) Dclre1a (s) St3gal5 (g) Pex11b (s) Pik3ap1 (g,s)	Pde4b (s) Crip2 (g) Eml4 (g) Zfp36l1 (g) Lrp5 (g,i) Map3k7ip2 (s) **Id3 (g,a,m)** **Dnmt3b (g)** Pkhd1 (g,s) **Cldn1 (g,i,m)** Inhba (g) Pdgfc (g) Clock (g) Insig2 (g,s,i) Pnkd (g)	Zfp36l1 (s,a) March7 (g) Ppp2r4 (s) **Prdm2 (g,s)** Irf6 (g) Cgn (g) **Id3 (g,s)** Cabc1 (g,s) Bach2 (g,s) Inhba (g) Nedd41 (s) Pkhd1 (g)	Lcn2 (s,i,m) **Tnfsf10 (s,a)** Tsc22d3 (g,s) Blnk (g) Ddit4 (g) Fbxo31 (g) Kcnk5 (s) Dpp8 (s) **Cebpb (g,s)** Errfi1 (g) Pctk3 (g,s) Pik3ap1 (g) Saa1 (g,s) Trim24 (g) Ak2 (s) Dnajb4 (g,i) Dclre1a (g) **Shc1 (s)** **Ctgf (g,s,a,i,m)** Pfn1 (g,i) **Bax (g,s)** Gmnn (g,s) Cebpd (g) **Casp3 (s)** Rarb (g,s) Bri3 (s) Gnpnat1 (s) Acads (s) Hyal1 (g,s) Saa2 (g,s) Angptl4 (g,a,i,m) Pklr(s) [e]**Gadd45b(s)**

Table 2.6 continued Connections Between 5 Cancer-related Processes and Genes, Including those which Carried Forward, that were Uniquely Active in B6C3F1 Mice Following Treatment with Phenobarbital (PB) for 2 Weeks[a]

Totals[d] **(out of 47 carry forward B6C3F1 genes)**	**9** g = 7, a = 0, m = 0, s = 5, i = 0	**2** g = 1, a = 1, m = 0, s = 1, i = 1	**1** g = 1, a = 0, m = 0, s = 0, i = 0	**5** g = 5, a = 0, m = 0, s = 4, i = 0
	D0H4S114 (g) Pfkfb3 (g) Dnaja1 (s) Pim3 (g,s) Hspa1b (s) Ppat (g) Nrg4 (g) Sh3bp2 (g,s) Pbef1 (g,s)	Ddah1 (g,a) Tff3 (s,i)	Tff3 (g)	Arl6ip5 (g,s) Fhit (g,s) Morc3 (g) Per1 (g,s) Per2 (g,s)
Totals[d] **(out of 281 unique B6C3F1, 2-week genes)**	**41** g = 30, a = 7, m = 4, s = 23, i = 6	**17** g = 14, a = 2, m = 2, s = 5, i = 4	**13** g = 10, a = 1, m = 0, s = 7, i = 0	**38** g = 26, a = 3, m = 3, s = 26, i = 5

[a]Uniquely active genes in livers of B6C3F1 mice at 2 weeks, including those that carried forward (i.e. exhibited similar expression changes, either **i**nduction of repression, at both 2 and 4 weeks), were identified as described in the Methods. Quantitative real-time PCR (qRT-PCR) was **p**erformed on a subset of these (see Appendix Table 2 for the complete data set), denoted here in **bolded font**, and genes whose expression **c**hanges were confirmed are underlined.

[b]Functional annotation revealed associations between key cancer-related processes (growth: g, survival: s, angiogenesis: a, invasion: i, and **m**etastasis: m) and many of the 281 total uniquely active genes at 2 weeks, which include genes observed only at 2 weeks, plus carry forward **g**enes.

[c]Gene symbols are listed in a particular column based on whether the literature indicates that the gene enhances or suppresses a particular process, **a**nd genes are further classified depending on whether their expression is induced (↑) or repressed (↓) by PB treatment. Note that a gene which **s**uppresses growth or survival can do so by promoting apoptosis and/or cell death.

[d]The total number of genes in each of the specific categories is depicted in **bold**. Those totals not listed in bold represent the genes, within a **c**ategory, that can participate in one or more cancer-related processes.

Table 2.7 Connections Between 5 Cancer-related Processes and Genes, Including those which Carried Forward, that were Uniquely Active in B6C3F1 Mice Following Treatment with Phenobarbital (PB) for 4 Weeks[a]

	Genes that ENHANCE growth, survival, angiogenesis, invasion, metastasis[b]		**Genes that SUPPRESS growth, survival, angiogenesis, invasion, metastasis**[b]	
	↑[c]	↓[c]	↓[c]	↑[c]
Totals[d] **(out of 86 unique B6C3F1, 4-week genes)**	**16** g = 8, a = 3, m = 1, s = 9, i = 3	**3** g = 3, a = 0, m = 0, s = 1, i = 0	**6** g = 5, a = 1, m = 0, s = 3, i = 0	**15** g = 10, a = 1, m = 1, s = 11, i = 3
	Hsph1 (g,s) **Mafb (g,s)** Thrsp (g,s) **Dnajb9 (s)** **Plk3 (g)** **Ppargc1a (a)** Ptp4a1 (g,i,m) Rnd3 (s) Bhlhb2 (s) **Ephb4 (g,s,a,i)** **Wee1 (s)** Bach1 (g) **Map3k5 (a)** **Map2k6 (i)** Tesk2 (s) Atp6v0a2 (g)	Fdft1 (g,s) Fgl1 (g) Arntl (g)	Ppap2c (s) Grk5 (g) **Fgl1 (g)** **Nr0b2/Shp (g,s)** Tsc22d1 (g) Osgin1 (g,s)	Efhd2 (s) **Ephb4 (g,s,i)** **Plk3 (g,s)** **Map3k5 (s)** **Gadd45a (g,s)** Hsph1 (s) Rnd3 (g,s) Mafb (g) Bhlhb2 (s) **Map2k6 (g,s,i,m)** **Wee1 (g)** Mme (g,a,i) **Ppargc1a (s)** Atp6v0a2 (g) Klf10 (g,s)
Totals[d] **(out of 47 carry forward B6C3F1 genes)**	**9** g = 7, a = 0, m = 0, s = 5, i = 0	**2** g = 1, a = 1, m = 0, s = 1, i = 1	**1** g = 1, a = 0, m = 0, s = 0, i = 0	**5** g = 5, a = 0, m = 0, s = 4, i = 0
	D0H4S114 (g) Pfkfb3 (g) Dnaja1 (s) Pim3 (g,s) Hspa1b (s) Ppat (g) Nrg4 (g) Sh3bp2 (g,s) Pbef1 (g,s)	Ddah1 (g,a) Tff3 (s,i)	Tff3 (g)	Arl6ip5 (g,s) Fhit (g,s) Morc3 (g) Per1 (g,s) Per2 (g,s)
Totals[d] **(out of 133 unique B6C3F1, 4-week genes)**	**25** g = 15, a = 3, m = 1, s = 14, i = 3	**5** g = 4, a = 1, m = 0, s = 2, i = 1	**7** g = 6, a = 0, m = 0, s = 3, i = 0	**20** g = 15, a = 1, m = 1, s = 15, i = 3

Table 2.7 continued Connections Between 5 Cancer-related Processes and Genes, Including those which Carried Forward, that were Uniquely Active in B6C3F1 Mice Following Treatment with Phenobarbital (PB) for 4 Weeks[a]

[a]Uniquely active genes in livers of B6C3F1 mice at 4 weeks, including those that carried forward (i.e. exhibited similar expression changes, either induction of repression, at both 2 and 4 weeks), were identified as described in the Methods. Quantitative real-time PCR (qRT-PCR) was performed on a subset of these (see Appendix Table 3 for the complete data set), denoted here in **bolded font**, and genes whose expression changes were confirmed are underlined.

[b]Functional annotation revealed associations between key cancer-related processes (growth: g, survival: s, angiogenesis: a, invasion: i, and metastasis: m) and many of the 133 total uniquely active genes at 4 weeks, which include genes observed only at 4 weeks, plus carry forward genes.

[c]Gene symbols are listed in a particular column based on whether the literature indicates that the gene enhances or suppresses a particular process, and genes are further classified depending on whether their expression is induced (↑) or repressed (↓) by PB treatment. Note that a gene which suppresses growth or survival can do so by promoting apoptosis and/or cell death.

[d]The total number of genes in each of the specific categories is depicted in **bold**. Those totals not listed in bold represent the genes, within a category, that can participate in one or more cancer-related processes.

Table 2.8 Kinase, Phosphatase, Phosphatase Activator (Regulatory Subunit), and Phosphatase Regulatory (Inhibitor) Genes Identified as Uniquely Active in Liver Tumor-Susceptible B6C3F1 Mice

	Gene[a]	Fold Change[b]	
		2 weeks[c]	4 weeks[c]
Kinases	Ak2	↑ 2.90	
	Ak3l1	↑ 2.18	
	Clk4	↑ 2.48	
	Mknk2	↑ 2.87	
	Pck1	↑ 2.68	
	Pctk3	↑ 2.99	
	Pi4kb	↑ 2.04	
	Pklr	↑ 2.04	
	Tk1	↑ 3.02	
	Camk1d	↓ 2.50	
	Pfkfb3	↑ 3.26	↑ 2.10
	Sbk1	↑ 3.75	↑ 2.16
	Adck5	↓ -2.11	↓ -2.54
	Map2k6*		↑ 2.16
	Map3k5*		↑ 2.79
	Plk3*		↑ 5.85
	Tesk2		↑ 2.25
	Taok3		↓ -2.20
	Grk5		↓ -2.27
	Pdk4		↓ -2.47
Phosphatases	Ptpn9	↓ -2.12	
	Pfkfb3	↑ 3.26	↑ 2.10
	Ptp4a1		↑ 3.46
	Ppap2c		↓ -2.19
Phosphatase Activator (Regulatory Subunit)	Ppp2r4	↓ -2.17	
Phosphatase Regulatory (Inhibitor) Subunit	Ppp1r3g	↑ 9.07	
	Ppp1r3b		↓ -2.17

[a] Uniquely active genes in B6C3F1 mice at 2 and/or 4 weeks, were identified based on microarray analysis, as described in the Methods. The expression changes of genes designated by asterisks (*) were confirmed by quantitative real-time PCR (Appendix Table 3).

[b] Fold change of gene expression (↑, induction or ↓,repression) based on microarray analysis.

[c] Time point at which the uniquely active gene was detected.

Table 2.9 Quantitative Real-time PCR (qRT-PCR) Analysis of Genes which Exhibited Unique Phenobarbital (PB)-induced Regions of Altered DNA methylation (RAMs) in Liver Tumor-Susceptible B6C3F1 Mice

Gene[a]	Genomic Location of Unique RAM[b]	Methylation Status at 2 and/or 4 Weeks[c]	Time Point of qRT-PCR	B6C3F1		C57BL/6		Summary of Methylation and Expression Statuses in B6C3F1
				Fold Change[d]	No. of Mice that Exhibited Change Outside 95% CI of Control Group[c]	Fold Change[d]	No. of Mice that Exhibited a Change Outside 95% CI of Control Group[c]	
Bcat2: branched chain aminotransferase 2, mitochondrial	Exonic (1.A.ii)	NewM	4 wk	↓ -1.38	--	n.c.	↑ 4	Unique expression change in B6C3F1 v. C57BL/6; apparent association between ↑ methylation levels and ↓ expression
Bcl2l13: BCL2-like 13 (apoptosis facilitator)	Intronic (1.A.iii)	4 wk: NewM	4 wk	↓ -1.83*	--	↓ -1.46	--	
Ube2d1: ubiquitin-conjugating enzyme E2D 1, UBC4/5 homolog (yeast)	> 2 and ≤ 10 kb upstream from TSS (1.B.ii)	2 wk: HypoM or NewM[f] 4 wk: NewM	4 wk	↓ -2.26*	--	↓ -1.48	--	
Srms: src-related kinase lacking..myristylation sites	Spans TSS and/or 5' UTR (1.A.i)	2 wk: HypoM or HyperM, and/or NewM[f]	2 wk	↓ -8.65^	--	↓ -3.31	--	Expression changes in B6C3F1 and C57BL/6 were not different; apparent association between ↑ methylation levels and ↓ expression or ↓ methylation levels and ↓ expression[g]
Trio: triple functional domain (PTPRF interacting)	Exonic (1.A.ii)	2 wk: HypoM or NewM[f] 4 wk: HypoM or HyperM[f]	4 wk	↓ -1.60^	--	↓ -1.44	--	
Ncor2: nuclear receptor co-repressor 2	Intronic (1.A.iii)	4 wk: NewM	4 wk	↓ -1.54[§]	--	↓ -2.02	--	Extent of expression change in B6C3F1 was less than that in the C57BL/6; apparent association between ↑ methylation levels and ↓ expression

Table 2.9 continued Quantitative Real-time PCR (qRT-PCR) Analysis of Genes which Exhibited Unique Phenobarbital (PB)-induced Regions of Altered DNA methylation (RAMs) in Liver Tumor-Susceptible B6C3F1 Mice

Anapc7: anaphase promoting complex subunit 7	$\leq$ 2 kb upstream from TSS (1.B.i)	4 wk: HypoM	4 wk	↓ -1.40	--	n.a.[h]	n.a.[h]	Expression levels were only evaluated in the B6C3F1[b], and a change (or an indication of) was observed; apparent association between ↓ methylation levels and ↓ expression
Ddx54: DEAD (Asp-Glu-Ala-Asp) box polypeptide 54	Intronic (1.A.iii)	2 wk: HypoM 4 wk: HypoM	4 wk	↓ -1.17	--	n.a.	n.a.	
Plekhf1: pleckstrin homology domain containing, family F (with FYVE domain) member 1	> 2 and $\leq$ 10 kb downstream from last exon/intron (1.C.ii)	2 wk: NewM 4 wk: HypoM	4 wk	↓ -1.47	--	n.a.	n.a.	
Ppp4c: protein phosphatase 4, catalytic subunit	Intronic (1.A.iii)	2 wk: HypoM	2 wk	n.c.	6: ↓ 4, ↑ 2	n.a.	n.a.	
Prickle2: prickle-like 2 (Drosophila)	> 2 and $\leq$ 10 kb upstream from TSS (1.B.ii)	2 wk: HypoM and/or NewM[f] 4 wk: HypoM	4 wk	n.c.	5: ↓ 4, ↑ 1	n.a.	n.a.	
Tcf4: transcription factor 4	Intronic (1.A.iii)	2 wk: HypoM and/or HyperM[f] 4 wk: HypoM	4 wk	↓ -1.51	--	n.a.	n.a.	
Tnk2: tyrosine kinase, non-receptor, 2	Intronic (1.A.iii)	4 wk: HypoM	4 wk	↓ -1.49	--	n.a.	n.a.	

Table 2.9 continued Quantitative Real-time PCR (qRT-PCR) Analysis of Genes which Exhibited Unique Phenobarbital (PB)-induced Regions of Altered DNA methylation (RAMs) in Liver Tumor-Susceptible B6C3F1 Mice

Cma1: chymase 1, mast cell	> 2 and ≤ 10 kb downstream from last exon/intron (1.C.ii)	4 wk: HypoM	4 wk	n.c.[1]	--	n/a	n/a	Expression levels were only evaluated in the B6C3F1[h]: no indication of an expression change was observed
Efnb2: ephrin B2	Intronic (1.A.iii)	2 wk: HypoM or NewM[f] 4 wk: HypoM or HyperM[f]	4 wk	n.c.	--	n/a	n/a	
Ptpro: protein tyrosine phosphatase, receptor type, O	Intronic (1.A.iii)	2 wk: HypoM and/or NewM[f] 4 wk: HypoM and/or HyperM[f]	4 wk	n.c.	--	n/a	n/a	
Ralgds: ral guanine nucleotide dissociation stimulator	Intronic (1.A.iii)	4 wk: HypoM	4 wk	n.c.	--	n/a	n/a	
Rxrb: retinoid X receptor beta	Intronic (1.A.iii)	4 wk: NewM	4 wk	n.c.	--	n/a	n/a	
Tgfbr2: transforming growth factor, beta receptor II	Intronic (1.A.iii)	4 wk: HypoM	4 wk	n.c.	--	n/a	n/a	

Table 2.9 continued Quantitative Real-time PCR (qRT-PCR) Analysis of Genes which Exhibited Unique Phenobarbital (PB)-induced Regions of Altered DNA methylation (RAMs) in Liver Tumor-Susceptible B6C3F1 Mice

[a]Genes identified from unique RAMs in the B6C3F1 mice, as compared to the relatively resistant C57BL/6, at 2 and/or 4 weeks (Phillips and Goodman, 2008).

[b]Genomic location of the RAM, based on a classification scheme in Appendix Figure 3. Abbreviations: TSS, transcriptional start site; UTR, untranslated region.

[c]PB-induced decreases in methylation (Hypomethylation, HypoM) and increases in methylation (Hypermethylation, HyperM and new methylation, NewM), as determined by Phillips and Goodman (2008).

[d]A fold change of gene expression (↑, up-regulation or ↓, down-regulation) is listed if it was statistically significant (Student's t-test, $p < 0.05$) in a treatment group (v. its time-matched control). If it was not significant, no change (n.c.) is listed. For *Bcl2l13* and *Ube2d1* (*), the fold change in the B6C3F1 was statistically greater than that in the C57BL/6 (Student's t-test, $p < 0.05$). *Srms* and *Trio* (^) exhibited fold changes in the B6C3F1 and C57BL/6 that were not statistically different (Student's t-test, $p < 0.05$). For *Ncor2* (§), the extent of the change in the B6C3F1 was statistically less than (Student's t-test, $p \leq 0.05$) that in the C57BL/6.

[e]If a fold change was not statistically significant, a gene was considered to show an 'indication of a change' if data from at least 3 of the 6 samples in the PB-treated group fell outside (above, ↑ or below, ↓) the 95% confidence interval (CI) of the control group data. If there was no indication of a change, or if a fold change was statistically significant, these data are not shown (--).

[f]Methylation status was ambiguous (i.e. could not be definitively determined), as described in detail in Phillips and Goodman (2008).

[g]The methylation statuses of *Srms* (at 2 weeks) and *Trio* (at 4 weeks) were ambiguous, so it was not possible to conclusively establish an association between the methylation and expression statuses.

[h]n.a. indicates that qRT-PCR was not performed. B6C3F1 expression data were generated for all of the genes at the indicated time points. However, C57BL/6 expression data were generated only if the B6C3F1 methylation and expression statuses appeared to be inversely correlated (i.e. decreased methylation levels were associated with increased expression, or increased methylation levels were associated with decreased expression), assuming that DNA methylation changes in key regions (e.g., regulatory elements) can control gene expression.

THESIS
E
142
340
THS

LIBRARY
Michigan State
University

PLACE IN RETURN BOX to remove this checkout from your record.
TO AVOID FINES return on or before date due.
MAY BE RECALLED with earlier due date if requested.

DATE DUE	DATE DUE	DATE DUE

5/08 K:/Proj/Acc&Pres/CIRC/DateDue.indd

IDENTIFICATION OF GENES INVOLVED IN TUMORIGENESIS THAT ARE DEREGULATED, WITH AN EMPHASIS ON ALTERED DNA METHYLATION

VOLUME II

By

Jennifer Marie Phillips

A DISSERTATION

Submitted to
Michigan State University
In partial fulfillment of the requirements
for the degree of

DOCTOR OF PHILOSOPHY

Biochemistry and Molecular Biology

2009

CHAPTER 3

ORPHAN NUCLEAR RECEPTOR CONSTITUTIVE ACTIVE/ANDROSTANE RECEPTOR (CAR)-MEDIATED ALTERATIONS IN DNA METHYLATION DURING PHENOBARBITAL (PB) PROMOTION OF LIVER TUMORIGENESIS

This chapter represents a manuscript that was published in *Toxicological Sciences* **96**, p. 72–82, 2007. The authors are Jennifer M. Phillips, Yukio Yamamoto, Masahiko Negishi, Robert R. Maronpot, and Jay I. Goodman.

ABSTRACT

Altered DNA methylation is an epigenetic mechanism that plays a key role in the carcinogenesis process, and the nongenotoxic rodent hepatocarcinogen phenobarbital (PB) alters the methylation status of DNA in mouse liver. The constitutive active/androstane nuclear receptor (CAR) mediates half of the PB-induced hepatic gene expression changes and it is essential for liver tumor promotion in PB-treated mice. Here, a technique involving methylation-sensitive restriction digestion, arbitrarily primed PCR, and capillary electrophoresis was utilized to detect PB-induced regions of altered DNA methylation (RAMs) in CAR wildtype (WT) mice that are sensitive to promotion by PB and resistant CAR knockout (KO) mice. The CAR WT mice developed preneoplastic lesions after 23 wk of PB treatment (precancerous) and liver tumors after 32 wk, while the CAR KO mice did not develop tumors (Yamamoto *et al.*, 2004). Our goal was to discern those RAMs which are playing important roles in tumor formation by comparing the RAMs that form in sensitive and resistant groups of mice. Using this novel approach, 42 unique RAMs were identified in the precancerous as compared to the CAR KO, 23 wk PB-treated tissue. Of these 42 RAMs, 14 carried forward to the tumor tissue, and additionally, 104 total unique RAMs were observed in the tumor tissue. These results indicate that unique RAMs occurred in the sensitive CAR WT mice and that a portion of these were seen in both the precancerous and tumor tissue. We hypothesize that these unique RAMs may be facilitating the tumorigenesis process, and these data support the view that DNA methylation plays a causative role in PB-induced tumorigenesis.

INTRODUCTION

The constitutive active/androstane receptor (CAR) is a member of the orphan nuclear receptor subfamily, which lacks known physiological ligands (Mohan and Heyman, 2003). CAR is expressed primarily in the liver and the small intestine, and at lower levels in heart, muscle, kidney, and lung tissue (Baes *et al.*, 1994). The role of CAR in detoxification is supported by the observations that it is activated by a variety of xenobiotics and mediates the upregulation of several phase I and II drug-metabolizing enzymes, e.g., CYP450s, glutathione S-transferases and UDP-glucuronosyltransferases (Ueda *et al.*, 2002a) in addition to drug transporters (Kast *et al.*, 2002; Assem *et al.*, 2004). CAR also contributes to the metabolism of endogenous compounds such as bilirubin, and steroid and thyroid hormones in response to exogenous agents (Kodama and Negishi, 2006), and its regulation of enzymes involved in energy metabolism is a component of the response to xenobiotic stress (Swales and Negishi, 2004). Finally, in addition to acting as a component of a transcription factor, CAR may interact with proteins leading to alteration of their function, e.g., CAR binding to the FoxO1 protein inhibits the ability of the latter to increase gluconeogenesis (Kodama and Negishi, 2006).

Phenobarbital (PB) is a prototypical nongenotoxic rodent liver tumor promoter that stimulates the expression of drug-metabolizing enzymes, in addition to causing hepatic hypertrophy and hyperplasia (Whysner, 1996). PB facilitates the translocation of CAR from the cytoplasm to the nucleus where it forms a heterodimer with the retinoid X receptor (RXR) which can bind to the PB-responsive element located within the promoter region of particular genes, e.g., *Cyp2b10*, leading to upregulation of their expression (Honkakoski *et al.*, 1998). Furthermore, microarray data from Ueda *et al.* (2002a)

indicate that PB alters the expression of 138 hepatic genes, increasing the expression of some while decreasing the expression of others, and approximately half of these changes are CAR-dependent. Thus, not all of the hepatic effects of PB are CAR-dependent. CAR also mediates PB-induced hepatomegaly (Wei *et al.*, 2000), and is essential for liver tumor promotion by PB in C3H/He mice following initiation with diethylnitrosamine (DEN) (Yamamoto *et al.*, 2004). Additionally, chronic activation of CAR by the potent PB-like inducer 1,4-Bis[2-(3,5-dichloropyridyloxy)]benzene (TCPOBOP) results in mouse liver tumor formation (Huang *et al.*, 2005).

Altered DNA methylation, an epigenetic mechanism which plays a key role in the regulation of gene expression, may play multiple roles in carcinogenesis (Counts and Goodman, 1995). The epigenetic DNA modification 5-methylcytosine accounts for approximately 3-5% of all DNA bases and is found at 70-80% of all CpG dinucleotides in the genome (Ehrlich *et al.*, 1982). Methylation at CpNpG sites also occurs in the mammalian genome (Clark *et al.*, 1995). Aberrant patterns of DNA methylation have been implicated in carcinogenesis. For example, the genomes of cancer cells are globally hypomethylated as compared to their normal counterparts (Gama-Sosa *et al.*, 1983) and decreased levels of methylation have been shown to cause activation of oncogenes such as *R-ras* and cyclin D2 (Nishigaki *et al.*, 2005; Oshimo *et al.*, 2003), in addition to chromosomal instability and increased tumor formation (Eden *et al.*, 2003; Gaudet *et al.*, 2003). Concurrently, GC-rich regions in the promoters of tumor suppressor genes in cancer cells become hypermethylated, resulting in gene silencing (Jones and Laird, 1999). Both mutation and epigenetic alterations are thought to play critical roles at all stages of the multistep/multistage model of the carcinogenesis process (Goodman and

Watson, 2002), which can be divided into experimentally determined stages, i.e., initiation, promotion, and progression (Dragan *et al.*, 1993).

Tumor promoters increase cell proliferation in target tissue and suppress apoptosis, thus facilitating the clonal expansion of initiated cells (Schulte-Hermann *et al.*, 1990). PB treatment alters hepatic DNA methylation status, and the effects, specifically hypermethylation of internal and external cytosines of 5' CCGG 3' sequences, are greater in liver tumor-prone as compared to resistant strains of mice (Watson and Goodman, 2002). In addition, unique PB-induced regions of altered methylation (RAMs) were identified in sensitive B6C3F1 mice as compared to relatively resistant C57BL/6 mice (Bachman *et al.*, 2006b). The comparison of RAMs that form in liver tumor-susceptible mice as compared to those that are relatively resistant results in the identification of RAMs that occur uniquely in the sensitive group and provides the opportunity to discern PB-induced methylation changes which may be crucial to the tumorigenesis process (Bachman *et al.*, 2006b).

In the current study, the methylation status of DNA was evaluated in mouse liver samples used by Yamamoto *et al.* (2004) where CAR wildtype (WT) and CAR knockout (KO) animals received one initiating dose of DEN followed by treatment with PB. CAR WT mice developed preneoplastic hepatic lesions after 23 wk and tumors after 32 wk of PB treatment, while the CAR KO mice did not form preneoplastic hepatic lesions after 23 wk of PB treatment and liver tumors were not observed after 32 wk of PB treatment (Yamamoto *et al.*, 2004). The PB-induced RAMs that occurred in the sensitive CAR WT mice were compared to those in the resistant CAR KO mice in order to evaluate the hypothesis that the RAMs that formed uniquely in the sensitive mice may play a role in

key events that occur during liver tumor formation. Our goal is to identify RAMs that play a role in mouse liver tumorigenesis by ascertaining those that occur uniquely in the sensitive CAR WT mice as compared to resistant CAR KO mice.

MATERIALS AND METHODS

Animals, Treatments and Tissue Samples

CAR KO (homozygous null) mice on a C57BL/6 background were backcrossed to C3H/HeNCrlBR mice (Charles River Laboratories, Wilmington, MA) (Yamamoto *et al.*, 2004). The C3H/He mouse is a strain that is highly susceptible to liver tumorigenesis (Buchmann *et al.*, 1991). The male mice used for these studies were housed in a specific pathogen-free facility and cared for in accordance with the National Institute of Health guidelines for the care and use of laboratory animals. CAR WT or CAR KO mice were injected with a single intraperitoneal dose of diethylnitrosamine (DEN), 90 mg/kg, at 5 wk of age and then administered drinking water (control) or 0.05% PB (w/w) in drinking water starting at 7 wk of age and continuing for 23 or 32 wk, resulting in the following groups of mice: CAR KO, 23 wk control, CAR KO, 23 wk PB, CAR WT, 23 wk control, CAR WT, 23 wk PB (precancerous tissue), and CAR WT, 32 wk PB (tumor tissue) (Yamamoto *et al.*, 2004). Animals were sacrificed at the end of the indicated timepoints, and their livers were quickly removed and frozen in liquid nitrogen. Liver samples were obtained from 6 mice in each experimental group. Tissue samples from the CAR WT, 23 wk PB group were taken from non-lesion areas of the liver, and 6 samples of tumor tissue were obtained.

Histopathology was performed. Tumors were selected based upon a limited availability for methylation studies, four adenomas and two carcinomas were selected. Thus, we were able to evaluate control tissue versus precancerous (CAR WT, 23 weeks PB) and precancerous tissue versus tumor tissue. However, due to the limited availability of samples, we were not able to evaluate specifically adenomas versus carcinomas.

Regarding the precancerous tissue (CAR WT, 23 weeks PB), there were no visible alterations, that is, no nodules and no adenomas (based upon histology of adjacent tissue). However, there could have been microscopic foci of cellular alteration in the frozen samples. Overall, the adjacent fixed specimens did occasionally have one or two small foci.

DNA isolation

Liver tissue was homogenized in 1ml of TRIzol® Reagent (Invitrogen, Carlsbad, CA). DNA was isolated via the manufacturer's protocol.

Evaluation of DNA Methylation Status by Arbitrarily Primed PCR and Capillary Electrophoresis

DNA methylation status was evaluated by an arbitrarily primed PCR and capillary electrophoresis procedure (Bachman *et al.*, 2006b). This technique permits the simultaneous evaluation of treatment-related hypomethylations (less methylation in a region that was methylated in control), hypermethylations (more methylation in a region that was methylated in control) and new methylations (methylation in a region that was not methylated in control) in numerous regions of the genome.

Restriction Digests

Each DNA sample was subjected to 3 separate double restriction digests that were performed in duplicate with a) a methylation-insensitive enzyme and b) a methylation-sensitive enzyme. Digestion with a methylation-insensitive enzyme, *RsaI* or *BfaI,* ensures complete digestion by the methylation-sensitive enzyme, *MspI, HpaII*, or *BssHII.*

Restriction digestion with *RsaI/MspI* and *RsaI/HpaII* was carried out as described previously (Bachman *et al.*, 2006b). *MspI* and *HpaII* recognize 5' CCGG 3' sites and cut between the internal cytosine and guanine. *MspI* will not restrict DNA if the external cytosine is methylated, while *HpaII* will not restrict DNA if the internal cytosine is methylated.

Restriction digestion with *BfaI/BssHII* was performed as described in a previous study (Bachman *et al.*, 2006b). *BssHII* recognizes 5' GCGCGC 3' sites and cuts between the first guanine and cytosine residues and will not restrict DNA if several combinations of cytosines in the sequence are methylated[1]. *BfaI* sites appear less frequently in CpG islands than RsaI sites and, thus, CpG islands are more intact following digestion of DNA with the former enzyme as compared to the latter (Shiraishi *et al.*, 1995). Therefore, the use of *BfaI* in combination with *BssHII*, a 6-base rare cutter with a GC-rich recognition sequence, provides an additional, important "window" into our DNA methylation status analysis which complements the data obtained from the *RsaI/MspI* and *RsaI/HpaII* digests.

Arbitrarily Primed PCR (AP-PCR) and Capillary Electrophoretic Separation of Products

AP-PCR and capillary electrophoresis were performed as described previously (Bachman *et al.*, 2006b), however two corrections were made: The 5 cycle stage of the AP-PCR reaction was followed by 30 cycles (not 40 cycles stated originally, as this was an error) of 94°C for 30 s (not 15 s stated originally, as this was an error), 55°C for 15 s, and 72°C for 1 min. The digested DNA was subjected to AP-PCR using a single arbitrary primer,

[1]http://rebase.neb.com/cgi-bin/msget?BssHII

5' AAC CCT CAC CCT AAC CCC GG 3' (Gonzalgo *et al.*, 1997) which was fluorescently labeled at the 5' end with HEX™ (Integrated DNA Technologies, Coralville, IA). This primer binds well to GC-rich regions and the 5' CCGG 3' sequence at its 3' end increases the probability of binding to the *MspI* and *HpaII* restriction sites, permitting the detection of methylation at the site of primer annealing and between sites of primer annealing. AP-PCR products were quantified using the ND-1000 UV-Vis Spectrophotometer (Nanodrop Technologies, Wilmington, DE).

Data Analysis

The results as size of PCR products, in base pairs, and their corresponding peak areas are analyzed using the Excel® program. A consensus, average peak area is calculated for each experimental group. This permits the consensus peak areas of one group to be compared with another to determine if there are differences in methylation at a particular PCR product size, and if so, these PCR products are considered to be regions of altered methylation (RAMs). In this study, 1) the CAR KO, 23 wk PB data were compared to the CAR KO, 23 wk control data, and 2) both the CAR WT, 23 wk PB (precancerous tissue) and CAR WT, 32 wk PB (tumor tissue) data were compared to the CAR WT, 23 wk control data. Treatment-related RAMs include: a) hypomethylations, both 100% decreases and decreases which are statistically significant when compared to control, b) hypermethylations which are increases that are statistically significant when compared to control and c) new methylations in which PCR product formed following treatment but did not form under control conditions. For each PCR product size, the consensus treated peak area was compared to the consensus control peak area using a Student's *t*-test

($p<0.05$). Each statistically significant difference was counted as a change in methylation (categorized as hypo- or hypermethylations) and only those methylation changes that were statistically significant are reported. All 100% hypomethylations were considered significant. Additionally, all new methylations, indicated by the formation of PCR product in the treated group and no product formation in the control group at a particular PCR product size, were considered significant. A detailed description of the data analysis procedure was described previously (Bachman *et al.*, 2006a; Bachman *et al.*, 2006b).

Assumptions

The following assumptions are made during the data analysis procedure: 1) each separate PCR product of a defined size represents a distinct region of the genome, 2) a region can include one or more recognition sequences for the specific methylation-sensitive restriction enzyme employed located between the annealing sites of the up- and down-stream primers; thus, the amount of each PCR product formed can be viewed as representing an "average" of the methylation status of the particular recognition sequences located between the up- and down-stream primers and 3) differences in the amount of each PCR product between the groups being compared represent the altered methylation status of a particular GC-rich region of DNA.

Statistical Analysis

In order to determine if the RAMs that occurred at the same PCR product size in 2 experimental groups are equivalent (common RAMs) or different (unique RAMs),

analysis of variance (ANOVA) tests ($p<0.05$) were performed. ANOVA tests analyze the difference between the means of 2 or more groups and an advantage over the use of multiple *t*-tests is the decreased probability of finding significance by chance. One-way ANOVA analysis was utilized to compare the magnitudes of the methylation changes that occurred at the same PCR product size in the CAR WT, 23 wk PB- (precancerous) and the CAR WT, 32 wk PB-treated (tumor) tissue because only one independent variable (i.e. duration of PB treatment) exists. Two-way ANOVA tests were executed to determine if the magnitudes of the RAMs that occurred at the same PCR product size as a result of PB treatment in the CAR WT, 23 wk and the CAR KO, 23 wk groups were equivalent or different because there are 2 independent variables (i.e. duration of PB treatment and mouse strain).

Common and Unique Regions of Altered Methylation (RAMs)

PCR products of identical size that exhibit methylation changes in 2 experimental groups (e.g., precancerous and CAR KO, 23 wk PB-treated tissue or tumor and precancerous tissue) are considered to be common RAMs. A region is considered to be a carry forward RAM if the methylation changes associated with the common RAM in the precancerous and tumor tissue occur in the same direction and are equivalent as determined by one-way ANOVA ($p<0.05$). RAMs in common between 2 experimental groups are considered to be unique RAMs if: 1) the methylation changes are opposite in direction (i.e. in the same region, a hypomethylation is elicited by one treatment and a hypermethylation occurs as a result of a second treatment), or 2) the changes in methylation occur in the same direction (i.e. both changes are hypermethylations) but the

extents of change are statistically different as determined by two-way, $p<0.05$ (for precancerous vs. CAR KO, 23 wk PB-treated tissue) or one-way ANOVA, $p<0.05$ (for tumor vs. precancerous tissue). In addition, RAMs are considered to be unique if they are observed only in a particular treatment group. For instance, a RAM may be observed only in the precancerous tissue (vs. CAR KO, 23 wk PB-treated tissue) or only in the tumor tissue (vs. precancerous tissue).

Percent Dissimilarity Calculations

Treatment Group vs. Control Group

The dissimilarity between control patterns of methylation and PB-induced patterns was calculated for 3 treatment vs. control groups (CAR KO, 23 wk PB vs. CAR KO, 23 wk control tissue, precancerous vs. CAR WT, 23 wk control tissue, and tumor vs. CAR WT, 23 wk control tissue). The total number of PCR products reporting in the control was added to the total number of unique PCR products (i.e. those PCR product sizes that were not formed under control conditions) reporting from treatment to obtain the total number of different sized PCR products reporting in the control and treatment groups. The total number of RAMs (hypomethylations, hypermethylations, and new methylations) in the treatment group divided by the total number of different sized PCR products that reported in the control and treatment group, expressed as a percent, equals the percent dissimilarity of the treatment as compared to the control pattern of methylation.

RESULTS

The procedure employed, which involves methylation-sensitive restriction digestion, arbitrarily primed PCR, and capillary electrophoresis, permits the simultaneous detection of treatment-related hypermethylations, hypomethylations, and "new" methylations throughout GC-rich regions of the genome. Administration of PB resulted in numerous RAMs in the livers of CAR WT mice treated for 23 wk, CAR KO mice treated for 23 wk and in liver tumors observed following treatment of CAR WT mice for 32 wk (Table 3.1 and Figures 3.1-3.3). The actual basic, underlying data for Table 3.1 and Figures 3.1-3.3 are located in the Appendix (Figures 3.1-3.3).

Treatment of WT mice with PB for 23 wk (precancerous tissue) and 32 wk (tumor tissue) resulted in the detection 47 and 129 RAMs, respectively (Table 3.1). Considerable increases of both hypomethylations and "new" methylations occurred, displaying greater then 2.6- and 4.3-fold increases, respectively, from precancerous to tumor tissue (Table 3.1). While the total number of RAMs detected in the precancerous and the CAR KO, 23 wk PB-treated tissue were approximately equal, the specific alterations differed. There were no hypermethylations observed in the CAR KO, 23 wk PB-treated tissue, while 10 occurred in the precancerous tissue. Furthermore, approximately twice the number of hypomethylations occurred in the CAR KO, 23 wk PB-treated tissue as in the precancerous tissue (Table 3.1).

In order to ascertain methylation changes that may play key roles in liver tumor formation in the CAR WT C3H/He mice, unique RAMs in the precancerous as compared to the CAR KO, 23 wk PB-treated tissue were first identified (Figure 3.1A). There were

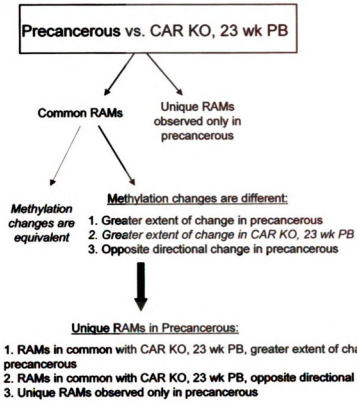
Table 3.1 GC-rich Regions of Altered Methylation (RAMs) in the Livers of C3H/He CAR WT and KO Mice Treated with 0.05% Phenobarbital for 23 or 32 Weeks

Treatment Group	Digest	RAMs Hypomethylation[a]	RAMs Hypermethylation[b]	RAMs "New" Methylation[c]	TOTAL
CAR KO, 23 wk 0.05% PB	MspI	5	0	12	17
	HpaII	13	0	3	16
	BssHII	21	0	0	21
Total[d]		**39**	**0**	**15**	**54**
CAR WT, 23 wk 0.05% PB (Precancerous)	MspI	1	4	10	15
	HpaII	6	6	2	14
	BssHII	13	0	5	18
Total[d]		**20**	**10**	**17**	**47**
CAR WT, 32 wk 0.05% PB (Tumor)	MspI	23	4	20	47
	HpaII	11	1	28	40
	BssHII	17	0	25	42
Total[d]		**51**	**5**	**73**	**129**

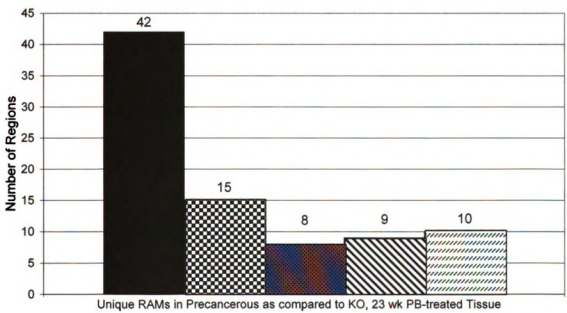
[a] Hypomethylated RAMs include both statistically significant ($p<0.05$) decreases and 100% decreases.
[b] Hypermethylated RAMs are only those increases which are statistically significant ($p<0.05$).
[c] New methylations indicate the formation of a PCR product following treatment due to a gain of methylation either at the site of primer annealing or between sites of primer annealing which was not present under control conditions.
[d] Total RAMs including hypomethylations, hypermethylations, and new methylations for all three methylation-sensitive restriction digests are reported for each treatment.

Figure 3.1 Identification of PB-Induced Unique Regions of Altered Methylation (RAMs) in the Precancerous as Compared to the CAR KO, 23 wk PB-Treated Tissue. The flowchart in (A) depicts the steps that are taken that allow for the identification of unique RAMs in precancerous (CAR WT, 23 wk PB) as compared to CAR KO, 23 wk PB-treated tissue. Steps that are relevant to discerning these RAMs are shown in normal font, while those that are not are shown in italics. RAMs are considered to be unique in the precancerous tissue if a region is in common between the two treatment groups and the magnitude of the methylation change in the precancerous tissue is greater than the change in the CAR KO, 23 wk PB-treated tissue as determined by two-way ANOVA analysis ($p<0.05$) or if the methylation changes at a common RAM occur in opposite directions (i.e., at a common RAM, a hypermethylation occurs in the precancerous tissue and a hypomethylation is observed in the CAR KO, 23 wk PB-treated tissue). Additionally, RAMs that are seen only in the precancerous tissue are considered to be unique. The unique RAMs in the precancerous as compared to the CAR KO, 23 wk PB-treated tissue (■) are depicted in (B). Hypomethylations (▩), hypermethylations (▩), new methylations (▩), and those RAMs in common between precancerous and CAR KO, 23 wk PB-treated tissue and which exhibit methylation changes that occur in opposite directions are represented (▩).

A.


Precancerous vs. CAR KO, 23 wk PB
Common RAMs
Unique RAMs observed only in precancerous
Methylation changes are equivalent
Methylation changes are different:
1. Greater extent of change in precancerous
2. Greater extent of change in CAR KO, 23 wk PB
3. Opposite directional change in precancerous
Unique RAMs in Precancerous:
1. RAMs in common with CAR KO, 23 wk PB, greater extent of change in precancerous
2. RAMs in common with CAR KO, 23 wk PB, opposite directional change
3. Unique RAMs observed only in precancerous

B.

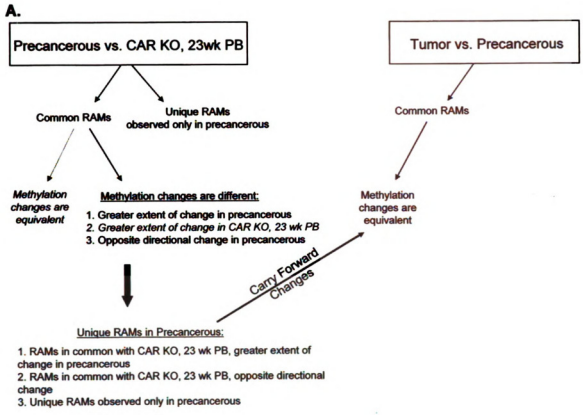

Number of Regions
45
40
35
30
25
20
15
10
5
0
42
15
8
9
10
Unique RAMs in Precancerous as compared to KO, 23 wk PB-treated Tissue

42 unique changes that occurred in the precancerous as compared to the CAR KO, 23 wk PB-treated tissue (Figure 3.1B).

From this pool of unique regions in the precancerous tissue, carry forward RAMs were discerned. Carry forward RAMs are those regions that were considered to be unique in the precancerous as compared to the CAR KO, 23 wk PB-treated tissue, were also observed in the tumor tissue, and whose methylation changes at a common RAM in the tumor and precancerous were equivalent as determined by one-way ANOVA, $p<0.05$ (Figure 3.2A). Of the 42 unique RAMs in the precancerous tissue as compared to the CAR KO, 23 wk PB-treated tissue, 14 (33%) carried forward to the tumor tissue (Figure 3.2B). These carry forward changes were primarily hypomethylations (71%), but 2 hypermethylations and 2 new methylations also were observed (Figure 3.2B).

Additionally, the total unique RAMs in the tumor tissue were detected (Figure 3.3A). Unique RAMs in the tumor tissue as compared to the precancerous tissue consist of common RAMs at which the methylation changes in the tumor tissue occur to a greater extent as determined by one-way ANOVA analysis ($p<0.05$), common RAMs with opposite directional changes in the tumor tissue (i.e. at a common RAM, PB induces a hypomethylation in the tumor tissue and a hypermethylation in the precancerous tissue), and unique RAMs observed only in the tumor tissue. Finally, to obtain the total unique RAMs in the tumor tissue, common RAMs in the tumor and CAR KO, 23 wk PB-treated tissue that exhibited equivalent methylation changes as determined by two-way ANOVA ($p<0.05$) were subtracted out, as methylation changes that occur in the CAR KO animals are most likely not critical for liver tumorigenesis.

Figure 3.2 Progressive Changes in Methylation: PB-Induced Regions of Altered Methylation (RAMs) which Carry Forward from Precancerous to Tumor Tissue in C3H/He CAR WT Mice. The flowchart in (a) demonstrates how carry forward RAMs from precancerous (CAR WT, 23 wk PB) to tumor (CAR WT, 32 wk PB) tissue are obtained. The steps that are relevant to the determination of these RAMs are shown in normal font, while those that are not are shown in italics. Carry forward RAMs are those regions which are unique in the precancerous as compared to the CAR KO, 23 wk PB-treated tissue, are also present in the tumor tissue, and whose methylation changes at this common RAM in the precancerous and tumor tissue are equivalent in magnitude as determined by two-way ANOVA analysis ($p<0.05$). Total carry forward RAMs (■) from precancerous to tumor tissue are depicted in (b). These RAMs are divided into hypomethylations (▩), hypermethylations (▩), and new methylations (▩).


A.
Precancerous vs. CAR KO, 23wk PB
Tumor vs. Precancerous
Common RAMs
Unique RAMs observed only in precancerous
Common RAMs
Methylation changes are equivalent
Methylation changes are different:
1. Greater extent of change in precancerous
2. Greater extent of change in CAR KO, 23 wk PB
3. Opposite directional change in precancerous
Methylation changes are equivalent
Carry Forward Changes
Unique RAMs in Precancerous:
1. RAMs in common with CAR KO, 23 wk PB, greater extent of change in precancerous
2. RAMs in common with CAR KO, 23 wk PB, opposite directional change
3. Unique RAMs observed only in precancerous

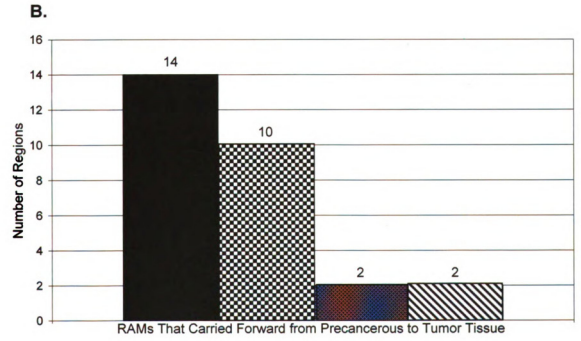
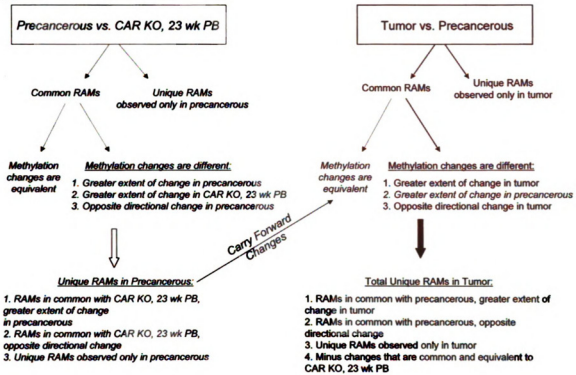
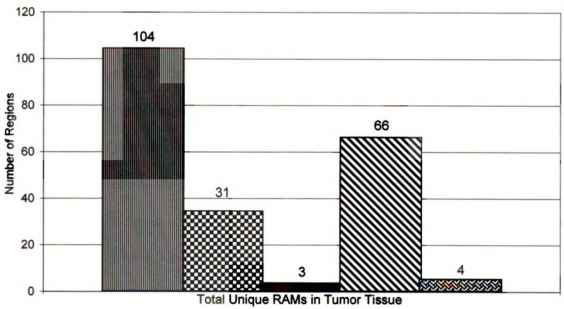

B.
Number of Regions
16
14
12
10
8
6
4
2
0
14
10
2
2
RAMs That Carried Forward from Precancerous to Tumor Tissue

Figure 3.3 Total Unique Regions of Altered Methylation (RAMs) That Occurred as a Result of PB Treatment in the Tumor as Compared to the Precancerous Tissue. The diagram used for the determination of total unique RAMs in the tumor (CAR WT, 32 wk PB) tissue is illustrated in (A). Steps that are relevant for determining these RAMs are shown in normal font, while those that are not are shown in italics. First, unique RAMs in the tumor as compared to the precancerous (CAR WT, 23 wk PB) tissue were ascertained. These include common RAMs with a greater extent of methylation change in the tumor tissue as determined by one-way ANOVA analysis ($p<0.05$), common RAMs in which the methylation changes occur in opposite directions, and those RAMs which are observed only in the tumor tissue. Then methylation changes that occurred at common RAMs in the tumor as compared to the CAR KO, 23 wk PB-treated tissue and were determined to be equivalent by two-way ANOVA analysis ($p<0.05$) were subtracted out to establish the total unique RAMs in the tumor tissue. These RAMs (▥), represented in (B), are segregated into hypomethylations (▩), hypermethylations (▩), new methylations (■), and those RAMs in common between the tumor and precancerous tissue with methylation changes that occurred in opposite directions (▩).

A.


Precancerous vs. CAR KO, 23 wk PB
Common RAMs
Unique RAMs observed only in precancerous
Methylation changes are equivalent
Methylation changes are different:
1. Greater extent of change in precancerous
2. Greater extent of change in CAR KO, 23 wk PB
3. Opposite directional change in precancerous
Carry Forward Changes
Unique RAMs in Precancerous:
1. RAMs in common with CAR KO, 23 wk PB, greater extent of change in precancerous
2. RAMs in common with CAR KO, 23 wk PB, opposite directional change
3. Unique RAMs observed only in precancerous
Tumor vs. Precancerous
Common RAMs
Unique RAMs observed only in tumor
Methylation changes are equivalent
Methylation changes are different:
1. Greater extent of change in tumor
2. Greater extent of change in precancerous
3. Opposite directional change in tumor
Total Unique RAMs in Tumor:
1. RAMs in common with precancerous, greater extent of change in tumor
2. RAMs in common with precancerous, opposite directional change
3. Unique RAMs observed only in tumor
4. Minus changes that are common and equivalent to CAR KO, 23 wk PB

B.


120
100
80
60
40
20
0
Number of Regions
104
31
3
66
4
Total Unique RAMs in Tumor Tissue

In total, 104 unique RAMs were observed in the tumor tissue (Figure 3.3B). New methylations accounted for 63% (66/104) of these changes, while hypomethylations represented 34% (35/104) and hypermethylations only 3% (3/104) of the total unique RAMs in the tumor (Figure 3.3B). Both the carry forward RAMs and the total unique RAMs in the tumor tissue may play critical mechanistic roles during the formation of liver tumors in the CAR WT C3H/He mice.

A diagram illustrating all of the data previously described is shown (Figure 3.4). Unique RAMs in the precancerous as compared to the CAR KO, 23 wk PB-treated tissue are depicted, and from these regions, carry forward changes from the precancerous to tumor tissue were determined. Finally, to obtain the total unique RAMs in the tumor tissue, 3 hypomethylations and 2 new methylations were subtracted out from the tallied unique RAMs in the tumor as compared to the precancerous tissue (Figure 3.4). These 5 RAMs were unique in the tumor as compared to the precancerous tissue and also were common RAMs between the tumor and CAR KO, 23 wk PB-treated tissue, with their associated methylation changes deemed to be equivalent by two-way ANOVA, $p<0.05$ (Figure 3.4). These RAMs have been excluded from the total unique RAMs in the tumor tissue because they are in common and equivalent between the precancerous mice and the CAR KO, 23 wk PB-treated mice that do not develop liver tumors, ***and thus are probably not relevant to the tumorigenesis process***. We understand that this a conservative approach and we recognize that the methylation changes that are equivalent in the CAR KO, 23 wk PB-treated and tumor tissue may be necessary but not sufficient for tumor development. It is important to note that all 4 of the unique RAMs in the tumor as compared to the precancerous tissue in which the methylation changes occurred in

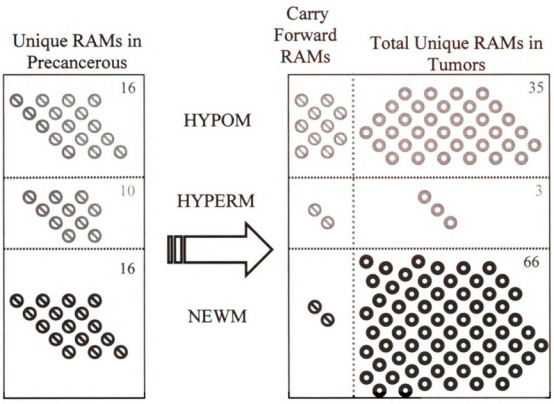


Figure 3.4 A Summary of Regions of Altered Methylation (RAMs) that Carry Forward from the Precancerous to the Tumor Tissue and Total Unique RAMs in the Tumor Tissue. The unique RAMs in the precancerous (CAR WT, 23 wk PB) as compared to the CAR KO, 23 wk PB-treated tissue are shown on the left (**O**). RAMs that carried forward in the CAR WT mice from precancerous to tumor (CAR WT, 32 wk PB) tissue are depicted (**O**) on the right. Total unique RAMs in the tumor tissue are represented on the far right (**O**). To obtain the total unique RAMs in the tumor tissue, common RAMs in the tumor as compared to the CAR KO, 23 wk PB-treated tissue which were equivalent as determined by two-way ANOVA analysis were subtracted from the unique RAMs in the tumor as compared to the precancerous tissue and are not shown here. All RAMs are divided into hypomethylations (HYPOM), hypermethylations (HYPERM), and new methylations (NEWM). It is important to note that the 4 RAMs in common between the tumor and the precancerous tissue which have methylation changes that are opposite in direction in the tumor and precancerous tissue (Figure 3.3B) were all hypomethylations in the tumor. Thus the 35 hypomethylations that are unique in the tumor tissue (Figure 3.4) include the 31 regions of hypomethylation (Figure 3.3B) added to the 4 RAMs in which methylation changes occurred in opposite directions in the tumor as compared to the precancerous tissue (Figure 3.3B). All 4 were hypomethylated in the tumor tissue and are tallied as such.

opposite directions (Figure 3.3B) were PB-elicited hypomethylations in the tumor tissue (as compared to an increase in methylation at the common region in the precancerous tissue) and are categorized as such (Figure 3.4).

The calculation of percent dissimilarity allows for the evaluation of PB-induced patterns of altered methylation in a treatment group as compared to a control group. Dissimilarity between the precancerous and the CAR WT, 23 wk control tissue was 47% but increased to 83% in the tumor tissue (Figure 3.5). This observation indicates that the methylation pattern became progressively aberrant with prolonged PB treatment. Furthermore, the CAR KO, 23 wk PB-treated tissue demonstrated 53% dissimilarity in its methylation pattern as compared to the CAR KO, 23 wk control tissue (Figure 3.5).

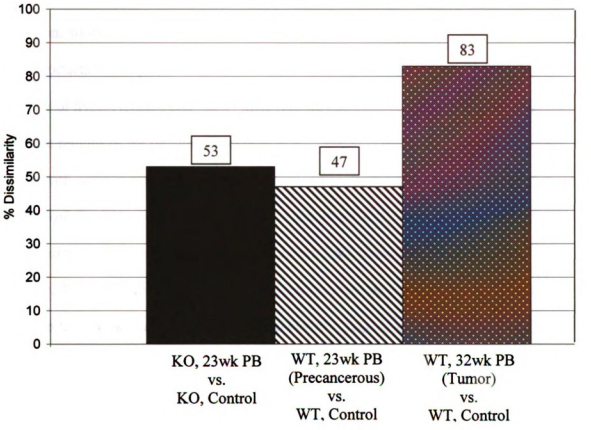


Figure 3.5 Determination of Percent Dissimilarity Between Precancerous vs. CAR WT, 23wk Control, Tumor vs. CAR WT, 23 wk Control, and CAR KO, 23 wk PB vs. CAR KO, 23 wk Control Tissue. Dissimilarity between patterns of methylation in a treatment group and its respective control group was calculated. For example, to determine how dissimilar the CAR KO, 23 wk PB-treated tissue is as compared to the CAR KO, 23 wk control tissue, the number of regions of altered methylation (including hypomethylations, hypermethylations, and new methylations) present in the CAR KO, 23 wk PB-treated tissue was divided by the total number of different sized PCR products reporting in the CAR KO, 23 wk PB-treated and CAR KO, 23 wk control groups and expressed as a percent. The same fundamental calculation was performed for the determination of percent dissimilarity in the precancerous (CAR WT, 23 wk PB) vs. CAR WT, 23 wk control tissue and in the tumor (CAR WT, 32 wk PB) vs. CAR WT, 23 wk control tissue.

DISCUSSION

We have developed an approach that involves methylation-sensitive restriction digestion, arbitrarily primed PCR, and capillary electrophoretic separation of the resulting PCR products which permits the detection of treatment-related changes in methylation, i.e. sites of hypo-, hyper-, and "new" methylation, that occur simultaneously throughout multiple regions of the genome (Bachman *et al.*, 2006b). DNA is subjected to a double digest with a non-methylation-sensitive enzyme plus one that is methylation-sensitive: *RsaI/MspI*, *RsaI/HpaII* or *BfaI/BssHII*. By evaluating CCGG sites, we are assessing the methylation status of approximately 7.45% of the CpG dinucleotides within the mouse genome, 4.37% of which are located within unique sequences and 3.08% of which are found in transposable elements (Fazzari and Greally, 2004). A significant advantage of using *MspI* and *HpaII* is that the methylation status at CpCpG sites as well as CpG sites are evaluated, respectively, affording the opportunity to complementarily assess a wider spectrum of methylation alterations. Restriction with *BfaI* leaves CpG islands more intact than *RsaI* (Shiraishi *et al.*, 1995) thus increasing the probability that subsequent digestion with the 6-base cutter *BssHII* will allow for the determination of the methylation status at sites within CpG islands. The combination of restriction digests employed permits a robust evaluation of methylation status along multiple regions of the genome.

The nongenotoxic rodent tumor promoter PB decreases global methylation levels to a greater extent in liver tumor-prone B6C3F1 as compared to resistant C57BL/6 mice (Counts and Goodman, 1996). Furthermore, higher levels of hypermethylation occurred at the internal and external cytosines of the recognition sequence 5' CCGG 3' in mice

that are more susceptible to liver tumorigenesis as compared to mice that are relatively resistant (C3H/He >> B6C3F1 > C57BL/6) (Watson and Goodman, 2002).

Using the aforementioned approach, we recently evaluated the effect of PB on the methylation status of DNA from B6C3F1 and C57BL/6 mice (Bachman *et al.*, 2006b). This method is an improvement over the polyacrylamide gel-based procedure used by Watson and Goodman (2002) because the current capillary electrophoresis-based technique permits a much more precise separation and quantification of the PCR products. Unique RAMs in the sensitive B6C3F1 mice were identified (Bachman *et al.*, 2006b). The primary advantage of comparing methylation changes that occur in sensitive vs. resistant mice is that the RAMs which may be most important for tumorigenesis (i.e. unique in the sensitive mice) are segregated out from those which arise only in the resistant group. This approach is conservative in the sense that we may be excluding some RAMs that are necessary but not sufficient for tumor development by "discarding" those that are in common and equivalent between B6C3F1 and C57BL/6 mice.

In the current study, another sensitive vs. resistant comparison was made between PB-induced RAMs that formed in the livers of sensitive CAR WT mice, which develop preneoplastic lesions after 23 wk and liver tumors after 32 wk of PB treatment, and the resistant CAR KO mice which do not develop liver lesions after 23 wk of promotion or tumors after 32 wk. RAMs were elicited in all 3 groups, indicating that PB induces methylation changes in these mice in both a CAR-dependent and CAR-independent manner (Table 3.1). These results are consistent with microarray data that shows that approximately half of the PB-induced gene expression changes that occur in mouse liver are CAR-dependent while the other half are CAR-independent (Ueda *et al.*, 2002a).

Furthermore, chronic activation of CAR causes tumor formation in mice (Huang *et al.*, 2005; Yamamoto *et al.*, 2004). All of these results are consistent with the concept that PB induces CAR-dependent and CAR-independent alterations, including methylation changes, in mouse liver. We hypothesize that PB-induced RAMs that occur uniquely in the CAR WT mice, especially those which carry forward from the 23 wk to 32 wk time points, may play key roles underlying promotion of liver tumorigenesis by PB.

More RAMs formed in the tumor as compared to the precancerous tissue, suggestive of a time-dependent relationship between duration of PB treatment and number of RAMs (Table 3.1). The unique RAMs observed in the precancerous and tumor tissue (Fig. 3.4) might facilitate tumorigenesis, especially those that carry forward from an early (precancerous) to a later (tumor) stage of tumorigenesis. It is important to recognize that the precancerous tissue is heterogeneous, comprised of both non-focal tissue and preneoplastic foci. By identifying methylation changes that carry forward from the precancerous to the tumor tissue, we are able to focus upon the crucial changes that most likely occur in both the preneoplastic and neoplastic lesions. Moreover, there were 104 total unique RAMs that formed in the tumor tissue, and this number does not include the 5 RAMs that were in common and equivalent between the KO, 23 wk PB-treated tissue and the tumor tissue, which were excluded in an effort to better focus upon the RAMs that were completely unique to the sensitive CAR WT mice (Fig. 3.3B). This observation supports the multistep/multistage model of tumorigenesis (Dragan *et al.*, 1993), during which there is a progressive accumulation of cells that have obtained heritable changes (i.e. genetic or epigenetic), which are critical for the selection and clonal expansion of initiated cells.

In addition to the possible involvement of mutations in key genes, epigenetic events have been implicated in the tumorigenesis process (Feinberg *et al.*, 2006; Goodman and Watson, 2002). Hypermethylation can downregulate the expression of tumor suppressor genes such as *MLH1*, *VHL*, and *RB1* (Jones and Laird, 1999) and hypomethylation can activate oncogenes (Nishigaki *et al.*, 2005; Oshimo *et al.*, 2003) plus increase genetic instability (Eden *et al.*, 2003) and tumor burden (Gaudet *et al.*, 2003). Thus, the presence of unique RAMs in the precancerous and tumor tissue as compared to the CAR KO, 23 wk-PB treated tissue, indicates that epigenetic alterations are involved in promotion of mouse liver tumors by PB.

CAR may mediate hypomethylation by blocking the methyltransferase enzymes from acting on DNA or recruiting proteins responsible for active demethylation (Bhattacharya *et al.*, 1999; Jost *et al.*, 2001; Zhu *et al.*, 2000). CAR could also induce hypomethylation by engaging cytidine deaminases, such as those from the Aid/Apobec family (Morgan *et al.*, 2004). Conversely, CAR may facilitate hypermethylation by recruiting methyltransferases, as in the case of GCNF and the resulting downregulation of *Oct-3/4* expression during gastrulation (Sato *et al.*, 2006). Additionally, CAR could mediate gene expression changes that affect enzymes involved in 1-carbon metabolism, thereby altering levels of methyl groups available for S-adenosylmethionine formation. For example, diets devoid of choline and methionine, compounds which serve as methyl-group donors for the DNA methyltransferase reaction, cause liver cancer in rodents (Ghoshal and Farber, 1984). CAR may also affect expression and/or activity of the DNA methyltransferases (Dnmt1, Dnmt3a, Dnmt3b).

The human isoform of CAR (hCAR) (Baes *et al.*, 1994) differs from its murine counterpart (mCAR) (Choi *et al.*, 1997) and structural variations seem to be responsible for some of the different responses of hCAR as compared to mCAR (Ueda *et al.*, 2002b). For instance, Kawamoto *et al.* (2000) found that estradiol and estrone activated mCAR but not hCAR. Additionally, mCAR and hCAR are both activated by PB (Moore *et al.*, 2000), but the PB-like inducer TCPOBOP is an agonist for mCAR and not hCAR (Moore *et al.*, 2000; Tzameli *et al.*, 2000). Conversely, the xenobiotic 6-(4-chlorophenyl-imidazo[2,1-*b*][1,3]thiazole-5-carbaldehyde *O*-(3,4-dichlorobenzyl)oxime is an agonist for hCAR but does not affect mCAR (Maglich *et al.*, 2003). There also are important species differences in terms of crosstalk between CAR and the xenobiotic-sensing pregnane X receptor (PXR). For example, TCPOBOP activates mCAR and hPXR but not hCAR or mPXR (Moore *et al.*, 2000). Similarly, clotrimazole can induce hPXR and inhibit hCAR but it does not affect mCAR (Moore *et al.*, 2000). Finally, androstanol serves as an inverse agonist for CAR, with its effects being greater in mCAR as compared to hCAR, while it activates both mPXR and hPXR (Moore *et al.*, 2000). Thus, there are important structural and regulatory differences between mCAR and hCAR. These distinctions might, in part, provide a mechanistic basis, possibly including differences in capacity to maintain normal patterns of DNA methylation, for the observation that PB, while being able to promote rodent liver tumors, is not a human carcinogen (Lamminpää *et al.*, 2002; Whysner *et al.*, 1996).

The question remains, "Why are humans more resistant to the effects of PB?" Part of the answer may lie downstream of CAR, in terms of the genes that are induced/repressed, some of which may be deregulated by methylation changes. Many of

the same tumor suppressors and oncogenes, such as pRB, p53, PTEN, and MLH1 (Herzig and Christofori, 2002), that are involved in a variety of human cancers are identical to those implicated in mouse tumorigenesis, and so while the same genes may be affected during human and mouse tumorigenesis, lesions may form only in mice due to differences in regulation of these genes, and altered methylation may be a component of this process. In general, humans are less susceptible to carcinogenesis as compared to rodents (Rangarajan and Weinberg, 2003). In this context, it should be noted that DNA methylation patterns are better preserved in human as compared to rodent cells in culture (reviewed in Goodman and Watson, 2002). Therefore, humans might be more comparable to the resistant KO mice in the sense that the methylation changes that occur in the CAR KO mice and any alterations in humans may not be as detrimental as those that arise in the CAR WT mice, and this could be a result of downstream differences in the RAMs caused by mCAR vs. hCAR.

The approach that our laboratory recently developed affords us the opportunity to detect treatment-related alterations in methylation, including sites of hyper-, hypo-, and "new" methylations. PB-elicited unique RAMs were identified in liver tumor-susceptible CAR WT mice as compared to the resistant CAR KO mice, and these changes, including unique RAMs in the precancerous and tumor tissue and especially those that carry forward from the early to the later time point, may play key roles in tumor formation in these mice. Currently, the PCR products that represent these key RAMs are being cloned, sequenced, and annotated in an attempt to identify specific, novel genes that are involved in the tumorigenesis process due to altered methylation.

ACKNOWLEDGEMENTS

J.M.P. is a predoctoral fellow supported by National Institutes of Health–National Institute of Environmental Health Sciences training grant No. T32-ES-7255. Research support, in the form of a gift, from the R.J. Reynolds Tobacco Company is acknowledged gratefully.

REFERENCES

Assem, M., Schuetz, E. G., Leggas, M., Sun, D., Yasuda, K., Reid, G., Zelcer, N., Adachi, M., Strom, S., Evans, R. M., Moore, D. D., Borst, P., and Schuetz, J. D. (2004) Interactions between hepatic *Mrp4* and *Sult2a* as revealed by the constitutive androstane receptor and *Mrp4* knockout mice. *J. Biol. Chem.* **21**, 22250-22257.

Bachman, A. N., Curtin, G. M., Doolittle, D. J., and Goodman, J. I. (2006a) Altered methylation in gene-specific and GC-rich regions of DNA is progressive and nonrandom during promotion of skin tumorigenesis. *Toxicol. Sci.* **91**, 406–418.

Bachman, A. N., Phillips, J. M, and Goodman J. I. (2006b) Phenobarbital induces progressive patterns of GC-rich and gene-specific altered DNA methylation in the liver of tumor-prone B6C3F1 Mice. *Toxicol. Sci.* **91**, 393-405.

Baes, M., Gulick, T., Choi, H. S., Martinoli, M. G., Simha, D., and Moore, D. D. (1994) A new orphan member of the nuclear hormone receptor superfamily that interacts with a subset of retinoic acid response elements. *Mol. Cell. Biol.* **14**, 1544-1152.

Bhattacharya, S. K., Ramchandani, S., Cervoni, N., and Szyf, M. (1999) A mammalian protein with specific demethylase activity for mCpG DNA. *Nature* **397**, 579-583.

Buchmann, A., Bauer-Hofmann, R., Mahr, J., Drinkwater, N. R., Luz, A., and Schwarz, M. (1991) Mutational activation of the c-Ha-*ras* gene in liver tumors of different rodent strains: correlation with susceptibility to hepatocarcinogenesis. *Proc. Natl. Acad. Sci.* **88**, 911-915.

Choi, H. S., Chung, M., Tzameli, I., Simha, D., Lee, Y. K., Seol, W., and Moore, D. D. (1997) Differential transactivation by two isoforms of the orphan nuclear hormone receptor CAR. *J. Biol. Chem.* **272**, 23565-23571.

Clark, S. J., Harrison, J., and Frommer, M. (1995) CpNpG methylation in mammalian cells. *Nat. Genet.* **10**, 20-27.

Counts, J. L. and Goodman, J. I. (1995) Alterations in DNA methylation may play a variety of roles in carcinogenesis. *Cell* **83**, 13-15.

Counts, J. L., Sarmiento, J. I., Harbison, M. L., Downing, J. C., McClain, R. M., and Goodman, J. I. (1996) Cell proliferation and global methylation status changes in mouse liver after phenobarbital and/or choline-devoid, methionine-deficient diet administration.

Carcinogenesis **17**, 1251-1257.

Dragan, Y. P, Sargent, L., Xu, Y. D., Xu, Y. H., and Pitot, H. C. (1993) The initiation promotion-progression model of rat hepatocarcinogenesis. *Proc. Soc. Exp. Biol. Med.* **202**, 16-24.

Eden, A., Gaudet, F., Waghmare, A., and Jaenisch, R. (2003) Chromosomal instability and tumors promoted by DNA hypomethylation. *Science* **300**, 455.

Ehrlich, M., Gama-Sosa, M. A., Huang, L. H., Midgett, R. M., Kuo, K. C., McCune, R. A., and Gehrke, C. (1982) Amount and distribution of 5-methylcytosine in human DNA from different types of tissues of cells. *Nucleic Acids Res.* **10**, 2709-2721.

Fazzari, M. J., and Greally, J. M. (2004) Epigenomics: Beyond CpG islands. *Nat. Rev. Genet.* **5**, 446-455.

Feinberg AP, Ohlsson R, Henikoff S. (2006) The epigenetic progenitor origin of human cancer. *Nat. Rev. Genet.* **7**, 21-33.

Gama-Sosa, M. A., Slagel, V. A., Trewyn, R. W., Oxenhandler, R., Kuo, K. C., Gehrke, C. W., and Ehrlich, M. (1983) The 5-methylcytosine content of DNA from human tumors. *Nucleic Acids Res.* **11**, 6883-6894.

Gaudet, F., Hodgson, J. G., Eden, A., Jackson-Grusby, L., Dausman, J., Gray, J. W., Leonhardt, H., and Jaenisch, R. (2003) Induction of tumors in mice by genomic hypomethylation. *Science* **300**, 489-492.

Ghoshal, A. K. and Farber, E. (1984) The induction of liver cancer by dietary deficiency of choline and methionine without added carcinogens. *Carcinogenesis* **5**, 1367-1370.

Gonzalgo, M. L., Liang, G., Spruck, C. H., III, Zingg, J. M., Rideout, W. M., III, and Jones, P. A. (1997) Identification and characterization of differentially methylated regions of genomic DNA by methylation-sensitive arbitrarily primed PCR. *Cancer Res.* **57**, 594-599.

Goodman, J. I., and Watson, R. E. (2002) Altered DNA methylation: a secondary mechanism involved in carcinogenesis. *Annu. Rev. Pharmacol. Toxicol.* **42**, 501-525.

Herzig, M. and Christofori, G. (2002) Recent advances in cancer research: mouse models of tumorigenesis. *Biochim. Biophys. Acta.* **1602**, 97-113.
Honkakoski, P., Zelko, I., Sueyoshi, T., and Negishi, M. (1998) The nuclear orphan receptor CAR-retinoid X receptor heterodimer activates the phenobarbital-responsive enhancer module of the *CYP2B* gene. *Mol. Cell. Biol.* **18**, 5652-5658.

Huang, W., Zhang, J., Washington, M., Liu, J., Parant, J. M., Lozano, G., Moore, D. D. (2005) Xenobiotic stress induces hepatomegaly and liver tumors via the nuclear receptor constitutive androstane receptor. *Mol. Endocrinol.* **19**, 1646-1653.

Jones, P.A., and Laird, P.W. (1999) Cancer epigenetics comes of age. *Nat. Genet.* **21**, 163-167.

Jost, J. P, Oakeley, E. J., Zhu, B., Benjamin, D., Thiry, S., Siegmann, M., and Jost, Y. C. (2001) 5-Methylcytosine DNA glycosylase participates in the genome-wide loss of DNA methylation occurring during mouse myoblast differentiation. *Nucleic Acids Res.* **29**, 4452-4461.

Kast, H. R., Goodwin, B., Tarr, P. T., Jones, S. A., Anisfeld, A. M., Stoltz, C. M., Tontonoz, P., Kliewer, S., Willson, T. M., and Edwards, P. A. (2002) Regulation of multidrug resistance-associated protein 2 (ABCC2) by the nuclear receptors pregnane X receptor, farnesoid X-activated receptor, and constitutive androstane receptor. *J. Biol. Chem.* **25**, 2908-2915.

Kawamoto, T., Kakizaki, S., Yoshinari, K., and Negishi, M. (2000) Estrogen activation of the nuclear orphan receptor CAR (constitutive active receptor) in induction of the mouse *Cyp2b10* gene. *Mol. Endocrinol.* **14**, 1897-1905.

Kodama, S. and Negishi, M. (2006) Phenobarbital confers its diverse effects by activating the orphan nuclear receptor CAR. *Drug Metab. Rev.* **38**, 75-87.

Lamminpää, A., Pukkala, E., Teppo, L., and Neuvonen, P. J. (2002) Cancer incidence among patients using antiepileptic drugs: a long-term follow-up of 28,000 patients. *Eur. J. Clin. Pharmacol.* **58**, 137–141.

Maglich, J. M., Parks, D. J., Moore, L. B., Collins, J. L., Goodwin, B., Billin, A. N., Stoltz, C. A., Kliewer, S. A., Lambert, M. H., Willson, T. M., and Moore, J. T. (2003) Identification of a novel human constitutive androstane receptor (CAR) agonist and its use in the identification of CAR target genes. *J. Biol. Chem.* **278**, 17277-83.

Mohan, R. and Heyman, R. A. (2003) Orphan nuclear receptor modulators. *Curr. Top. Med. Chem.* **3**, 1637-1647.

Moore, L. B., Parks, D. J., Jones, S. A., Bledsoe, R. K., Consler, T. G., Stimmel, J. B., Goodwin, B., Liddle, C., Blanchard, S. G., Willson, T. M., Collins, J. L., and Kliewer, S. A. (2000) Orphan nuclear receptors constitutive androstane receptor and pregnane X receptor share xenobiotic and steroid ligands. *J. Biol. Chem.* **275**, 15122-15127.

Morgan, H. D., Dean, W., Coker, H. A., Reik, W., and Petersen-Mahrt, S. K. (2004) Activation-induced cytidine deaminase deaminates 5-methylcytosine in DNA and is expressed in pluripotent tissues: implications for epigenetic reprogramming. J. Biol. Chem. 279, 52353-60.

Nishigaki, M., Aoyagi, K., Danjoh, I., Fukaya, M., Yanagihara, K., Sakamoto, H., Yoshida, T., and Sasaki, H. (2005) Discovery of aberrant expression of *R-RAS* by cancer-linked DNA hypomethylation in gastric cancer using microarrays. *Cancer Res.* **65**, 2115-2124.

Oshimo, Y., Nakayama, H., Ito, R., Kitadai, Y., Yoshida, K., Chayama, K., and Yasui,

W. (2003) Promoter methylation of cyclin D2 gene in gastric carcinoma. *Int. J. Oncol.* **23**, 1663-1670.
Rangarajan, A. and Weinberg, R. A. (2003) Opinion: Comparative biology of mouse versus human cells: modelling human cancer in mice. *Nat. Rev. Cancer* **3**, 952-959.

Sato, N., Kondo, M., and Arai, K. (2006) The orphan nuclear receptor GCNF recruits DNA methyltransferase for *Oct-3/4* silencing. *Biochem. Biophys. Res. Commun.* **344**, 845-851.

Schulte-Hermann, R., Timmermann-Trosiener, I., Barthel, G., and Bursch, W. (1990) DNA synthesis, apoptosis, and phenotypic expression as determinants of growth of altered foci in rat liver during phenobarbital promotion. *Cancer Res.* **50**, 5127-5135.

Shiraishi, M., Lerman L. S., and Sekiya T. (1995) Preferential isolation of DNA fragments associated with CpG islands. *Proc. Natl. Acad. Sci.* **92**, 4229-4233.

Swales, K. and Negishi, M. (2004) CAR, driving into the future. *Mol. Endocrinol.* **18**, 1589-1598.

Tzameli, I., Pissios, P., Schuetz, E. G., and Moore, D. D. (2000) The xenobiotic compound 1,4-bis[2-(3,5-dichloropyridyloxy)]benzene is an agonist ligand for the nuclear receptor CAR. *Mol. Cell. Biol.* **20**, 2951-2958.

Ueda, A., Hamadeh, H. K., Webb, H. K., Yamamoto, Y., Sueyoshi, T., Afshari, C. A., Lehmann, J. M., and Negishi, M. (2002a) Diverse roles of the nuclear orphan receptor CAR in regulating hepatic genes in response to phenobarbital. *Mol. Pharmacol.* **61**, 1-6.

Ueda, A., Kakizaki, S., Negishi, M., and Sueyoshi, T. (2002b) Residue threonine 350 confers steroid hormone responsiveness to the mouse nuclear orphan receptor CAR. *Mol. Pharmacol.* **61**, 1284-1288.

Watson, R. E. and Goodman, J. I. (2002) Effects of phenobarbital on DNA methylation in GC-rich regions of hepatic DNA from mice that exhibit different levels of susceptibility to liver tumorigenesis. *Toxicol. Sci.* **68**, 51-58.

Whysner, J., Ross, P. M., and Williams, G. M. (1996) Phenobarbital mechanistic data and risk assessment: enzyme induction, enhanced cell proliferation, and tumor promotion. *Pharmacol. Ther.* **71**, 53-91.

Yamamoto, Y., Moore, R., Goldsworthy, T. L., Negishi, M., and Maronpot, R. R. (2004) The orphan nuclear receptor constitutive active/androstane receptor is essential for liver tumor promotion by phenobarbital in mice. *Cancer Res.* **64**, 7197-7200.

Zhu, B., Zheng, Y., Angliker, H., Schwarz, S., Thiry, S., Siegmann, M., and Jost, J. P. (2000) 5-Methylcytosine DNA glycosylase activity is also present in the human MBD4 (G/T mismatch glycosylase) and in a related avian sequence. *Nucleic Acids Res.* **28**, 4157-4165.

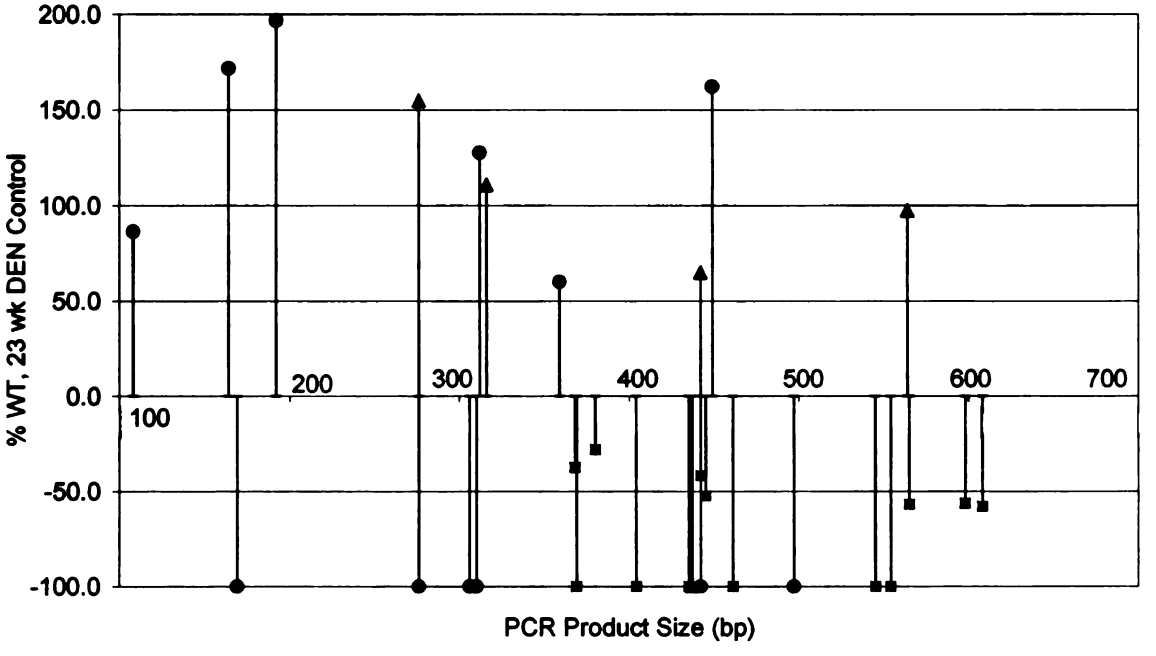
CHAPTER 3 APPENDIX

The appendix contains a series of figures which provide the actual, basic underlying data for Table 3.1 and Figures 3.1–3.3. These figures provide the data for RAMs whose methylation changes were (1) statistically significant (hypomethylations, hypermethylations), (2) complete 100% hypomethylations and (3) new methylations. Data are depicted for the CAR KO, 23 wk PB-treated, precancerous (CAR WT, 23 wk PB-treated), and tumor (CAR WT, 32 wk PB-treated) tissue.

Figure 3.6 GC-Rich Regions of Altered DNA Methylation: Comparison of Diethylnitrosamine (DEN)-Initiated, 0.05% phenobarbital (PB)-promoted Precancerous Tissue (CAR Wildtype, 23 wk DEN/PB) to Control (CAR Wildtype, 23 wk DEN). *RsaI/MspI* (triangles), *RsaI/HpaII* (circles), and *BfaI/BssHII* (squares) restriction digestion and AP-PCR was performed on DNA isolated from C3H/He CAR WT mouse liver initiated with a single dose of DEN, and then administered water or 0.05% PB (w/w) for 23 wk. Regions of hypomethylation and hypermethylation are evident (A). Regions of new methylation resulting from PB treatment are shown in terms of peak area for each PCR product size (B). The y-axis scale was expanded in order to facilitate visualization of all data points. Subsequently, 2 regions of new methylation whose peak areas exceeded the scale of the chart were labeled with their corresponding peak areas (C). A table tallying the regions of altered methylation for each treatment is shown as an inset in each figure. Regions of hypomethylation and hypermethylation are expressed in terms of the treated mean for each PCR product size as a percent of the control mean for each PCR product size. All changes projecting below the x-axis represent decreases in methylation (hypomethylation) while all of those above the x-axis represent increases in methylation (hypermethylation). All 100% hypomethylations are considered to be significant, and only the hypermethylations and partial hypomethylations that were significantly different from control values (Student's *t*-test, $p<0.05$) are shown.

A.

Digest	Hypomethylated RAMs	Hypermethylated RAMs	TOTAL RAMs
MspI ▲	1	4	5
HpaII ●	6	6	12
BssHII ■	13	0	13



Peak Area (Peak Area Units)

5

0

2

Figure 3.6 continued **GC-Rich Regions of Altered DNA Methylation: Comparison of Diethylnitrosamine (DEN)-Initiated, 0.05% phenobarbital (PB)-promoted Precancerous Tissue (CAR Wildtype, 23 wk DEN/PB) to Control (CAR Wildtype, 23 wk DEN).**

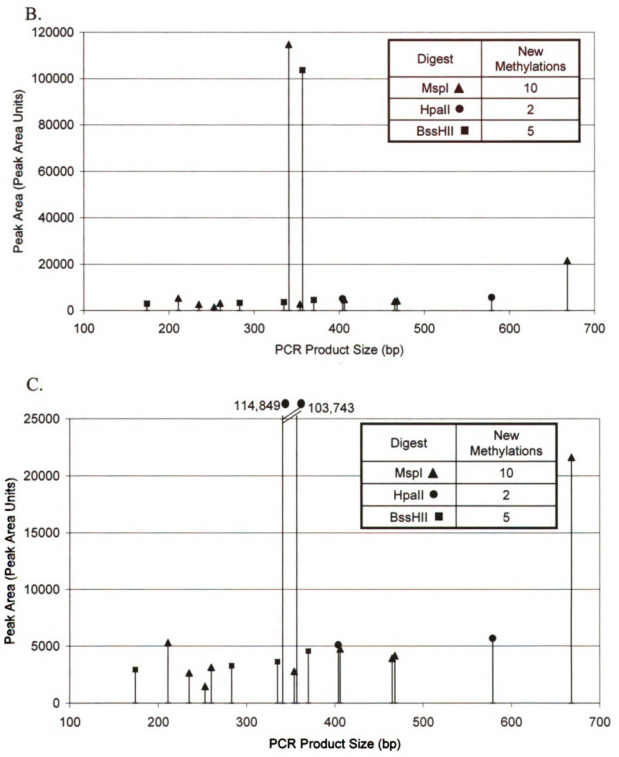


Figure 3.7 GC-Rich Regions of Altered DNA Methylation: Comparison of Diethylnitrosamine (DEN)-Initiated, 0.05% Phenobarbital (PB)-promoted Tumor Tissue (CAR Wildtype, 32 wk DEN/PB) to Control (CAR Wildtype, 23 wk DEN). *RsaI/MspI* (triangles), *RsaI/HpaII* (circles), and *BfaI/BssHII* (squares) restriction digestion and AP-PCR was performed on DNA isolated from C3H/He CAR WT mouse liver initiated with a single dose of DEN, and then administered water or 0.05% PB (w/w) for 32 wk. Regions of hypomethylation and hypermethylation are evident (A). The y-axis scale was expanded in order to facilitate visualization of all data points. Subsequently, 1 region of hypermethylation whose percent consensus control exceeded the scale of the chart was labeled with its corresponding value (B). Regions of new methylation resulting from PB treatment are shown in terms of peak area for each PCR product size (C). A table tallying the regions of altered methylation for each treatment is shown as an inset in each figure. Regions of hypomethylation and hypermethylation are expressed in terms of the treated mean for each PCR product size as a percent of the control mean for each PCR product size. All changes projecting below the x-axis represent decreases in methylation (hypomethylation) while all of those above the x-axis represent increases in methylation (hypermethylation). All 100% hypomethylations are considered to be significant, and only the hypermethylations and partial hypomethylations that were significantly different from control values (Student's t-test, $p<0.05$) are shown.

A.

Digest	Hypomethylated RAMs	Hypermethylated RAMs	TOTAL RAMs
MspI ▲	23	4	27
HpaII ●	11	1	12
BssHII ■	17	0	17

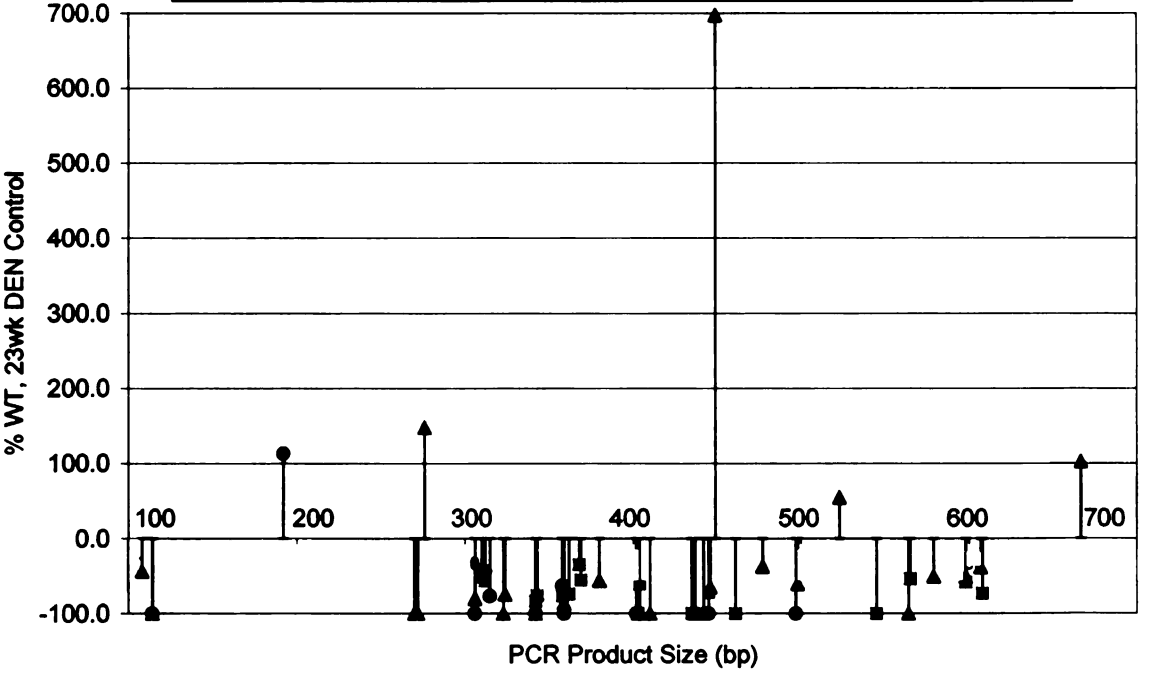
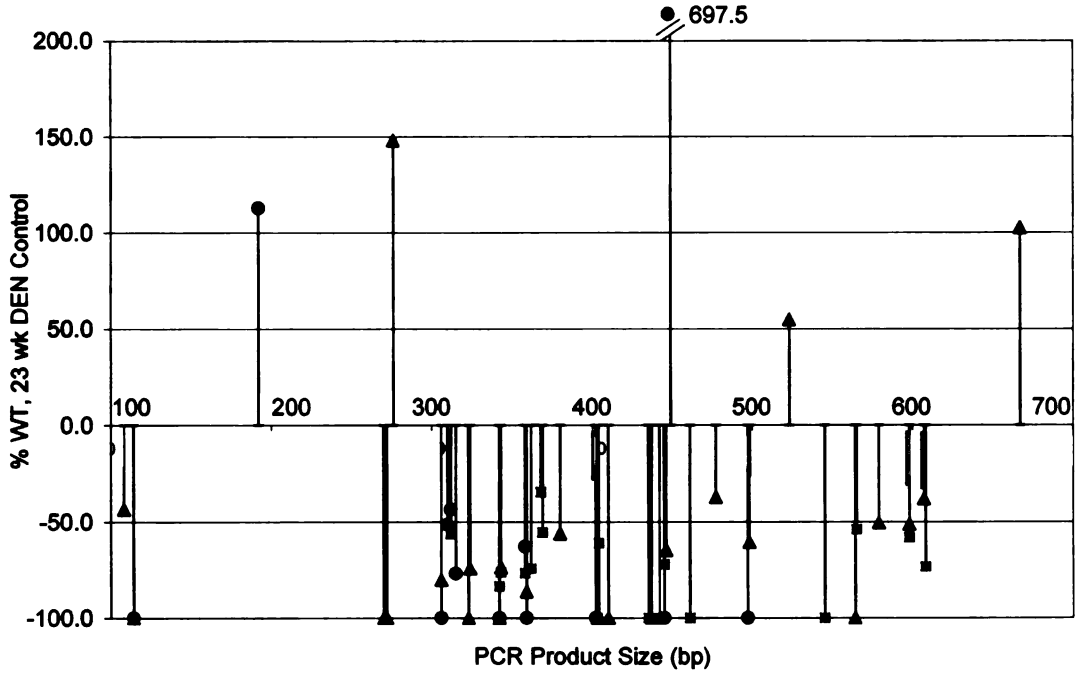


Figure 3.7 continued **GC-Rich Regions of Altered DNA Methylation: Comparison of Diethylnitrosamine (DEN)-Initiated, 0.05% Phenobarbital (PB)-promoted Tumor Tissue (CAR Wildtype, 32 wk DEN/PB) to Control (CAR Wildtype, 23 wk DEN).**

B.

Digest	Hypomethylated RAMs	Hypermethylated RAMs	TOTAL RAMs
MspI ▲	23	4	27
HpaII ●	11	1	12
BssHII ■	17	0	17



C.

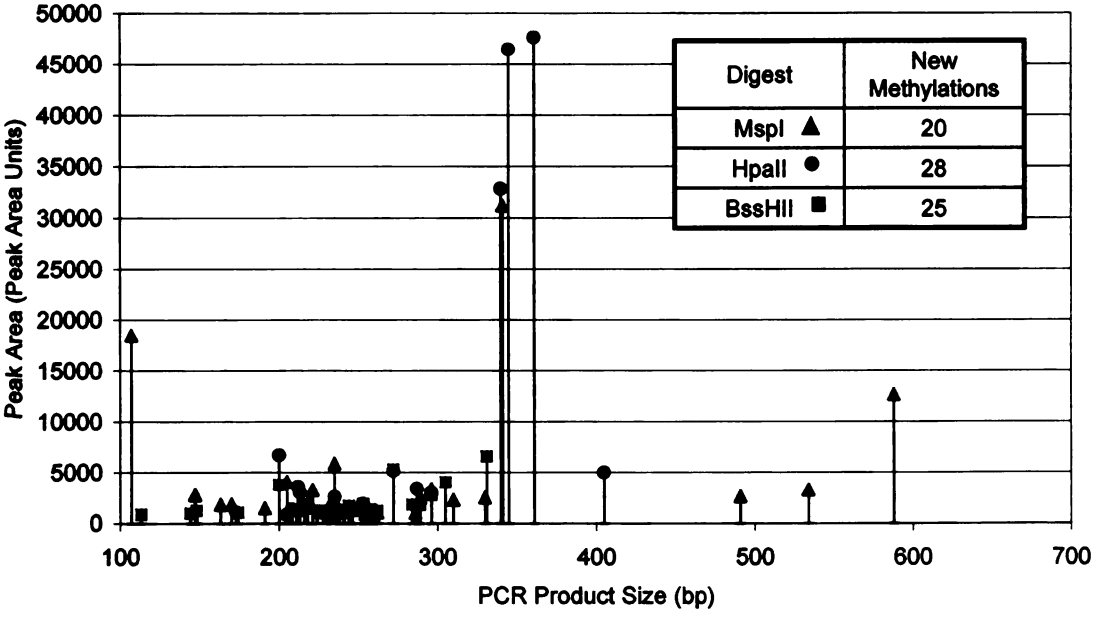


Figure 3.8 GC-Rich Regions of Altered DNA Methylation: Comparison of Diethylnitrosamine (DEN)-Initiated, 0.05% Phenobarbital (PB)-promoted CAR Knockout (KO) Tissue (CAR KO, 23 wk DEN/PB) to Control (CAR KO, 23 wk DEN). *RsaI/MspI* (triangles), *RsaI/HpaII* (circles), and *BfaI/BssHII* (squares) restriction digestion and AP-PCR was performed on DNA isolated from C3H/He CAR KO mouse liver initiated with a single dose of DEN and then administered water or 0.05% PB (w/w) for 23 wk. Regions of hypomethylation and hypermethylation are evident (A). Regions of new methylation resulting from PB treatment are shown in terms of peak area for each PCR product size (B). The y-axis scale was expanded in order to facilitate visualization of all data points. Subsequently, 1 region of new methylation whose peak area exceeded the scale of the chart were labeled with its corresponding peak area (C). A table tallying the regions of altered methylation for each treatment is shown as an inset in each figure. Regions of hypomethylation and hypermethylation are expressed in terms of the treated mean for each PCR product size as a percent of the control mean for each PCR product size. All changes projecting below the x-axis represent decreases in methylation (hypomethylation) while all of those above the x-axis represent increases in methylation (hypermethylation). All 100% hypomethylations are considered to be significant, and only the hypermethylations and partial hypomethylations that were significantly different from control values (Student's *t*-test, $p<0.05$) are shown.

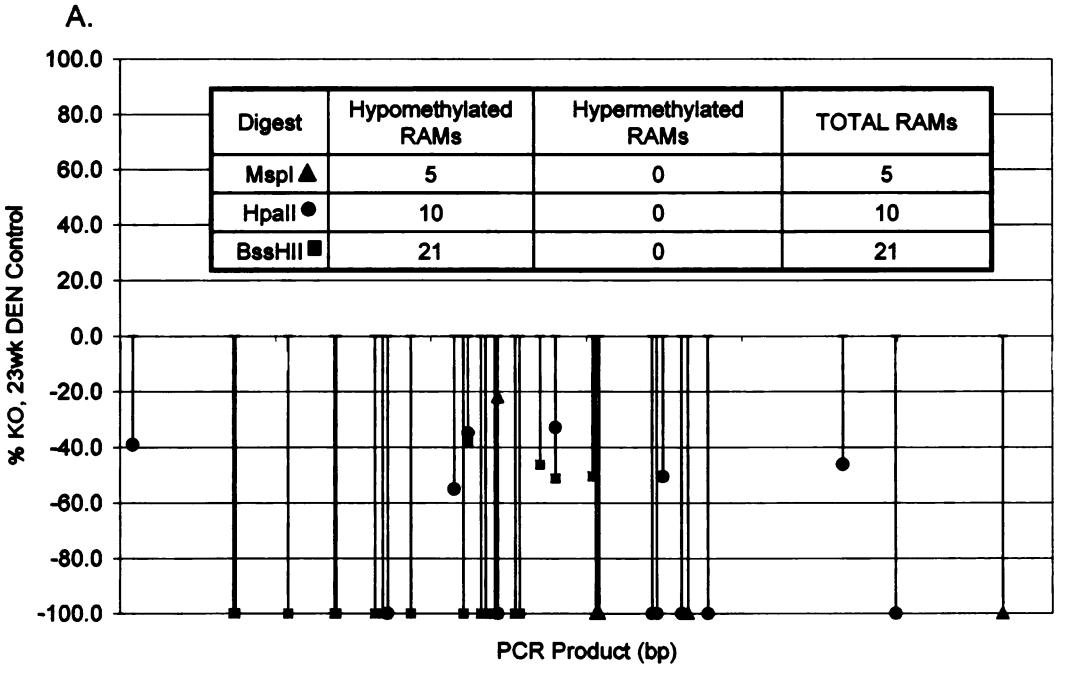
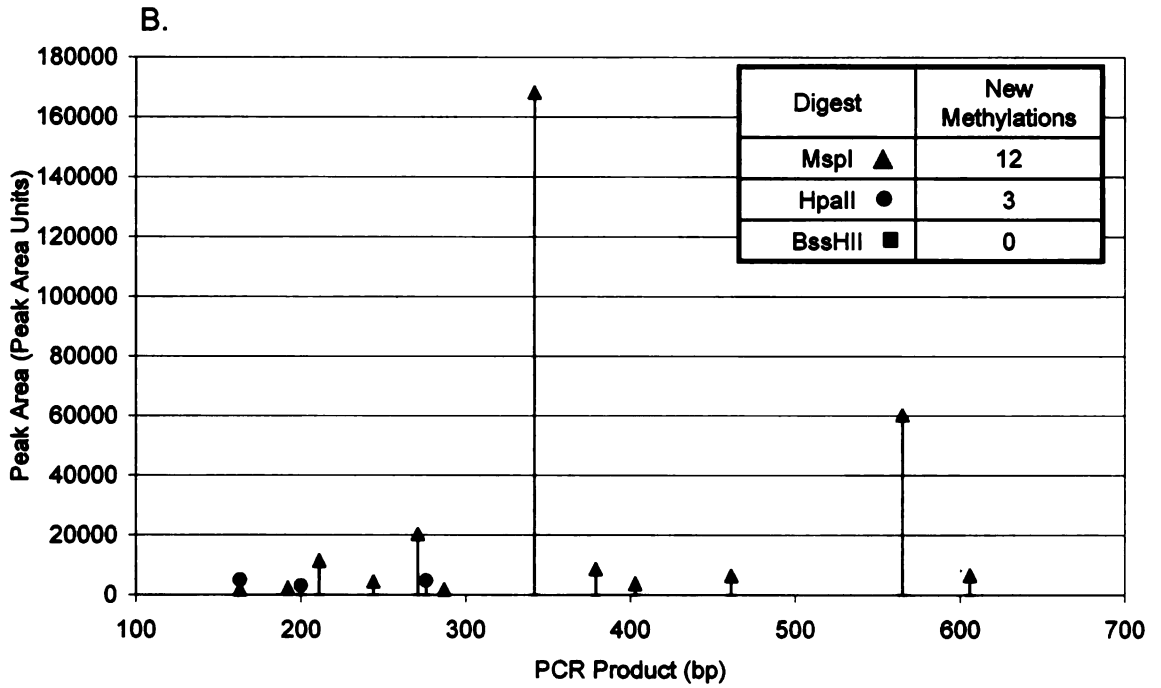
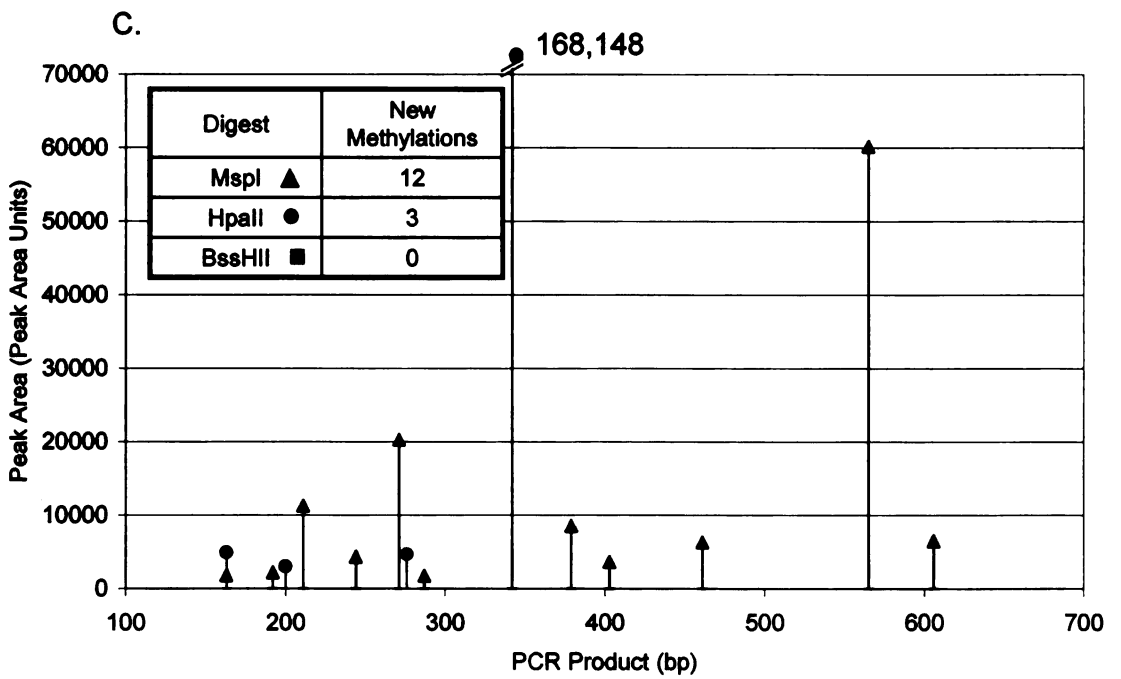


Figure 3.8 continued **GC-Rich Regions of Altered DNA Methylation: Comparison of Diethylnitrosamine (DEN)-Initiated, 0.05% Phenobarbital (PB)-promoted CAR Knockout (KO) Tissue (CAR KO, 23 wk DEN/PB) to Control (CAR KO, 23 wk DEN).**





CHAPTER 4

MULTIPLE GENES EXHIBIT PHENOBARBITAL (PB)-INDUCED CONSTITUTIVE ACTIVE/ANDROSTANE RECEPTOR (CAR)-MEDIATED DNA METHYLATION CHANGES DURING LIVER TUMORIGENESIS AND IN LIVER TUMORS

This chapter represents a manuscript that is in press for publication (as of March 2009) in *Toxicological Sciences*. The authors are Jennifer M. Phillips and Jay I. Goodman.

ABSTRACT

The constitutive active/androstane receptor (CAR) mediates responses to the nongenotoxic rodent liver tumor promoter phenobarbital (PB), including certain gene expression changes, hepatomegaly, and tumor formation. Aberrant DNA methylation represents epigenetic events that can play multiple roles in tumorigenesis. Previously, 146 unique PB-induced regions of altered DNA methylation (RAMs) were observed in liver-tumor susceptible CAR wildtype (WT) mice (in 23 weeks, precancerous tissue and 32 weeks, tumor tissue), as compared to the resistant knockout (KO). We believe that at least some of these might be key for tumorigenesis (Phillips *et al.*, 2007). In the current study, cloning and annotation of a subset (82%) of the unique RAMs revealed 47 genes exhibiting altered methylation; 17 are already implicated in cancer or related processes and, thus, we have identified 30 "new" candidate genes that might be involved in carcinogenesis due to an epigenetic alteration. These may contribute to tumor development through their involvement in angiogenesis, apoptosis, epithelial-mesenchymal cell transition, growth/survival, and invasion/migration/metastasis. We have also, previously, discerned unique PB-elicited RAMs in liver tumor-prone B6C3F1 mice, as compared to the relatively resistant C57BL/6 strain, at 2 or 4 weeks (Bachman *et al.*, 2006b), and identified 51 genes exhibiting altered methylation (Phillips and Goodman, 2008). Importantly, 11 of these genes were identified from identical, unique RAMs discerned in both the sensitive B6C3F1 and CAR WT mice, thus representing an initial, potential candidate "fingerprint" which might serve as a biomarker for PB-induced tumorigenesis. These 2 studies reveal "new" genes whose epigenetic statuses changed uniquely in liver tumor-susceptible mice (B6C3F1 and CAR WT), as compared to their

resistant counterparts (C57BL/6 and CAR KO, respectively), within a continuum of PB-induced tumorigenesis.

INTRODUCTION

The constitutive active/androstane nuclear receptor (CAR) is expressed primarily in the liver and mediates transcription of drug-metabolizing enzymes, e.g., cytochrome P450 (CYP) 2B10 and CYP3A11, plus NADPH-cytochrome reductase (Ueda *et al.*, 2002), the UDP-glucuronosyltransferase UGT1A1 (Sugatani *et al.*, 2001) and glutathione S-transferases (Huang *et al.*, 2003). Thus, CAR plays a key role in the metabolism and excretion of xenobiotics and endobiotics (e.g., bilirubin and bile acids), in addition to xenobiotic-induced changes in energy metabolism (reviewed in Konno *et al.*, 2008).

Phenobarbital (PB), the prototypical nongenotoxic rodent liver tumor promoter, causes liver hyperplasia and hypertrophy, and induces xenobiotic-metabolizing enzymes (Whysner *et al.*, 1996). A promoting dose of PB increases DNA synthesis and decreases apoptosis in murine hepatocytes (Kolaja *et al.*, 1996b), and initially stimulates hepatocyte proliferation (Counts *et al.*, 1996; Kolaja *et al.*, 1996a). Ha-*ras* mutations are infrequent in PB-induced mouse liver tumors (Fox *et al.*, 1990; Rumsby *et al.*, 1991), however, hypomethylation of Ha-*ras* (Vorce and Goodman, 1991) and increased expression occurs (Counts *et al.*, 1997). Additionally, connexin32 (the major gap junction-forming protein in liver) is required for promotion by PB (Moennikes *et al.*, 2000).

PB and PB-like compounds (e.g., 1,4-bis[2-(3,5-dichloropyridyloxy)]benzene, TCPOBOP) activate CAR (reviewed in Swales and Negishi, 2004). CAR is required for PB-induced hepatomegaly and *Cyp2b10* gene expression in mouse liver (Wei *et al.*, 2000), and chronic CAR activation in response to PB or TCPOBOP results in hepatocarcinogenesis (Huang *et al.*, 2005). Importantly, CAR is essential for tumor promotion by PB in diethylnitrosamine (DEN)-initiated C3H/He mice (Yamamoto *et al.*,

2004). Microarray data analysis of PB-treated CAR wildtype (WT) and knockout (KO) mice indicated that of 138 genes (out of 8,736 total genes/expressed sequence tags, ESTs) whose expression was altered, only approximately half of these changes were CAR-dependent (Ueda *et al.*, 2002). In response to PB treatment, CAR translocates from the cytoplasm to the nucleus, heterodimerizes with retinoid X receptor (RXR), and binds to and activates transcriptional elements (e.g., PB-responsive enhancer modules) to affect gene expression (Honkakoski *et al.*, 1998; Kawamoto *et al.*, 1999; Sueyoshi *et al.*, 1999). Nuclear translocation of CAR can be blocked by an inhibitor of protein phosphatase 2A (PP2A) (Kawamoto *et al.*, 1999), while a subunit of protein phosphatase 1, PPP1R16A, can inhibit protein phosphatase 1-beta (PP1β), resulting in CAR translocation (Sueyoshi *et al.*, 2008). Additionally, CAR-mediated induction of the *Cyp2b10* gene can be blocked by a Ca^{2+}/calmodulin-dependent kinase inhibitor, without affecting nuclear accumulation (Yamamoto *et al.*, 2003). These results suggest that both phosphorylation and dephosphorylation events contribute to CAR activation. We speculate that enhancement of PP2A and/or inhibition of PP1β plays a role in the mechanism by which PB stimulates nuclear translocation of CAR.

DNA methylation is an epigenetic mechanism regulating transcription which, when altered, may lead to tumorigenesis. For instance, hypomethylation can activate oncogenes, while hypermethylation can silence tumor suppressors (Esteller, 2008; Goodman and Watson, 2002). Therefore, aberrant methylation, in addition to mutation, can play critical roles during all stages of tumor formation, e.g., by facilitating the progressive clonal expansion of subpopulations which possess growth advantages over neighboring cells (Goodman and Watson, 2002). While the detailed mechanisms of PB-

induced altered DNA methylation remain to be elucidated, liver tumor-sensitive B6C3F1 mice, as compared to resistant C57BL/6, appear to be "defective" with regard to the ability to preserve normal methylation patterns (Watson and Goodman, 2002). Indeed, PB causes the formation of unique regions of altered DNA methylation (RAMs) in B6C3F1, compared to C57BL/6, mice at 2 and 4 weeks of treatment (Bachman *et al.*, 2006b). Cloning and annotation of these unique RAMs revealed changes in methylation which occurred within genes that are known to play important roles in tumorigenesis (e.g., angiogenesis, invasion, metastasis, and epithelial-mesenchymal cell transition), plus genes which had not previously been linked to cancer, thus providing insight regarding specific genes which may play a role in PB-induced tumorigenesis due to altered DNA methylation (Phillips and Goodman, 2008).

In an analogous fashion to Bachman *et al.* (2006b), Phillips *et al.* (2007) compared DNA methylation patterns in liver tumor-susceptible C3H/He CAR WT mice and resistant CAR KO mice. Unique RAMs in the livers of CAR WT mice initiated with DEN and treated with PB for 23 (precancerous tissue) or 32 (tumor tissue) weeks, compared to CAR KO mice initiated with DEN and treated with PB for 23 weeks, were identified. Methylation changes also occurred in the CAR KO, PB-treated mice, suggesting, analogous to gene expression changes observed in Ueda *et al.* (2002), that DNA methylation changes are both CAR –dependent and –independent. We hypothesize that a subset of the unique RAMs in the precancerous and tumor tissue are important for facilitating tumorigenesis. In this study, unique RAMs detected in the precancerous and tumor tissue (Phillips *et al.*, 2007) were cloned and annotated to discern the particular genes involved and how they might contribute to tumorigenesis, e.g., common cellular

targets of the genes of interest were identified in order to picture how they might interact to affect critical signaling pathways, leading to key alterations in phenotype. While Phillips and Goodman (2008) focused upon genes involved in PB-induced tumor formation at very early treatment times (i.e. 2 and 4 weeks), the current study elucidated genes involved at later times, when foci (23 week, PB-treated CAR WT) and tumors (32 week, PB-treated CAR WT) are apparent. Taken together, these 2 studies (the aforementioned B6C3F1-C57BL/6 study, and the current CAR study) lead to the identification of genes whose methylation statuses changed uniquely in liver tumor-susceptible mice (B6C3F1 and CAR WT), as compared to their resistant counterparts (C57BL/6 and CAR KO, respectively), within a continuum of PB-induced tumorigenesis.

MATERIALS AND METHODS

Animals, Treatments and Tissue Samples

The DNA employed for these studies was isolated from the same liver samples used by Phillips *et al.* (2007), and these samples were provided by Yamamoto *et al.* (2004). CAR WT or CAR KO mice, on a C3H/He background (which is highly susceptible to liver tumorigenesis (Buchmann *et al.*, 1991)), were injected with a single intraperitoneal dose of diethylnitrosamine (DEN), 90 mg/kg, at 5 weeks of age and then administered drinking water (control) or 0.05% PB (w/w) in drinking water starting at 7 weeks of age and continuing for 23 or 32 weeks, resulting in the following groups: CAR KO, 23 week control, CAR KO, 23 week PB, CAR WT, 23 week control, CAR WT, 23 weeks PB (precancerous tissue), and CAR WT, 32 week PB (tumor tissue) (Yamamoto *et al.*, 2004).

Protocol Employed for the Annotation of PB-induced Unique RAMs in Precancerous and Tumor Tissue

The RAMs cloned and annotated in the current study were previously detected via an approach involving methylation-sensitive restriction digestion, arbitrarily primed PCR (AP-PCR), and capillary electrophoresis (CE) (p. 184 of this dissertation), a technique described in detail by Bachman *et al.* (2006a). The following comparisons were previously made between experimental groups: 1) the CAR KO, 23 week PB data were compared to the CAR KO, 23 week control data, and 2) both the CAR WT, 23 week PB (precancerous tissue) and CAR WT, 32 week PB (tumor tissue) data were compared to the CAR WT, 23 week control data. For each specific PCR product size that was observed in control v. PB-treated an individual Student's t-test was performed to evaluate

whether or not there was a statistical ($p < 0.05$) difference in the peak area. Additionally, new methylations (PCR products which were observed in the PB-treated and not in control), as well as 100% hypomethylations (PCR products which were observed in control but not seen at all in PB-treated), were viewed as being "significant" (Bachman *et al.*, 2006a).

For the methylation analysis performed by Phillips *et al.* (2007), whole liver from 4 of the 5 (not including the WT, 32-week PB) groups was utilized; the precancerous liver tissue (WT, 23-week PB) contained no tumors, however, based upon histology of adjacent tissue, there are expected to be very numerous microscopic foci of cellular alteration diffused throughout the tissue. Importantly, DNA was isolated from individual liver tumors that developed in the WT, 32-week PB group.

The 23-week PB-treated mice are 30 weeks of age (PB treatment started when the animals were 7 weeks old), and the 32-week mice are 39 weeks of age. Thus, the mice were past the juvenile development stage and not into old age, and at an age where a reasonable degree of stability of methylation might be anticipated over a 9-week period.

Cloning and Sequencing of AP-PCR Products

AP-PCR products were first cloned using an in-gel approach to identify in what regions of the genome the PB-induced unique precancerous and tumor RAMs occurred. The AP-PCR products and a 100 base pair DNA ladder (Invitrogen, Carlsbad, CA) were electrophoresed through a 3% NuSieve® GTG® low melting temperature agarose gel (Lonza Biosciences, Basel, Switzerland). Portions of the gel that contained PCR products within 100 base pair size ranges were excised, melted and used for in-gel

cloning reactions prepared with the pGEM®-T Easy Vector Kit (Promega, Madison, WI). Clones that contained PCR product inserts were purified and sequenced at the Research Technology and Support Facility at Michigan State University. Sequencing reactions were prepared using either SP6 or T7 sequencing primers (as described in the pGEM®-T Easy Vector Technical Manual; Promega, Madison, WI) and subsequently run on an ABI 3730*xl* Genetic Analyzer.

Comparison of the Sizes of Cloned and Sequenced AP-PCR Products to the Sizes of Unique RAMs

After the sequences were obtained, the sizes of the cloned products were compared to the sizes of the unique RAMs in order to determine which cloned products represented unique precancerous and tumor RAMs. In many instances, it can be confidently stated that a particular cloned product represents a single RAM and as such, the methylation status of that RAM is unambiguous. However, the raw data analysis performed to establish if a RAM occurred in a treatment group as compared to its respective control group (Phillips *et al.*, 2007) is based upon the understanding that the ABI 3130 Genetic Analyzer capillary electrophoresis instrument does not detect PCR product sizes with 100% accuracy. Therefore, in certain instances during the analysis of the raw data, PCR product sizes were combined. Six animals per experimental group were used and restriction digestions were performed in duplicate, followed by AP-PCR, for a total of 12 reactions. If multiple PCR product sizes within 2 base pairs of one another displayed product in less than half of the 12 AP-PCR reactions, these products were considered to be "identical" and were subsequently combined. This procedure has implications for analysis of the cloning data. For example, 2 RAMs occurred uniquely in the tumor tissue

as a result of *RsaI/HpaII* digestion: a hypomethylation at 402 bp and a carry forward new methylation at 404 bp (p. 200 of this dissertation). A carry forward methylation change is a unique RAM that was observed in both precancerous and tumor tissue. A PCR product of 404 bp was cloned, and a BLAT search showed that the product spans an intronic region within the transmembrane protein 132d (*Tmem132d*) gene (Table 4.1). Due to our basic data analysis $\pm$ 2 bp assumption, the methylation status of *Tmem132d* is ambiguous; it could represent the hypomethylated RAM at 402 bp or the newly methylated carry forward RAM at 404 bp.

Additionally, the use of 3 different methylation-sensitive enzyme pairs could also reveal multiple methylation statuses of a particular gene. In the case of dipeptidylpeptidase 10 (*Dpp10*), *RsaI/HpaII* digestion revealed a hypomethylated RAM while *RsaI/MspI* digestion demonstrated a carry forward hypermethylated RAM in the precancerous tissue (Table 4.1). Thus, *Dpp10* could represent one or both of these RAMs since different restriction digestions were utilized, each of which reveals information regarding the methylation patterns of different cytosines at and within the sites of primer annealing. The "methylation status" data column in Table 4.1 reflects these 2 situations, (e.g., Hypo/New for a single gene, in a particular tissue).

Analysis of Sequenced AP-PCR Products

The sequences were subjected to BLAT database searches of the mouse genome (UCSC Genome Browser, July 2007 mouse assembly, http://genome.ucsc.edu/cgi-bin/hgBlat?command=start&org=mouse) in order to ascertain in which regions of the genome the unique PB-induced precancerous and tumor RAMs occurred. The BLAT

program aligns a nucleotide or amino acid sequence to an index of an entire animal genome. For DNA sequence queries, BLAT can detect sequence alignments of 95% or greater similarity of regions with lengths of 25 or more base pairs. Additional information about the genomic region/gene is listed, including, but not limited to: gene information, sequence conservation between species, GC percentage, and the location of single nucleotide polymorphisms and repeat elements. The unique RAMs were classified according to a scheme that indicates where, in relation to a gene (e.g., within an intron, within an exon, upstream of the transcriptional start site), they are located. RAMs were also categorized by chromosomal location and gene function. Gene Ontology information for Figure 4.10 was obtained from http://www.geneontology.org/.

The functions of the genes identified using BLAT searches were investigated via Pathway Studio® 5.0 (Ariadne Genomics, Rockville, MD). In this fashion, connections between each individual gene and other genes, cellular processes, or disease states were elucidated. An example of this type of analysis is located in Figure 4.11. In addition, common targets and common regulators of genes identified from unique RAMs in both the precancerous and tumor tissue were discerned. Pathway Studio® 5.0 was also utilized to uncover documented links between unique precancerous and tumor RAMs and cancer-related processes, including angiogenesis, apoptosis, epithelial-mesenchymal cell transition (EMT), migration/invasion/metastasis and growth and survival.

Comparison of Genes/Genomic Regions Identified From Unique PB-Induced RAMs that Formed in Both CAR WT (Precancerous Liver and/or Liver Tumor) to Genes/Genomic Regions Identified From Unique PB-induced RAMs in Liver Tumor-Susceptible B6C3F1 Mice (2 and/or 4 Weeks)

We previously identified 170 total unique RAMs in livers of tumor-susceptible B6C3F1 mice treated with 0.05 % (w/w) PB for 2 or 4 weeks, as compared to the resistant C57BL/6 stock (Bachman *et al.*, 2006b), and PCR products representing 90 of these 170 (53%) RAMs were cloned and subjected to BLAT searches that resulted in 51 annotated genes (Phillips and Goodman, 2008). Unique B6C3F1 RAMs at 2 and 4 weeks, which corresponded to identical genes and uncharacterized regions (i.e. regions of DNA greater than 10 kb away from an annotated gene) observed in the current study, were compared to the unique CAR precancerous and tumor RAMs, in order to determine whether the methylation patterns of common genes/uncharacterized regions observed in both studies were altered similarly or differently by PB treatment. Since 3 different restriction digestions were utilized, multiple RAMs might represent the same gene/uncharacterized region.

The following criteria needed to be met in order for a gene/uncharacterized genomic region identified from a PB-induced RAM to be viewed as being in common between the studies: 1) the RAM must have been cloned in both the B6C3F1 (2 and/or 4 weeks PB) and CAR WT (precancerous and/or tumor) mice, and 2) the unique RAMs in the B6C3F1 and CAR WT mice must have aligned to the same region of the genome. Hypermethylated RAMs (significant increases, Student's t-test, $p < 0.05$) and newly methylated RAMs are considered to be increases in methylation, while hypomethylated RAMs (both 100% decreases, and those which are significant, Student's t-test, $p < 0.05$) are considered to be decreases. Genes and uncharacterized genomic regions, identified from identical, unique PB-induced RAMs that formed in both CAR WT (precancerous

liver and/or liver tumor) and B6C3F1 (2 and/or 4 week treated), are listed in Table 4.3 and Table 4.4, respectively.

Cloning and sequencing revealed 2 observations regarding criterion number 2 (above). First, following digestion with the same methylation-sensitive restriction enzyme, PCR products occasionally formed which: a) represented distinct RAMs that differed by more than 2 bp in multiple groups (B6C3F1, 2- and/or 4-week, and CAR WT, precancerous liver and/or liver tumor); and b) aligned to the same region of the genome. Secondly, following digestion with the same methylation-sensitive restriction enzyme, PCR products occasionally formed which: a) represented distinct RAMs that were within 2 bp of one another (e.g., unique RAMs at 315 and 317 bp) in multiple groups (B6C3F1, 2- and/or 4-week, and CAR WT, precancerous liver and/or liver tumor); and b) aligned to the same region of the genome. Thus, for a particular restriction digestion, unique RAMs in the B6C3F1 and CAR WT mice that were within 2 bp of one another or more than 2 bp apart, which were represented by PCR products that aligned to the same region of the genome, were considered to be one RAM. This is evident in Table 4.3 and Table 4.4. The following is an example of situation number one, above. A PCR product, representing a 464 bp RAM that was identified after *RsaI/MspI* digestion and AP-PCR, was cloned in the B6C3F1 mice at 4 weeks, and aligned to *Bcat2* (Table 4.3). Similarly, in the CAR precancerous tissue, a PCR product, representing a 468 bp RAM that was identified after *RsaI/MspI* digestion and AP-PCR, was cloned in the CAR precancerous tissue, and aligned to the same region of *Bcat2* (Table 4.3). While the 2 RAMs were not within 2 bp of one another, the sequencing results clearly demonstrated that the PCR products aligned to the same region of the genome. Therefore, these RAMs were

considered to be one RAM. The following is an example of situation number two, above. For *Ddx54* (Table 4.3), 2 distinct RAMs (M315 in precancerous tissue, and M317 in the B6C3F1 mice at 4 weeks) that the cloned PCR products represent were within 2 bp of one another. Therefore, these RAMs were considered to be one RAM.

RESULTS

PCR products were cloned that represent 119 (82%) of the 146 total unique RAMs previously detected in the livers of male C3H/He CAR WT mice treated with a tumor-promoting dose of PB for 23 (precancerous tissue) or 32 (tumor tissue) weeks, as compared to resistant CAR KO mice, including 14 carry forward RAMs (i.e. those which were observed in both the precancerous and tumor tissue) (p. 200 of this dissertation) (Phillips *et al.*, 2007). These RAMs were annotated via the BLAT sequence alignment tool, and 47 genes were discerned (Table 4.1). Two genes (*Ttll9* and *Wscd1*) are listed twice because in each situation, 2 PCR products of different sizes aligned to 2 distinct, separate regions of the same gene. RAMs were also classified based on their location relative to an annotated gene (Table 4.1 and Fig. 4.8) and chromosomal distribution (Fig. 4.9). All of the annotated genes were subsequently investigated via an informatic approach in order to determine the function of the gene, in addition to any genes which are common targets and/or regulators of the unique RAMs of interest in the precancerous and tumor tissue. A functional summary of these RAMs (Fig. 4.10), plus 1 representative pathway of a unique precancerous and tumor RAM, is presented in Fig. 4.11.

Many (59 of the 75 total genes and genomic regions) annotated RAMs could unambiguously be assigned a specific methylation status (Table 4.1). Unambiguous carry forward hypomethylations were observed in both the precancerous and tumor tissue: annexin A4 (*Anxa4*), coiled-coil domain containing 134 (*Ccdc134*), exosome component 2 (*Exosc2*), RIKEN cDNA 1700027D21 gene (*1700027D21Rik*), and c-abl oncogene 1, receptor tyrosine kinase (*Abl1*). Hypomethylated RAMs that occurred only in the tumor tissue included cellular retinoic acid binding protein 1 (Crabp1), nudC

Table 4.1 Genes and Genomic Regions Identified from Unique Phenobarbital (PB)-induced RAMs in C3H/He Constitutive Active/Androstane Receptor (CAR) Wildtype (Precancerous Liver and/or Liver Tumors), as Compared to Resistant PB-Treated Knockout Mice, were Cloned and Subjected to BLAST-like Alignment Tool (BLAT) Searches

Methylation Status[a]		Gene Name	Gene Symbol	Accession Number	Genomic Location[d]	Normal Function	Potential Role in Tumorigenesis
Precan.[b]	Tumor[c]						
	Hypo (M)[e]	Cellular retinoic acid binding protein 1	*Crabp1*	NM_013496	1.A.ii	Retinoic acid (RA) metabolism (1)[f]	Methylation-associated silencing in esophageal carcinoma (2)
	Hypo (M)	NudC domain containing 3	*Nudcd3*	NM_173748	1.A.ii	Dynein stabilization and cell viability (3)	--
	Hypo (M)	Protein kinase C, epsilon	*Prkce*	NM_011104	1.A.iii	Inhibition of apoptosis (4) and cell proliferation (5)	Transformation (6) and cancer cell proliferation (7)
	Hypo (M)	p53 and DNA damage regulated 1	*Pdrg1*	NM_178939	1.C.ii	Facilitates ultraviolet radiation-induced cell death (8)	--
	Hypo (M)	Solute carrier family 11 (proton-coupled divalent metal ion transporters), member 2	*Slc11a2*	NM_008732	1.A.iii	Divalent cation transport (9)	Overexpressed during the progression of esophageal adenocarcinoma (10)
	Hypo (M)	Spermatogenesis associated 21	*Spata21*	NM_177867	1.B.i	Unknown	--
	Hypo (M)	Tubulin tyrosine ligase-like family, member 9 (381 bp)	*Ttll9*	NM_029064	1.A.ii	α-tubulin-preferring glutamyl ligase (11)	--
	Hypo (B)	Solute carrier family 38, member 9	*Slc38a9*	NM_178746	1.A.iii	Unknown	--
Hypo (B)[g]	**Hypo (B)**	Annexin A4	*Anxa4*	NM_013471	1.A.i	Ca^{2+}-regulated protein involved in ion conductance (12) and membrane permeability (13)	Promotes migration in a model system of renal carcinoma (14)
Hypo (B)	**Hypo (B)**	Coiled-coil domain containing 134	*Ccdc134*	NM_172428	1.A.i	Secretory protein that inhibits ERK and JNK activation (15)	Expressed in a variety of human tumor tissues (15)
Hypo (B)	**Hypo (B)**	Exosome component 2	*Exosc2*	NM_144886	1.C.i	Putative exosome component (16)	--
Hypo (M)	**Hypo (M)**	RIKEN cDNA 1700027D21 gene	*1700027D 21Rik*	NM_029661	1.C.i	Unknown	--
Hypo (B)	**Hypo (B)**	c-abl oncogene 1, receptor tyrosine kinase	*Abl1*	NM_009594	1.B.ii	Cell cycle arrest (17), apoptosis (18), and DNA synthesis in response to growth factors (19)	Various oncogenes are derived from c-abl (20)
Hypo (H)	**Hypo (H)** or Hypo (H)[h]	DNA segment, Chr 13, Wayne State University 177, expressed	*D13Wsu1 77e*	NM_178605	1.B.i	Unknown	--
Hypo (H)	**Hypo (H)** or Hypo (H)[h]	HIG1 domain family, member 2A	*Higd2a*	NM_025933	1.A.i	Unknown	--
Hyper (M)	Hypo (B)	Dead box polypeptide 54	*Ddx54*	NM_028041	1.A.iii	Corepressor of nuclear receptors (21)	--
Hyper (H)	Hyper (M)	Yip1 interacting factor homolog A (S. cerevisiae)	*Yif1a*	NM_026553	1.A.ii	In yeast, functions in endoplasmic reticulum-to-Golgi transport (22)	--
New (M)		Branched chain aminotransferase 2, mitochondrial	*Bcat2*	NM_009737	1.A.ii	Metabolism of branched chain amino acid (23)	--

Table 4.1 continued Genes and Genomic Regions Identified from Unique Phenobarbital (PB)-induced RAMs in C3H/He Constitutive Active/Androstane Receptor (CAR) Wildtype (Precancerous Liver and/or Liver Tumors), as Compared to Resistant PB-Treated Knockout Mice, were Cloned and Subjected to BLAST-like Alignment Tool (BLAT) Searches

New (M)		Ubiquinol-cytochrome c reductase (6.4 kD) subunit	*Uqcr*	NM_025650	I.A.i	Unknown	--
New (M)		Zinc finger and BTB domain containing 8 opposite strand	*Zbtb8os*	NM_025970	I.A.iii	Unknown	--
New (B)	New (B)	Chimerin (chimaerin) 2	*Chn2*	NM_023543	I.A.iii	Regulation of smooth muscle cell proliferation/migration (24) and T-cell responses (25)	Inhibition of proliferation in breast cancer cells (26)
New (B)	New (B)	RIKEN cDNA 1520401A03 gene	*1520401A03Rik*	NM_177132	I.A.iii	Unknown	--
New (M)	New (M)	Sine oculis-related homeobox 3 homolog (Drosophila)	*Six3*	NM_011381	I.A.ii	Homeobox gene involved in brain (27) and ocular (28) development	--
	New (B)	A disintegrin-like and metallopeptidase (reprolysin type) with thrombospondin type 1 motif, 17	*Adamts17*	NM_001033877	I.A.iii	Unknown	--
	New (H)	Annexin A2	*Anxa2*	NM_007585	I.A.iii	Osteoblastic mineralization (29), signal transduction (30) and proliferation (31)	Expression in prostate cancer cells inhibits migration (32)
	New (H)	BTB (POZ) domain containing 11	*Btbd11*	NM_028709	I.A.iii	Potential role in nervous system development (33)	--
	New (H)	Chemokine (C-C- motif) receptor 4	*Ccr4*	NM_009916	I.A.iii	Normal immunity (34)	Tumor immunity (34)
	New (B,H)[i]	Calsyntenin 2	*Clstn2*	NM_022319	I.A.iii	Potential role in synaptic transmission (35)	--
	New (B,H)[i]	Folliculin	*Flcn*	NM_146018	I.A.iii	Potential role in energy and/or nutrient sensing (36)	Potential tumor suppressor (37)
	New (M)	Glutamate decarboxylase-like 1	*Gadl1*	XM_135211	I.A.iii	Unknown	--
	New (B)	Hect domain and RLD 3	*Herc3*	NM_028705	I.A.ii	Binds to and is regulated by ubiquitin (38)	--
	New (B)	Like-glycosyltransferase	*Large*	NM_010687	I.A.iii	Posttranslational protein modification (39), brain development (40)	Located within a critical region that is deleted in meningiomas (41)
	New (B)	Leucine rich repeat and Ig domain containing 2	*Lingo2*	NM_175516	I.A.iii	Unknown	--
	New (H,M)[i]	Src-related kinase lacking C- and N-terminal myristylation sites	*Srms*	NM_011481	I.A.i	Nonreceptor tyrosine kinase (42)	--
	New (B,H)[i]	Transcription factor 4	*Tcf4*	NM_013685	I.A.iii	Wnt signaling (43)	Expression increased in cancer (44,45)
	New (B)	Tubulin tyrosine ligase-like family, member 9 (208 bp)	*Ttll9*	NM_029064	I.A.ii	α-tubulin-preferring glutamyl ligase (11)	--
	New (M)	WD repeat domain 17	*Wdr17*	NM_028220	I.A.iii	Potential role in eye development (46)	--
	New (H)	Zinc finger and SCAN domain containing 22	*Zscan22*	NM_001001447	I.A.i	Unknown	--

Table 4.1 continued Genes and Genomic Regions Identified from Unique Phenobarbital (PB)-induced RAMs in C3H/He Constitutive Active/Androstane Receptor (CAR) Wildtype (Precancerous Liver and/or Liver Tumors), as Compared to Resistant PB-Treated Knockout Mice, were Cloned and Subjected to BLAST-like Alignment Tool (BLAT) Searches

	New (H)	RIKEN cDNA A430078G23 gene	*A430078G23R tk*	NM_001033378	I.B.i	Unknown	--
	Hypo (B,H,M) and/or New (H)[h,i]	Protein tyrosine phosphatase, receptor type O	*Ptpro*	NM_011216	I.A.iii	Transmembrane protein tyrosine phosphatase (47)	Tumor suppressor (47)
New (M)	Hypo (M)	WSC domain containing 1 (407 bp)	*Wscd1*	NM_177618	I.A.iii	Unknown	--
Hypo (H) and/or **Hyper (M)**[i]	**Hyper (M)**	Dipeptidylpeptidase 10	*Dpp10*	NM_199021	I.A.iii	Regulation of K^+-gated voltage channels (48)	--
Hypo (H) and/or **Hyper (M)**[i]	**Hyper (M)**	Tyrosine kinase non-receptor 2	*Tnk2*	NM_016788	I.A.iii	Intracellular kinase that might be involved in growth/movement (49)	Invasion and metastasis (50)
Hypo (B) and/or Hyper (M)[i]	**Hypo (B)** and/or Hypo (M)[i]	Ephrin B2	*Efnb2*	NM_010111	I.A.iii	Vascular development, angiogenesis in adult mice (51)	Angiogenesis and invasion (51-53)
New (H)	**New (H)** or Hypo (H)[h]	Predicted gene, EG622408	*EG622408*	NM_001037914	I.C.i	Unknown	--
Hypo (H) or Hyper (H)[h]	Hypo (B,H) and/or New (M)[i]	Prickle-like 2 (Drosophila)	*Prickle2*	NM_001081146	I.B.ii	Tissue/planar polarity via the WNT/PCP signaling pathway (54)	Expression detected in gastric and uterine cancers (55)
Hypo (B) and/or Hyper (M)[i]	**Hypo (B)** and/or Hypo (M)[i]	Triple functional domain (PTPRF interacting)	*Trio*	XM_001474968	I.A.ii	Coordination of cytoskeleton remodeling (56)	Growth, invasion, tumorigenicity (57)
New (M) and/or **New (H)**[i]	Hypo (M,H) and/or **New (H)**[h,i]	Transmembrane protein 132d	*Tmem132d*	NM_172885	I.A.iii	Unknown	--
Hyper (H) and/or New (B)[i]	Hypo (B,H,M) and/or New (H)[h,i]	WSC domain containing 1 (359-361 bp)	*Wscd1*	NM_177618	I.A.iii	Unknown	--
Hypo in Precan. or Tumor (B/H/M)		Uncharacterized[j]	5 RAMs	--	2	--	--
Hyper in Precan. or Tumor (B/H/M)		Uncharacterized	3 RAMs	--	2	--	--
New in Precan. or Tumor (B/H/M)		Uncharacterized	9 RAMs	--	2	--	--

Table 4.1 continued Genes and Genomic Regions Identified from Unique Phenobarbital (PB)-induced RAMs in C3H/He Constitutive Active/Androstane Receptor (CAR) Wildtype (Precancerous Liver and/or Liver Tumors), as Compared to Resistant PB-Treated Knockout Mice, were Cloned and Subjected to BLAST-like Alignment Tool (BLAT) Searches

Methylation statuses are opposite in Precan. vs. Tumor		Uncharacterized	1 RAM	--	2	--	--
Precan. status is ambiguous[h,i]		Uncharacterized	2 RAMs	--	2	--	--
	Tumor status is ambiguous[h,i]	Uncharacterized	3 RAMs	--	2	--	--
Hypo (B)	Hypo (M)	Multiple gene hits[k]	442-445 bp	Various	3	Various	Various
New (M)		Multiple gene hits[k]	462 bp	Various	3	Various	Various
	New (M)	Uncharacterized[j]	491 bp	--	4	--	--

[a]The methylation status of a region of the genome, as determined by Phillips *et al.* (2007), in the treatment group as compared to the control group: hypomethylations are decreases which were statistically significant (Student's t-test, $p < 0.05$) plus complete 100% decreases, hypermethylations are increases which were statistically significant (Student's t-test, $p < 0.05$), and new methylations were increases, in which specific PCR products formed in the treatment but not in the control group.

[b]Methylation statuses of regions of the genome in precancerous tissue (23 weeks of PB treatment)

[c]Methylation statuses of regions of the genome in tumor tissue (32 weeks of PB treatment)

[d]Genomic location relative to the transcriptional start site

[e]The letter in parentheses indicates which methylation-sensitive restriction enzyme (*BssHII*, *HpaII* or *MspI*) led to the identification of the RAM

[f]The numbers in parentheses correspond to references which are listed in the manuscript that is in press.

[g]**Carry forward RAM (listed in bold) was observed in both the precancerous and tumor tissue.**

[h]Indicates that the region of the genome might be represented by 1 of 2 RAMs that formed via the same restriction digestion and the reason for this uncertainty is explained in the Methods

[i]The region of the genome might be represented by more than 1 RAM because different restriction digestions (e.g., *Hpa*II and/or *Msp*I and/or *BssH*II) led to the identification of multiple RAMs represented by PCR products that aligned to the same region of the genome. With the exception of *Efnb2* and *Trio*, "and/or" indicates that at least 2 of these RAMs exhibited changes in opposite direction.

[j]The uncharacterized genomic regions that these RAMs represent are greater than 10 kb away from an annotated gene.

[k]BLAT showed multiple top hits for the particular PCR product and the sequence associates with a specific repeat element.

containing 3 (*Nudcd3*), protein kinase C, epsilon (*Prkce*), p53 and DNA damage regulated 1 (*Pdrg1*), solute carrier family 11 (proton-coupled divalent metal ion transporters), member 2 (*Slc11a2*), spermatogenesis associated 21 (*Spata21*), tubulin tyrosine ligase-like family, member 9, 381 bp (*Ttll9*), solute carrier family 38, member 9 (*Slc38a9*), dead box polypeptide 54 (*Ddx54*), and WSC domain containing 1, 407 bp (*Wscd1*).

RAMs that were unambiguously assigned a hypermethylated status in the precancerous tissue included dead box polypeptide 54 (*Ddx54*) and Yip1 interacting factor homolog A (S. cerevisiae) (*Yif1a*). In the tumor tissue, Yip1 interacting factor homolog A (S. cerevisiae) (*Yif1a*) was hypermethylated. Furthermore, unambiguous new methylations in the precancerous tissue were branched chain aminotransferase 2, mitochondrial (*Bcat2*), ubiquinol-cytochrome c reductase (6.4 kD) subunit (*Uqcr*), zinc finger and BTB domain containing 8 opposite strand (*Zbtb8os*), chimerin (chimaerin) 2 (*Chn2*), RIKEN cDNA 1520401A03 gene (*1520401A03Rik*), sine oculis-related homeobox 3 homolog (Drosophila) (*Six3*), and WSC domain containing 1, 407 bp (*Wscd1*). Newly methylated RAMs in the tumor tissue included chimerin (chimaerin) 2 (*Chn2*), RIKEN cDNA 1520401A03 gene (*1520401A03Rik*), sine oculis-related homeobox 3 homolog (Drosophila) (*Six3*), A disintegrin-like and metallopeptidase (reprolysin type) with thrombospondin type 1 motif, 17 (*Adamts17*), annexin A2 (*Anxa2*), BTB (POZ) domain containing 11 (*Btbd11*), chemokine (C-C- motif) receptor 4 (*Ccr4*), calsyntenin 2 (*Clstn2*), folliculin (*Flcn*), glutamate decarboxylase-like 1 (*Gadl1*), Hect domain and RLD 3 (*Herc3*), like-glycosyltransferase (*Large*), leucine rich repeat and Ig domain containing 2 (*Lingo2*), src-related kinase lacking C- and N-terminal myristylation

sites (*Srms*), transcription factor 4 (*Tcf4*), tubulin tyrosine ligase-like family, member 9, 208 bp (*Ttll9*), WD repeat domain 17 (*Wdr17*), zinc finger and SCAN domain containing 22 (*Zscan22*) and RIKEN cDNA A430078G23 gene (*A430078G23Rik*). There were no unambiguous hypermethylated or newly methylated RAMs that carried forward from the precancerous to the tumor tissue.

As described in the methods, some genes and genomic regions, which are greater than 10 kb away from a known gene, are tentatively classified as having multiple methylation statuses in the precancerous and/or tumor tissue (21%, 16 of the 75 total genes and genomic regions). Table 4.1 indicates the methylation statuses and particular treatment periods at which these genes displayed altered methylation. The genes were: DNA segment, Chr 13, Wayne State University 177, expressed (*D13Wsu177e*), HIG1 domain family, member 2A (*Higd2a*), protein tyrosine phosphatase, receptor type O (*Ptpro*), dipeptidylpeptidase 10 (*Dpp10*), tyrosine kinase nonreceptor 2 (*Tnk2*), ephrin B2 (*Efnb2*), predicted gene, EG622408 (*EG622408*), prickle-like 2 (Drosophila) (*Prickle2*), triple functional domain, PTPRF interacting (*Trio*), transmembrane protein 132d (*Tmem132d*), and WSC domain containing 1, 359-361 bp (*Wscd1*).

There were 3 PCR products which each associated with multiple "hits" that displayed the highest BLAT scores (i.e. numerous genomic regions showed the fewest mismatches as compared to the sequence of interest), indicating that any of one of the various regions could correspond to the PCR product sequence. While all of the top hits for a particular PCR product represented regions on different chromosomes, the product aligned to the identical repetitive element. Therefore, these 3 RAMs (442-445, 462 and 491 bp) appear to be linked to a different, specific repetitive element, and we are unable

to determine with certainty which genomic region the unique RAM represents. BLAT searches revealed that regions of the genome (including the aforementioned 491 bp region), represented by 24 RAMs, are uncharacterized (i.e. located more than 10 kb away from an annotated gene). Of these 24 RAMs, the methylation statuses of 18 were unambiguous and therefore could be classified as either hypo- (5 RAMs), hyper- (3 RAMs) or new- (10 RAMs) methylations at a particular time point. One of the 24 uncharacterized RAMs could be assigned a specific methylation in both the precancerous and tumor tissue; the changes were opposite in direction (i.e. the precancerous RAM was hypomethylated and the tumor RAM was newly methylated). Finally, for 5 out of the 24 uncharacterized RAMs, the methylation status in the precancerous tissue (2 RAMs) or the tumor tissue (3 RAMs) was ambiguous.

The Pathway Studio® 5.0 informatic program was used to identify common targets and regulators of these genes in precancerous and tumor tissue. Figure 4.1 depicts the common targets of several of the genes of interest in the precancerous tissue. Genes identified from PB-induced RAMs discerned in precancerous liver (Table 4.1) which do not possess targets that are in common with any of the other precancerous genes are not represented in Figure 4.1. Common targets of the genes identified from PB-induced RAMs discerned in tumor tissue are depicted in Figure 4.2. For example, cyclin D1 (CCND1) is a common target of ABL1, CRABP1, PRKCE, and TCF4, and similarly, v-akt murine thymoma viral oncogene homolog 1 (AKT1) is a common target of ABL1, EFNB2, PRKCE, and TCF4. In this way, potential targets of multiple genes of interest were ascertained in order to determine whether common cellular processes might be affected which could more efficiently facilitate tumorigenesis. Additionally, common

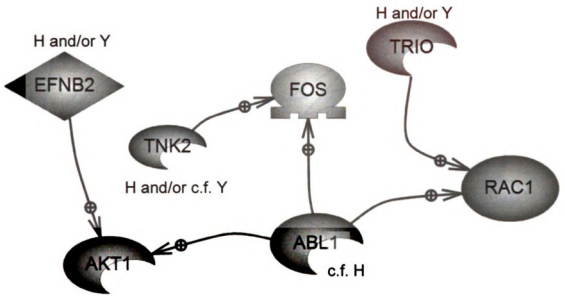


Figure 4.1 Common Targets of Genes Identified from Unique Regions of Altered DNA Methylation (RAMs) in Phenobarbital (PB)-induced Precancerous Liver Tissue from C3H/He Constitutive Active/Androstane Receptor (CAR) Wildtype Mice. An informatics approach was utilized to discern targets of 2 or more genes identified from unique PB-induced RAMs in precancerous tissue (23 weeks). Unique RAMs are hypomethylated (H) or hypermethylated (Y). A combination of letters (e.g., H and/or Y) indicates an ambiguous methylation status. RAMs that carried forward (c.f.), i.e. were observed in both precancerous and tumor tissue, are denoted. The arrows point towards the common targets, which are unlabeled. Positive (—●➔) effects are shown. The shapes of the entities represent the specific class of molecules to which a gene belongs: extracellular proteins or nuclear receptors (⬭), ligands (◇), kinases (◠), and transcription factors (⬭).

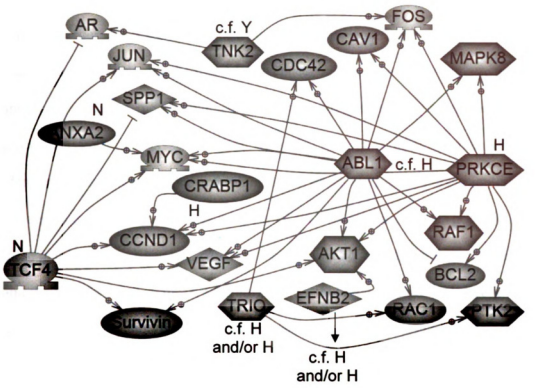


Figure 4.2 Common Targets of Genes Identified from Unique Regions of Altered DNA Methylation (RAMs) in Phenobarbital (PB)-induced Liver Tumor Tissue from C3H/He Constitutive Active/Androstane Receptor (CAR) Wildtype Mice. An informatics approach was utilized to discern targets of 2 or more genes identified from unique PB-induced RAMs in tumor tissue (32 weeks). Unique RAMs are hypomethylated (H), hypermethylated (Y) or newly methylated (N). A combination of letters (e.g., c.f. H and/or H) indicates an ambiguous methylation status. RAMs that carried forward (c.f.), i.e. were observed in both precancerous and tumor tissue are denoted. The arrows point towards the common targets, which are unlabeled. Positive (—•➤) and negative (—⊣) effects are shown. The shapes of the entities represent the specific class of molecules to which a gene belongs: extracellular proteins or nuclear receptors (⬭), ligands (◇), kinases (⬭) and transcription factors (Ω).

regulators of genes of interest in the precancerous and tumor tissue were identified (Fig. 4.12). In order to elucidate how these genes might be contributing to tumorigenesis, interconnections between them and 5 key cancer-related processes (angiogenesis, apoptosis, epithelial-mesenchymal cell transition, migration/invasion/metastasis and growth/survival) were discerned (Figs. 4.3-4.7). The genes of interest that were identified in the precancerous and tumor tissue which are linked to a particular process are depicted separately within each figure. Table 4.2 summarizes the potential effects of these genes on tumorigenesis, based on their connections to the aforementioned processes and their methylation statuses, assuming that methylation changes affect gene expression (e.g., increases in methylation silence expression and decreases in methylation facilitate expression).

As described in the Methods, unique B6C3F1 RAMs at 2 and 4 weeks (identified in Bachman *et al.*, 2006b; annotated in Phillips and Goodman, 2008), which corresponded to identical genes and uncharacterized genomic regions (i.e. regions of DNA greater than 10 kb away from an annotated gene observed in the current study, were compared to the unique CAR precancerous and tumor RAMs, in order to determine whether the methylation patterns of common genes/genomic regions seen in both studies were altered similarly or differently by PB treatment. Eleven genes (*Bcat2, Ddx54, Efnb2, Prickle2, Ptpro, Srms, Tcf4, Tnk2, Trio, Wscd1* and *Zscan22*), identified from unique RAMs, were observed in both groups of mice (Table 4.3). Five genes were identified from RAMs whose methylation statuses either clearly increase (*Bcat2*: M464-468 and *Zscan22*: H238-239) or clearly decrease (*Ddx54:* B312-315, *Ptpro*: B341-342, and *Wscd1*: M358-359) in both the B6C3F1 and CAR WT mice. Three genes were

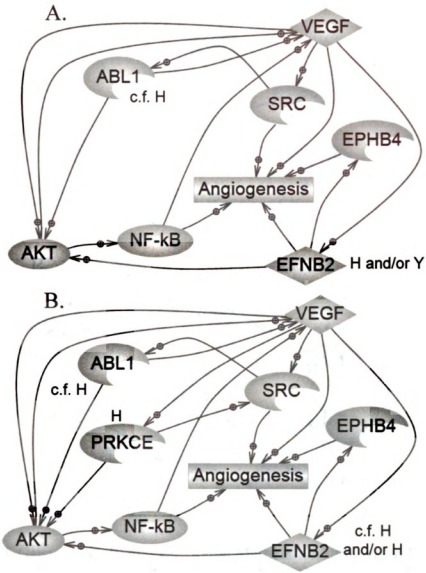


Figure 4.3 Genes which Exhibited Altered Methylation Uniquely in Phenobarbital (PB)-induced Precancerous and Liver Tumor Tissue and which are Potentially Involved in the Regulation of Angiogenesis. An informatics approach was utilized to discern relationships between angiogenesis and genes identified from unique RAMs in precancerous (A) and tumor (B) tissue. Unique RAMs are denoted by their methylation status: hypomethylation (H) or hypermethylation (Y). A combination of letters (e.g., H and/or Y) indicates an ambiguous methylation status, and carry forward (c.f.) RAMs are noted. Positive (—•➤) regulation is shown. The shapes of the entities represent the specific class of molecules to which a gene belongs: extracellular proteins or nuclear receptors (⬭), ligands (◇) and kinases (◠).

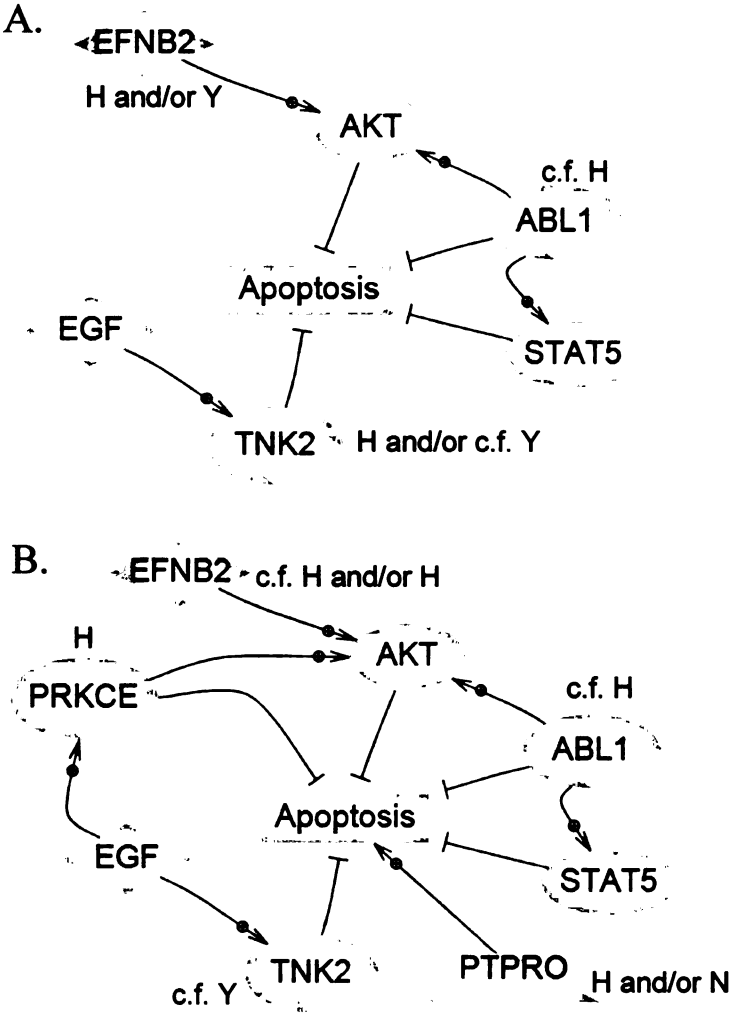


Figure 4.4 Genes which Exhibited Altered Methylation Uniquely in Phenobarbital (PB)-induced Precancerous and Liver Tumor Tissue and which are Potentially Involved in the Regulation of Apoptosis. An informatics approach was utilized to discern relationships between apoptosis and genes identified from unique RAMs in precancerous (A) and tumor (B) tissue. Unique RAMs are denoted by their methylation status: hypomethylation (H), hypermethylation (Y), or new methylation (N). A combination of letters (e.g., H and/or N) indicates an ambiguous methylation status, and carry forward (c.f.) RAMs are noted. Positive (—●→) and negative (—⊣) regulation is shown. The shapes of the entities represent the specific class of molecules to which a gene belongs: extracellular proteins or nuclear receptors (⬭), ligands (◇), kinases (◜) and phosphatases (◢ ◣).

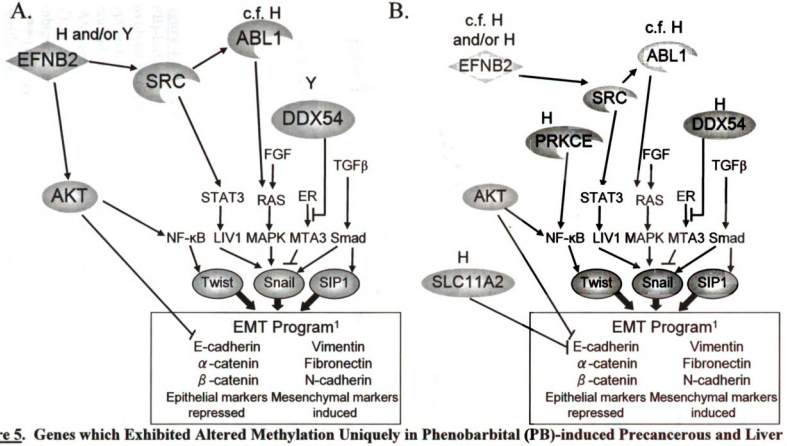


Figure 5. Genes which Exhibited Altered Methylation Uniquely in Phenobarbital (PB)-induced Precancerous and Liver Tumor Tissue and which are Potentially Involved in the Regulation of Epithelial-Mesenchymal Cell Transition (EMT). An informatics approach was utilized to discern relationships between EMT and genes identified from unique RAMs in precancerous (A) and tumor (B) tissue. Unique RAMs are denoted by their methylation statuses: hypomethylation (H) and hypermethylation (Y). A combination of letters (e.g., H and/or Y) indicates an ambiguous methylation status, and carry forward (c.f.) RAMs are noted. Positive (⟶) and negative (⟞) regulation is shown. The shapes of the entities represent the specific class of molecules to which a gene belongs: extracellular proteins or nuclear receptors ( ), ligands ( ), and kinases ( ). [1]The annotated RAMs depicted have been superimposed on a modification of a schematic of the EMT program (Zvaifler, 2006).

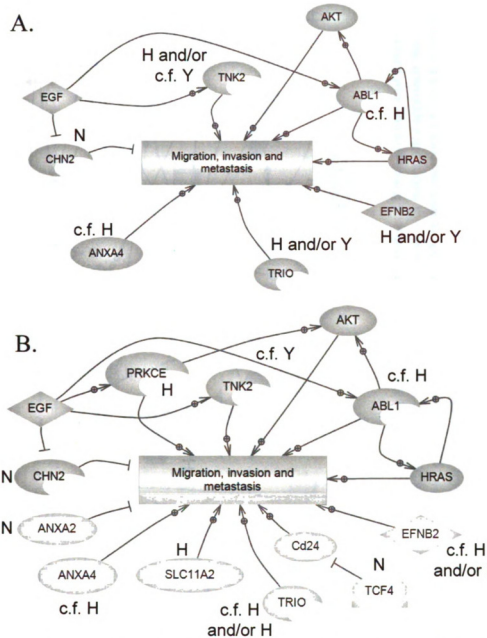


Figure 4.6 Genes which Exhibited Altered Methylation Uniquely in Phenobarbital (PB)-induced Precancerous and Liver Tumor Tissue and which are Potentially Involved in the Regulation of Migration, Invasion and Metastasis. An informatics approach was utilized to discern relationships between migration/invasion/metastasis and genes identified from unique RAMs in precancerous (A) and tumor (B) tissue. Unique RAMs are denoted by their methylation status: hypomethylation (H), hypermethylation (Y), or new methylation (N). A combination of letters (e.g., H and/or Y) indicates an ambiguous methylation status, and carry forward (c.f.) RAMs are denoted. Positive (—•→) and negative (—⊣) regulation is shown. The shapes of the entities represent the specific class of molecules to which a gene belongs: extracellular proteins or nuclear receptors ( ), ligands ( ), transcription factors ( ), and kinases ( ).

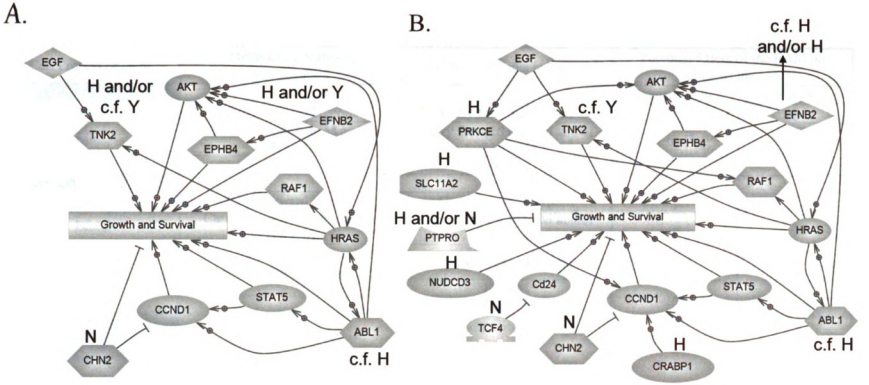


Figure 4.7 Genes which Exhibited Altered Methylation Uniquely in Phenobarbital (PB)-induced Precancerous and Liver Tumor Tissue and which are Potentially Involved in the Regulation of Growth and Survival. An informatics approach was utilized to discern relationships between growth/survival and genes identified from unique RAMs in precancerous (A) and tumor (B) tissue. Unique RAMs are denoted by their methylation status: hypomethylation (H), hypermethylation (Y), or new methylation (N). A combination of letters (e.g., H and/or Y) indicates an ambiguous methylation status, and carry forward (c.f.) RAMs are denoted. Positive (—•→) and negative (—⊣) regulation is shown. The shapes of the entities represent the specific class of molecules to which a gene belongs: extracellular proteins or nuclear receptors (⬭), ligands (◇), kinases (⬭), phosphatases (▲) and transcription factors (⬭).

Table 4.2 Genes Identified from Unique Phenobarbital (PB)-induced RAMs in C3H/He Constitutive Active/Androstane Receptor (CAR) Wildtype (Precancerous Liver and/or Liver Tumors), as Compared to Resistant CAR Knockout Mice, and their Potential Functional Significance in Tumorigenesis

Cell Process or Gene[a]	Methylation Status in Precancerous[b]	Methylation Status in Tumors[c]	Potential Effect of the RAM on Indicated Process[d]	
ANGIOGENESIS			Precancerous	Tumor
Abl1[e]	Carry forward HypoM	Carry forward HypoM	↑[f]	↑
Efnb2	Carry forward HypoM and/or HyperM	Carry forward HypoM and/or HypoM	↑ or ↓[g]	↑
Prkce		HypoM		↑
APOPTOSIS				
Abl1	Carry forward HypoM	Carry Forward HypoM	↓	↓
Efnb2	Carry forward HypoM and/or HyperM	Carry forward HypoM and/or HypoM	↓ or ↑	↓
Tnk2	HypoM and/or carry forward HyperM	Carry forward HyperM	↓ or ↑	↑
Prkce		HypoM		↓
Ptpro		HypoM and/or NewM		↑ or ↓
EPITHELIAL-MESENCHYMAL TRANSITION				
Abl1	Carry forward HypoM	Carry Forward HypoM	↑	↑
Ddx54	HyperM	HypoM	↓	↑
Efnb2	Carry forward HypoM and/or HyperM	Carry forward HypoM and/or HypoM	↑ or ↓	↑
Prkce		HypoM		↑
Slc11a2		HypoM		↑
GROWTH/ SURVIVAL				
Abl1	Carry forward HypoM	Carry Forward HypoM	↑	↑
Chn2	NewM	NewM	↑	↑
Efnb2	Carry forward HypoM and/or HyperM	Carry forward HypoM and/or HypoM	↑ or ↓	↑

Downloaded from http://journals.lww.com/anesthesiology/Fulltext/2019/01000/Anesthesiology_Publication_Info_for_Authors.1.aspx by guest on 01/31/2019

Table 4.2 continued Genes Identified from Unique Phenobarbital (PB)-induced RAMs in C3H/He Constitutive Active/Androstane Receptor (CAR) Wildtype (Precancerous Liver and/or Liver Tumors), as Compared to Resistant CAR Knockout Mice, and their Potential Functional Significance in Tumorigenesis

Tnk2	HypoM and/or carry forward HyperM	Carry forward HyperM	↑ or ↓	↓
Crabp1		HypoM		↑
Nudcd3		HypoM		↑
Prkce		HypoM		↑
Ptpro		HypoM and/or NewM		↓ or ↑
Slc11a2		HypoM		↑
Tcf4		NewM		↑
MIGRATION/INVASION /METSTASIS				
Abl1	Carry forward HypoM	Carry Forward HypoM	↑	↑
Anxa4	Carry forward HypoM	Carry Forward HypoM	↑	↑
Chn2	NewM	NewM	↑	↑
Efnb2	Carry forward HypoM and/or HyperM	Carry forward HypoM and/or HypoM	↑ or ↓	↑
Tnk2	HypoM and/or carry forward HyperM	Carry forward HyperM	↑ or ↓	↓
Trio	HyperM and/or Carry forward HypoM	HypoM and/or Carry forward HypoM	↓ or ↑	↑
Anxa2		NewM		↑
Prkce		HypoM		↑
Slc11a2		HypoM		↑
Tcf4		NewM		↑

[a]Genes which were identified from one or more unique RAMs discerned in precancerous and tumor tissue; [b]Methylation statuses of genes in precancerous tissue (23 weeks of PB treatment); [c]Methylation statuses of genes in tumor tissue (32 weeks of PB treatment); [d]Based on methylation status(es) of the genes (assuming that methylation changes affect gene expression, e.g., increases in methylation silence expression and decreases in methylation facilitate expression), and the relationships between the genes and a cellular process (Figs. 4.3-4.7); [e]Specific relationships between a gene and cellular process are depicted in Figs. 4.3-4.7; [f]A ↑ symbol indicates a potential positive effect (including positive regulation, and inhibition of negative regulation) of the RAM on a cellular process; [g]A ↓ symbol indicates a potential negative effect (including negative regulation, and inhibition of positive regulation) of the RAM on a cellular process.

Table 4.3 Genes Identified from Identical, Unique Phenobarbital (PB)-induced RAMs that Formed in Both CAR Wildtype (Precancerous Liver and/or Liver Tumors) and B6C3F1 (2 and/or 4 Week Treated) Mice

Gene (Genomic Classification)	Considered to be one RAM[c]	Methylation Status			
		B6C3F1[a]		CAR Wildtype[b]	
		2 week	4 week	Precancerous	Tumor
Bcat2: Branched chain aminotransferase 2, mitochondrial (1.A.ii: Exonic)	M464-468		$\uparrow^{N}$ (M464)[d]	$\uparrow^{N}$ (M468)	
Ddx54: Dead box polypeptide 54 (1.A.iii: Intronic)	M315-317[e]		↓ (M317)[f]	↑ (M315)	
	B312-315[e]		↓ (B315)		↓ (B312)
Efnb2: Ephrin B2 (1.A.iii: Intronic)	M564-566	↓ (M566) or $\uparrow^{N}$ (M565)[g]		↑ (M564)	↓ (M564)
Prickle2: Prickle-like 2 (Drosophila) (1.B.ii: > 2 and ≤ 10 kb upstream of TSS)	H310-312[e]	↓ (H312)	↓ (H310)	↓ (H310) or ↑ (H312)[g]	↓ (H312)
	B310-312[e]	$\uparrow^{N}$ (B310)	↓ (B310)		↓ (B312)
Ptpro: Protein tyrosine phosphatase, receptor type O (1.A.iii: Intronic)	H340-343[e]	↓ (H341) or $\uparrow^{N}$ (H343)[g]			↓ (H342) or $\uparrow^{N}$ (H340)[g]
	B341-342[e]	↓ (B341)	↓ (B341)		↓ (B342)
Srms: src-related kinase lacking C-terminal regulatory tyrosine and N-terminal myristylation sites (1.A.i: Spans TSS and/or 5' UTR)	M202-206	↑ (M202) or ↓ (M206)[g]			$\uparrow^{N}$ (M205)
Tcf4: Transcription factor 4 (1.A.iii: Intronic)	H200[e]	↓ (H200)			$\uparrow^{N}$ (H200)
	B200[e]	↑ (B200)	↓ (B200)		$\uparrow^{N}$ (B200)
Tnk2: Tyrosine kinase non-receptor 2 (1.A.iii: Intronic)	M275-276		↓ (M275)	↑ (M276)	↑ (M276)
Trio: Triple functional domain (PTPRF interacting) (1.A.ii: Exonic)	M564-566	↓ (M566) and $\uparrow^{N}$ (M565)[g]		↑ (M564)	↓ (M564)
Wscd1: WSC domain-containing 1 (359-361 bp) (1.A.iii: Intronic)	M358-359[e]		↓ (M358)		↓ (M359)
	B357-358[e]		↑ (B357)	$\uparrow^{N}$ (B357)	↓ (B358)
Zscan22: Zinc finger and SCAN domain containing 22 (1.A.i.: Spans TSS and/or 5' UTR)	H238-239		$\uparrow^{N}$ (H238 or H239)[h]		$\uparrow^{N}$ (H238)

Table 4.3 continued Genes Identified from Identical, Unique Phenobarbital (PB)-induced RAMs that Formed in Both CAR Wildtype (Precancerous Liver and/or Liver Tumors) and B6C3F1 (2 and/or 4 Week Treated) Mice

[a]Unique RAMs that formed in livers of B6C3F1 mice upon 2 or 4 weeks of 0.05% (w/w) PB treatment.
[b]Unique RAMs that formed in C3H/He CAR WT mice (precancerous or tumor tissue).
[c]A unique RAM (e.g., H200) is listed as a single letter, which indicates the methylation-sensitive restriction enzyme (*BssHII*, *HpaII* or *MspI*) which led to the identification of the RAM, plus the size(s), in base pairs, of the unique RAMs detected. If more than 1 size is listed (e.g., M564-566), these represent the span of the RAM sizes in the B6C3F1 and CAR WT groups, as noted in parentheses in the "methylation status" column. The rationale for considering multiple RAMs of similar sizes to be one RAM is detailed within the Materials/Methods.
[d]The presence of an arrow, plus the RAM size, indicates that the unique RAM was discerned in a specific group of mice. Increases in methylation (hypermethylated RAMs: those which are significant, Student's t-test, $p < 0.05$, and newly methylated RAMs, where PCR product formed in the treatment but not the control group) are collectively represented by an upwards arrow (↑); A^N depicts a new methylation, while hypermethylations remain as unlabeled upwards arrows.
[e]Since 3 different restriction digestions were utilized, more than 1 RAM might represent a single gene.
[f]Decreases in methylation (hypomethylated RAMs, both 100% decreases, and those which are significant, Student's t-test, $p < 0.05$) are collectively represented by a downwards arrow (↓).
[g]The methylation status is ambiguous (e.g., newly methylated M565 or hypomethylated M566 might represent *Efnb2*).
[h]The gene might be represented by 1 of 2 RAMs which exhibited the same direction of change (e.g., both are new methylations).

identifie

group

Bill 4 (

Bill (

a 2 wee

CAR to

prevaric

inspec

Prick

identif

RAM

and th

ident

124

grou

Bill

ame

Ma

ide

we

identified from RAMs whose methylation statuses are clearly opposite (e.g., increases in 1 group and decreases in another) in at least 1 B6C3F1 group and 1 CAR WT group: *Ddx54* (M315-317), *Tcf4* (H200) and *Tnk2* (M275-276). *Prickle2* (B310-312) and *Tcf4* (B200) were identified from RAMs in the B6C3F1 whose methylation statuses increase at 2 weeks, decrease at 4 weeks, and either increase (*Tcf4*) or decrease (*Prickle2*) in the CAR tumor tissue. *Wscd1* (B357-358) was identified from RAMs in the CAR precancerous and tumor tissue whose methylation statuses increase and decrease, respectively, and also increase in the B6C3F1 at 4 weeks. Finally, *Efnb2* (M564-566), *Prickle2* (H310-312), *Ptpro* (H340-343), *Srms* (M202-206) and *Trio* (M564-566) were identified from a RAM in at least 1 group whose methylation status is unclear (i.e. 2 RAMs formed in the same group and the methylation changes are opposite in direction), and thus, it is uncertain whether the altered methylation patterns in these 5 genes, identified from 5 RAMs, are similar across groups of B6C3F1 and CAR WT mice.

Six uncharacterized genomic regions on 6 different chromosomes (271-272, 288, 324, 370, 378-379 and 575-576 bp), identified from unique RAMs, were observed in both groups of mice (Table 4.4). Two regions were identified from RAMs whose methylation statuses clearly decrease (271-272 bp: M270-272 and 378-379 bp: M378-380) in both the B6C3F1 and CAR WT mice. Two regions were identified from RAMs whose methylation statuses are clearly opposite (i.e. increases in 1 group and decreases in another) in at least 1 B6C3F1 group and 1 CAR WT group: 288 bp (M286) and 324 bp (M323-326). Regions 271-272 bp (B269-272) and 575-576 bp (M577-579) were identified from RAMs in the B6C3F1 whose methylation statuses are opposite at 2 and 4 weeks, and either increase (271-272 bp) or decrease (575-576 bp) in the CAR tumor

tissue. Finally, regions 271-272 bp (H269-272) and 370 bp (B368-370) were identified from a RAM in 1 group whose methylation status is unclear (e.g., 2 RAMs formed in the same group and the methylation changes are opposite in direction), and thus, it is uncertain whether the altered methylation in these 2 cases is similar across groups of B6C3F1 and CAR WT mice.

DISCUSSION

The methodology employed in this study to evaluate PB-induced altered methylation represents an unbiased approach in the sense that the genes/genomic regions evaluated are not predetermined, i.e. methylation changes are detected first, followed by the identification of the genes/genomic regions exhibiting the changes. RAMs were detected using DNA isolated from whole liver tissue for 4 of the experimental groups (CAR WT 23-week control, CAR KO 23-week control, CAR WT 23-week PB/precancerous and CAR KO 23-week PB). DNA from individual liver tumors was analyzed for the 5th group, CAR WT 32-week PB. It is vital to focus upon whole animal studies, as compared to *in vitro* models only. Firstly, interactions between various cell types are likely to be essential for tumorigenesis, and whole animals also possess an intact immune system, e.g., secretion of IL-6 by macrophages facilitates DEN-induced hepatocarcinogenesis (Naugler *et al.*, 2007) and stromal fibroblasts can promote tumor growth (Orimo *et al.*, 2005). Secondly, the origin of liver tumor cells is unclear. Cancer cell precursors are likely hepatocytes, which can proliferate in response to treatment with mitogens such as PB (Counts *et al.*, 1996; Kolaja *et al.*, 1996a), or partial hepatectomy (Steer, 1995), and adult human (Takahashi *et al.*, 2007) and murine embryonic (Wernig *et al.*, 2007) fibroblasts can be reprogrammed, producing induced pluripotent stem (iPS) cells. Importantly, iPS cells were generated from adult murine hepatocytes following transduction with only four genes, Oct 3/4, Sox2, Klf4, and c-Myc (Aoi *et al.*, 2008). The reprogramming of adult pancreatic exocrine cells into induced β-cells via expression of 3 transcription factors: Ngn3, Pdx1 and Mafa (Zhou *et al.*, 2008) provides a basis for speculating that liver cancer progenitor cells could arise directly from normal liver cells

without reverting to a stem cell state. Additionally, PB treatment can inhibit hepatocyte proliferation, providing an opportunity for those cells which "lose" responsiveness to this inhibition to, possibly, form the initial clones of precancerous cells (reviewed in Counts *et al.*, 1996). The suggestion that hepatocytes are liver tumor cell precursors is not incompatible with the notion that tumor cells might originate from stem cell transformation (Reya *et al.*, 2001).

A limited number of genes have been associated with mouse liver tumorigenesis, i.e. CAR (Huang *et al.*, 2005; Yamamoto *et al.*, 2004), β-catenin (Aydinlik *et al.*, 2001; Strathmann *et al.*, 2006), *c-Myc* (Vorce and Goodman, 1991), Ha-*ras* (Counts *et al.*, 1997; Vorce and Goodman, 1991; Wiseman *et al.*, 1986), Ki-*ras* (Vorce and Goodman, 1991), and *Raf* (Ray *et al.*, 1994). Previously, 146 total unique RAMs were observed in liver-tumor susceptible PB-treated CAR WT mice (precancerous and tumor tissue), as compared to their resistant KO counterpart and we suggested that at least some of these changes might be playing critical roles in the carcinogenesis process (Phillips *et al.*, 2007). In this study, cloning and annotation of a subset (82%) of these unique RAMs revealed 47 genes which might contribute to tumorigenesis due to their altered DNA methylation statuses; 17 have previously been implicated in cancer or related processes (Table 4.1). Thus, we have identified 30 "new" candidate genes which might be involved in PB-induced carcinogenesis.

We recently identified 170 unique RAMs in liver tumor-prone B6C3F1, as compared to relatively resistant C57BL/6, mice upon treatment with 0.05% PB (w/w) for 2 or 4 weeks (Bachman *et al.*, 2006b); subsequent cloning and annotation of these RAMs uncovered 51 genes that exhibited altered methylation (Phillips and Goodman, 2008).

The combined data from these 2 model systems have revealed the formation of unique RAMs in liver tumor-sensitive mice at early (i.e. 2 and 4 weeks) as well as later (i.e. 23 weeks, precancerous and 32 weeks, tumor tissue) treatment time points, and thus, we have: 1) evaluated methylation changes which occur within a continuum of PB-induced liver tumorigenesis, and 2) identified the genes/genomic regions that harbor these modifications.

Strikingly, there were multiple RAMs cloned in both the CAR WT and B6C3F1 mice which aligned to the exact same genomic regions and exhibited unique alterations in methylation in livers of both groups of tumor-susceptible mice, i.e. B6C3F1 and CAR WT. Specifically, 11 genes were identified from identical, unique PB-induced RAMs that formed in both C3H/He CAR WT (precancerous liver and/or liver tumor) and B6C3F1 (2 and/or 4 week treated) mice (Table 4.3). Importantly, these similarities were observed regardless of the stock/strain of mice. While 6 of these genes (*Efnb2*, *Prickle2*, *Ptpro*, *Tcf4*, *Tnk2* and *Trio*) have previously been shown to be involved in cancer or cancer-related processes (Table 4.1; example pathway in Fig. 4.13), the remaining 5 (*Bcat2*, *Ddx54*, *Srms*, *Wscd1* and *Zscan22*) are of particular interest because they represent "new" candidate genes potentially involved in both relatively early and late stages of tumorigenesis. The androgen receptor (*AR*) and *Akt1* are common targets (Fig. 4.14), while *Egf* is a common regulator (Fig. 4.15), of a subset of the 6 cancer-related genes. For some of these common genes (*Ddx54*: M315-317, *Tcf4*: H200, and *Tnk2*: M275-76), the change in methylation status at the 2/4 week time point(s) does not occur in the same direction (e.g., hypomethylation v. hypermethylation) as that seen in the

precancerous/tumor tissue, indicating the possibility for them to have a different role during early, as compared to late, stages of tumorigenesis.

Based on these data, it is conceivable that an "altered methylation fingerprint," consisting of a subset of the genes which exhibited PB-induced altered methylation uniquely in the liver tumor-sensitive mice, could be developed and utilized as a biomarker to identify PB-like nongenotoxic liver tumor promoters at relatively early times following treatment. Preliminary candidates for the "altered methylation fingerprint" are those genes, presented in Table 4.3, which revealed identical methylation changes in both the B6C3F1 and CAR WT mice: *Bcat2*: M464-468, *Ddx54*: B312-315, *Ptpro*: B341-342, *Wscd1*: M358-359, and *Zscan22*: 238-239. A second tier of potential genes that might contribute to an "altered methylation fingerprint" includes 3 genes (identified from 4 RAMs) which occurred in both the B6C3F1 and CAR WT mice; RAMs from at least 1 time point in each group exhibited similar methylation changes, however, an additional group showed an opposite or ambiguous change (e.g., from Table 4.3: *Prickle2*: H310/312, excluding the ambiguous precancerous RAM, *Prickle2*: B310-312, excluding the B6C3F1, 2 week RAM, *Tcf4*: B200, excluding the B6C3F1, 4 week RAM, and *Wscd1*: B357-358, excluding the tumor RAM).

While the genes exhibiting unique PB-induced altered methylation patterns in the precancerous and tumor tissue may individually be playing crucial roles during tumorigenesis (e.g., hypermethylation of a growth suppressor or hypomethylation of an oncogene), analysis of total hepatic DNA, or DNA isolated from individual tumors, does not allow us to conclude whether the changes occurred in one, or multiple, cell populations. Since it is possible that these modifications arose in different populations, it

is constructive to consider the overarching pathways (e.g., angiogenesis) in which these genes participate (Table 4.2; Figs. 4.3-4.7). Similar observations were made by Jones *et al.* (2008) and Parsons *et al.* (2008), who showed that core signaling pathways were genetically altered in pancreatic cancer and glioblastoma, respectively. Importantly, while the particular mutations varied among tumor samples of a specific cancer type (i.e. different genes were affected, depending on the sample), the altered genes participate in the same pathways. Likewise, epigenetic deregulation of certain pathways by numerous genes identified from unique RAMs might more efficiently facilitate tumor formation. Importantly, several unique precancerous RAMs are involved in 5 distinct processes, however, more unique RAMs in the tumor tissue potentially affect these same pathways (Figs. 4.3-4.7), suggesting that altered methylation plays progressively critical roles during tumor development. Additionally, common targets of multiple genes identified from unique RAMs in the precancerous (Fig. 4.1) and tumor (Fig. 4.2) tissue suggest that common processes might be influenced, e.g., AKT1 is a common target of 4 genes identified from unique RAMs in the tumor tissue (Fig. 4.2: *Abl1*, *Efnb2*, *Prkce* and *Tcf4*).

Of the 5 the processes in which multiple genes identified from unique precancerous and tumor RAMs are involved (Figs. 4.3-4.7), 4 of them (angiogenesis, EMT, growth/survival, and invasion/metastasis) are also converged upon by unique B6C3F1 RAMs at 2 or 4 weeks of PB treatment (Fig. 4 in Phillips and Goodman, 2008). Furthermore, common targets (AKT1, CCND1, FOS, JUN, PTK2, and VEGF) of unique precancerous and/or tumor RAMs (Figs. 4.1 and 4.2) are also targets of unique B6C3F1, 4 week RAMs (Fig. 3 in Phillips and Goodman, 2008). These data, combined with the finding that several common genes in the B6C3F1 (2 and 4 weeks) and CAR WT (23 and

32 weeks) mice exhibited PB-induced altered methylation (Table 4.3), indicate the importance of early modifications which might ultimately influence expression and drive tumorigenesis.

Many genes exhibit point mutations, deletions or amplifications in various cancers (Jones *et al.*, 2008; Parsons *et al.*, 2008). However, the integration of genetic and epigenetic data is crucial to understanding the molecular basis of the disease (McLendon *et al.*, 2008), and our data highlight the significance of DNA methylation as an epigenetic mechanism underlying tumorigenesis. It is known that C3H/He and B6C3F1 mice are more susceptible to liver tumors as compared to the C57BL/6 strain (Becker *et al.*, 1982). In response to PB treatment, methylation patterns are altered to a greater extent in the sensitive groups, including higher levels of hypermethylation (C3H/He >> B6C3F1 > C57BL/6), and thus, it is hypothesized that the inability of these animals to maintain normal methylation patterns is responsible, at least in part, for their differential liver tumor susceptibilities (Watson and Goodman, 2002). While the fundamental genes underlying liver cancer in mice and humans are likely the same, rodents exhibit an increased susceptibility to tumorigenesis (Rangarajan and Weinberg, 2003). Also, it has been observed that methylation patterns in rodent cells are less stable than in human cells (reviewed in Goodman and Watson, 2002). Therefore, a difference between humans and rodents might exist with regard to the regulation of epigenetic control, including DNA methylation, resulting in enhanced sensitivity to tumor formation in the latter.

PB causes hepatic hypertrophy and hyperplasia (Whysner *et al.*, 1996), and PB-treated CAR WT, but not CAR KO, mice exhibit an increase in liver mass due to mitogenesis and cellular hypertrophy (Wei *et al.*, 2000). Thus, hypomethylation could

result from replication-dependent, passive demethylation (Howlett and Reik, 1991). Hypomethylated RAMs might occur via physical blocking of cis elements and/or trans-acting factors (e.g., DNA methyltransferases, DNMTs, or methyl-binding proteins) by CAR itself, e.g., the presence of CAR on DNA could sterically hinder the binding of DNMT1. Active demethylation (reviewed in Ooi and Bestor, 2008) might also decrease 5-methylcytosine levels. Increases in methylation (i.e. hyper- and new- methylations) could be mediated by the recruitment of de novo DNMTs (i.e. 3A and 3B) and/or methyl-binding proteins to DNA by CAR, similar to the orphan nuclear receptor GCNF recruitment of de novo methyltransferases, resulting in *Oct-3/4* silencing (Sato *et al.*, 2006). Moreover, CAR might mediate PB-induced expression changes in proteins that could alter methylation status: DNMTs (Goll and Bestor, 2005), proteins involved in demethylation (Ooi and Bestor, 2008), methyl-binding proteins (Lopez-Serra and Esteller, 2008) and/or enzymes involved in regulating levels of *S*-adenosylmethionine (SAM), the primary methyl-donor for DNMT reactions (Ulrey *et al.*, 2005).

The current study focused upon PB-induced RAMs that formed uniquely in liver tumor-sensitive CAR WT (precancerous liver and/or liver tumor tissue), as compared to resistant CAR KO, mice, and the genes identified from these RAMs can function in processes that are important for tumor development, including angiogenesis, apoptosis, EMT, growth/survival, and migration/invasion/metastasis. These data, plus the results from analogous work in which PB-elicited unique RAMs at 2 and 4 weeks in susceptible B6C3F1, as compared to relatively resistant C57BL/6, mice were discerned (Bachman *et al.*, 2006b) and annotated (Phillips and Goodman, 2008), allowed us to identify genes whose methylation statuses were altered uniquely in sensitive animals within a

continuum of PB-induced liver tumorigenesis. A subset of these, as discussed above, represent our initial, preliminary candidate "altered methylation fingerprint" which might be employed as a biomarker to identify PB-like nongenotoxic liver tumor promoters at relatively early times following treatment. Common genes observed at both early (B6C3F1) and later (CAR WT) time points of treatment (Table 4.3), which exhibited unique PB-induced alterations in methylation, participate in the same key processes, indicating that methylation changes at early times are critical for tumor formation. Thus, the current study represents an important step forward towards our goal of enhancing our understanding of genes and pathways involved in PB-induced tumorigenesis. Expression analysis (both quantitative real-time PCR and microarrays) is currently being performed on RNA isolated from the same liver tissue used in the current study and our study involving a comparison of the effects of PB (following 2 or 4 wk of treatment) on liver tumor susceptible B6C3F1 mice as compared to the relatively resistant C57BL/6 (Phillips and Goodman, 2008).

ACKNOWLEDGEMENTS

C3H/He CAR wildtype and knockout mouse liver tissue was graciously provided by Drs. Masahiko Negishi and Robert Maronpot (National Institute of Environmental Health Sciences). Predoctoral fellowship support for J.M.P was received from the National Institutes of Health/National Institute of Environmental Health Sciences training grant No. T32-ES-7255. Research support, in the form of a gift, from the R.J. Reynolds Tobacco Company is acknowledged gratefully.

REFERENCES

Aoi, T., Yae, K., Nakagawa, M., Ichisaka, T., Okita, K., Takahashi, K., Chiba, T., and Yamanaka, S. (2008) Generation of pluripotent stem cells from adult mouse liver and stomach cells. *Science* **321**, 699-702.

Aydinlik, H., Nguyen, T. D., Moennikes, O., Buchmann, A, and Schwarz, M. (2001) Selective pressure during tumor promotion by phenobarbital leads to clonal outgrowth of β-catenin-mutated mouse liver tumors. *Oncogene* **22**, 7812–7816.

Bachman, A. N., Kamendulis, L. M., and Goodman, J. I, (2006a) Diethanolamine and phenobarbital produce an altered pattern of methylation in GC-rich regions of DNA in B6C3F1 mouse hepatocytes similar to that resulting from choline deficiency. *Toxicol. Sci.* **90**, 317–325.

Bachman, A. N., Phillips, J. M, and Goodman J. I. (2006b) Phenobarbital induces progressive patterns of GC-rich and gene-specific altered DNA methylation in the liver of tumor-prone B6C3F1 mice. *Toxicol. Sci.* **91**, 393-405.

Becker, F. F. (1982) Morphological classification of mouse liver tumors based on biological characteristics. *Cancer Res.* **42**, 3918–3923.

Buchmann, A., Bauer-Hofmann, R., Mahr, J., Drinkwater, N. R., Luz, A., and Schwarz, M. (1991) Mutational activation of the c-Ha-*ras* gene in liver tumors of different rodent strains: Correlation with susceptibility to hepatocarcinogenesis. *Proc. Natl. Acad. Sci. U.S.A.* **88**, 911–915.

Counts, J. L., McClain, R. M., and Goodman, J. I. (1997). Comparison of effect of tumor promoter treatments on DNA methylation status and gene expression in B6C3F1 and C57BL/6 mouse liver and in B6C3F1 mouse liver tumors. *Mol. Carcinog.* **18**, 97-106.

Counts, J. L., Sarmiento, J. I., Harbison, M. L., Downing, J. C., McClain, R. M., and Goodman, J. I. (1996). Cell proliferation and global methylation status changes in mouse liver after phenobarbital and/or choline-devoid, methionine-deficient diet administration. *Carcinogenesis* **17**, 1251-1257.

Esteller, M. (2008) Epigenetics in cancer. *N. Engl. J. Med.* **358**, 1148-1159.

Fox, T. R., Schumann, A. M., Watanabe, P. G., Yano, B. L., Maher, V. M., McCormick, J. J. (1990) Mutational analysis of the H-*ras* oncogene in spontaneous C57BL/6 x C3H/He mouse liver tumors and tumors induced with genotoxic and nongenotoxic hepatocarcinogens. *Cancer Res.* **50**, 4014-4019.

Goll, M. G., and Bestor, T. H. (2005) Eukaryotic cytosine methyltransferases. *Annu. Rev. Biochem.* **74**, 481-514.

Goodman, J.I., and Watson, R.E. (2002). Altered DNA methylation: A secondary mechanism involved in carcinogenesis. *Annu. Rev. Pharmacol. Toxicol.* **42**, 501-525.

Honkakoski, P., Zelko, I., Sueyoshi, T., and Negishi, M. (1998) The nuclear orphan receptor CAR-retinoid X receptor heterodimer activates the phenobarbital-responsive enhancer module of the *CYP2B* gene. *Mol. Cell. Biol.* **18**, 5652-5658.

Howlett, S. K., and Reik, W. (1991) Methylation levels of maternal and paternal genomes during preimplantation development. *Development* **113**, 119-127.

Huang, W., Zhang, J., Chua, S. S., Qatanani, M., Han, Y., Granata, R., and Moore, D. D. (2003) Induction of bilirubin clearance by the constitutive androstane receptor (CAR). *Proc. Natl. Acad. Sci. U S A.* **100**, 4156-4161.

Huang, W., Zhang, J., Washington, M., Liu, J., Parant, J. M., Lozano, G., Moore, D. D. (2005) Xenobiotic stress induces hepatomegaly and liver tumors via the nuclear receptor constitutive androstane receptor. *Mol. Endocrinol.* **19**, 1646-1653.

Jones, S., Zhang, X., Parsons, D. W., Lin, J. C., Leary, R. J., Angenendt, P., Mankoo, P., Carter, H., Kamiyama, H., Jimeno, A., Hong, S. M., Fu, B., Lin, M. T., Calhoun, E. S., Kamiyama, M., Walter, K., Nikolskaya, T., Nikolsky, Y., Hartigan, J., Smith, D. R., Hidalgo, M., Leach, S. D., Klein, A. P., Jaffee, E. M., Goggins, M., Maitra, A., Iacobuzio-Donahue, C., Eshleman, J. R., Kern, S. E., Hruban, R. H., Karchin, R., Papadopoulos, N., Parmigiani, G., Vogelstein, B., Velculescu, V. E., and Kinzler, K. W. (2008) Core signaling pathways in human pancreatic cancers revealed by global genomic analyses. *Science* **321**, 1801-1806.

Kawamoto, T., Sueyoshi, T., Zelko, I., Moore, R., Washburn, K., and Negishi, M. (1999) Phenobarbital-responsive nuclear translocation of the receptor CAR in induction of the *CYP2B* gene. *Mol. Cell. Biol.* **19**, 6318-6322.

Kolaja, K. L., Stevenson, D. E., Johnson, J. T., Walborg, E. F., Jr., and Klaunig, J. E. (1996a) Subchronic effects of dieldrin and phenobarbital on hepatic DNA synthesis in mice and rats. *Fundam. Appl. Toxicol.* **29**, 219-228.

Kolaja, K. L., Stevenson, D. E., Walborg Jr., E. F., and Klaunig J. E. (1996b). Dose dependence of phenobarbital promotion of preneoplastic hepatic lesions in F344 rats and B6C3F1 mice: effects on DNA synthesis and apoptosis. *Carcinogenesis* **17**, 947-954.

Konno, Y., Negishi, M., and Kodama, S. (2008) The roles of nuclear receptors CAR and PXR in hepatic energy metabolism. *Drug Metab. Pharmacokinet.* **23**, 8-13.

Lopez-Serra, L., and Esteller, M. (2008) Proteins that bind methylated DNA and human cancer: reading the wrong words. *Br. J. Cancer* **98**, 1881-1885.

McLendon, R., Friedman, A., Bigner, D., Van Meir, E. G., Brat, D. J., Mastrogianakis, G. M., Olson, J. J., Mikkelsen, T., Lehman, N., Aldape, K., *et al.* (2008) Comprehensive genomic characterization defines human glioblastoma genes and core pathways. *Nature* **455**, 1061-1068.

Moennikes, O., Buchmann, A., Romualdi, A., Ott, T., Werringloer, J., Willecke, K., and Schwarz, M. (2000). Lack of phenobarbital-mediated promotion of hepatocarcinogenesis in connexin32-null mice. *Cancer Res.* **15**, 5087-5091.

Naugler, W. E, Sakurai, T., Kim, S., Maeda, S., Kim, K., Elsharkawy, A. M., and Karin, M. (2007) Gender disparity in liver cancer due to sex differences in MyD88-dependent IL-6 production. *Science* **317**, 121–124.

Ooi, S. K., and Bestor, T. H. (2008) The colorful history of active DNA demethylation. *Cell* **133**, 1145-1148.

Orimo, A., Gupta, P. B., Sgroi, D. C., Arenzana-Seisdedos, F., Delaunay, T., Naeem, R., Carey, V. J., Richardson, A. L., and Weinberg, R. A. (2005) Stromal fibroblasts present in invasive human breast carcinomas promote tumor growth and angiogenesis through elevated SDF-1/CXCL12 secretion. *Cell* **121**, 335-348.

Parsons, D. W., Jones, S., Zhang, X., Lin, J. C., Leary, R. J., Angenendt, P., Mankoo, P., Carter, H., Siu, I. M., Gallia, G. L., Olivi, A., McLendon, R., Rasheed, B. A., Keir, S., Nikolskaya, T., Nikolsky, Y., Busam, D. A., Tekleab, H., Diaz, L. A. Jr., Hartigan, J., Smith, D. R., Strausberg, R. L., Marie, S. K., Shinjo, S. M., Yan, H., Riggins, G. J., Bigner, D. D., Karchin, R., Papadopoulos, N., Parmigiani, G., Vogelstein, B., Velculescu, V. E., and Kinzler, K. W. (2008) An integrated genomic analysis of human glioblastoma multiforme. *Science* **321**, 1807-1812.

Phillips, J. M., and Goodman, J. I. (2008) Identification of genes that may play critical roles in phenobarbital (PB)-induced liver tumorigenesis due to altered DNA methylation. *Toxicol. Sci.* **104**, 86-99.

Phillips, J. M., Yamamoto, Y., Negishi, M., Maronpot, R. R., and Goodman, J. I. (2007) Orphan nuclear receptor constitutive active/androstane receptor-mediated alterations in

DNA methylation during phenobarbital promotion of liver tumorigenesis. *Toxicol. Sci.* **96**, 72-82.

Rangarajan, A., and Weinberg, R. A. (2003) Comparative biology of mouse versus human cells: Modeling human cancer in mice. *Nat. Rev. Cancer* **3**, 952–959.

Ray, J. S., Harbison, M. L., McClain, R. M., and Goodman, J. I. (1994) Alterations in the methylation status and expression of the *raf* oncogene in phenobarbital-induced and spontaneous B6C3F1 mouse live tumors. *Mol. Carcinog.* **9**, 155–166.

Reya, T., Morrison, S. J., Clarke, M. F., and Weissman, I. L. (2001) Stem cells, cancer, and cancer stem cells. *Nature* **414**, 105–111.

Rumsby, P. C., Barrass, N. C., Phillimore, H. E., and Evans, J. G. (1991) Analysis of the Ha-*ras* oncogene in C3H/He mouse liver tumours derived spontaneously or induced with diethylnitrosamine or phenobarbitone. *Carcinogenesis* **12**, 2331-2336.

Sato, N., Kondo, M., and Arai, K. (2006) The orphan nuclear receptor GCNF recruits DNA methyltransferase for *Oct-3/4* silencing. *Biochem. Biophys. Res. Commun.* **344**, 845-851.

Steer, C.J. (1995) Liver regeneration. *FASEB J.* **9**, 1396-1400.

Strathmann, J., Schwarz, M., Tharappel, J. C., Glauert, H. P., Spear, B. T., Robertson, L. W., Appel, K. E., and Buchmann, A. (2006) PCB 153, a non-dioxin-like tumor promoter, selects for β-catenin (*Catnb*)-mutated mouse liver tumors. *Toxicol. Sci.* **93**, 34-40.

Sueyoshi, T., Kawamoto, T., Zelko, I., Honkakoski, P., and Negishi, M. (1999) The repressed nuclear receptor CAR responds to phenobarbital in activating the human *CYP2B6* gene. *J. Biol. Chem.* **274**, 6043-6046.

Sueyoshi, T., Moore, R., Sugatani, J., Matsumura, Y., and Negishi, M. (2008) PPP1R16A, the membrane subunit of protein phosphatase 1β, signals nuclear translocation of the nuclear receptor constitutive active/androstane receptor. *Mol. Pharmacol.* **73**, 1113-1121.

Sugatani, J., Kojima, H., Ueda, A., Kakizaki, S., Yoshinari, K., Gong, Q. H., Owens, I. S., Negishi, M., and Sueyoshi, T. (2001) The phenobarbital response enhancer module in the human bilirubin UDP-glucuronosyltransferase *UGT1A1* gene and regulation by the nuclear receptor CAR. *Hepatology* **33**, 1232-1238.

Swales, K. and Negishi, M. (2004) CAR, driving into the future. *Mol. Endocrinol.* **18**, 1589-1598.

Takahashi, K., Tanabe, K., Ohnuki, M., Narita, M., Ichisaka, T., Tomoda, K., and Yamanaka, S. (2007) Induction of pluripotent stem cells from adult human fibroblasts by

defined factors. *Cell* **131**, 861-872.

Ueda, A., Hamadeh, H. K., Webb, H. K., Yamamoto, Y., Sueyoshi, T., Afshari, C. A., Lehmann, J. M., and Negishi, M. (2002) Diverse roles of the nuclear orphan receptor CAR in regulating hepatic genes in response to phenobarbital. *Mol. Pharmacol.* **61**, 1-6.

Ulrey, C. L., Liu, L., Andrews, L. G., and Tollefsbol, T. O. (2005) The impact of metabolism on DNA methylation. *Hum. Mol. Genet.* **14** Spec No 1:R139-147.

Vorce, R. L., and Goodman, J. I. (1991). Hypomethylation of *ras* oncogenes in chemically induced and spontaneous B6C3F1 mouse liver tumors. *Toxicol. Environ. Health.* **34**, 367-384.

Watson, R. E. and Goodman, J. I. (2002). Effects of phenobarbital on DNA methylation in GC-rich regions of hepatic DNA from mice that exhibit different levels of susceptibility to liver tumorigenesis. *Toxicol. Sci.* **68**, 51-58.

Wei, P., Zhang, J., Egan-Hafley, M., Liang, S., and Moore, D. D. (2000). The nuclear receptor CAR mediates specific xenobiotic induction of drug metabolism. *Nature* **407**, 920-923.

Wernig, M., Meissner, A., Foreman, R., Brambrink, T., Ku, M., Hochedlinger, K., Bernstein, B. E., and Jaenisch, R. (2007) In vitro reprogramming of fibroblasts into a pluripotent ES-cell-like state. *Nature* **448**, 318–324.

Whysner, J., Ross, P. M., and Williams, G. M. (1996) Phenobarbital mechanistic data and risk assessment: enzyme induction, enhanced cell proliferation, and tumor promotion. *Pharmacol. Ther.* **71**, 53-91.

Wiseman, R.W., Stowers, S. J., Miller, E. C., Anderson, M. W., and Miller, J. A. (1986) Activating mutations of the c-Ha-*ras* protooncogene in chemically induced hepatomas of the male B6C3 F1 mouse. *Proc. Natl. Acad. Sci. U.S.A.* **83**, 5825–5829.

Yamamoto, Y., Kawamoto, T., and Negishi, M. (2003) The role of the nuclear receptor CAR as a coordinate regulator of hepatic gene expression in defense against chemical toxicity. *Arch. Biochem. Biophys.* **409**, 207-211.

Yamamoto, Y., Moore, R., Goldsworthy, T. L., Negishi, M., and Maronpot, R. R. (2004) The orphan nuclear receptor constitutive active/androstane receptor is essential for liver tumor promotion by phenobarbital in mice. *Cancer Res.* **64**, 7197-7200.

Zhou, Q., Brown, J., Kanarek, A., Rajagopal, J., and Melton, D. A. *In vivo* reprogramming of adult pancreatic exocrine cells to β-cells. *Nature* **455**, 627-632.

Zvaifler, N. J. (2006) Relevance of the stroma and epithelial-mesenchymal transition (EMT) for the rheumatic diseases. *Arthritis Res. Ther.* **8**, 210-220.

CHAPTER 4 APPENDIX

The appendix consists of a series of figures which provide a summary of the genomic locations (Fig. 4.8), chromosomal alignments (Fig. 4.9) and functions (Fig. 4.10) of the genes/genomic regions identified from unique RAMs in CAR WT mice. Additionally, there is 1 example of an informatic pathways of a unique CAR WT RAM (Fig. 4.11), and common cellular regulators of genes identified from unique RAMs in precancerous and tumor tissue (Fig. 4.12). An example of a pathway diagram of genes identified from unique PB-induced RAMs observed in CAR WT and B6C3F1 mice is depicted in Fig. 4.13. Common targets and regulators of genes identified from unique PB-induced RAMs observed in CAR WT and B6C3F1 mice are found in Figs. 4.14 and 4.15, respectively. Identical genomic regions identified from unique PB-induced RAMs observed in CAR WT and B6C3F1 mice are presented in Table 4.1. Note that these data are a subset of the total Supplementary Information that can be found in the version of this manuscript that is in press for publication to *Toxicological Sciences* (as of March 2009).

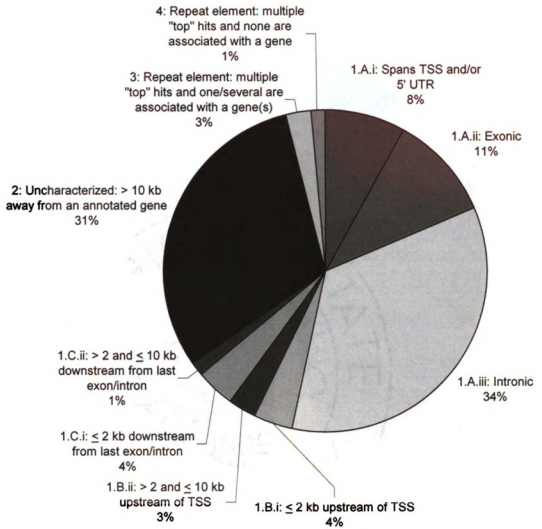


Figure 4.8 The Distribution of Genomic Locations of the Annotated (Including Uncharacterized Regions) Phenobarbital (PB)-induced Unique Regions of Altered DNA Methylation (RAMs) in C3H/He Constitutive Active/Androstane Receptor (CAR) Precancerous and Liver Tumor Tissue. The genomic locations of the annotated (including uncharacterized regions) RAMs are presented based on the classification scheme on page 71 of this dissertation.

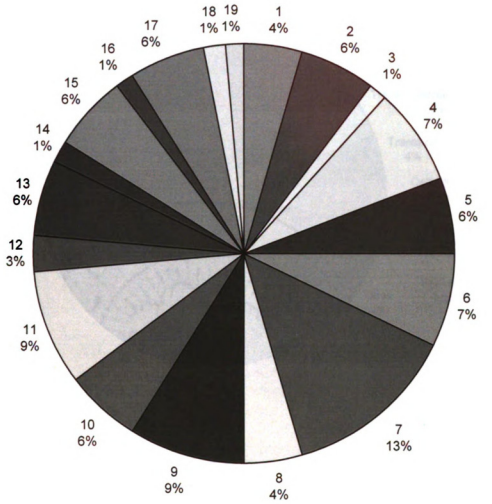


Figure 4.9 The Chromosomal Distribution of the Annotated (Including Uncharacterized Regions) Phenobarbital (PB)-induced Unique Regions of Altered DNA Methylation (RAMs) in C3H/He Constitutive Active/Androstane Receptor (CAR) Precancerous and Liver Tumor Tissue. The chromosomes proceed from 1 to 19, in a clockwise fashion. None of the RAMs aligned to the X or Y chromosomes.

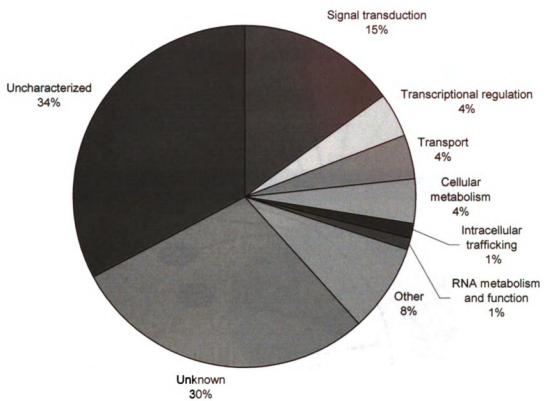


Figure 4.10 Functional Breakdown of the Genomic Regions that Represent Unique PB-induced Regions of Altered DNA Methylation (RAMs) in C3H/He Constitutive Active/Androstane Receptor (CAR) Wildtype Mice (Precancerous and Liver Tumor Tissue). The genomic regions, including genes, representing unique RAMs were broken down into 12 categories, 10 of which are based on Gene Ontology (GO) functional information. For genes in the "unknown" category, no information about them exists in the literature. Regions in the "uncharacterized" category align to the mouse genome greater than 10 kilobases away from an annotated gene.

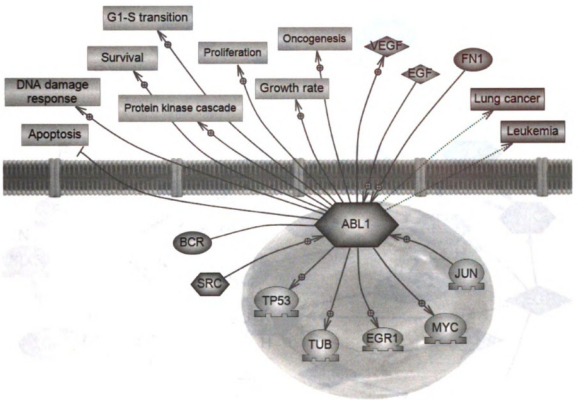


Figure 4.11 Informatics Analysis of c-Abl Oncogene 1, Receptor Tyrosine Kinase (*Abl1*) Which Represents a Unique Carry Forward Hypomethylated RAM in both the Precancerous and Liver Tumor Tissue. The protooncogene *Abl1* encodes a cytoplasmic and nuclear protein tyrosine kinase that has been implicated in a variety of cellular processes, including oncogenesis. Solid arrows indicate positive (—➤) or negative (—⊣) regulation, while dotted arrows (⇢) indicate involvement in disease states. The shapes of the entities represent a specific class of molecules to which a gene belongs: extracellular proteins or nuclear receptors ( ), ligands ( ), kinases ( ) and transcription factors ( ).

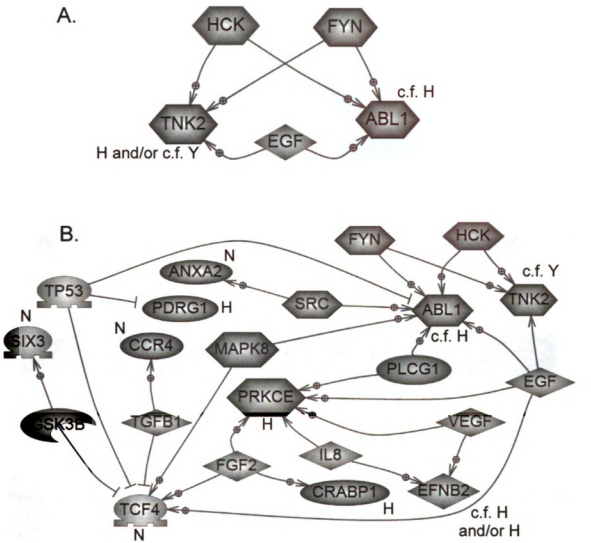


Figure 4.12 Common Regulators of Genes that were Identified from Unique Phenobarbital (PB)-induced Regions of Altered DNA Methylation (RAMs) in C3H/He Constitutive Active/Androstane Receptor (CAR) Wildtype Precancerous and Liver Tumor Tissue. An informatic approach was utilized to discern regulators that affect 2 or more genes identified from unique PB-induced RAMs in precancerous tissue (23 weeks, in A) and liver tumor tissue (32 weeks, in B). Unique RAMs are hypomethylated (H), hypermethylated (Y), or newly methylated (N). A combination of letters (e.g., H and/or Y) represents a RAM with an ambiguous methylation status in the tumor tissue, and carry forward (c.f.) RAMs are notted. The arrows point away from the common regulator (unlabeled) and towards the unique RAM; positive (—➤) and negative (—⊣) regulation is shown. The shapes of the entities represent a specific class of molecules to which a gene belongs: extracellular proteins or nuclear receptors ( ), ligands ( ), kinases ( ), and transcription factors ( ).

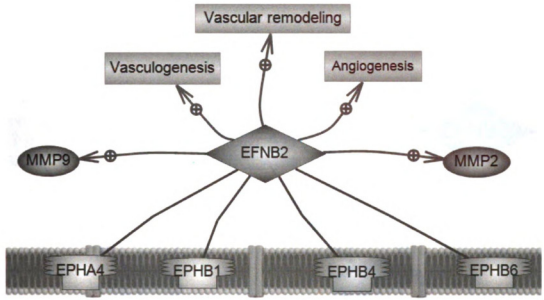


Figure 4.13 Informatic Analysis of Ephrin B2 (*Efnb2*), a Gene Identified from Identical, Unique Phenobarbital (PB)-induced RAMs that Formed in Both C3H/He CAR Wildtype (Precancerous Liver and/or Liver Tumors) and B6C3F1 (2 and/or 4 Weeks) Mice. *Efnb2* encodes a ligand that is involved in angiogenesis. The methylation statuses of this gene in CAR WT and B6C3F1 mice are listed in Table 3. Solid arrows indicate positive (—●→) regulation, while lines lacking arrowheads (———) indicate direct interactions. The shapes of the entities represent a specific class of molecules to which a gene belongs: extracellular proteins (⬭), ligands (◇), and membrane receptors (⬭).

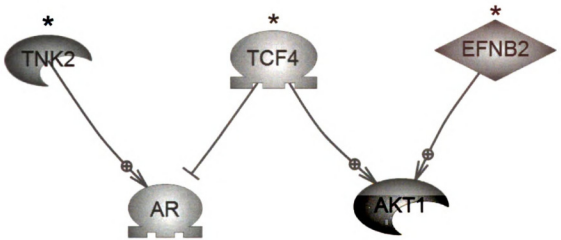


Figure 4.14 Common Targets of Genes Identified from Identical, Unique Phenobarbital (PB)-induced RAMs that Formed in Both C3H/He CAR Wildtype (Precancerous Liver and/or Liver Tumors) and B6C3F1 (2 and/or 4 Weeks) Mice. An informatics approach was utilized to discern targets of 2 or more genes identified from identical, unique PB-induced regions of altered DNA methylation (*) in liver tumor-susceptible CAR WT and B6C3F1 mice. The arrows point towards the common targets (no asterisks); positive (—➤) and negative (—⊣) regulation is shown. The shapes represent the specific class of molecules to which a gene belongs: ligands ( ), kinases ( ), and transcription factors ( ). Table 3 contains the methylation statuses of *Efnb2, Tcf4,* and *Tnk2* in CAR WT and B6C3F1 mice.

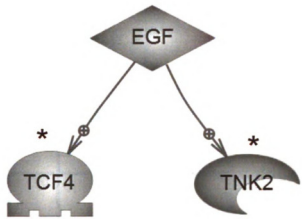


Figure 4.15 Common Regulator of Genes Identified from Identical, Unique Phenobarbital (PB)-induced RAMs that Formed in Both C3H/He CAR Wildtype (Precancerous Liver and/or Liver Tumors) and B6C3F1 (2 and/or 4 Weeks) Mice. An informatics approach was utilized to discern regulators that affect 2 or more genes identified from identical, unique PB-induced regions of altered DNA methylation (*) in liver tumor-susceptible CAR WT and B6C3F1 mice. The arrows point away from the common regulator (no asterisk); positive (→) regulation is shown. The shapes represent a specific class of molecules to which a gene belongs: ligands ( ), kinases ( ), and transcription factors ( ). Table 3 contains the methylation statuses of *Tcf4* and *Tnk2* in CAR WT and B6C3F1 mice.

Table 4.4 Uncharacterized Genomic Regions Identified from Identical, Unique Phenobarbital (PB)-induced RAMs that Formed in Both C3H/He Constitutive Active Androstane Receptor (CAR) Wildtype (Precancerous Liver and/or Liver Tumors) and B6C3F1 (2 and/or 4 Weeks) Mice[a]

Cloned size of uncharacterized region (Chromosome)	Methylation Status[b]				
		B6C3F1		CAR WT	
	Considered to be one RAM[c]	2 wk	4 wk	Precan.	Tumor
271-272 bp (3)	H269-272[d]	↓ (H270) or ↑^{N} (H269)[e]			↑^{N} (H272)
	M270-272[d]		↓ (M271)		↓ (M270 or M272)[f]
	B269-272[d]	↑^{N} (B272)	↓ (B269)		↑^{N} (B272)
288 bp (9)	M286		↓ (M286)		↑^{N} (M286)
324 bp (1)	M323-326		↑^{N} (M326)		↓ (M323 or M324)[f]
370 bp (5)	B368-370		↓ (B369)	↓ (B368, B369) or ↑^{N} (B370)[e]	↓ (B368)
378-379 bp (7)	M378-380		↓ (M378)		↓ (M380)
575-576 bp (2)	M577-579	↓ (M577)	↑ (M577)		↓ (M579)

Table 4.4 Uncharacterized Genomic Regions Identified from Identical, Unique Phenobarbital (PB)-induced RAMs that Formed in Both C3H/He Constitutive Active Androstane Receptor (CAR) Wildtype (Precancerous Liver and/or Liver Tumors) and B6C3F1 (2 and/or 4 Weeks) Mice[a]

[a]In order to determine whether the methylation patterns of identical uncharacterized genomic regions observed in both studies were altered similarly or differently by PB treatment, unique B6C3F1 RAMs induced by 2 and 4 weeks PB (0.05% (w/w)), and unique RAMs in CAR precancerous and tumor tissue representing these identical regions, were compared.
[b]Increases in methylation (hypermethylated RAMs: those which are significant, Student's t-test, $p < 0.05$, and newly methylated RAMs) are collectively represented by an upwards arrow (↑). A superscript "N" depicts a new methylation; hypermethylations are upwards arrows which remain unlabeled. Decreases in methylation (hypomethylated RAMs, both 100% decreases, and those which are significant, Student's t-test, $p < 0.05$) are collectively represented by a downwards arrow (↓).
[c]A unique RAM (e.g., M286) is listed as a single letter, which indicates the methylation-sensitive restriction enzyme (BssHII, HpaII or MspI) used, plus the size(s), in base pairs, of the unique RAMs detected. If more than 1 size (e.g., H269-272) is listed, these represent the span of the RAM sizes in the B6C3F1 and CAR WT groups, as noted in parentheses in the "methylation status" column. A detailed description of the rationale for considering multiple RAMs of similar sizes to be one RAM is detailed within the Materials/Methods.
[d]Since 3 different restriction digestions were utilized, more than 1 RAM might represent an uncharacterized region.
[e]The methylation status is ambiguous (e.g., in the B6C3F1 mice at 2 weeks, newly methylated H269 or hypomethylated H270 could represent the 271-272 bp uncharacterized region).
[f]The uncharacterized region might be represented by 1 of 2 RAMs, which exhibit the same methylation status (e.g., both are decreases).

CHAPTER 5

THE CONSTITUTIVE ACTIVE/ANDROSTANE RECEPTOR (CAR) FACILITATES UNIQUE PHENOBARBITAL (PB)-INDUCED EXPRESSION CHANGES OF GENES INVOLVED IN KEY PATHWAYS IN PRECANCEROUS LIVER AND LIVER TUMORS

This chapter represents a manuscript that was submitted in March 2009 to *Toxicological Sciences*. The authors are Jennifer M. Phillips, Lyle D. Burgoon, and Jay I. Goodman.

ABSTRACT

Our overall goal is to elucidate progressive changes, in expression and methylation status, of genes which play key roles in phenobarbital (PB)-induced liver tumorigenesis, with an emphasis on their potential to affect signaling through critical pathways involved in the regulation of cell growth and differentiation. PB-elicited unique expression changes of genes, including some of those identified previously as exhibiting regions of altered DNA methylation (Phillips and Goodman, 2009a), were discerned in precancerous liver tissue and/or individual liver tumors from susceptible constitutive active/androstane receptor (CAR) wildtype (WT) v. resistant CAR knockout (KO) mice. Many of these function in crucial cancer-related processes, e.g., angiogenesis, apoptosis, cell cycle, DNA methylation, Hedgehog signaling, invasion/metastasis, Notch signaling, and Wnt signaling. Furthermore, a subset of the uniquely altered genes contained CAR response elements (CAREs). This included *Gadd45b*, a coactivator of CAR and apoptosis inhibitor, and 2 DNA methyltransferases (*Dnmt1*, *Dnmt3a*). The presence of CAREs in Dnmts suggests a potential direct link between PB and altered DNA methylation. The current data are juxtaposed with the effects of PB on DNA methylation and gene expression that occurred uniquely in liver tumor-prone B6C3F1 mice, as compared to the resistant C57BL/6, following 2- or 4-wk of treatment (Phillips and Goodman, 2008 and 2009b). Collectively, these data reveal a comprehensive view of PB-elicited molecular alterations (i.e. changes in gene expression and DNA methylation) that can facilitate hepatocarcinogenesis. Notably, candidate genes for initial "fingerprints" of early and late stages of PB-induced tumorigenesis are proposed.

INTRODUCTION

Epigenetic alterations (e.g., DNA methylation), in addition to mutation, play crucial roles during the multistep/multistage process of tumorigenesis (Esteller, 2007; Loeb and Harris, 2008). Indeed, both hypermethylation and hypomethylation are critical mechanisms that facilitate tumor development (Counts and Goodman, 1995; Grønbaek *et al.*, 2007). Furthermore, genes with diverse functions (e.g., cell cycle control, differentiation) participate in signaling that varies dramatically in cancer cells, as compared to normal cells (Weinstein, 2000). For example, physiological dependence upon (i.e. addiction to) increased levels and/or activity of specific genes can be essential for leading to and maintaining the transformed phenotype (Weinstein, 2002). Ultimately, the progressive accumulation of changes results in the acquisition of 6 major features of a tumor that control its malignant growth (Hanahan and Weinberg, 2000).

Our overall goal is to elucidate progressive changes, in expression and methylation status, of genes that play key roles in phenobarbital (PB)-induced liver tumorigenesis, with an emphasis on their potential to affect signaling through critical pathways involved in the regulation of cell growth and differentiation. Treatment with a 0.05% (w/w) promoting dose of PB, a nongenotoxic rodent hepatocarcinogen (Whysner *et al.*, 1996), causes liver tumors in 100% of susceptible B6C3F1 and C3H/He mice after 12 months, but none in the resistant C57BL/6 mice after 18 months (Becker, 1982).

In order to shed light upon potential mechanisms involved in PB-induced tumorigenesis at very early times, we performed an extensive microarray analysis of RNA from tumor-prone B6C3F1 and relatively resistant C57BL/6 mice, treated for 2 and 4 weeks with PB, focusing upon genes whose expression was altered uniquely in the

susceptible group (Phillips and Goodman, 2009b). A subset of the genes can affect angiogenesis, the epithelial-mesenchymal cell transition, and invasion/metastasis, plus the cell cycle and apoptosis, which is consistent with the observations that PB stimulates proliferation (Counts *et al.*, 1996; Kolaja *et al.*, 1996a), and suppresses apoptosis (Kolaja *et al.*, 1996b). We hypothesize that at least some of these initial changes could impart selective clonal advantages to cells.

PB causes the formation of unique regions of altered DNA methylation (RAMs) in the same livers of these tumor-prone B6C3F1 mice v. the relatively C57BL/6, at 2 and 4 weeks (Bachman *et al.*, 2006). Annotation of these regions uncovered 51 genes, many of which are involved in cancer-related processes (Phillips and Goodman, 2008). Taken together, our expression and methylation analyses have provided a more comprehensive picture of unique PB-elicited molecular alterations in susceptible B6C3F1 mice which might facilitate hepatocarcinogenesis as early as 2 and 4 weeks.

The constitutive active/androstane receptor (CAR) mediates many of the effects of PB. However, microarray analysis of C3H/He CAR wildtype (WT) and knockout (KO) mice revealed that only approximately half of the PB-elicited alterations in gene expression observed were dependent upon CAR, indicating that PB also functions through CAR-independent mechanisms (Ueda *et al.*, 2002). Importantly, CAR up-regulates growth arrest and DNA-damage-inducible 45 beta (*GADD45B*) (Yamamoto and Negishi, 2008), a gene which can inhibit TNF-α/JNK-induced apoptosis (Papa *et al.*, 2004).

CAR is required for liver tumor formation elicited by PB (Huang *et al.*, 2005; Yamamoto *et al.*, 2004). C3H/He CAR WT mice, initiated with diethylnitrosamine

(DEN), develop precancerous lesions after 23 weeks of PB promotion and tumors after 32 weeks, while CAR KO mice do not (Yamamoto *et al.*, 2004). PB also induces unique RAMs in CAR WT mice (precancerous liver and/or individual liver tumors), as compared to the CAR KO (Phillips *et al.*, 2007). Annotation of the regions that exhibited these unique methylation changes revealed 47 genes, many of which participate in crucial cancer-associated pathways (e.g., growth, angiogenesis, epithelial-mesenchymal cell transition) (Phillips and Goodman, 2009a).

Here, we have expanded upon our assessment of unique methylation changes in CAR precancerous liver and/or individual liver tumors by evaluating the expression of genes identified from these RAMs, plus 3 DNA methyltransferases (Dnmts). Additionally, an extensive microarray analysis was performed using RNA isolated from the same tissues of the susceptible CAR WT and resistant CAR KO mice, in order to discern genes, as well as overarching cellular processes and signaling pathways, that were perturbed uniquely during later stages of PB-induced tumor development. Finally, a search for putative CAR response elements (CAREs), a subset of PB response elements, within genes whose methylation and/or expression patterns were altered uniquely in the CAR WT mice, including 3 Dnmt genes, was carried out.

The gene expression results presented here complement data obtained from the annotation of genes identified from unique RAMs in precancerous liver and/or liver tumors from PB-treated CAR WT mice (Phillips and Goodman, 2009a), as well as the elucidation of genes whose expression and/or methylation statuses were altered uniquely in PB-treated susceptible B6C3F1 mice, at 2 and/or 4 weeks (Phillips and Goodman, 2008; Phillips and Goodman, 2009b). Combined, these data sets provide insight into

progressive alterations of genes that are involved in signaling pathways and cellular processes that might function throughout a continuum of PB-induced liver tumorigenesis. Significantly, candidate genes for initial "fingerprints" of early, as well as late, stages of PB-induced tumor formation are proposed, based upon the expression and methylation changes of genes ascertained in these studies.

MATERIALS AND METHODS

Animals, Treatments and Tissue Samples

The RNA employed for these studies was isolated from the same liver samples used by Phillips *et al.* (2007) for analysis of DNA methylation. These livers were originally provided by Yamamoto *et al.* (2004). CAR WT or CAR KO mice, on a C3H/He background (which is highly susceptible to liver tumorigenesis (Buchmann *et al.*, 1991)), were injected with a single intraperitoneal dose of diethylnitrosamine (DEN), 90 mg/kg, at 5 weeks of age and then administered drinking water (control) or 0.05% PB (w/w), a liver tumor-promoting dose, in drinking water starting at 7 weeks of age and continuing for 23 or 32 weeks, resulting in the following groups: CAR KO, 23-week control, CAR KO, 23-week PB, CAR WT, 23-week control, CAR WT, 23-week PB (precancerous liver tissue), and CAR WT, 32-week PB (individual liver tumors) (Yamamoto *et al.*, 2004). Whole liver from 4 of the 5 (not including the CAR WT, 32-week PB) groups was utilized; the precancerous liver tissue (CAR WT, 23-week PB) contained no tumors, however, based upon histology of adjacent tissue, there are expected to be numerous microscopic foci of cellular alteration diffused throughout the tissue. Importantly, RNA was isolated from individual liver tumors that developed in the CAR WT, 32-week PB group.

RNA Isolation and Preparation

In a dounce homogenizer, frozen liver samples were homogenized in 1 ml TRIzol® Reagent (Invitrogen, Carlsbad, CA) per 100 mg tissue. Total RNA from each group (N = 6) was isolated via the manufacturer's protocol and stored at -80°C until use.

Upon removal from -80°C, the RNA samples were purified with the Qiagen RNeasy Mini Kit (Qiagen, Valencia, CA) according to the manufacturer's protocol. Samples were eluted in diethyl pyrocarbonate (DEPC)-treated water, and RNA integrity was evaluated on the Agilent 2100 Bioanalyzer using 5 ng sample aliquots and the RNA 6000 Pico Lab-on-a-Chip (Agilent Technologies, Santa Clara, CA). The presence of 2 distinct peaks, representing 18S and 28S rRNA levels, were indicative of high quality samples. Data from the Agilent Bioanalyzer quality control measure revealed that 3 RNA samples (1 CAR WT, 23-week control mouse, 1 CAR KO 23-week control mouse, and 1 CAR KO, 23-week PB-treated mouse) were degraded, and these 3 samples were excluded from further analysis. The purity (A260/A280 ratios) and concentrations of the RNA samples were determined via the NanoDrop™ 8000 spectrophotometer (Thermo Scientific, Wilmington, DE).

Microarray Analysis

All procedures were performed according to standard protocols found within the Affymetrix Genechip® Expression Analysis Technical Manual (Affymetrix, Santa Clara, CA).

RNA Labeling and Fragmentation

The One-Cycle Target Labeling and Control Reagent kit (Affymetrix, Santa Clara, CA) was utilized for first- and second- strand cDNA synthesis plus double-stranded cDNA sample cleanup, and synthesis plus cleanup of biotin-labeled cRNA, of 27 samples (N = 6, for the WT, 23-week PB-treated (precancerous liver tissue), and CAR

WT, 32-week PB-treated (individual liver tumors) groups, plus N = 5 for the WT, 23-week control, KO, 23-week control, and KO, 23-week PB-treated groups). To start, 1 μg of total RNA was used for the generation of double-stranded cDNA. The cDNA was then used as a template for the synthesis of biotinylated cRNA. The size distribution and yield of the labeled cRNA products were evaluated on the Agilent 2100 Bioanalyzer using 5 ng sample aliquots and the RNA 6000 Pico Lab-on-a-Chip (Agilent Technologies, Santa Clara, CA). Subsequently, 15 μg of labeled cRNA was fragmented to a range of 35-200 bp in a 40 μl volume reaction (40mM Tris-acetate at pH 8.1, 100mM potassium acetate, and 30mM magnesium acetate) at 94°C for 35 min. The size distribution of the fragmented cRNA was assessed on the Agilent 2100 Bioanalyzer using 5 ng sample aliquots and the RNA 6000 Pico Lab-on-a-Chip (Agilent Technologies, Santa Clara, CA).

Hybridization, Washing, Staining, and Scanning

Fifteen μg of fragmented cRNA was hybridized to a GeneChip® Mouse Genome 430 2.0 Array (Affymetrix, Santa Clara, CA), containing more than 45,000 probe sets representing over 34,000 genes. The instrumentation utilized for the washing and scanning of the chips is operated by the GeneChip® Operating Software (GCOS, Affymetrix, Santa Clara, CA), version 3.1. After hybridization cocktails were removed, arrays were washed and stained on an Affymetrix Fluidics 450 station, and subsequently scanned using the Affymetrix GeneChip® Scanner 3000 7G, in order to detect hybridization signals. From the resulting image files (DAT file), GCOS computes cell

intensity data (CEL file), which is further analyzed to determine differential gene expression patterns.

Data Analysis

Data from Affymetrix GeneChip CEL files were normalized using GC Robust Multi-array Average (GCRMA) (Wu *et al.*, 2004). Boxplots and Principal Components Analysis (PCA) were employed to assess data quality. A CDF file established by Dai *et al.* (2005), containing more accurate gene/transcript definitions (as compared to those from Affymetrix) based on up-to-date Entrez Gene information, was utilized (Mouse430, version 9.0, from (http://brainarray.mbni.med.umich.edu/Brainarray/Database/CustomCDF/CDF_download_v9.asp). Based upon these new probe set definitions, data was generated for 16,475 genes (as compared to more than 45,000 features representing over 34,000 genes, as indicated by Affymetrix). All statistical analyses were performed in R (v2.6.1) using Bioconductor (2.1).

Identification of Uniquely Active Genes in Liver Tumor-Susceptible CAR WT Mice, as Compared to the Resistant CAR KO

A "consensus" list of CAR WT, 23-week control genes was created in order to focus upon those that demonstrated a high degree of internal consistency of expression within the group. For each gene, the 99% confidence interval (CI) of normalized intensity values of the 5 samples from the CAR WT, 23-week control group was calculated. If at least 4 out of the 5 samples in the control group exhibited expression levels that fell within the 99% CI, these genes were deemed to have the potential to be

differentially expressed (i.e. active) in precancerous liver tissue and/or individual liver tumors (v. WT, 23-week control). In this fashion, the original 16,475 genes derived from the CDF file (for which expression data was initially generated, see above), was reduced to a pool of 13,733. For each gene (out of the 13,733), the average expression level in the CAR WT, 23-week control group was calculated using the normalized expression values from all 5 control samples, and this value was compared to its expression level in each individual precancerous liver tissue sample and individual liver tumor. A gene was considered to be active in the precancerous liver tissue or individual liver tumors (v. CAR WT, 23-week control) based upon meeting 2 criteria: 1) at least 3, of the 6 total, samples in each PB-treated group exhibited expression levels that fell outside (all above or all below) the 99% CI of the control group data, and 2) it exhibited a $\geq$ 2-fold change in expression (up- or down-regulated) as compared to the average expression level of the control group. The average expression level in precancerous liver tissue or individual liver tumors was calculated for each active gene.

In an analogous fashion, a "consensus" list of CAR KO, 23-week control group genes was created. First, for each gene, the 99% confidence interval (CI) of normalized intensity values of the 5 samples from the CAR KO, 23-week control group was calculated. If at least 4 out of the 5 samples in the control group exhibited expression levels that fell within the 99% CI, these genes were deemed to have the potential to be active in liver tissue from the KO, 23-week PB-treated mice (v. KO, 23-week control). In this fashion, the original 16,475 genes derived from the CDF file (for which expression data was initially generated, see above), was reduced to a pool of 12,264. For each gene (out of the 12,264), the average expression level in the CAR KO, 23-week control group

was calculated using the normalized expression values from all 5 control samples, and this value was compared to its expression level in each liver sample from the KO, 23-week PB-treated group. A gene was considered to be active in the CAR KO, 23-week PB-treated group based upon meeting 2 criteria: 1) at least 3, of the 5 total, samples in the PB-treated group exhibited expression levels that fell outside (all above or all below) the 99% CI of the control group, and 2) it exhibited a $\geq$ 2-fold change in expression (up- or down-regulated) as compared to the average expression level of the control group. The average expression level in the CAR KO, 23-week PB-treated group was calculated for each active gene.

Once the active genes in the precancerous liver tissue (v. CAR WT, 23-week control), individual liver tumors (v. CAR WT, 23-week control), and CAR KO, 23-week PB-treated (v. KO, 23-week control) groups were ascertained, uniquely active genes in precancerous and tumor tissue, as compared to liver tissue from the CAR KO, 23-week PB-treated group, were discerned. The active genes in the precancerous liver tissue and liver tissue from the CAR KO, 23-week PB-treated group were compared to one another, and similarly, active genes in the individual liver tumors and CAR KO, 23-week PB-treated group were compared to one another. In order to focus on major differences, common genes observed in both the PB-treated CAR WT (precancerous liver tissue or individual liver tumors) and CAR KO groups that exhibited expression changes in the same direction (i.e. induced or repressed in both) were not given further consideration. Thus, the genes considered to be uniquely active in precancerous liver tissue or individual liver tumors, as compared to liver tissue from CAR KO, 23-week PB-treated, included: 1) common active genes whose expression changes were opposite (e.g., induction in the

precancerous liver tissue or individual liver tumors, and repression in liver from the CAR KO, 23-week PB-treated group), and 2) genes which were active only in the precancerous liver tissue or individual liver tumors. In an analogous manner, uniquely active genes in liver tissue from the CAR KO, 23-week PB-treated group, as compared to the precancerous liver tissue and individual liver tumors, were elucidated.

Finally, the uniquely active genes in precancerous liver tissue were compared to those in individual liver tumors. Genes whose expression was altered uniquely in precancerous liver tissue, as compared to individual liver tumors, included: 1) those whose expression changes were opposite (e.g., induction in the precancerous tissue, and repression in the tumors), and 2) those that were active only in the precancerous tissue. Similarly, genes whose expression was altered uniquely in individual liver tumors, as compared to precancerous liver tissue, included: 1) those whose expression changes were opposite (e.g., induction in the tumors, and repression in the precancerous tissue), and 2) those that were active only in the individual liver tumors. Finally, uniquely active "carry forward" genes were those whose expression changed in the same direction in both precancerous liver tissue and individual liver tumors.

Additionally, in order to be progressively more stringent, core groups of uniquely active genes were identified in precancerous liver tissue and individual liver tumors based on at least 5/6 and 6/6 samples exhibiting expression levels outside of the 99% CI of the control group data, in addition to being $\geq$ 2-fold up- or down-regulated.

Quantitative Real-time PCR (qRT-PCR) Analysis

Expression levels of 3 groups of genes were investigated via qRT-PCR: 1) a subset of 22 genes (listed in Table 5.4) that were uniquely active in precancerous liver tissue and/or individual liver tumors, including 4 uniquely active carry forward genes, 2 genes that were active in both precancerous liver tissue and individual liver tumors that exhibited opposite expression changes, and 16 genes that were active only in individual liver tumors; 2) a subset of 16 genes (listed in Table 5.6) identified from unique RAMs in precancerous liver tissue and/or individual liver tumors, as compared to 23-week PB-treated CAR KO mice, as discerned by Phillips and Goodman (2009a); and 3) 3 DNA methyltransferase (Dnmt) genes (*Dnmt1, Dnmt3a, Dnmt3b*). The genes in Groups 1 and 3, above, were chosen for analysis based on their interesting, potentially cancer-related, documented functions, and the possibility that they affect pertinent signaling pathways (e.g., the 3 genes from Group 3 are involved in establishing DNA methylation patterns). The genes in Group 2 can also influence key pathways, and many were selected because they exhibited identical PB-induced RAMs in liver tumor-susceptible CAR WT and B6C3F1 mice (Phillips and Goodman, 2009a).

Reverse Transcription of RNA

RNA, from the same samples used for microarray analysis (with the exception of 1 tumor sample, for which the RNA was entirely depleted during microarray analysis, and could not be utilized for qRT-PCR, thus the N of the tumor samples decreased from 6 to 5), were treated with amplification grade DNAse I enzyme (Invitrogen, Carlsbad, CA) to eliminate contaminating genomic DNA. Each reaction, containing 1 μg of RNA, 10X DNase I Reaction Buffer, 2 U DNase I, and DEPC-treated water (Ambion Inc., Austin,

TX) up to 10 µl, was incubated for 15 min. at room temperature. DNAse I was inactivated by adding 1 µl of 25 mM EDTA solution and subsequently heating the reactions for 10 min. at 65°C. Reverse transcription reactions containing DNAse I-treated RNA were prepared with reagents from the High Capacity cDNA Reverse Transcription Kit (Applied Biosystems, Foster City, CA). Each reaction contained 1 µg RNA, 10X reverse transcription buffer, 25X dNTP mix (100 mM), 10X random primers, 50 U MultiScribe™ reverse transcriptase, and RNAse-free water, up to 20 total µl. Reactions were incubated at 25°C for 10 min., 37°C for 120 min., and 85°C for 5 s. All samples were stored at 4°C until needed.

Primers for qRT-PCR

Primers were designed using the web-based Primer3 program, v. 0.4.0 (http://frodo.wi.mit.edu/primer3/input.htm) and synthesized by the Macromolecular Structure Facility at Michigan State University. The sizes of the amplicons ranged from 100-140 bp and the primers were 20mers; all other parameters (e.g., melting temperature) remained on the default settings. The majority of primers were designed such that the amplicon spanned an intron-exon junction near the 3' end of the gene of interest. This was confirmed using GenBank sequence information, and also, in most instances, the UCSC In-Silico PCR web-based tool (July 2007 build, http://genome.ucsc.edu/cgi-bin/hgPcr?command=start). This was done so as to preclude the possibility that the expression data could be attributed to contamination with genomic DNA. Furthermore, we are attempting to not simply confirm the microarray data but are extending this to evaluate proper splicing, i.e. this represents a stringent attempt to evaluate changes in

expression of functional mRNAs. Names and symbols, accession numbers, forward and reverse primer sequences of genes chosen for qRT-PCR analysis, plus amplicon sizes, are listed in Supplementary Tables S1A (selected genes that were uniquely active in precancerous liver tissue and/or individual liver tumors, based on microarray analysis) and S1B (selected genes identified from unique RAMs, plus 3 Dnmt genes) in the submitted manuscript.

qRT-PCR Assays

Reactions were prepared with *Power* SYBR® Green PCR Master Mix (Applied Biosystems, Foster City, CA), according to the manufacturer's protocol, with each reaction containing 1 μl of cDNA from the aforementioned reverse transcription reaction (with the exception of 18S reactions, which contained 1 μl of 1:100 diluted cDNA), 1X *Power* SYBR® Green PCR Master Mix, 0.3 μM of both the forward and reverse primers (with the exception of *Dnmt3b*, 0.1 μM) , and DEPC-treated water (Ambion Inc., Austin, TX) up to 50 μl. PCR amplification of duplicate reactions was conducted in MicroAmp™ 96-well Optical Plates (Applied Biosystems, Foster City, CA) using the Applied Biosystems 7500 Real-Time PCR System, with the following thermal cycling conditions: 50°C for 2 min., 95°C for 10 min., and 40 cycles of 95°C for 15 s plus 60°C for 1 min. A dissociation protocol was run for each primer pair to ensure that a single product formed, and agarose gel electrophoresis of amplified products was performed to verify amplicon size.

Before samples were analyzed, standard curves for each gene were generated from purified amplicons. Standard curve samples (spanning 10^2 to 10^8 copies) for a

particular gene were included on the appropriate sample plate so that the absolute quantitation method, which compares the threshold cycle of an unknown sample against a standard curve with known copy numbers, could be used to determine mRNA expression levels. The copy number of the gene of interest for each sample was standardized to that of the 18S rRNA gene to control for differences in RNA quantity, quality, and reverse transcription efficiency. Finally, fold changes in the treatment groups (v. controls), were calculated. The following comparisons were made: 1) precancerous liver tissue (N = 6) v. CAR WT, 23-week control group (N = 5), 2) individual liver tumors (N = 5) v. CAR WT, 23-week control group, and 3) CAR KO, 23-week PB-treated group (N = 5) v. CAR KO, 23-week control group (N = 5). Statistical outliers were excluded from the final fold change calculations following their identification by the Grubbs' test ($p < 0.05$, http://www.graphpad.com/quickcalcs/Grubbs1.cfm). Significance was determined via a Student's t-test ($p < 0.05$). A change was considered to be unique in precancerous liver tissue and/or individual liver tumors (as compared to liver tissue from the CAR KO, 23-week PB-treated group) if: 1) it was in an opposite direction, or 2) it changed to a greater extent (Student's t-test, $p < 0.05$). However, in those cases where there was not a statistically significant change in expression in the treated group, if the expression (either up or down) of the gene in at least 3 samples was outside of the 95% CI of the control group, it was considered to show an 'indication of a change' in expression.

Functional Analysis of Uniquely Active Genes in Precancerous Liver Tissue and/or Individual Liver Tumors

The Database for Annotation, Visualization and Integrated Discovery (DAVID), version 6 (Dennis *et al.*, 2003; http://david.abcc.ncifcrf.gov/), was utilized to obtain functional information about the uniquely active genes in precancerous liver tissue and individual liver tumors. Functional annotation clustering (focused on Gene Ontology terms), one of several DAVID tools available, grouped genes in the precancerous liver tissue and individual liver tumors, separately, into distinct categories which were based upon cellular processes (e.g., angiogenesis) or activity (e.g., oxidoreductase activity). Furthermore, DAVID was used to overlay these genes onto pathways from the Kyoto Encyclopedia of Genes and Genomes (KEGG) database, thus enhancing our understanding of these data. The Pathway Studio® 6.0 informatics program (Ariadne Genomics, Rockville, MD) was used to confirm selected information obtained from DAVID (e.g., multiple relationships depicted in Figs. 5.2-5.5 and Supplementary Figs. S4-S14), and to discern additional connections between genes and pathways/processes of interest.

Identification of Constitutive Active/Androstane Receptor Response Elements (CAREs)

CAREs are a subset of PB-responsive elements (PBREMs) since 1) CAR-independent effects of PB have been observed (Ueda *et al.*, 2002), and thus it is presumed that other classes of cis elements modulate those effects, and 2) there might exist elements which are necessary, but not sufficient, for transcriptional regulation by CAR. Seven *bona fide* constitutive androstane receptor response elements (CAREs) were identified from the literature (Chen *et al.*, 2003; Gerbal-Chaloin *et al.*, 2002; Goodwin *et*

al., 2002; Honkakoski *et al.*, 1998; Sueyoshi *et al.*, 1999; Sugatani *et al.*, 2001) and used to construct a position weight matrix (PWM). The criteria for *bona fide* CAREs are that the elements are functional in a reporter gene assay and have been shown to bind to CAR by either gel shift or chromatin immunoprecipitation assays. Additionally, there had to be a match between the sequences of the elements reported in the literature and the most recent build, i.e. compilation of genome sequence and annotation data at a particular point in time, of the human, mouse, or rat genome. The matrix similarity score threshold used was 0.80, i.e. the identified CAREs were at least 80% similar to the consensus cis element.

The search for CAREs was performed within genes from the 3 groups described above (a subset of uniquely active genes in precancerous liver tissue and/or individual liver tumors that were selected for confirmation by qRT-PCR, a subset of genes identified from unique RAMs in precancerous liver tissue and/or individual liver tumors whose expression levels were evaluated by qRT-PCR, and 3 Dnmt genes). Potential/possible regulatory regions (-10,000 bp relative to the transcription start site through the 5'-untranslated region) for the genes selected for analysis were obtained from the UCSC genome database (http://genome.ucsc.edu). These regulatory regions were analyzed using previously described methods (Sun *et al.*, 2004).

RESULTS

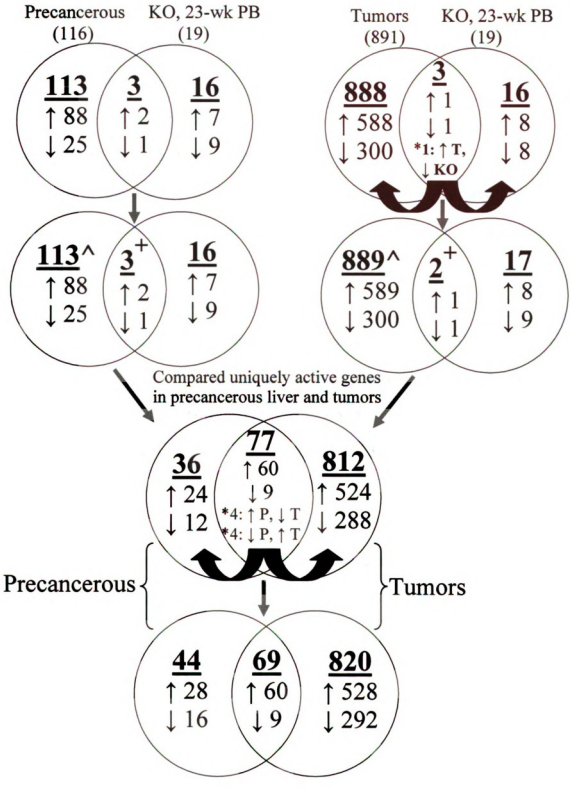
The complete microarray data set is presented as Supplementary Table S2A. Generally, mice within a particular experimental group (e.g., precancerous liver tissue) exhibited similar expression patterns (Fig. 5.6). The distribution of these data are positively skewed (i.e. towards zero), indicative of a good microarray experiment, while some outlying data points for each individual mouse were observed (Fig. 5.7). For the CAR WT, 23-week control and CAR KO, 23-week control mice, "consensus" gene lists were made (Supplementary Tables S2B and S2C, respectively, in the submitted manuscript) and active genes in the PB-treated mice were identified from them. PCA revealed distinct differences in gene expression patterns, based upon treatment and strain (Fig. 5.6).

Identification of Uniquely Active Genes

Active genes in the 3 PB-treated groups, as compared to their respective controls (precancerous liver tissue v. WT, 23-week control; individual liver tumors v. WT, 23-week control; and KO, 23-week PB-treated v. KO, 23-week control), were discerned (Fig. 5.1). Lists of the active genes represented in the Venn diagrams (Fig. 5.1) can be found in Supplementary Tables S3A-I in the submitted manuscript.

PB treatment altered the expression of 116 and 19 genes in precancerous liver tissue and liver tissue from CAR KO 23-week PB-treated mice, respectively (Fig. 5.1). Comparison of these active genes revealed 3 that exhibited the same direction of fold change (2 induced and 1 repressed) in both groups, and therefore, these were not considered further. Thus, 113 genes (88 induced and 25 repressed) were uniquely active

Figure 5.1 Identification of Uniquely Active Genes in Precancerous Liver Tissue and/or Individual Liver Tumors, as Compared to Liver Tissue from Tumor-Resistant Constitutive Active/Androstane Receptor (CAR) Knockout (KO) Mice. Microarray analysis was utilized to discern genes which were differentially expressed, i.e., active (↑, up-regulated or ↓, down-regulated). A gene was considered to be active based on meeting 2 criteria: 1) at least 3, of the 5 or 6 total, samples in each PB-treated group exhibited expression levels that fell outside the 99% confidence interval (CI) of the normalized intensity values of the respective control group, and 2) it exhibited a $\geq$ 2-fold change in expression (up- or down-regulated) as compared to the average expression level of the control group. Uniquely active genes (^) in precancerous liver tissue (P) and/or individual liver tumors (T), as compared to liver tissue from CAR KO, 23-week PB-treated mice, were discerned by excluding genes that exhibited changes which occurred in the same direction (+). Genes that exhibited changes in opposite directions, depicted by asterisks (*), were considered to be uniquely active in each group. Of the 933 total uniquely active genes, 44 were altered in precancerous liver tissue, 820 were altered in individual liver tumors, and 69 were altered in the same direction in both tissues. Gene lists are found in Supplementary Tables S3A-I in the submitted manuscript. Additionally, in order to be progressively more stringent, core groups of uniquely active genes were identified in precancerous liver tissue and individual liver tumors based on at least 5/6 and 6/6 samples.


Precancerous (116)
KO, 23-wk PB (19)
113 ↑88 ↓25
3 ↑2 ↓1
16 ↑7 ↓9
Tumors (891)
KO, 23-wk PB (19)
888 ↑588 ↓300
3 ↑1 ↓1 *1: ↑T, ↓KO
16 ↑8 ↓8
113^ ↑88 ↓25
3+ ↑2 ↓1
16 ↑7 ↓9
889^ ↑589 ↓300
2+ ↑1 ↓1
17 ↑8 ↓9
Compared uniquely active genes in precancerous liver and tumors
36 ↑24 ↓12
77 ↑60 ↓9 *4: ↑P, ↓T *4: ↓P, ↑T
812 ↑524 ↓288
Precancerous
Tumors
44 ↑28 ↓16
69 ↑60 ↓9
820 ↑528 ↓292

in precancerous liver tissue. Conversely, 16 genes (7 induced and 9 repressed) were uniquely active in liver tissue from CAR KO, 23-week PB-treated mice, as compared to precancerous liver tissue.

PB altered the expression of 891 genes in individual liver tumors (Fig. 5.1). When these were compared to the 19 active genes in CAR KO, 23-week PB-treated mice, 3 genes were in common (Fig. 5.1). Two exhibited fold changes that occurred in the same direction (1 induced and 1 repressed) in both groups, and therefore, were not considered further. The third gene exhibited opposite changes, and hence, was considered to be uniquely active in each group. Furthermore, the expression of 888 and 16 genes was altered in individual liver tumors, and liver tissue from CAR KO, 23-week PB-treated mice, respectively. Thus, 889 uniquely active genes (589 induced and 300 repressed) were discerned in individual liver tumors, while 17 (8 induced and 9 repressed) were identified in liver tissue from CAR KO, 23-week PB-treated mice (Fig. 5.1).

Comparison of the 113 (precancerous liver tissue) and 889 (individual liver tumors) uniquely active genes revealed 77 that overlapped (Fig. 5.1). Sixty genes were up-regulated in both groups and 9 were down-regulated in both groups (Supplementary Table S3G), while 8 exhibited opposite expression changes: 4 were induced in precancerous liver tissue and repressed in individual liver tumors, and 4 were repressed in precancerous liver tissue and induced in individual liver tumors. These 8 genes were considered to be uniquely active in each group. In summary, 69 uniquely active genes carried forward (i.e. were induced or repressed in both groups), while 44 genes were

altered uniquely in precancerous liver tissue and 820 were altered uniquely in individual liver tumors (Fig. 5.1). In total, PB elicited unique expression changes of 933 genes in precancerous liver tissue and/or individual liver tumors (Fig. 5.1).

The validity of these microarray data is substantiated by the observation that the expression of PB-induced genes, encoding drug-metabolizing enzymes and drug transporters, whose transcription is mediated by CAR, e.g., *Cyp2b10, Por, Abcc4* (Assem *et al.*, 2004; Ueda *et al.*, 2002), was up-regulated in treated CAR WT, but not KO mice. Additional PB-inducible drug-metabolizing enzymes, e.g., *Cyp2b9* and *Cyp2b13* (Nemoto and Sakurai, 1995; Stupans *et al.*, 1984) were also up-regulated only in CAR WT mice. Importantly, as would be expected, all of these genes comprised a subset of the 69 uniquely active carry forward genes.

Venn diagrams, showing the numbers of genes that were uniquely active in precancerous liver tissue and/or individual liver tumors, based on at least 5/6 and 6/6 samples exhibiting expression levels outside of the 99% CI of the normalized intensity values of the control group, in addition to being $\geq$ 2-fold up- or down-regulated, are located in Figure 5.8, and genes are listed in Supplementary Tables S4A-J in the submitted manuscript. Genes that were uniquely active in at least 5/6 precancerous liver tissue samples and 5/6 individual liver tumors, 51 and 385, respectively, were identified (Fig. 5.8) and are listed in Supplementary Tables S4A and S4B. Comparison of these genes revealed 402 total active genes: 34 carried forward, while 17 were altered uniquely in precancerous liver tissue and 351 were altered uniquely in individual liver tumors.

Genes that were active in all 6 of the precancerous liver tissue samples and all 6 of individual tumors, 35 and 94, respectively, were identified (Fig. 5.8) and are listed in

Supplementary Tables S4F and S4G. Comparison of these genes revealed 106 total active genes: 23 carried forward, while 12 were altered uniquely in precancerous liver tissue, and 71 were altered uniquely in individual liver tumors. Functional annotation and pathway analysis was performed on all 933 active genes in precancerous liver tissue and individual liver tumors, based on at least 3/6 total samples from PB-treated mice exhibiting a change. Additionally, genes that were active in 5/6 total samples are noted in the pathways (Figs. 5.2-5.5 and Supplementary Figs. S4-S14 in the submitted manuscript).

Twenty-two of the 933 uniquely active genes identified by microarray analysis in the precancerous liver tissue and/or individual liver tumors were selected for confirmation of their expression statuses by qRT-PCR (Table 5.4). The expression statuses of 4 carry forward genes were confirmed. Two genes that exhibited changes in opposite directions in the precancerous liver tissue and individual liver tumors were evaluated. The expression of *Cdh1* was confirmed only in precancerous liver tissue, and that of *Fgf21* was confirmed only in individual liver tumors. However, *Fgf21* exhibited a statistically significant decrease in precancerous liver tissue (v. its control). Of 16 genes that were uniquely active only in individual liver tumors, all of their expression statuses were confirmed. While none of these was identified as being uniquely active in precancerous liver tissue based on microarray analysis, unique expression changes were detected by qRT-PCR for 4 of them (*Bmp8b, Gadd45b, Mdm2, Tgfbr2*), and 2 genes (*Mapk3* and *Pdgfa*) exhibited indications of unique expression changes (Table 5.4).

Functional Analysis of Uniquely Active Genes

Functional annotation clustering by DAVID segregated the 933 total uniquely active genes in precancerous liver tissue and/or individual liver tumors into groups based on common biological processes and molecular functions (selected examples in Supplementary Tables S6A-S in the submitted manuscript). Numerous uniquely active genes participate in key cellular processes and signaling pathways that can influence tumor development. The genes are depicted in pathways/processes in Figures 5.2-5.5 and in Supplementary Information (Figs. S4-S14 in the submitted manuscript).

PB altered the expression of genes that can positively or negatively regulate cell cycle progression (e.g., *Cdc2a, Ccnd1, Gadd45a, Gadd45b, Gmnn, Mdm2, Wee1)* (Fig. 5.2). Additional genes demonstrate connections to the cell cycle and growth (Supplementary Fig. S4). The induction and repression of genes involved in apoptosis (e.g., *Casp1, Gadd45a, Gadd45b, Gas1, Myc*, and *p21*) was observed (Fig. 5.2; Supplementary Fig. S5)

Furthermore, genes linked to MAPK signaling were altered (Fig. 5.2; Supplementary Fig. S6). Notably, *Mapk3 (*also known as *Erk1)* was induced. Growth factors which are known to stimulate MAPK cascades (e.g., *Fgf21* and *Pdgfa*), as well as downstream targets of MAPK activation (e.g., *Ddit3, Jun, Mknk2, Myc*), were also affected.

Figure 5.3 depicts uniquely active genes that are involved in multiple cancer-related processes: angiogenesis (e.g., *Angptl6, Cxcr7, Cyr61, Esam1, Pdgfa*), cytoskeleton organization/dynamics (e.g., *Diap2, F2r, Gna12, Rras, Rock2*), and cell-to-cell or cell-to-matrix adhesion (*Cd36, Cd44, Cdh1, Icam1, Lmo7*). Additional genes that contribute to these 3 processes are illustrated in Supplementary Figures S7-S9.

Figure 5.2 The Expression and/or Methylation Statuses of Genes Involved in the Cell Cycle, Apoptosis, and Mitogen-activated Protein Kinase (MAPK) Signaling were Altered in Precancerous and Tumor Tissue. Microarray analysis was employed to identify uniquely active genes in precancerous liver tissue (P) and/or individual liver tumors (T), as described in the Methods. Functional annotation of 933 uniquely active genes (Fig. 1; Supplementary Tables S3G-I in the submitted manuscript) was performed. Genes that were active in at least 5/6 precancerous liver samples and/or 5/6 individual liver tumors are denoted (§) next to the relevant tissue (P or T). Expression was up-regulated (↑), down-regulated (↓), or changed in opposite directions. AKT1 (white symbol), while not altered in response to PB, is included because it 'links' EFNB2 to apoptosis. The tissue (P or T) is underlined one time if the expression change was confirmed by qRT-PCR, two times if qRT-PCR revealed a unique expression change which was not detected by microarray analysis, or three times if there was an indication of a unique expression change (see Methods). qRT-PCR analysis of *Fgf21* expression confirmed its up-regulation in individual liver tumors, while there was a statistically significant decrease in expression in the precancerous tissue (^). Genes not selected for confirmation by qRT-PCR lack underlining and asterisks. If a gene, identified from a unique PB-induced region of altered DNA methylation (RAM) in precancerous liver tissue and/or individual liver tumors (Chapter 4), exhibited a unique expression change based on qRT-PCR, this is denoted by an asterisk (*), while an indication of a unique expression change is represented by 2 asterisks (**). Additional connections between uniquely altered genes and the cell cycle, apoptosis, and MAPK signaling are depicted in Supplementary Figs. S4-S6 in the submitted manuscript. Positive (·····➤) or negative (—┤) regulation is illustrated, and the shapes of the entities represent the specific class of molecules to which the gene belongs: extracellular proteins ( ), ligands ( ), kinases ( ), transcription factors ( ), and membrane receptors ( ).

↑T§
RRAS
↑P,↑T§
PDGFA
↑P,↑T§
TGFBR2
↑T§
JUN
↑T§
MKNK2
↑T
MRAS
↑P,↑I
MAPK3
↓P
GNA12
↑T§
EGFR
MAPK
↑P,↑I
GADD45A
↑P,↑T§
DDIT3
↓P^^§, ↑T§
FGF21
↑P,↑T§
GADD45B
↑P,↑I
CCND1
↑T§
CDC2A
↑T
CDT1
↑T
E2F3
Cell Cycle
↑T
GMNN
↑T
MCM5
↑P,↑I
MDM2
↑T§
WEE1
↑I
TCF4
↑T*
NUDCD3
↑T**
↑P*,↑T*
ABL1
↑P,
↓T
GAS1
↑T
WWOX
↓T
p21
↑T
MYC
↑P,↑I
Apoptosis
↑T§
AHR
↑I
CASP1
↑P,↑T
PHLDA1
↑T
SHF
↑P**,↑T**
TNK2
AKT1
↑P**,↑T*
EFNB2

Figure 5.3 The Expression and/or Methylation Statuses of Genes Involved in Angiogenesis, Cytoskeleton Organization/Dynamics, and Adhesion were Altered in Precancerous and Tumor Tissue. Microarray analysis was employed to identify uniquely active genes in precancerous liver tissue (P) and/or individual liver tumors (T), as described in the Methods. Functional annotation of 933 uniquely active genes (Fig. 1; Supplementary Tables S3G-I in the submitted manuscript) was performed. Genes that were active in at least 5/6 precancerous liver tissue samples and/or 5/6 individual liver tumors are denoted (§) next to the relevant tissue (P or T). Expression was up-regulated (↑), down-regulated (↓), or changed in opposite directions. The tissue (P or T) is underlined one time if the expression change was confirmed by qRT-PCR or three times if there was an indication of a unique expression change (see Methods). qRT-PCR analysis of *Cdh1* confirmed its up-regulation in precancerous liver tissue, but not its down-regulation in individual liver tumors (≠). Genes not selected for confirmation by qRT-PCR lack underlining and asterisks. If a gene, identified from a unique PB-induced region of altered DNA methylation (RAM) in precancerous liver tissue and/or individual liver tumors (Chapter 4), exhibited a unique expression change based on qRT-PCR, this is denoted by an asterisk (*), while an indication of a unique expression change is represented by 2 asterisks (**). *Anxa2* (∞) was uniquely active in individual liver tumors (Supplementary Table S3I in the submitted manuscript) and exhibited a unique RAM. Additional connections between uniquely altered genes and angiogenesis, cytoskeleton organization/dynamics, and adhesion are depicted in Supplementary Figs. S7-S9 in the submitted manuscript. Positive (·····➢) or negative (——┤) regulation is illustrated, and the shapes of the entities represent the specific class of molecules to which the gene belongs: extracellular proteins (⬭), ligands (◇), kinases (◠), and membrane receptors (⊓).

Cytoskeleton Organization/Dynamics
Angiogenesis
Adhesion
↓P
GNA12
↑T
FGD1
↑P,↑T§
F2R
↓T§
EGFR
↑T§
DIAP2
↑P**,↑T**
TNK2
↑P**,↑T*
EFNB2
↑P,↑T§
PDGFA
↑T
IHH
↑T§
ESAM1
↑T§
CXCR7
↑P§,↑T§
ABL1
↑P*,↑T*
TRIO
↑P**,↑T*
PFN2
↑T
ROCK2
↑T§
RRAS
↑T§
FMN1
↓T
FAT1
↑T§
CD36
↑T§
CD44
↑P§,↓T#
CDH1
COL1A2
↑T
ICAM1
↑T
LMO7
↑T§
RELN
↓T
TGFBI
↓T
CYR61
↑T
ANXA2
↑T§,∞
ANGPTL6
↑T§
CD97
↑T
NRP1
↓T§
ENG
↓T

Significantly, genes involved in 5 major developmental pathways (epithelial-mesenchymal cell transition, EMT; Hedgehog; Notch; transforming growth factor-beta, TGF-β, and Wnt) were uniquely active in precancerous liver tissue and/or individual liver tumors (Fig. 5.4; Supplementary Figs. S10-S14). Additionally, uniquely active kinase, phosphatase and phosphatase regulatory (inhibitor) subunit genes are presented in Table 5.5.

Expression of DNA Methyltransferase (Dnmt) Genes

Expression data of *Dnmt1, Dnmt3a* and *Dnmt3b* are presented in Table 5.1. There was a 2-fold increase in the expression of *Dnmt1* in individual liver tumors. Though not statistically significant, there was an indication of up-regulation of *Dnmt1* expression in precancerous liver tissue and in liver tissue from CAR KO, 23-wk PB-treated mice, as evidenced by 3/6 total samples in the precancerous group, and 3/5 total samples in the CAR KO, 23-week PB-treated group exhibiting expression levels that fell above the 95% CI of their respective control group data. The expression of *Dnmt3a* was increased in both precancerous liver tissue (1.27-fold) and individual liver tumors (2.29-fold), while there was no expression change in the CAR KO, 23-week PB-treated group. The expression of *Dnmt3b* was not altered.

Expression of Genes Identified from Unique PB-Induced RAMs

In addition to evaluating the effects of PB on global gene expression, we were also interested in assessing the expression of a subset of genes previously shown to exhibit unique PB-induced RAMs in precancerous liver tissue and/or individual liver

Figure 5.4 The Expression and/or Methylation Statuses of Genes Involved in Pathways Associated with Development and Differentiation were Altered in Precancerous and Tumor Tissue. Microarray analysis was employed to identify uniquely active genes in precancerous liver tissue (P) and/or individual liver tumors (T), as described in the Methods. Functional annotation of 933 uniquely active genes (Fig. 1; Supplementary Tables S3G-I in the submitted manuscript) was performed. Genes that were active in at least 5/6 precancerous liver samples and/or 5/6 individual liver tumors are denoted (§) next to the relevant tissue (P or T). Expression was up-regulated (↑), down-regulated (↓), or changed in opposite directions. The tissue (P or T) is underlined one time if the expression change was confirmed by qRT-PCR, two times if qRT-PCR revealed a unique expression change which was not detected by microarray analysis, or three times if there was an indication of a unique expression change (see Methods). There was an indication of up-regulation of *Wnt5a* expression in precancerous liver tissue (^). Genes not selected for confirmation by qRT-PCR lack underlining and asterisks. If a gene, identified from a unique PB-induced unique region of altered DNA methylation (RAM) in precancerous liver tissue and/or individual liver tumors (Chapter 4), exhibited a unique expression change based on qRT-PCR, this is denoted by an asterisk (*), while an indication of a unique expression change is represented by 2 asterisks (**). Additional connections between uniquely altered genes and pathways that are instrumental in development and differentiation (epithelial-mesenchymal cell transition, EMT; Hedgehog; Notch; transforming growth factor-beta, TGF-beta) are depicted in Supplementary Figures S10-S14 in the submitted manuscript. Positive (·····➔) or negative (——┤) regulation is illustrated, and the shapes of the entities represent the specific class of molecules to which the gene belongs: extracellular proteins ( ), ligands ( ), kinases ( ), transcription factors ( ), and membrane receptors ( ).

Development and Differentiation
WNT
WIF1
PRICKLE2
WISP1
NKD1
JUN
AXIN2
CCND1
TGF-beta
BMP8b
DCN
FST
TGFBR2
TGFBR3
GAS1
WNT5A
TCF4
MYC
ID2
ID3
Hedgehog
CSNK1E
SMO
IHH
Notch
RFNG
DTX4
TRIO
EFNB2
ABL1
EMT
EGFR
MAPK3

Table 5.1 Quantitative Real-time PCR (qRT-PCR) Analysis of the Expression of 3 DNA Methyltransferase (Dnmt) Genes

Gene	Experimental Group[a]	Fold Change[b]	No. of Mice that Exhibited a Change Outside 95% CI of Control Group[c]
Dnmt1: DNA methyltransferase 1	KO, 23 wk PB	n.c.	↑ 3
	Precancerous	n.c.	4: ↑ 3, ↓ 1
	Tumors	↑ 2.00	--
Dnmt3a: DNA methyltransferase 3a	KO, 23 wk PB	n.c.	--
	Precancerous	↑ 1.27	--
	Tumors	↑ 2.29	--
Dnmt3b: DNA methyltransferase 3b	KO, 23 wk PB	n.c.	--
	Precancerous	n.c.	--
	Tumors	n.c.	--

[a] Phenobarbital (PB) was administered to constitutive active/androstane receptor (CAR) wildtype (WT) mice for 23 weeks (precancerous liver tissue) or 32 weeks (individual liver tumors), and to CAR knockout (KO) mice for 23 weeks.

[b] A fold change of gene expression (↑, up-regulation) is listed if it was statistically significant (Student's t-test, $p < 0.05$) in a treatment group (v. its control). If it was not significant, no change (n.c.) is listed. Comparisons were made as described in the Methods.

[c] If a fold change was not statistically significant, a gene was considered to show an indication of a change if at least 3 samples from the PB-treated group exhibited expression that was outside (above, ↑ or below, ↓) the 95% confidence interval (CI) of the control group data. If there was no indication of a change, or if a fold change was statistically significant, these data are not shown (--).

tumors (Phillips and Goodman, 2009a). qRT-PCR was employed to evaluate expression of 16 of these genes, using RNA isolated from the same tissues in which the unique RAMs were ascertained (Table 5.6). In this manner, complementary data from our gene expression and DNA methylation studies were depicted (Figs. 5.2-5.5). Genes that exhibited only a PB-induced change in methylation are shown in Supplementary Figs. S4-S5, S7, and S9.

Presence of CAREs

Thirty genes, whose expression and/or methylation statuses were altered uniquely (with the exception of *Dnmt3b*) in precancerous liver tissue and/or individual liver tumors, contained at least 1 putative CARE within 10 kb upstream of their transcriptional start sites (Table 5.2; base sequences of the putative CAREs are listed in Supplementary Table S9 in the submitted manuscript). Of these, 26 (including *Gadd45a*, *Gadd45b*, *Tgfbr2, Dnmt1, Dnmt3a*, and *Dnmt3b*) were subjected to qRT-PCR analysis (Table 5.1; Appendix Tables 5.4 and 5.6).

Comparison of Current Data with Analogous Data Obtained from B6C3F1 Mice

In a previous series of studies, we evaluated unique gene expression changes and the presence of CAREs, and performed functional annotation of genes of interest in liver tumor-prone B6C3F1 mice, as compared to the relatively resistant C57BL/6, following treatment with a tumor-promoting dose of PB for 2 and 4 weeks (Phillips and Goodman, 2009b). It is instructive to now compare these data with the analogous data reported in the current manuscript: the expression of 3 Dnmt genes (Table 5.3), genes identified from

Table 5.2 Expression of Genes that Contain Putative Constitutive Active/Androstane Receptor Response Elements (CAREs)[A,B]

Gene[C]		Precancerous or Liver Tumors	Microarray Analysis[D]	qRT-PCR Analysis[E]	Methylation Change[F]	No. of Putative CAREs
Exhibited Expression Changes Based on Microarray Analysis[G]	*Bmp8b*	Precancerous	ND[J]	↑		1
		TUMORS	↑	↑		
	Cdh1	**PRECANCEROUS**	↑	↑		2
		Tumors	↓	n.s.[K]		
	Fgf21	**PRECANCEROUS**	↓	↓[L]		2
		TUMORS	↑	↑		
	Gadd45a[H]	Precancerous	↑	↑		2
		Tumors	↑	↑		
	Gadd45b[H]	Precancerous	ND[J]	↑		4
		TUMORS	↑	↑		
	Id3	**TUMORS**	↓	n.p.[M]		1
	Mapk3	Precancerous	ND[J]	n.s.[K]		1
		Tumors	↑	↑		
	Mdm2	Precancerous	ND[J]	↑		4
		Tumors	↑	↑		
	Myc	Precancerous	↑	↑		1
		Tumors	↑	↑		
	Tgfbr2[I]	Precancerous	ND[J]	↑		1
		TUMORS	↑	↑		
	Wisp1	**PRECANCEROUS**	↑	↑		1
		TUMORS	↑	↑		
	Casp1	Tumors	↑	↑		1
	Cbs[H]	Tumors	↓	n.p.[M]		3
	Ccnd1	Tumors	↑	↑		1

Table 5.2 continued Expression of Genes that Contain Putative Constitutive Active/Androstane Receptor Response Elements (CAREs)[A,B]

	Cdc2a	**TUMORS**	↑	↑		2
	Ddit3	**TUMORS**	↑	↑		1
	Jun	**TUMORS**	↑	↑		2
	Nkd1	**TUMORS**	↑	↑		1
	Wee1[H]	**TUMORS**	↑	n.p.[M]		5
DNA methyltransferases[N]	*Dnmt1*	Precancerous	ND[J]	n.s.[K]		3
		Tumors	ND[J]	↑		
	Dnmt3a	Precancerous	ND[J]	↑		2
		Tumors	ND[J]	↑		
	Dnmt3b	Precancerous	ND[J]	n.s.[K]		1
		Tumors	ND[J]	n.s.[K]		
	Abl1	Precancerous	ND[J]	↑	c.f. HypoM	2
		Tumors	ND[J]	↑	c.f. HypoM	
	*Anxa2**	Tumors	↑	n.p.[M]	NewM	1
	Bcat2[I]	Precancerous	ND[J]	↑	NewM	2
	Ddx54[I]	Precancerous	ND[J]	n.s.[K]	HyperM	1
		Tumors	ND[J]	↑	HypoM	
	Nudcd3	Tumors	ND[J]	n.s.[K]	HypoM	2
	Prickle2[I]	Precancerous	ND[J]	n.s.[K]	HypoM or HyperM^	1
		Tumors	ND[J]	n.s.[K]	HypoM and/or NewM^	
	Slc11a2	Tumors	ND[J]	↑	HypoM	1
	Srms[I]	Tumors	ND[J]	n.s.[K]	NewM	4

Table 5.2 continued Expression of Genes that Contain Putative Constitutive Active/Androstane Receptor Response Elements (CAREs)[A,B]

[A]Putative CAREs are located 10 kb upstream of the transcriptional start site.

[B]We used the same position weight matrix and 80% stringency cut-off (as described in Methods) on 25,000 randomly constructed sequences of 10 kb in length and found that, on average, there were only 0.561 CAREs found per sequence (across all 25,000 sequences). The probability of a gene having more than 1 CARE is 10.8%, while the probability of having more than 2, 3, or 4 CAREs is 2.2%, 0.38%, and 0.044%, respectively. The probability of not having any CAREs is 57.4%. We view the informatic approach for identification of CAREs as hypothesis generating.

[C]Genes that exhibited unique phenobarbital (PB)-elicited expression (current chapter) and/or methylation (Chapter 4) changes in precancerous liver tissue and/or individual liver tumors. *Anxa2* (*) was uniquely active and newly methylated.

[D]Expression changes (↑, up-regulation and ↓, down-regulation) of uniquely active genes that were identified based on microarray analysis (as described in the Methods). A tissue in **CAPITAL, BOLDED FONT** indicates that the gene was active in at least 5/6 total precancerous liver samples or 5/6 total individual liver tumors.

[E]Expression changes (↑, up-regulation and ↓, down-regulation) based on qRT-PCR. An arrow indicates that a change in the PB-treated group (v. its control) was statistically significant (Student's t-test, $p < 0.05$), and also unique as compared to expression in liver tissue from CAR knockout (KO), 23-week PB-treated mice (as described in the Methods).

[F]PB-induced decreases in methylation (Hypomethylation, HypoM) and increases in methylation (Hypermethylation, HyperM and new methylation, NewM), as determined in Chapter 4. Carry forward (c.f.) changes were observed in both precancerous liver tissue and individual liver tumors. In 2 instances (^), the methylation status was ambiguous (i.e. could not be definitively determined).

[G]Detailed confirmatory qRT-PCR data are found in Appendix Table 1.

[H]Also exhibited unique expression change in livers of tumor-prone B6C3F1 mice v. the relatively resistant C57BL/6, treated with PB for 2 or 4 weeks (Chapter 2).

[I]Also exhibited unique RAM in livers of tumor-prone B6C3F1 mice v. the relatively resistant C57BL/6, treated with PB for 2 or 4 weeks (Chapter 2).

[J]ND (not detected) indicates that the gene was not active.

[K]The fold change in the PB-treated group is not significant (n.s.) v. its control (Student's t-test, $p < 0.05$).

[L]The fold changes in precancerous liver tissue and liver tissue from CAR KO, 23-week PB-treated mice were not statistically different (Student's t-test, $p < 0.05$).

[M]qRT-PCR was not performed (n.p.).

[N]Detailed qRT-PCR data are found in Table 1.

[O]Detailed qRT-PCR data are found in Appendix Table 3.

Table 5.3 Quantitative Real-Time PCR (qRT-PCR) Analysis of Expression of 3 DNA Methyltransferase (Dnmt) Genes in 2 Types of Liver Tumor-Susceptible Mice

Gene	B6C3F1 fold change[a]		CAR WT fold change[b]	
	2 weeks PB	4 weeks PB	Precancerous	Tumors
Dnmt1: DNA methyltransferase 1	↓ -1.47	↓ -1.49	n.c.[c]	↑ 2.00
Dnmt3a: DNA methyltransferase 3a	↓ -1.60	↓ -1.81	↑ 1.27	↑ 2.29
Dnmt3b: DNA methyltransferase 3b	↓ -6.60	↓ -2.00	n.c.[c]	n.c.[c]

[a]Fold changes of gene expression in livers of phenobarbital (PB)-treated B6C3F1 mice at 2 and 4 weeks (v. their respective controls). All changes (↑, up-regulation and ↓, down-regulation) are statistically significant (Student's t-test, $p < 0.05$), and are considered to be unique as compared to expression in livers of PB-treated relatively resistant C57BL/6 mice (Chapter 4).

[b]Fold changes of gene expression in PB-treated CAR wildtype (WT) mice (precancerous liver tissue and individual liver tumors) v. their control. The changes are statistically significant (Student's t-test, $p < 0.05$), and are considered to be unique as compared to expression in liver tissue from CAR KO, 23-week PB-treated mice (Table 1).

[c]No change (n.c.) indicates that a fold change was not statistically significant.

identical RAMs (Table 5.7), uniquely active genes, based on microarray analysis (a subset is listed in Table 6.2 on p. 358; Supplementary Tables S11A-C in the submitted manuscript), the presence of CAREs (Table 5.2), and pathways and processes (Table 6.3, p. 359).

DISCUSSION

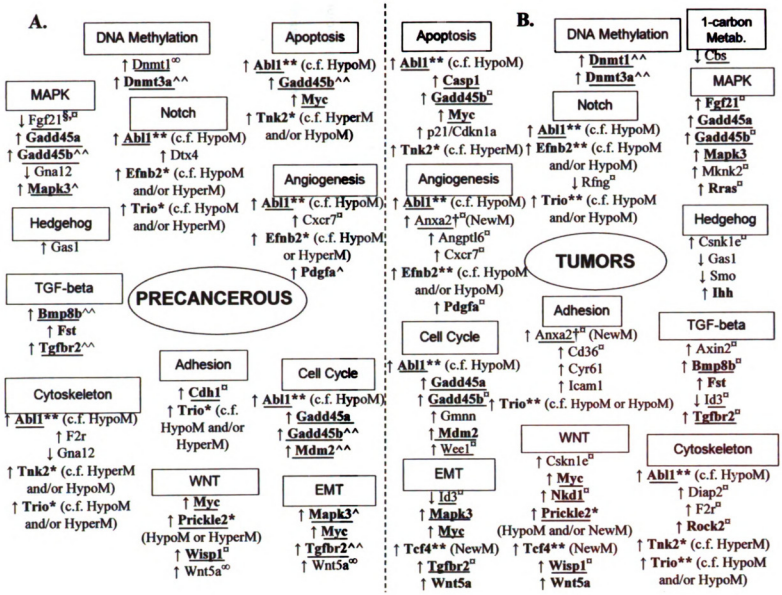
Our overall goal is to elucidate progressive changes, in expression and methylation status, of genes which play key roles during PB-induced liver tumorigenesis, with an emphasis on their potential to affect signaling through critical pathways involved in the regulation of cell growth and differentiation. In a series of key studies (Phillips and Goodman, 2008; Phillips and Goodman, 2009a; Phillips and Goodman, 2009b) plus the current one, we have discerned unique PB-elicited alterations, in DNA methylation and gene expression, that occurred in 2 types of liver tumor-prone mice. This was accomplished by "subtracting" out those which were also observed in their tumor-resistant counterparts. Indeed, PB induced RAMs in tissue from kidney (a non-target organ) as well as liver tissue from relatively tumor-resistant C57BL/6 mice (Bachman *et al.*, 2006) and tumor-resistant CAR KO mice (Phillips *et al.*, 2007). Therefore, the use of this "subtraction approach" was necessary in order to provide novel insight regarding key molecular events that transpired during tumorigenesis across a broad time-line of PB treatment (i.e. 2 and 4 weeks, to precancerous liver tissue and, finally, individual liver tumors). This permitted us to focus on critical genes and how they might interact to contribute to tumorigenesis.

The present report expands upon our previous work involving CAR WT and KO mice, in which genes that exhibited unique PB-induced RAMs in precancerous liver tissue and/or individual liver tumors were identified (Phillips and Goodman, 2009a). An extensive analysis of expression culminated in the elucidation of genes (including several identified from unique RAMs) whose transcription was altered uniquely in precancerous liver tissue and/or individual liver tumors v. liver tissue from resistant CAR KO, 23-week

PB-treated mice. Remarkably, these data sets are complementary, as genes whose expression and/or methylation statuses changed uniquely in response to PB are involved in many of the same cancer-associated signaling pathways and cellular processes (Fig. 5.5; Supplementary Figs. S4-S14 in the submitted manuscript).

In an analogous fashion, we have demonstrated that unique methylation (Phillips and Goodman, 2008) and gene expression (Phillips and Goodman, 2009b) changes occurred in tumor-susceptible B6C3F1 mice v. their relatively resistant C57BL/6 counterpart, at 2 and/or 4 weeks of PB treatment. Importantly, genes exhibiting unique alterations in both types of susceptible mice are involved in many of the same fundamental signaling pathways and cellular processes at both early (i.e. 2 and 4 weeks) and later (23 weeks, precancerous liver tissue and 32 weeks, individual liver tumors) times (Table 6.3, p. 359). Early events, including DNA methylation changes, might cause a cell to become addicted to (i.e., dependent on) oncogenic signaling pathways that are necessary for transformation (Baylin and Ohm, 2006), and this strengthens support for our assertion that changes observed at 2 and 4 weeks could facilitate selective clonal expansion, which is characteristic of tumor formation (Feinberg *et al.*, 2006). We have provided a view of the progressive nature of the multistage model of carcinogenesis, as genes whose expression (e.g., *Gadd45b, Cxcr7, Kcnk1*) or methylation statuses (e.g., *Prickle2, Ptpro, Zscan22*) changed at 2 and/or 4 weeks remained deregulated in precancerous liver tissue and/or individual liver tumors (Tables 6.1 and 6.2, pp. 357-358). Those genes whose expression changed only in individual liver tumors are listed in Supplementary Table S3I in the submitted manuscript. Indeed, genes that were altered at

Figure 5.5 Summary of Signaling Pathways and Processes Involving Genes that Exhibited Unique Expression and/or Methylation Changes in Precancerous and Tumor Tissue. PB induced unique regions of altered DNA methylation (RAMs), including hypomethylations (HypoM), hypermethylations (HyperM), and new methylations (NewM), in tumor-susceptible constitutive active/androstane receptor (CAR) wildtype (WT) mice at 23 (precancerous liver tissue, in A) and/or 32 (individual liver tumors, in B) weeks (Chapter 3). Carry forward (c.f.) RAMs were observed in both tissues. If a gene, identified from a unique RAM (Chapter 4), exhibited a unique expression change (induction, ↑ or repression, ↓) based on qRT-PCR, this is denoted by bolded font and 2 asterisks (**), while an indication of a unique expression change is represented by bolded font and 1 asterisk (*). As described in the Methods, microarray analysis was employed to identify uniquely active genes in precancerous liver tissue and/or individual liver tumors. Indicated genes (¤) were active in at least 5/6 precancerous liver samples or at least 5/6 individual liver tumors. Expression of uniquely active genes was confirmed (bolded) by qRT-PCR. In precancerous liver tissue, qRT-PCR revealed a statistically significant decrease in *Fgf21* expression (§) and an indication of up-regulation of *Wnt5a* and *Dnmt1* expression (∞). Genes not selected for confirmation by qRT-PCR are listed in unbolded font and lack symbols. *Anxa2* (†) exhibited a unique RAM and was uniquely active in the individual liver tumors. A gene whose unique expression change was revealed only by qRT-PCR is denoted by bolded font and 2 carrots (^^), while a gene that exhibited an indication of a unique change is denoted by bolded font and 1 carrot (^). A line underneath a gene indicates that at least 1 putative CAR response element (CARE) was found within 10 kb upstream of the transcriptional start site (Table 2). Abbreviations: metab., metabolism; EMT, epithelial-mesenchymal cell transition; MAPK, mitogen-activated protein kinase; TGF-beta, transforming growth factor-beta.


A.
DNA Methylation
↑ Dnmt1∞
↑ Dnmt3a^^
MAPK
↓ Fgf21$,¤
↑ Gadd45a
↑ Gadd45b^^
↓ Gna12
↑ Mapk3^
Notch
↑ Abl1** (c.f. HypoM)
↑ Dtx4
↑ Efnb2* (c.f. HypoM and/or HyperM)
↑ Trio* (c.f. HypoM and/or HyperM)
Apoptosis
↑ Abl1** (c.f. HypoM)
↑ Gadd45b^^
↑ Myc
↑ Tnk2* (c.f. HyperM and/or HypoM)
Angiogenesis
↑ Abl1** (c.f. HypoM)
↑ Cxcr7¤
↑ Efnb2* (c.f. HypoM or HyperM)
↑ Pdgfa^
Hedgehog
↑ Gas1
TGF-beta
↑ Bmp8b^^
↑ Fst
↑ Tgfbr2^^
PRECANCEROUS
Adhesion
↑ Cdh1¤
↑ Trio* (c.f. HypoM and/or HyperM)
Cytoskeleton
↑ Abl1** (c.f. HypoM)
↑ F2r
↓ Gna12
↑ Tnk2* (c.f. HyperM and/or HypoM)
↑ Trio* (c.f. HypoM and/or HyperM)
Cell Cycle
↑ Abl1** (c.f. HypoM)
↑ Gadd45a
↑ Gadd45b^^
↑ Mdm2^^
WNT
↑ Myc
↑ Prickle2* (HypoM or HyperM)
↑ Wisp1¤
↑ Wnt5a∞
EMT
↑ Mapk3^
↑ Myc
↑ Tgfbr2^^
↑ Wnt5a∞
B.
Apoptosis
↑ Abl1** (c.f. HypoM)
↑ Casp1
↑ Gadd45b¤
↑ Myc
↑ p21/Cdkn1a
↑ Tnk2* (c.f. HyperM)
Angiogenesis
↑ Abl1** (c.f. HypoM)
↑ Anxa2↑¤ (NewM)
↑ Angptl6¤
↑ Cxcr7¤
↑ Efnb2** (c.f. HypoM and/or HypoM)
↑ Pdgfa¤
Cell Cycle
↑ Abl1** (c.f. HypoM)
↑ Gadd45a
↑ Gadd45b¤
↑ Gmnn
↑ Mdm2
↑ Wee1¤
EMT
↓ Id3¤
↑ Mapk3
↑ Myc
↑ Tcf4** (NewM)
↑ Tgfbr2¤
↑ Wnt5a
DNA Methylation
↑ Dnmt1^^
↑ Dnmt3a^^
Notch
↑ Abl1** (c.f. HypoM)
↑ Efnb2** (c.f. HypoM and/or HypoM)
↓ Rfng¤
↑ Trio** (c.f. HypoM and/or HypoM)
TUMORS
Adhesion
↑ Anxa2↑¤ (NewM)
↑ Cd36¤
↑ Cyr61
↑ Icam1
↑ Trio** (c.f. HypoM or HypoM)
WNT
↑ Cskn1c¤
↑ Myc
↑ Nkd1¤
↑ Prickle2* (HypoM and/or NewM)
↑ Tcf4** (NewM)
↑ Wisp1¤
↑ Wnt5a
1-carbon Metab.
↓ Cbs
MAPK
↑ Fgf21¤
↑ Gadd45a
↑ Gadd45b¤
↑ Mapk3
↑ Mknk2¤
↑ Rras¤
Hedgehog
↑ Csnk1e¤
↓ Gas1
↓ Smo
↑ Ihh
TGF-beta
↑ Axin2¤
↑ Bmp8b¤
↑ Fst
↓ Id3¤
↑ Tgfbr2¤
Cytoskeleton
↑ Abl1** (c.f. HypoM)
↑ Diap2¤
↑ F2r¤
↑ Rock2¤
↑ Tnk2* (c.f. HyperM)
↑ Trio** (c.f. HypoM and/or HypoM)

both the early and late time points are particularly compelling candidates for direct involvement in tumorigenesis. Furthermore, in a hypothesis driven fashion, these genes can serve as the substrate for developing a "fingerprint" for PB-like, nongenotoxic rodent hepatocarcinogens. Efforts have been made to identify gene expression signatures of nongenotoxic rodent hepatocarcinogenesis in mice (Iida *et al.*, 2005), and rats (Fielden *et al.*, 2007), which are not as responsive to PB-induced tumorigenesis as the susceptible mouse strains. Our approach for elucidating gene expression changes that might be useful biomarker candidates is more appropriate than what is in the literature currently because we "subtracted out" alterations that occurred in the PB-treated resistant CAR KO mice, and thus, are focusing on changes in precancerous liver tissue and/or individual liver tumors that are likely to be related directly to tumorigenesis.

The phosphorylation and de-phosphorylation of proteins is intimately involved in numerous signaling pathways. Thus, it is interesting to note that genes which encode kinases, phosphatases, protein phosphatase regulatory (inhibitor) subunits and/or protein phosphatase activators (regulatory subunit) were uniquely active in precancerous liver tissue and/or individual liver tumors (Table 5.5) and in B6C3F1 mice following 2- or 4-weeks of treatment with PB (Supplementary Table S8 in Phillips and Goodman, 2009b). In this context, it is important to reflect on how the activation of CAR is dependent on kinases and phosphatases. CAR is sequestered in the cytoplasm by HSP90 in mouse hepatocytes (Yoshinari *et al.*, 2003) and HSP90 plus the cochaperone cytoplasmic CAR retention protein (CCRP) in human hepatocytes (Kobayashi *et al.*, 2003). In response to PB treatment, CAR translocates from the cytoplasm to the nucleus, heterodimerizes with retinoid X receptor (RXR), and binds to transcriptional elements (e.g., PB-responsive

enhancer modules) to affect gene expression (Honkakoski *et al.*, 1998; Kawamoto *et al.*, 1999; Sueyoshi *et al.*, 1999). Specifically, PB causes recruitment of protein phosphatase 2A (PP2A) to the CAR:HSP90 cytoplasmic complex (Yoshinari *et al.*, 2003). Okadaic acid, a phosphatase inhibitor which can inhibit PP2A, blocks the PB-induced nuclear translocation of CAR (Kawamoto *et al.*, 1999). CAR-mediated induction of the *Cyp2b10* gene can be blocked by KN-62 (a Ca^{2+}/calmodulin-dependent kinase inhibitor) without affecting nuclear accumulation (Yamamoto *et al.*, 2003), which suggests that CAR is activated in the nucleus by a phosphorylation event. The mechanism underlying PB-induced translocation of CAR from the cytoplasm to the nucleus appears to entail interaction of CAR with a homodimer of the membrane-associated subunit of protein phosphatase 1, PPP1R16A (R16A). The R16A residues dimerize at a region containing protein kinase A phosphorylation sites. Additionally, R16A can inhibit protein phosphatase 1-beta (PP1β), which can inhibit CAR translocation (Sueyoshi *et al.*, 2008). We speculate that enhancement of PP2A and/or inhibition of PP1β plays a role in the mechanism by which PB stimulates nuclear translocation of CAR.

Rodents are more prone to tumor development than humans (Rangarajan and Weinberg, 2003). However, in our opinion, the basic genes involved in tumorigenesis are likely to be largely the same in both species. Therefore, it is reasonable to hypothesize that differences in regulation of gene activity can contribute to this species disparity in susceptibility. A fundamental difference between murine and human CAR is their responsiveness to a range of agonists and inverse agonists, which might be attributable to structural variations (Stanley *et al.*, 2006). Thus, the relative sensitivity of mice to carcinogenesis might, in part, be due to distinct regulatory mechanisms and/or

structural features of mCAR. Moreover, it has been demonstrated that methylation patterns in rodent cells are less stable than those in human cells (reviewed in Goodman and Watson, 2002), so differences in epigenetic control (e.g., DNA methylation) between the species could, in part, underlie the enhanced propensity of rodents, as compared to humans, to develop cancer.

A key question is, what is responsible for the difference in susceptibility between the tumor-prone and tumor-resistant mice? Proliferation alone is not the answer, as PB treatment for 1 and 2 weeks increases levels in both the susceptible B6C3F1 and relatively resistant C57BL/6 mice (Counts *et al.*, 1996). CAR is clearly involved, since PB-treated CAR KO mice do not develop liver tumors (Yamamoto *et al.*, 2004). However, there appears to be other downstream events that are requisite for transformation because the induction of genes encoding drug-metabolizing enzymes, indicative of a functional CAR protein, occurred in both the B6C3F1 and C57BL/6 mice at 2 and 4 weeks (Phillips and Goodman, 2009b).

Gadd45b is a likely candidate gene, as its overexpression can enhance CAR-mediated transcription (Yamamoto and Negishi, 2008). At 2 weeks of PB treatment, *Gadd45b* appears to be up-regulated to a greater extent in B6C3F1 mice v. the C57BL/6 (Phillips and Goodman, 2009b), and it is also uniquely up-regulated in precancerous liver tissue and individual liver tumors (Table 5.4). Therefore, increased *Gadd45b* expression might be a crucial factor involved in the ability of PB to promote tumorigenesis, especially since it can function as an inhibitor of apoptosis (Papa *et al.*, 2004) which is one of the hallmark effects of PB (Kolaja *et al.*, 1996b; Whysner *et al.*, 1996). Additional genes of interest in this regard are those that harbor CAREs and exhibit PB-

elicited altered methylation and/or expression statuses (Table 5.2; Table 2 in Phillips and Goodman, 2009b).

Differential expression of Dnmts (Table 5.3: decreases in *Dnmt1*, *3a* and *3b* at 2 and 4 weeks; increase in *Dnmt3a* in precancerous liver tissue; and increases in *Dnmt1* and *3a* in individual liver tumors) is suggestive of distinct roles that seem to be dependent on the stage of tumorigenesis. Furthermore, all 3 Dnmts contain at least 1 CARE (Table 5.2), which implies that CAR potentially regulates their transcription, thus suggesting a direct link between PB and altered DNA methylation. However, Dnmts in all mice are expected to contain CAREs. Therefore, other factors (e.g., single nucleotide polymorphisms in the CAREs, proteins that target CAR, co-activators and co-repressors of CAR) might contribute to the differences in expression. Nevertheless, the unique PB-elicited expression changes of Dnmts in susceptible mice might influence the formation of RAMs, a subset of which could foster tumor development.

In vivo studies are essential for advancing our understanding of the complex carcinogenesis process. Numerous stromal components, such as matrix metalloproteinases, can influence malignant behavior (Marx, 2008). Moreover, inflammation-related signaling can contribute to tumorigenesis, e.g., IL-6 production by macrophages facilitates DEN-initiated liver tumor formation (Naugler *et al.*, 2007). Significantly, our use of whole liver tissue (including precancerous liver) and individual liver tumors derived from PB-treated mice enabled the detection of changes that occurred within the context of the microenvironment, and potentially, within multiple cell types.

In summary, we have performed extensive investigations (spanning 4 studies: Phillips and Goodman, 2008; Phillips and Goodman, 2009a; Phillips and Goodman,

2009b; the current report) of PB-elicited molecular alterations, i.e. DNA methylation and gene expression changes, that occurred uniquely in liver tumor-susceptible mice, as compared to their tumor-resistant counterparts. This approach, involving 2 distinct model systems comprised of PB-treated mice whose exposure periods spanned a continuum of PB-induced hepatocarcinogenesis, has proven to be effective for identifying genes that might be mechanistically critical for tumor development. As a direct result of these analyses, numerous genes are presented that could contribute to tumorigenesis by virtue of their deregulation in response to PB. Many of these genes participate in processes (Table 6.3, p. 359, and listed in parentheses below) that are capable of contributing to the acquisition of the 6 basic features of a tumor (Hanahan and Weinberg, 2000): 1) self-sufficiency in growth signals (cell cycle, growth, survival, and MAPK signaling), 2) insensitivity to anti-growth signals (cell cycle, growth, survival, TGF-β signaling, and differentiation-related pathways, i.e. Hedgehog, Notch, Wnt), 3) evasion of apoptosis (apoptosis and survival), 4) sustained angiogenesis (angiogenesis), 5) tissue invasion and metastasis (invasion, metastasis, EMT, adhesion and cytoskeleton organization/dynamics), and 6) limitless replicative potential (cell cycle, growth, survival), plus an inflammatory microenvironment (acute inflammatory response, in Supplementary Table S6O), as emphasized by Mantovani (2009). Significantly, DNA methylation and gene expression changes that could be utilized in the development of a "fingerprint" of PB exposure are presented (Supplementary Table S14; a subset of these are listed in Table 6.2, p. 358). Collectively, these data provide novel insight regarding the detailed picture of gene expression and DNA methylation changes that underlie PB-induced liver tumorigenesis.

ACKNOWLEDGEMENTS

Predoctoral fellowship support for J.M.P was received from the National Institutes of Health/National Institute of Environmental Health Sciences training grant No. T32-ES-7255. Research support, in the form of an unrestricted gift, from the R.J. Reynolds Tobacco Company is acknowledged gratefully. We thank the Michigan State University Research Technology and Support Facility for technical assistance with the microarray experiments.

REFERENCES

Assem, M., Schuetz, E. G., Leggas, M., Sun, D., Yasuda, K., Reid, G., Zelcer, N., Adachi, M., Strom, S., Evans, R. M., Moore, D. D., Borst, P., and Schuetz, J. D. (2004) Interactions between hepatic *Mrp4* and *Sult2a* as revealed by the constitutive androstane receptor and *Mrp4* knockout mice. *J. Biol. Chem.* **279**, 22250-22257.

Bachman, A. N., Phillips, J. M, and Goodman J. I. (2006). Phenobarbital induces progressive patterns of GC-rich and gene-specific altered DNA methylation in the liver of tumor-prone B6C3F1 mice. *Toxicol. Sci.* **91**, 393-405.

Baylin, S. B., and Ohm, J. E. (2006) Epigenetic gene silencing in cancer - a mechanism for early oncogenic pathway addiction? *Nat. Rev. Cancer* **6**, 107-116.

Becker, F.F. (1982). Morphological classification of mouse liver tumors based on biological characteristics. *Cancer Res.* **42**, 3918-3923.

Buchmann, A., Bauer-Hofmann, R., Mahr, J., Drinkwater, N. R., Luz, A., and Schwarz, M. (1991) Mutational activation of the c-Ha-*ras* gene in liver tumors of different rodent strains: Correlation with susceptibility to hepatocarcinogenesis. *Proc. Natl. Acad. Sci. U.S.A.* **88**, 911–915.

Chen, Y., Ferguson, S. S., Negishi, M., and Goldstein, J. A. (2003) Identification of constitutive androstane receptor and glucocorticoid receptor binding sites in the *CYP2C19* promoter. *Mol. Pharmacol.* **64**, 316-324.

Counts, J. L., and Goodman, J. I. (1995) Alterations in DNA methylation may play a variety of roles in carcinogenesis. *Cell* **83**, 13-15.

Counts, J. L., Sarmiento, J. I., Harbison, M. L., Downing, J. C., McClain, R. M., and Goodman, J. I. (1996). Cell proliferation and global methylation status changes in mouse liver after phenobarbital and/or choline-devoid, methionine-deficient diet administration. *Carcinogenesis* **17**, 1251-1257.

Dai, M., Wang, P., Boyd, A. D., Kostov, G., Athey, B., Jones, E. G., Bunney, W. E., Myers, R. M., Speed, T. P., Akil, H., Watson, S. J., and Meng, F. (2005) Evolving

gene/transcript definitions significantly alter the interpretation of GeneChip data. *Nucleic Acids Res.* **33**, e175.

Dennis, G. Jr., Sherman, B. T., Hosack, D. A., Yang, J., Gao, W., Lane, H. C., Lempicki, R. A. (2003) DAVID: Database for Annotation, Visualization, and Integrated Discovery. *Genome Biol.* **4**, P3.

Esteller, M. (2007) Epigenetic gene silencing in cancer: the DNA hypermethylome. *Hum. Mol. Genet.* **16** Spec No 1, R50-59.

Feinberg, A. P., Ohlsson, R., and Henikoff, S. (2006) The epigenetic progenitor origin of human cancer. *Nat. Rev. Genet.* **7**, 21-33.

Fielden, M. R., Brennan, R., and Gollub, J. (2007) A gene expression biomarker provides early prediction and mechanistic assessment of hepatic tumor induction by non-genotoxic chemicals. *Toxicol. Sci.* **99**, 90-100.

Gerbal-Chaloin, S., Daujat, M., Pascussi, J. M., Pichard-Garcia, L., Vilarem, M. J., and Maurel, P. (2002) Transcriptional regulation of *CYP2C9* gene. Role of glucocorticoid receptor and constitutive androstane receptor. *J. Biol. Chem.* **277**, 209-217.

Goodman, J. I., and Watson, R. E. (2002) Altered DNA methylation: a secondary mechanism involved in carcinogenesis. *Annu. Rev. Pharmacol. Toxicol.* **42**, 501-525.

Goodwin, B., Hodgson, E., D'Costa, D. J., Robertson, G. R., and Liddle, C. (2002) Transcriptional regulation of the human *CYP3A4* gene by the constitutive androstane receptor.
Mol. Pharmacol. **62**, 359-365.

Grønbaek, K., Hother, C., and Jones, P. A. (2007) Epigenetic changes in cancer. *APMIS (Acta Pathologica, Microbiologica et Immunologica Scandinavica)* **115**, 1039-1059.

Hanahan, D., and Weinberg, R. A. (2000) The hallmarks of cancer. *Cell* **100**, 57-70.

Honkakoski, P., Zelko, I., Sueyoshi, T., and Negishi, M. (1998) The nuclear orphan receptor CAR-retinoid X receptor heterodimer activates the phenobarbital-responsive enhancer module of the *CYP2B* gene. *Mol. Cell. Biol.* **18**, 5652-5658.

Huang, W., Zhang, J., Washington, M., Liu, J., Parant, J. M., Lozano, G., Moore, D. D. (2005) Xenobiotic stress induces hepatomegaly and liver tumors via the nuclear receptor constitutive androstane receptor. *Mol. Endocrinol.* **19**, 1646-1653.

Iida, M., Anna, C. H., Holliday, W. M., Collins, J. B., Cunningham, M. L., Sills, R. C., Devereux, T. R. (2005) Unique patterns of gene expression changes in liver after treatment of mice for 2 weeks with different known carcinogens and non-carcinogens. *Carcinogenesis* **26**, 689-699.

Kawamoto, T., Sueyoshi, T., Zelko, I., Moore, R., Washburn, K., and Negishi M. (1999) Phenobarbital-responsive nuclear translocation of the receptor CAR in induction of the *CYP2B* gene. *Mol. Cell. Biol.* **19**, 6318-6322.

Kobayashi, K., Sueyoshi, T., Inoue, K., Moore, R., and Negishi, M. (2003) Cytoplasmic accumulation of the nuclear receptor CAR by a tetratricopeptide repeat protein in HepG2 cells. *Mol. Pharmacol.* **64**, 1069-1075.

Kolaja, K. L., Stevenson, D. E., Johnson J. T., Walborg, Jr., E. F., and Klaunig, J. E. (1996a) Subchronic effects of dieldrin and phenobarbital on hepatic DNA synthesis in mice and rats. *Fundam. Appl. Toxicol.* **29**, 219-228.

Kolaja, K. L., Stevenson, D. E., Walborg Jr., E. F., and Klaunig J. E. (1996b). Dose dependence of phenobarbital promotion of preneoplastic hepatic lesions in F344 rats and B6C3F1 mice: effects on DNA synthesis and apoptosis. *Carcinogenesis* **17**, 947-954.

Loeb, L. A., and Harris, C. C. (2008) Advances in chemical carcinogenesis: a historical review and prospective. *Cancer Res.* **68**, 6863-6872.

Mantovani, A. (2009) Cancer: Inflaming metastasis. *Nature* **457**, 36-37.

Marx, J. (2008) Cancer biology. All in the stroma: cancer's Cosa Nostra. *Science* **320**, 38-41.

Naugler, W. E, Sakurai, T., Kim, S., Maeda, S., Kim, K., Elsharkawy, A. M., and Karin, M. (2007) Gender disparity in liver cancer due to sex differences in MyD88-dependent IL-6 production. *Science* **317**, 121–124.

Nemoto, N., and Sakurai, J. (1995) Glucocorticoid and sex hormones as activating or modulating factors for expression of Cyp2b-9 and Cyp2b-10 in the mouse liver and hepatocytes. *Arch. Biochem. Biophys.* **319**, 286-292.

Papa, S., Zazzeroni, F., Bubici, C., Jayawardena, S., Alvarez, K., Matsuda, S., Nguyen, D. U., Pham, C. G., Nelsbach, A. H., Melis, T., De Smaele, E., Tang, W. J., D'Adamio, L., and Franzoso, G. (2004) Gadd45β mediates the NF-κB suppression of JNK signalling by targeting MKK7/JNKK2. *Nat. Cell. Biol.* **6**, 146-153.

Phillips, J. M., Yamamoto. Y,, Negishi, M., Maronpot, R. R., and Goodman, J. I. (2007). Orphan nuclear receptor constitutive active/androstane receptor-mediated alterations in DNA methylation during phenobarbital promotion of liver tumorigenesis. *Toxicol. Sci.* **96**, 72-82.

Phillips, J. M., and Goodman, J. I. (2008) Identification of genes that may play critical roles in phenobarbital (PB)-induced liver tumorigenesis due to altered DNA methylation. *Toxicol. Sci.* **104**, 86-99.

Phillips, J. M., and Goodman, J. I. (2009a) Multiple genes exhibit phenobarbital (PB)-induced constitutive active/androstane receptor (CAR)-mediated DNA methylation changes during liver tumorigenesis and in liver tumors. *Toxicol. Sci.*, accepted for publication.

Phillips, J. M., and Goodman, J. I. (2009b) Phenobarbital (PB) elicits unique, early changes in the expression of hepatic genes that affect critical pathways in tumor-prone B6C3F1 mice. *Toxicol. Sci.*, submitted for publication.

Rangarajan, A., and Weinberg, R. A. (2003) Opinion: Comparative biology of mouse versus human cells: modelling human cancer in mice. *Nat. Rev. Cancer* **3**, 952-959.

Stanley, L. A., Horsburgh, B. C., Ross, J., Scheer, N., and Wolf, C. R. (2006) *Drug Metab. Rev.* PXR and CAR: nuclear receptors which play a pivotal role in drug disposition and chemical toxicity. **38**, 515-597.

Stupans, I., Ikeda, T., Kessler, D. J., and Nebert, D. W. (1984) Characterization of a cDNA clone for mouse phenobarbital-inducible cytochrome P-450b. *DNA* **3**, 129-137.

Sueyoshi, T., Kawamoto, T., Zelko, I., Honkakoski, P., and Negishi, M. (1999) The repressed nuclear receptor CAR responds to phenobarbital in activating the human *CYP2B6* gene. *J. Biol. Chem.* **274**, 6043-6046.

Sueyoshi, T., Moore, R., Sugatani, J., Matsumura, Y., and Negishi, M. (2008) PPP1R16A, the membrane subunit of protein phosphatase 1β, signals nuclear translocation of the nuclear receptor constitutive active/androstane receptor. *Mol. Pharmacol.* **73**, 1113-1121.

Sugatani, J., Kojima, H., Ueda, A., Kakizaki, S., Yoshinari, K., Gong, Q. H., Owens, I. S., Negishi, M., and Sueyoshi, T. (2001) The phenobarbital response enhancer module in the human bilirubin UDP-glucuronosyltransferase *UGT1A1* gene and regulation by the nuclear receptor CAR. *Hepatology* **33**, 1232-1238.

Sun, Y. V., Boverhof, D. R., Burgoon, L. D., Fielden, M. R., and Zacharewski, T. R. (2004) Comparative analysis of dioxin response elements in human, mouse and rat genomic sequences.
Nucleic Acids Res. **32**, 4512-4523.

Tomida, S., Yanagisawa, K., Koshikawa, K., Yatabe, Y., Mitsudomi, T., Osada, H., and Takahashi, T. (2007) Identification of a metastasis signature and the DLX4 homeobox protein as a regulator of metastasis by combined transcriptome approach. *Oncogene* **26**, 4600-4608.

Ueda, A., Hamadeh, H. K., Webb, H. K., Yamamoto, Y., Sueyoshi, T., Afshari, C. A., Lehmann, J. M., and Negishi, M. (2002) Diverse roles of the nuclear orphan receptor CAR in regulating hepatic genes in response to phenobarbital. *Mol. Pharmacol.* **61**, 1-6.

Weinstein, I. B. (2000) Disorders in cell circuitry during multistage carcinogenesis: the role of homeostasis. *Carcinogenesis* **4**, 857-864.

Weinstein, I. B. (2002) Addiction to oncogenes--the Achilles heal of cancer. *Science* **297**, 63-64.

Whysner, J., Ross, P. M., and Williams, G. M. (1996). Phenobarbital mechanistic data and risk assessment: enzyme induction, enhanced cell proliferation, and tumor promotion. *Pharmacol. Ther.* **71**, 53-91.

Wu, Z., Irizarry, R. A., Gentleman, R., Martinez-Murillo, F., and Spencer, F. (2004) A model
based background adjustment for oligonucleotide expression arrays. *J. Am. Stat. Assoc.* **99**, 909-917.

Yamamoto, Y., Kawamoto, T., and Negishi, M. (2003) The role of the nuclear receptor CAR as a coordinate regulator of hepatic gene expression in defense against chemical toxicity.Arch *Biochem. Biophys.* **409**, 207-211.

Yamamoto, Y., Moore, R., Goldsworthy, T. L., Negishi, M., and Maronpot, R. R. (2004) The orphan nuclear receptor constitutive active/androstane receptor is essential for liver tumor promotion by phenobarbital in mice. *Cancer Res.* **64**, 7197-7200.

Yamamoto, Y., and Negishi, M. (2008) The antiapoptotic factor growth arrest and DNA-damage-inducible 45 β regulates the nuclear receptor constitutive active/androstane receptor-mediated transcription. *Drug Metab. Dispos.* **36**, 1189-1193.

Yoshinari, K., Kobayashi, K., Moore, R., Kawamoto, T., and Negishi, M. (2003) Identification of the nuclear receptor CAR:HSP90 complex in mouse liver and recruitment of protein phosphatase 2A in response to phenobarbital. *FEBS Lett.* **548**, 17-20.

CHAPTER 5 APPENDIX

Data within the appendix consist of: Principal Component Analysis of the microarray data (Fig. 5.6), box plot depicting the distribution of microarray data (Fig. 5.7), Venn diagrams depicting numbers of genes that were uniquely active in precancerous liver tissue and/or individual liver tumors in at least 5/6 or 6/6 total mice per group (Fig. 5.8), data from qRT-PCR assays of uniquely active genes (identified by microarray analysis) in precancerous and/or individual liver tumors (Table 5.4), uniquely active kinase, phosphatase, and phosphatase regulatory (inhibitor) genes that are candidates for involvement in PB-induced CAR activation (Table 5.5), qRT-PCR expression data of genes identified from unique RAMs in precancerous liver tissue and/or individual liver tumors (Table 5.6), and qRT-PCR expression data of genes identified from identical, unique RAMs in B6C3F1 (2 and/or 4 weeks) and CAR WT (precancerous liver tissue and/or individual liver tumors) mice (Table 5.7). Note that these data are a subset of the total Supplementary Information that can be found in the version of this manuscript that was submitted to *Toxicological Sciences* in March 2009.

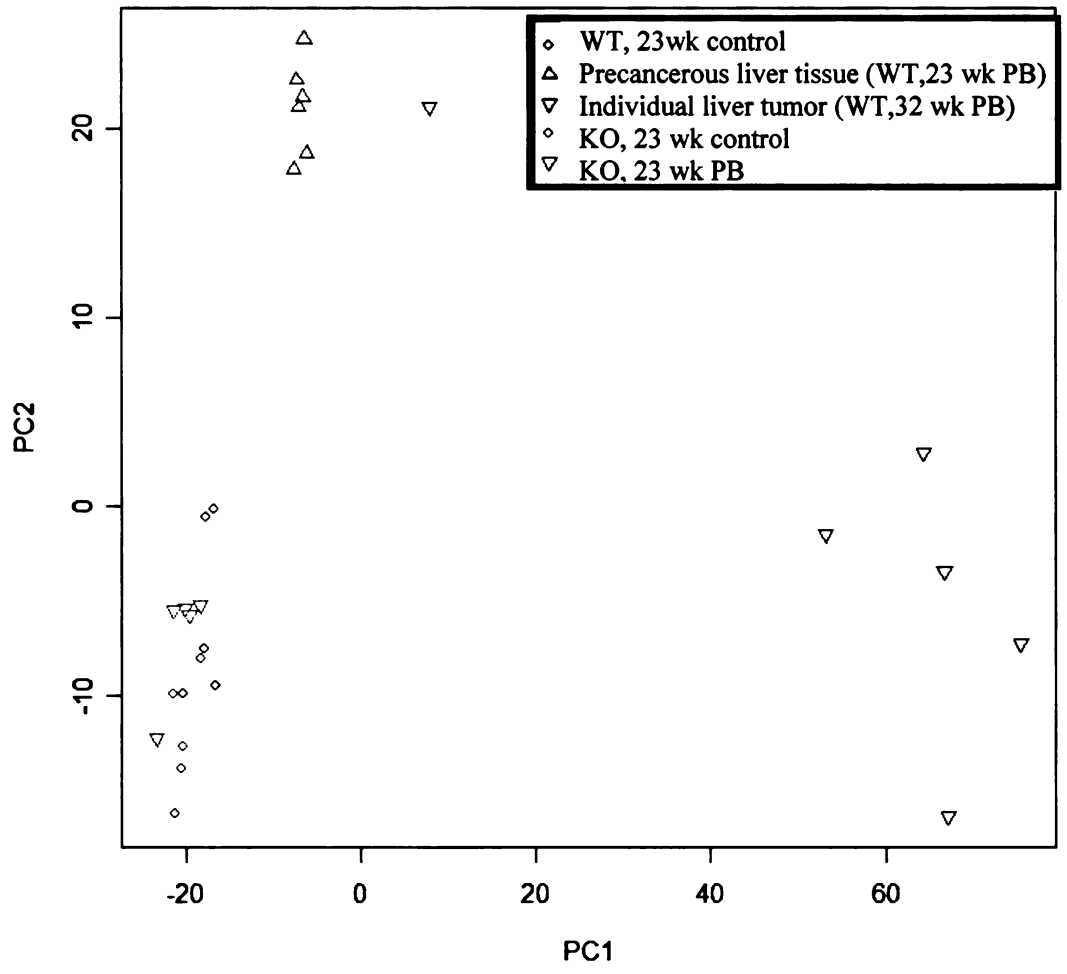


Figure 5.6 Principle Component Analysis (PCA) of Gene Expression Patterns Exhibited in Tissue Samples from Constitutive Active/Androstane Receptor (CAR) Wildtype (WT) and Knockout (KO) Mice. Microarray analysis was performed on RNA isolated from 5 groups of tissues which were obtained from livers of control and phenobarbital (PB)-treated mice: WT, 23 wk control, N=5; precancerous liver tissue (WT, 23 wk PB), N=6; individual liver tumors (WT, 32 wk PB), N=6; KO, 23 wk control, N=5; and KO, 23 wk PB, N=5. PCA is a dimension reduction technique that creates axes through the data (Principal Components; PC) that account for variability within the data set. PC1 accounts for the largest variance, PC2 is orthogonal to PC1 and accounts for the next largest variance, and so forth, until all of the variance is explained. Similarities and differences of overall gene expression patterns are evident. This image is presented in color.

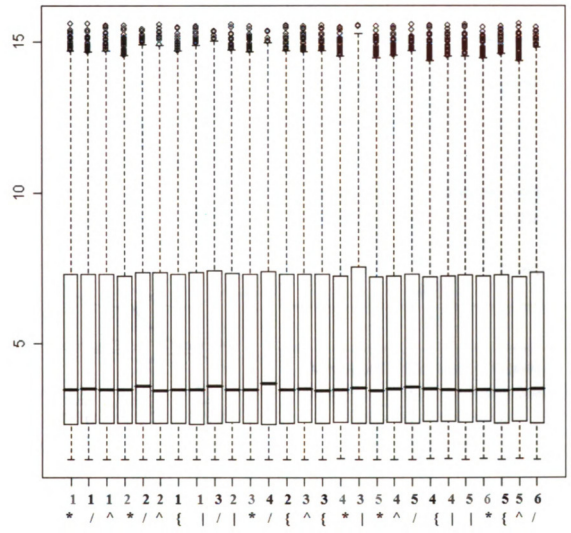


Figure 5.7 Distribution of Microarray Data that were Generated using RNA Isolated from Constitutive Active/Androstane Receptor (CAR) Wildtype (WT) and Knockout (KO) Mouse Tissues. Microarray analysis was performed on RNA isolated from 5 groups of tissues which were obtained from livers of control and phenobarbital (PB)-treated mice: WT, 23 wk control, N=5 (^); precancerous liver tissue (WT, 23 wk PB), N=6 (*); individual liver tumors (WT, 32 wk PB), N=6 (/); KO, 23 wk control, N=5 (|); and KO, 23 wk PB, N=5 ({). A "box-and-whisker" plot was utilized to express the distribution of the data. The individual samples are listed along the bottom of the figure, and the normalized intensity values (in log2 form), representing expression levels, are listed along the left-hand side. The white bars represent the interquartile range (IQR), which extends from the 25th to the 75th percentiles, and the horizontal black bars within the IQR represent the median value. The "whiskers" end at + 1.5 * IQR units. Every dot (o) beyond the "whiskers" reflects an outlying data point.

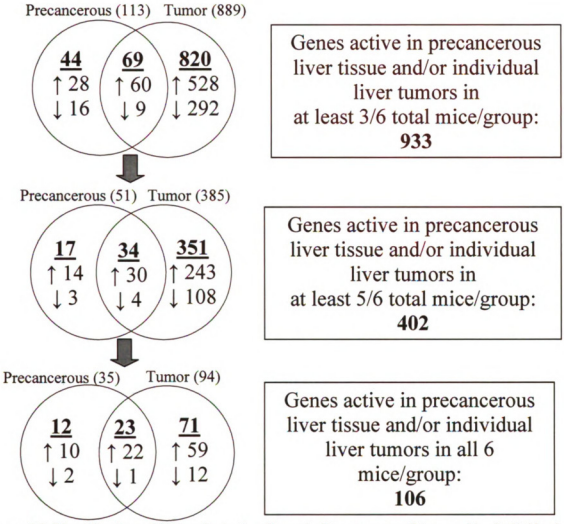


Figure 5.8 Identification of Uniquely Active Genes in Precancerous Liver and/or Individual Liver Tumors. Microarray analysis was employed to identify uniquely active genes in precancerous liver tissue and/or individual liver tumors based on at least 3/6 samples exhibiting expression levels outside of the 99% confidence interval (CI) of the normalized intensity values of the control group, in addition to being $\geq$ 2-fold up- or down-regulated. Comparison of 113 uniquely active genes in precancerous liver tissue and 889 uniquely active genes in individual liver tumors revealed a total of 933: 69 carried forward (i.e. were uniquely induced or repressed in both groups), while 44 were altered uniquely in precancerous liver tissue and 820 were altered uniquely in individual liver tumors (Fig. 1). In order to be progressively more stringent, core groups of uniquely active genes were identified based on at least 5/6 and 6/6 samples exhibiting expression levels outside of the 99% CI of the normalized intensity values of the control group data, in addition to being $\geq$ 2-fold up- or down-regulated. Comparison of 51 genes that were uniquely active in at least 5/6 precancerous liver samples and 385 genes that were uniquely active in at least 5/6 individual liver tumors revealed a total of 402: 34 genes carried forward, while 17 genes were altered uniquely in precancerous liver tissue and 351 genes were altered uniquely in individual liver tumors. Finally, comparison of 35 genes that were uniquely active in all 6 precancerous liver samples and 94 genes that were uniquely active in at all 6 individual liver tumors revealed a total of 106: 23 genes carried forward, while 12 genes were altered uniquely in precancerous liver tissue and 71 genes were altered uniquely in individual liver tumors. Gene lists are found within Supplementary Information in the submitted manuscript.

Table 5.4 Quantitative Real-time PCR (qRT-PCR) Analysis of the Expression of 22 Genes that were Uniquely Active in Precancerous Liver Tissue and/or Individual Liver Tumors

Uniquely Active Gene[a]	Fold Change Based on Microarray Analysis[b]			qRT-PCR Data								
				Mean Fold Change in PB-treated Group[c]			No. of animals above upper limit of 95% CI of control group[d]			No. of animals below lower limit of 95% CI of control group[d]		
	P	T	K	P	T	K	P	T	K	P	T	K
Bmp8b	--	↑10.66	--	↑ 1.84	↑ 229.4	n.c.	5	5	0	0	0	3
Casp1	--	↑ 4.31	--	n.c	↑ 2.63	n.c.	0	4	0	0	0	2
Ccnd1	--	↑ 6.39	--	n.c	↑ 5.91	↓ -1.94	2	4	0	0	0	5
Cdc2a	--	↑ 9.21	--	n.c.	↑ 11.55	n.c.	1	5	0	0	0	1
Cdh1	↑ 3.50	↓ -5.02↑	--	↑ 3.17	n.c.	n.c.	6	1	1	0	1	1
Fgf21	↓ -2.70↑	↑ 6.67	--	↓ -7.08[§]	↑ 3.06	↓ -3.94[§]	0	4	0	6	1	5
Fst +	↑ 2.45	↑ 5.49	--	↑ 2.60	↑ 4.28	↓ -2.91	6	5	0	0	0	4
Ddit3	--	↑ 5.21	--	n.c.	↑ 3.83	n.c.	1	4	1	2	1	1
Gadd45a +	↑ 3.37	↑ 2.90	--	↑ 1.75	↑ 2.68	n.c.	4	5	0	0	0	2
Gadd45b	--	↑ 7.34	--	↑ 9.51	↑ 24.34	n.c.	6	5	0	0	0	3
Ihh	--	↑ 3.11	--	n.c.	↑ 4.40	n.c.	1	5	2	1	0	0
Jun	--	↑ 5.36	--	n.c.	↑ 3.50	n.c.	0	4	2	0	0	2
Mapk3	--	↑ 2.25	--	n.c.	↑ 2.61	↓ -1.56	3*	4	0	0	0	5
Mdm2	--	↑ 2.44	--	↑ 1.70	↑ 2.67	n.c.	5	5	1	0	0	0
Myc +	↑ 3.68	↑ 4.23	--	↑ 1.78	↑ 4.88	↓ -1.22	6	5	0	0	0	4
Nkd1	--	↑ 7.90	--	n.c.	↑ 36.89	n.c.	2	5	1	1	0	3
Pdgfa	--	↑ 5.25	--	n.c.	↑ 5.19	↓ -1.88	3*	5	0	2	0	4
Rock2	--	↑ 3.87	--	n.c.	↑ 3.05	n.c.	0	5	0	1	0	2

Table 5.4 continued Quantitative Real-time PCR (qRT-PCR) Analysis of the Expression of 22 Genes that were Uniquely Active in Precancerous Liver Tissue and/or Individual Liver Tumors

Rras	--	↑3.03	--	n.c.	↑2.79	↓-3.22	2	4	0	0	0	5
Tgfbr2	--	↑4.40	--	↑1.79	↑5.59	n.c.	5	5	0	0	0	3
Wisp1 +	↑12.38	↑37.80	--	↑12.92	↑34.93	↓-2.57	6	5	0	0	0	3
Wnt5a	--	↑3.17	--	n.c.	↑3.29	n.c.	3	4	3	0	0	0

[a]Twenty-two uniquely active genes in precancerous liver tissue and/or individual liver tumors, a subset of the 933 identified based on microarray analysis (as described in the Methods), were chosen for confirmation of their expression statuses by qRT-PCR. Genes highlighted in gray were active in at least 5/6 total precancerous liver samples (unbolded and underlined), at least 5/6 individual liver tumors (unbolded), or at least 5/6 precancerous liver and 5/6 tumor samples (**bolded**). Uniquely active carry forward genes (i.e. those up- or down-regulated in both precancerous liver tissue and individual liver tumors) are denoted by a plus sign (+).

[b]Fold changes of gene expression (based on microarray analysis) are expressed as a change in a phenobarbital (PB)-treated group v. its control (comparisons were made as described in the Methods). All changes, with the exception of 2 (†), were confirmed by qRT-PCR. Fold changes (up-regulation, ↑ and down-regulation, ↓) in precancerous liver tissue (**P**), individual liver tumors (**T**), and liver tissue from constitutive active/androstane receptor (CAR) knockout, 23-week PB-treated mice (**K**) are listed. (--) indicates that a gene was not active.

[c]All fold changes listed are statistically significant in a PB-treated group v. its control (Student's t-test, $p < 0.05$). No change (n.c.) indicates that the fold change was not significant. qRT-PCR revealed unique expression changes that were not detected by microarray analysis (highlighted in gray). For *Fgf21*, the fold change in precancerous liver tissue was not statistically different from the fold change in liver tissue from CAR KO, 23-week PB-treated mice, Student's t-test, $p < 0.05$ (*).

[d]The 95% confidence interval (CI) of the control group data was calculated, and the number of samples (out of 6 total for precancerous liver and individual liver tumors, and 5 total for CAR KO) from a PB-treated group that fell outside the 95% CI are listed. Highlighted in gray are those circumstances where data from at least 3 of the precancerous samples that fell outside the 95% CI of the control group data were considered an 'indication' of an expression change. An asterisk (*) denotes an indication of a unique change.

Table 5.5 Kinase, Phosphatase, and Phosphatase Regulatory (Inhibitor) Subunit Genes Identified as Uniquely Active in Precancerous Liver Tissue and/or Individual Liver Tumors[a]

	Gene[b]	Fold Change[c]	
		Precancerous[d]	Tumors[d]
Kinases	Tie1	↑ 3.56	
	Dyrk3		↑ **13.21**
	Pdk4[e]		↑ **11.97**
	Nek2		↑ **10.33**
	Aurka		↑ **7.00**
	Hunk		↑ **5.79**
	Prkg2		↑ **5.40**
	Rock2		↑ **3.87**
	Csnk1e		↑ **3.72**
	Frk		↑ 3.59
	Mknk2[f]		↑ **3.34**
	Pdxk		↑ **3.14**
	Limk1		↑ 2.84
	Pklr[f]		↑ 2.74
	Nagk		↑ 2.41
	Pi4k2b		↑ 2.28
	Mapk3		↑ 2.25
	Flt4		↓ **-3.00**
	Sgk1		↓ **-3.20**
	Grk5[f]		↓ -3.21
	Camkk2		↓ **-3.61**

Table 5.5 continued Kinase, Phosphatase, and Phosphatase Regulatory (Inhibitor) Subunit Genes Identified as Uniquely Active in Precancerous Liver Tissue and/or Individual Liver Tumors[a]

	Dclk3		↓ -3.88
	Zap70		↓ **-5.47**
	Ak3l1[e]		↓ **-5.89**
	Pck1[e]		↓ -12.49
Phosphatases	Ppap2c[e]		↑ 4.76
	Alpl		↑ 3.35
	Dusp14		↑ 3.17
	Dusp3		↑ 2.41
	Ppm1l		↓ -2.20
	Ptprb		↓ -2.80
	Ppm1m		↓ -3.88
	G6pc		↓ **-6.26**
Phosphatase Regulatory (Inhibitor) Subunit	Ppp1r14a	↓ -2.54	↓ **-3.07**

[a]No kinase or phosphatase genes were active in the CAR KO mice treated with PB for 23 weeks; [b]Uniquely active genes in precancerous liver tissue and individual liver tumors were identified based on microarray analysis, as described in the Methods; [c]Fold change of gene expression (↑, induction or ↓, repression); [d]Tissue in which the uniquely active gene was detected. Fold changes of genes that were uniquely active in 5/6 samples (**bolded font**) or 6/6 samples (highlighted in gray) are denoted; [e]Genes highlighted in gray and listed in normal font were also active in tumor-susceptible B6C3F1 mice at 2 or 4 weeks, and exhibited an opposite direction of change (Chapter 2); [f]Genes highlighted in gray and listed in **bolded font** were also active in tumor-susceptible B6C3F1 mice at 2 or 4 weeks and exhibited the same direction of change (Chapter 2).

Table 5.6 Quantitative Real-time PCR (qRT-PCR) Analysis of Expression of Genes That Exhibited Unique Phenobarbital (PB)-induced Regions of Altered DNA Methylation (RAMs)

Gene[a]	Genomic Location of Unique RAM[b]	Methylation Status in Precancerous Liver (Pre) or Tumors[c]	Precancerous or Tumors		KO, 23 wk PB		Summary of Methylation and Gene Expression Statuses
			Fold Change[d]	No. of Mice that Exhibited a Change Outside 95% CI of Control Group[e]	Fold change[d]	No. of Mice that Exhibited a Change Outside 95% CI of Control Group[e]	
Anxa4: annexin A4	Spans TSS and/or 5' UTR (1.A.i)	Tumors: c.f. HypoM	n.c.	↑ 3	↓ -1.47	--	Unique expression change (or an indication of) in precancerous liver and/or tumors: apparent association between ↓ methylation and ↑ expression
Abl1: c-abl oncogene 1, receptor tyrosine kinase	> 2 and ≤ 10 kb upstream from TSS (1.B.ii)	Pre: c.f. HypoM	↑ 1.33	--	n.c.	--	
		Tumors: c.f. HypoM	↑ 2.09	--			
Ddx54: DEAD (Asp-Glu-Ala-Asp) box polypeptide 54	Intronic (1.A.iii)	Tumors: HypoM	↑ 1.33	--	↓ -1.54	--	
Efnb2: ephrin B2	Intronic (1.A.iii)	Tumors: c.f. HypoM and/or HypoM[f]	↑ 3.30	--	↓ -1.40	--	
Nudcd3: NudC domain containing 3	Exonic (1.A.ii)	Tumors: HypoM	n.c.	4: ↑ 3, ↓ 1	n.c.	↓ 3	
Slc11a2: solute carrier family 11 (proton-coupled divalent metal ion transporters), member 2	Intronic (1.A.iii)	Tumors: HypoM	↑ 1.46	--	n.c.	5: ↑ 1, ↓ 4	
Trio: triple functional domain (PTPRF interacting)	Exonic (1.A.ii)	Tumors: c.f. HypoM and/or HypoM[f]	↑ 2.54	--	n.c.	5: ↑ 1, ↓ 4	

Table 5.6 continued Quantitative Real-time PCR (qRT-PCR) Analysis of Expression of Genes That Exhibited Unique Phenobarbital (PB)-induced Regions of Altered DNA Methylation (RAMs)

Bcat2: branched chain aminotransferase 2, mitochondrial	Exonic (1.A.ii)	Pre: NewM	↑ 1.24	--	n.c.	--	Unique expression change (or an indication of) in precancerous liver or tumors: apparent association between ↑ methylation and ↑ expression
Ddx54: DEAD (Asp-Glu-Ala-Asp) box polypeptide 54	Intronic (1.A.iii)	Pre: HyperM	n.c.	4: ↑ 3, ↓ 1	↓ -1.54	--	
Tcf4: transcription factor 4	Intronic (1.A.iii)	Tumors: NewM	↑ 4.42	--	n.c.	--	
Tnk2: tyrosine kinase, non-receptor, 2	Intronic (1.A.iii)	Tumors: c.f. HyperM	n.c.	↑ 4	n.c.	--	
Efnb2: ephrin B2	Intronic (1.A.iii)	Pre: c.f. HypoM and/or HyperM[f]	n.c.	↑ 4	↓ -1.40	--	Indication of a unique expression change in precancerous liver and/or tumors: ambiguous methylation status and ↑ expression
Prickle2: prickle-like 2 (Drosophila)	> 2 and ≤ 10 kb upstream from TSS (1.B.ii)	Pre: HypoM or HyperM[f]	n.c.	↑ 3	n.c.	--	
		Tumors: HypoM and/or NewM[f]	n.c.	5: ↑ 3, ↓ 2			
Tnk2: tyrosine kinase, non-receptor, 2	Intronic (1.A.iii)	Pre: c.f. HyperM and/or Hypo[f]	n.c.	↑ 4	n.c.	--	
Trio: triple functional domain (PTPRF interacting)	Exonic (1.A.ii)	Pre: c.f. HypoM and/or HyperM[f]	n.c.	↑ 3	n.c.	5: ↑ 1, ↓ 4	

Table 5.6 continued Quantitative Real-time PCR (qRT-PCR) Analysis of Expression of Genes That Exhibited Unique Phenobarbital (PB)-induced Regions of Altered DNA Methylation (RAMs)

Anxa4: annexin A4	Spans TSS and/or 5' UTR (1.A.i)	Pre: c.f. HypoM	n.c.	--	↓ -1.47	--	No indication of an expression change in precancerous liver or tumors
Chn2: chimerin (chimaerin) 2	Intronic (1.A.iii)	Pre: NewM	n.c.	--	n.c.	↓ 3	
		Tumors: NewM	n.c.	--			
Crabp1: cellular retinoic acid binding protein 1	Exonic (1.A.ii)	Tumors: HypoM	n.c.	--	↓ -3.81	--	
Ptpro: protein tyrosine phosphatase, receptor type, O	Intronic (1.A.iii)	Tumors: HypoM and/or NewM[f]	n.c.	--	n.c.	--	
Prkce: protein kinase C, epsilon	Intronic (1.A.iii)	Tumors: HypoM	n.c.	--	n.c.	--	
Srms: src-related kinase lacking C-terminal regulatory tyrosine and N-terminal myristylation sites	Spans TSS and/or 5' UTR (1.A.i)	Tumors: NewM	n.c.	--	n.c.	3: ↑ 4, ↓ 1	

[a]Genes identified from unique PB-induced RAMs in precancerous liver tissue and/or individual liver tumors v. liver tissue from tumor-resistant constitutive active/androstane receptor (CAR) knockout (KO), 23-week PB-treated mice (Chapter 4)

[b]Genomic location of a RAM, based on a classification scheme on p. 71. Abbreviations: TSS, transcriptional start site; UTR, untranslated region

[c]PB-induced decreases in methylation (Hypomethylation, HypoM) and increases in methylation (Hypermethylation, HyperM and new methylation, NewM) (Chapter 4). Carry forward (c.f.) changes were observed in both precancerous liver tissue and individual liver tumors

[d]A fold change of gene expression (↑, up-regulation or ↓, down-regulation) is listed if it was statistically significant (Student's t-test, $p < 0.05$). If it was not significant, no change (n.c.) is listed. Comparisons were made as described in the Methods

[e]If a fold change was not statistically significant, a gene was considered to show an indication of a change if at least 3 samples in the PB-treated group exhibited expression that was outside (above, ↑ or below, ↓) the 95% confidence interval (CI) of the control group data. If there was no indication of a change, or if a fold change was statistically significant, these data are not shown (--)

[f]Methylation status was ambiguous (i.e. could not be definitively determined) (Chapter 4). For *Efnb2* and *Trio* in the individual liver tumors, a decrease in methylation occurred; what was ambiguous was whether the hypomethylation represented a carry forward change.

Table 5.7 Quantitative Real-Time PCR Analysis (qRT-PCR) of Expression of Genes Identified from Identical, Unique Phenobarbital (PB)-induced Regions of Altered DNA Methylation (RAMs) in 2 Types of Liver Tumor-Prone Mice

		B6C3F1 Mice				CAR WT Mice			
Gene[a] (Location of RAM)[b]	RAM Sizes[c]	2 weeks PB		4 weeks PB		Precancerous Liver		Liver Tumors	
		Methylation[d]	Express.[e]	Methylation[d]	Express.[e]	Methylation[d]	Express.[e]	Methylation[d]	Express.[e]
Bcat2: Branched chain aminotransferase 2, mitochondrial (1.A.ii: Exonic)	M464-468			↑[N] (M464)	↓ -1.38	↑[N] (M468)	↑ 1.24		
Ddx54: Dead box polypeptide 54 (1.A.iii: Intronic)	M315-317			↓ (M317)	↓ -1.17	↑ (M315)	n.c.		↑ 1.33
	B312-315			↓ (B315)				↓ (B312)	
Prickle2: Prickle-like 2 (Drosophila) (1.B.ii: > 2 and ≤ 10 kb upstream from TSS)	H310-312			↓ (H310)	n.c.	↓ (H310) or ↑ (H312)[f]	n.c.	↓ (H312)	n.c.
	B310-312			↓ (B310)				↓ (B312)	
Ptpro: protein tyrosine phosphatase, receptor type, O (1.A.iii: Intronic)	B341-342			↓ (B341)	n.c.			↓ (B342)	n.c.
Srms: src-related kinase lacking C-terminal regulatory tyrosine and N-terminal myristylation sites (1.A.i: Spans TSS and/or 5' UTR)	M202-206	↑ (M202) or ↓ (M206)[f]	↓ -8.65					↑[N] (M205)	n.c.
Tcf4: Transcription factor 4 (1.A.iii: Intronic)	B200			↓ (B200)	↓ -1.51			↑[N] (B200)	↑ 4.42
Tnk2: Tyrosine kinase non-receptor 2 (1.A.iii: Intronic)	M275-276			↓ (M275)	↓ -1.49	↑ (M276)	n.c.	↑ (M276)	n.c.

Table 5.7 continued Quantitative Real-Time PCR Analysis (qRT-PCR) of Expression of Genes Identified from Identical, Unique Phenobarbital (PB)-induced Regions of Altered DNA Methylation (RAMs) in 2 Types of Liver Tumor-Prone Mice

[a]Genes identified from identical unique PB-induced RAMs in tumor-susceptible B6C3F1 mice (2 and/or 4 weeks) and constitutive active/androstane receptor (CAR) wildtype (WT) mice (precancerous liver tissue and/or individual liver tumors) (Chapter 4)
[b]Genomic location of a RAM, based on a classification scheme on p. 71. Abbreviations: TSS, transcriptional start site; UTR, untranslated region
[c]A unique RAM (e.g., B200) is represented by a letter (indicative of the restriction enzyme that led to the identification of the RAM: *BssHII*, *HpaII* or *MspI*), followed by its size, in base pairs. Separation by a hyphen (e.g., B341-342) indicates the span of RAM sizes were detected in multiple groups. The use of multiple enzymes occasionally resulted in 2 RAMs (e.g., H310-312 and B310-312) that represented a single gene.
[d]A unique RAM (e.g., B200) is represented by a letter (indicative of the restriction enzyme that led to the identification of the RAM: *BssHII*, *HpaII* or *MspI*), followed by its size, in base pairs. Increases in methylation include hypermethylations (↑) and new methylations ($\uparrow^{N}$). Decreases in methylation include hypomethylations (↓)
[e]A fold change of gene expression (↑, up-regulation and ↓, down-regulation) is listed if it was statistically significant (Student's t-test, $p < 0.05$) in a treatment group (v. its control). If it was not significant, no change (n.c.) is listed. Data from precancerous liver tissue and individual liver tumors are found in Appendix Table 3, while those from B6C3F1 mice are found in Chapter 2.
[f]Methylation status was ambiguous, i.e. not definitively determined (as described in Chapter 4).

SUMMARY

Specific Aims

Each of the following specific aims, constituting 3 separate but related projects, was experimentally assessed, and the overall results are summarized in italics.

PROJECT 1 (Chapters 1 and 2): Identification of genes that exhibit unique phenobarbital (PB)-induced hepatic methylation and/or expression changes in liver tumor-susceptible B6C3F1 mice, as compared to relatively resistant C57BL/6 mice, at 2 and 4 weeks of treatment.

a) To ascertain key genes that exhibit unique regions of altered DNA methylation (RAMs) in susceptible B6C3F1 mice at 2 and 4 weeks: **Chapter 1**

Of the 170 unique PB-induced regions of altered DNA methylation (RAMs) that were discerned in liver tumor-susceptible B6C3F1 mice, as compared to their relatively resistant C57BL/6 counterparts, at 2 and 4 weeks (Bachman et al., *2006), cloning and annotation of 90 of them (53%) revealed 51 genes that harbored methylation changes. Functional analysis of the genes demonstrated connections to cancer-related processes, including growth and survival, angiogenesis, epithelial-mesenchymal cell transition, invasion, and metastasis, suggesting that they are capable of affecting tumorigenesis, while others represent "new" candidate genes which have been not previously associated with the disease. It is possible that, in response to PB treatment, changes in some of these genes are early events that contribute to the formation of tumors that are destined to become evident at later time points.*

b) To determine how expression of key genes (identified from unique RAMs in B6C3F1 mice, as discerned in Aim 1a) relates to their methylation statuses, and if transcript levels are altered uniquely in B6C3F1 mice: **Chapter 2**

*Of the 19 genes tested (out of 51 total genes identified), 3 of them (*Bcat2, Bcl2l13, Ube2d1*) were newly methylated and repressed at 4 weeks, and these expression patterns were unique as compared to the changes observed in the C57BL/6 mice. Two genes,* Srms *(2 weeks) and* Trio *(4 weeks) possessed ambiguous (i.e. not able to be definitively determined) methylation statuses and the extent of their repression was not significantly different from that observed in the C57BL/6 groups.* Ncor2 *was newly methylated and repressed in the B6C3F1, but the extent of the repression was significantly less than that in the C57BL/6. For 13 genes assayed only in the B6C3F1 mice, 7 genes were hypomethylated and repressed (or showed an indication of repression), while expression levels of the remaining 6 did not change. Since many of these genes are associated with cancer-related processes, PB treatment could alter their methylation statuses, subsequently influence expression levels, and possibly facilitate clonal expansion that contributes to tumorigenesis.*

c) To determine if expression levels of 3 DNA methyltransferase (Dnmt) genes change uniquely in B6C3F1 mice at 2 and 4 weeks of PB treatment: **Chapter 2**

At both 2 and 4 weeks, Dnmt1, Dnmt3a, *and* Dnmt3b *were repressed uniquely in B6C3F1 mice, as compared to the C57BL/6, indicating that PB-elicited expression changes of Dnmt genes might represent one mechanism by which the unique B6C3F1 RAMs formed.*

d) To perform microarray analysis and subsequently elucidate unique gene expression changes in B6C3F1 mice, at 2 and 4 weeks: **Chapter 2**

Unique expression changes were seen in tumor-prone B6C3F1 mice, as compared to the C57BL/6, at 2 (281) and 4 (133) weeks, including 47 whose expression was altered in the same direction at both time points. Subsets of these can participate in cellular processes and signaling pathways that have previously been implicated in tumorigenesis, suggesting that PB-elicited gene expression changes which occurred uniquely in the susceptible mice could directly contribute to carcinogenesis. Furthermore, genes involved in 1-carbon metabolism, which can impact DNA methylation patterns, were disrupted uniquely in the B6C3F1, providing evidence of a mechanism of PB-induced altered DNA methylation in the susceptible mice.

e) To identify putative CAR response cis elements (CAREs) within selected genes, including 3 Dnmt's, whose methylation and/or expression statuses are altered uniquely in B6C3F1 mice due to 2 and/or 4 weeks of PB treatment: **Chapter 2**

CAREs were located within 30 genes that were altered uniquely in response to PB treatment: 9 genes identified from RAMs (for 8/9, there was an expression change (or indication of) in B6C3F1 mice at 2 or 4 weeks; of the 8, 3 changes were unique in the B6C3F1); 18 uniquely active (i.e. differentially expressed) genes at 2 or 4 weeks, based on microarray analysis (for 13, expression changes were confirmed by qRT-PCR); and 3 Dnmt's (for all 3, expression was altered uniquely in B6C3F1 mice at 2 and 4 weeks). These data support the notion that CAR mediates early PB-elicited expression changes, including those of genes that are involved in cancer-related processes, and those that are capable of regulating methylation patterns.

PROJECT 2 (Chapters 3, 4, and 5): Identification of genes that exhibit unique PB-induced methylation and/or expression changes in liver tumor-susceptible CAR wildtype (WT) mice at 23 (precancerous liver) and 32 (liver tumors) weeks of treatment, as compared to tumor-resistant CAR knockout (KO) mice at 23 weeks.

a) To compare changes in GC-rich methylation patterns in tumor-susceptible CAR WT and resistant KO mice, and to discern unique RAMs in the CAR WT groups (both precancerous liver and liver tumors): **Chapter 3**

PB elicited 146 unique RAMs in CAR WT mice, as compared to the CAR KO, including 14 changes which "carried forward," i.e. were observed in both precancerous liver and liver tumors. Some of these CAR-dependent alterations might contribute to tumor development in the susceptible WT mice.

b) To ascertain key genes that exhibit unique RAMs in precancerous liver and/or liver tumors: **Chapter 4**

Cloning and annotation of 119 of the 146 (82%) total unique RAMs uncovered 47 genes that harbored methylation changes in precancerous and/or tumor tissue. Functional investigation of these genes revealed that many participate in cancer-related processes, including growth and survival, apoptosis, angiogenesis, epithelial-mesenchymal cell transition, cytoskeleton dynamics, and adhesion, indicating that they are capable of influencing tumor development. For others, there is no evidence linking the genes to the disease, and thus, they could be considered "new" candidate genes of PB-induced tumorigenesis, based upon their altered methylation statuses.

c) To determine how expression of key genes (identified from unique RAMs in CAR WT mice, as discerned in Aim 2b) relates to their methylation statuses, and if

transcript levels are altered uniquely in precancerous liver and/or liver tumors: **Chapter 5**

*Of the 16 genes tested (out of 47 total genes identified) that exhibited unique RAMs in precancerous liver and/or liver tumors, 7 of them (*Abl1, Anxa4, Ddx54, Efnb2, Nudcd3, Slc11a2, Trio*) were hypomethylated and demonstrated increased expression levels (or an indication of) in the same tissue, and these were unique as compared to expression in liver tissue from PB-treated CAR KO mice. Four of the genes (*Bcat2, Ddx54, Tcf4, Tnk2*), exhibited increased methylation and elevated expression levels (or an indication of) in the same tissue, and these levels were unique as compared to those in liver tissue from PB-treated CAR KO mice. The methylation statuses of 4 genes (*Efnb2, Prickle2, Tnk2, Trio*) were ambiguous (i.e. not definitively determined) in either precancerous liver or liver tumors, and there was an indication of unique induction of expression. There were several that did not exhibit an expression change. Overall, these data indicate that altered methylation might regulate the observed expression changes in precancerous liver and/or liver tumors, and based upon the documented roles of many of these genes in cancer-related processes, could possibly facilitate tumorigenesis.*

d) To determine if expression levels of 3 Dnmt genes change uniquely in precancerous liver and/or liver tumors: **Chapter 5**

Dnmt1 *(in precancerous liver) and* Dnmt3a *(in precancerous liver and liver tumors) were induced uniquely, as compared to liver from PB-treated CAR KO mice. This suggests that expression changes of certain Dnmt genes might be a mechanism by which PB uniquely affects methylation statuses in susceptible CAR WT mice.*

e) To perform microarray analysis and subsequently elucidate unique gene expression changes in precancerous liver and/or liver tumors: **Chapter 5**

Unique expression changes were ascertained in precancerous liver (113) and liver tumors (889), as compared to livers from CAR KO, 23-week PB-treated mice, which included 8 whose directions of change were opposite. Additionally, expression of 69 genes was altered in the same direction in both tissues. Functional annotation of these genes revealed that many are involved in cellular processes and signaling pathways that are associated with tumorigenesis. Therefore, at least some of them might be critical for PB-induced tumor development.

f) To identify putative CAREs within selected genes, including 3 Dnmt's, whose methylation and/or expression statuses are altered uniquely in precancerous liver and/or liver tumors: **Chapter 5**

CAREs were located within 30 genes that were altered uniquely in response to PB: 8 genes identified from RAMs (for 7/8, there was a unique change in expression (or an indication of) in precancerous liver and/or liver tumors v. liver tissue from PB-treated CAR KO mice); 19 uniquely active genes in precancerous liver and/or liver tumors, based on microarray analysis (for 16, expression changes were confirmed by qRT-PCR; 3 were not selected for confirmation), and 3 Dnmt genes (for Dnmt1 *and* Dnmt3a, *expression was altered uniquely in precancerous liver and/or liver tumors). These results support the notion that, in tumor-susceptible mice, CAR mediates PB-elicited expression changes of genes that are capable of driving tumorigenesis (based on their cancer-related functions), in addition to those that regulate DNA methylation patterns.*

<u>PROJECT 3 (Chapters 4 and 5)</u>: Comparison of genes that exhibit unique PB-elicited altered methylation and/or gene expression changes in both types of liver tumor-susceptible mice, at early (i.e. 2 and 4 weeks) and late (i.e. 23 weeks, precancerous liver and 32 weeks, liver tumors) time points.

a) To compare genes that exhibit unique RAMs in both the PB-treated susceptible B6C3F1 and CAR WT mice: **Chapter 4**

*PB treatment induced RAMs in 11 common genes (*Bcat2, Ddx54, Efnb2, Prickle2, Ptpro, Srms, Tcf4, Tnk2, Trio, Wscd1, Zscan22*) in both types of susceptible mice, including 5 (*Bcat2, Ddx54, Ptpro, Wscd1, Zscan22*) whose methylation levels either increased or decreased at both early and later times. Therefore, these represent preliminary candidate genes for the development of an "altered DNA methylation fingerprint" of PB promotion (Table 6.1).*

b) To compare the expression of genes that exhibit unique RAMs, plus 3 Dnmt's, in both PB-treated susceptible B6C3F1 and CAR WT mice: **Chapter 5**

*Considering a subset of the 11 aforementioned genes in which an expression change (or indication of a change) was observed in both types of mice, 5 (*Bcat2, Ddx54, Prickle2, Tcf4, Tnk2*) exhibited a decrease in B6C3F1 mice at 4 weeks, while they exhibited an increase in precancerous liver and/or liver tumors (Table 6.1). RAMs induced by PB within* Bcat2, Ddx54, and Prickle2 *might have influenced expression levels that were evident subsequent to 4 weeks and were evident in precancerous liver and/or tumors, since their transcription (but not methylation statuses) changed between early and later times. For* Tcf4 *and* Tnk2, *decreased methylation levels at 4 weeks might suppress expression, while increased levels might induce expression in precancerous liver and/or*

liver tumors. Assuming these methylation changes control transcription, and the observed expression changes affect tumorigenesis (based upon documented, cancer-related functions), the roles of these genes in tumor formation likely vary during initial, as compared to later stages.

Furthermore, Dnmt1, Dnmt3a, *and* Dnmt3b *were uniquely repressed in B6C3F1 mice at 2 and 4 weeks, while* Dnmt3a *(precancerous liver and liver tumors) and* Dnmt1 *(liver tumors) were induced uniquely (Table 6.2). Therefore, DNMT enzymes might establish methylation patterns differently during early v. later stages of tumorigenesis.*

c) To compare genes whose expression is altered uniquely, based on microarray analysis, in both the PB-treated susceptible B6C3F1 and CAR WT mice: **Chapter 5** *The uniquely altered genes in B6C3F1 mice at 2 and/or 4 weeks (367) and CAR WT mice, in precancerous liver and/or liver tumors (933), were compared. Expression levels of 69 genes were altered in the same direction and 26 in opposite directions, in at least 1 group of B6C3F1 and at least 1 group of CAR WT mice. Additionally, 5 genes exhibited the same direction of change in 2 groups of mice, but showed a divergent alteration in a third group. Functional annotation demonstrated that genes such as* Cxcr7, Gadd45a, *and* Gadd45b *(induced in both susceptible groups, Table 6.2), possess critical, tumorigenesis-related functions. Therefore, genes altered in both types of susceptible mice might facilitate the selective clonal expansion of cells during very early phases of PB promotion (i.e. 2 and 4 weeks), ultimately resulting in the precancerous lesions and frank tumors that arise at later time points (i.e. 23 and 32 weeks). Significantly, multiple cancer-related processes and signaling pathways involve genes whose methylation and/or expression statuses were perturbed by PB in both types of tumor-prone mice.*

Table 6.1 Expression of Genes Identified from Identical Phenobarbital (PB)-induced Regions of Altered DNA Methylation (RAMs) in 2 Types of Liver Tumor-Prone Mice

Gene[a] (Location of RAM)[b]	B6C3F1 Mice		CAR WT Mice			
	4 weeks PB		Precancerous Liver		Liver Tumors	
	Methyl.[c]	Express.[d]	Methyl.[c]	Express.[d]	Methyl.[c]	Express.[d]
***Bcat2*:** Branched chain aminotransferase 2, mitochondrial (Exonic)	$\uparrow^{N}$ (M)	↓ -1.38*	$\uparrow^{N}$ (M)	↑ 1.24		
***Ddx54*:** Dead box polypeptide 54 (Intronic)	↓ (M) ↓ (B)	↓ -1.17*	↑ (M)	↑ 3, ↓ 1	 ↓ (B)	↑ 1.33*
***Prickle2*:** Prickle-like 2 (Drosophila) (> 2 and ≤ 10 kb upstream from TSS)	↓ (H) ↓ (B)	↓ 4, ↑ 1			↓ (H) ↓ (B)	↑ 3, ↓ 2
***Ptpro*:** Protein tyrosine phosphatase, receptor type,O (Intronic)	↓ (B)	n.c.			↓ (B)	n.c.
***Tcf4*:** Transcription factor 4 (Intronic)	↓ (B)	↓ -1.51*			$\uparrow^{N}$ (B)	↑ 4.42*
***Tnk2*:** Tyrosine kinase non-receptor 2 (Intronic)	↓ (M)	↓ -1.49*	↑ (M)	↑ 4	↑ (M)	↑ 4
[e]***Wscd1*:** WSC domain-containing 1 (Intronic)	↓ (M)				↓ (M)	
[e]***Zscan22*:** Zinc finger and SCAN domain containing 22 (Spans TSS)	$\uparrow^{N}$ (H)				$\uparrow^{N}$ (H)	

[a]Genes identified from identical PB-induced RAMs that occurred uniquely in tumor-susceptible B6C3F1 mice (4 weeks) and constitutive active/androstane receptor (CAR) wildtype (WT) mice (precancerous liver and/or liver tumors) v. their resistant counterparts (Chapter 4).

[b]Genomic location of a RAM. TSS, transcriptional start site.

[c]Increases in methylation include hypermethylations (↑) and new methylations ($\uparrow^{N}$). Decreases in methylation are hypomethylations (↓). RAMs in gray exhibited the same direction of change in both types of mice. A letter indicates the restriction enzyme (*BssHII*, *HpaII*, *MspI)* used to detect the RAM.

[d]A fold change of gene expression (↑, up-regulation and ↓, down-regulation), based on quantitative real-time PCR, is statistically significant (Student's t-test, $p < 0.05$) if denoted by an asterisk (*). If a fold change was not statistically significant, it is not listed, however, a gene was considered to show an indication of a change if at least 3, out of 6 total, samples from the PB-treated group fell outside (either above, ↑ or below, ↓) the 95% confidence interval of the control group data. No change (n.c.) denotes that there was no indication of a change; [e]Expression was not evaluated.

Table 6.2 Genes Exhibiting Phenobarbital (PB)-elicited Altered Expression in 2 Types of Liver Tumor-Prone Mice[a]

Gene	Early[b]		Late[c]	
	B6C3F1		CAR WT	
	2 weeks PB	4 weeks PB	Precancerous	Tumors
Ddah1	↓	↓	↓	
Slc41a2	↓	↓	↓	
Maff	↑	↑		↑
Slc16a7	↑	↑		↑
BC016495	↑	↑		↑
Tsku	↑	↑		↑
Tars	↓	↓		↓
Clpx	↓	↓		↓
Nrg4	↑	↑		↓
D0H4S114	↑	↑		↓
Sds	↑	↑		↓
Avpr1a	↓	↓		↑
Dnmt1	↓	↓		↑
Kcnk1	↑	↑	↑	↑
Cyp2d12	↑	↑	↑	↑
Dnmt3a	↓	↓	↑	↑
Gadd45a		↑	↑	↑
Por		↑	↑	↑
Srxn1		↑	↑	↑
Tcfcp2l1		↑	↑	↑
BC089597		↓	↓	↓
Cxcr7	↑		↑	↑
Gadd45b	↑		↑	↑
Gna14	↑		↑	↑
Rarb	↑		↑	↑
Cib3	↑		↑	↑
Slco1a4	↑		↑	↑
6430706D22Rik	↑		↑	↑
Serpina9	↓		↓	↓
Serpina4-ps1	↓		↓	↓
Slc13a2	↑		↑	↓
Thrsp		↑	↑	
Mfsd11		↑	↑	
Ces6		↑	↑	
EG624219		↓	↓	

[a]Up-regulated (↑) or down-regulated (↓) gene expression, based on microarray and/or quantitative real-time PCR (qRT-PCR) analysis; [b]Unique gene expression changes in PB-treated liver tumor-susceptible B6C3F1 mice v. the relatively resistant C57BL/6, at 2 and 4 weeks, were discerned (Chapter 2); [c]Unique gene expression changes in PB-treated liver tumor-susceptible constitutive active/androstane receptor (CAR) wildtype (WT) mice (23 weeks, precancerous liver and 32 weeks, liver tumors) v. the resistant CAR knockout (KO) at 23 weeks, were discerned (Chapter 5).

Table 6.3 Common Signaling Pathways and Cellular Processes Involving Genes that Exhibited Methylation and/or Expression Changes in 2 Types of Liver-Tumor Prone Mice

Pathway or Process	Genes Altered in B6C3F1 Mice[a]		Genes Altered in CAR WT Mice[b]	
	2 weeks PB	4 weeks PB	Precancerous	Tumors
Adhesion	√	√	√	√
Angiogenesis	√	√	√	√
Apoptosis	√	√	√	√
1-Carbon Metabolism	√	√	--[c]	√
Cell Cycle / Growth / Survival	√	√	√	√
Cytoskeleton Organization / Dynamics	√	√	√	√
DNA methylation	√	√	√	√
Epithelial-mesenchymal cell transition	√	√	√	√
Hedgehog signaling	--[c]	--[c]	√	√
Invasion / Metastasis	√	√	√	√
MAPK signaling	√	√	√	√
Notch signaling	√	√	√	√
TGF-β signaling	√	√	√	√
Wnt signaling	√	√	√	√

[a] A (√) indicates the involvement of genes that exhibited unique regions of altered DNA methylation, RAMs (Chapter 1), and/or expression changes (Chapter 2) in livers of tumor-susceptible B6C3F1 mice v. the relatively resistant C57BL/6, treated with phenobarbital (PB) for 2 and 4 weeks.

[b] A (√) indicates the involvement of genes that exhibited unique RAMs (Chapter 4) and/or expression changes (Chapter 5) in livers of PB-treated constitutive active/androstane receptor (CAR) wildtype (WT) mice (precancerous liver and/or liver tumors) v. the tumor-resistant CAR knockout (KO) mice (23 weeks).

[c] (--) indicates that none of the genes of interest participate in a pathway/process.

DISCUSSION

Three complementary projects, comprising 5 distinct chapters of this dissertation, were designed to test the overall hypothesis: genes that are deregulated uniquely in liver tumor-susceptible, as compared to resistant mice, are among those that are mechanistically important for tumorigenesis. Two separate model systems were utilized to discern molecular alterations (i.e. DNA methylation and gene expression changes) that occurred uniquely in 2 different types of tumor-prone mice, as compared to their resistant counterparts. Many of the genes that exhibited PB-elicited changes play documented roles in cancer-related processes, and thus, the previously presented results strongly support the overall hypothesis.

The following 5 aspects of this research are those that I believe to be the most significant contributions to the fields of epigenetics and tumorigenesis:

1) The use of two model systems (each consisting of a group of liver tumor-prone and tumor-resistant mice) to elucidate unique molecular alterations in tumor-susceptible mice, across a continuum of PB treatment, is an extremely effective approach for assessing changes which are critical for tumor development.

A powerful aspect of this research was the ability to compare alterations that occurred in tumor-susceptible, as compared to tumor-resistant mice. In this fashion, one can focus upon key changes in genes that might directly contribute to carcinogenesis. B6C3F1 mice are susceptible to PB-induced liver tumor formation, as compared to the relatively resistant C57BL/6 (Becker, 1982), and similarly, CAR WT mice develop tumors in response to a DEN-initiation/PB-promotion regimen, while CAR KO mice do not (Yamamoto *et al.*, 2004). Unique changes in DNA methylation and gene expression

were discerned in each sensitive group, as compared to their resistant counterpart, in order to identify genes that, by virtue of their deregulation, might enhance the aberrant clonal expansion of cells that ultimately contributes to tumor formation.

It is common to encounter studies that focus upon molecular changes that arise towards the end stages of carcinogenesis (e.g., frank tumors). While this is undoubtedly an important avenue to pursue, it is necessary to explore earlier stages of the disease in order to develop a more comprehensive understanding of the tumorigenesis process. One truly novel component of my research involved ascertaining early events that transpired during periods of PB treatment which are not characterized by the presence of tumors. For example, in addition to liver tumors (CAR WT, 32 weeks PB), precancerous liver (CAR WT, 23 weeks PB), containing numerous microscopic foci of cellular alteration diffused throughout the tissue, was examined. Tumors evolve from the step-wise clonal expansion of initiated cells (Feinberg, 2006), and thus, early changes are critical. As such, the use of precancerous liver was a valuable asset for the evaluation of such alterations.

Furthermore, liver tissue was analyzed from mice treated with PB for even shorter periods (i.e. 2 and 4 weeks), at times when cellular proliferation is increased (Counts *et al.*, 1996; Kolaja *et al.*, 1996a), but far earlier than when tumors are present. Therefore, another innovative aspect of my research was the inclusion of these very early times to identify unique changes in tumor-susceptible mice that might be important for the growth of tumors that are destined to become evident at later times of PB exposure: 8 months, with DEN treatment (Yamamoto *et al.*, 2004) and 12 months, without (Becker, 1982). In this manner, two distinct model systems were utilized to evaluate unique molecular

events (alterations in DNA methylation and gene expression) in tumor-prone, as compared to tumor-resistant mice, within a continuum of PB treatment. This approach provided an effective means of exploring genes and signaling pathways that might be involved in tumorigenesis.

2) Both increases and decreases in methylation represent key events that occur during tumor development.

Typically, changes in methylation status are elucidated on a gene-by-gene basis within pre-determined genomic regions (e.g., bisulfite sequencing). Less frequently, genome-wide techniques, primarily limited to CpG islands (e.g., restriction landmark genome scanning, RLGS and amplification of inter-methylated sites, AIMS), are also utilized to detect methylation changes. I used a novel methodology involving methylation-sensitive restriction digestion, arbitrarily primed PCR (AP-PCR), and capillary electrophoresis, to evaluate PB-induced methylation patterns within CpG islands (mainly using the restriction enzyme *BssHII*), as well as at non-island CpG (*HpaII*) and CpCpG (*MspI*) sites. This technique, which is "unbiased" in the sense that regions to be assayed were not pre-selected, enables the simultaneous detection of an array of changes, including both increases (hypermethylation and "new" methylations), as well as decreases (hypomethylations), within GC-rich regions throughout the genome. This approach is quantitative (i.e. the extents of methylation changes were determined), as well as highly accurate and sensitive.

Using this method, our laboratory previously elucidated unique PB-induced RAMs in susceptible B6C3F1 mice, as compared to the relatively resistant C57BL/6, at 2 and 4 weeks (Bachman *et al.*, 2006). This work is analogous to the study described in

Chapter 3, in which unique RAMs were discerned in PB-treated tumor-prone CAR WT mice (precancerous liver and liver tumors), as compared to the tumor-resistant CAR KO. The elucidation of "carry forward" RAMs (i.e. changes observed in both tissues) is consistent with a fundamental principle of carcinogenesis, that is, the accumulation of heritable changes which result in proliferative growth advantages, and the subsequent selective clonal expansion of initiated cells. Importantly, PB caused both increases and decreases in methylation levels, and considered together with data that demonstrate roles for both types of alterations in cancer (Esteller, 2008), my results indicate that at least some of the observed RAMs might be crucial for tumor formation.

Thus, it was of paramount importance to discern the genes in which these methylation changes occurred. Chapters 1 and 4 describe the cloning and annotation of genes that harbored the unique RAMs discerned in the tumor-susceptible B6C3F1 (51 genes) and CAR WT (47 genes) mice, respectively. A large body of literature describes the identification of genes disrupted by hypermethylation, including those involved in a variety of cellular processes which are relevant to tumorigenesis: cell cycle, apoptosis, invasion, transcriptional regulation, tyrosine kinase signaling, and Wnt signaling, among others (Esteller, 2007b). Many of the genes identified from unique RAMs in the B6C3F1 and CAR WT mice have documented roles in cancer-related processes, including the cell cycle, apoptosis, angiogenesis, epithelial-mesenchymal cell transition, invasion, metastasis, and multiple signaling pathways (i.e. Wnt, Notch, and TGF-β). Thus, my data both reinforce and build upon previous observations, with regard to tumorigenesis-associated pathways that are affected by altered methylation, and significantly,

demonstrate that changes in specific genes within these pathways occur at very early time points of PB treatment.

The literature is more limited with respect to the characterization of hypomethylated oncogenes, whose induction can facilitate tumor development (Wilson *et al.*, 2007). Many genes in both susceptible types of mice (B6C3F1 and CAR WT) exhibited PB-elicited decreases in methylation, and thus, my research has markedly added to a list of genes that, due to their hypomethylated states and documented functions in cancer-related processes, could potentially contribute to tumorigenesis. Notably, I have also shown that genes not previously linked to altered DNA methylation and/or tumorigenesis exhibited unique methylation statuses in the tumor-prone mice, resulting in many "new" candidate genes that might be involved in PB-induced carcinogenesis.

3) Uniquely altered genes, and cancer-related pathways/processes in which they are involved, were discerned in PB-treated liver tumor-susceptible mice.

The mechanisms underlying PB-induced tumorigenesis, as indicated in the introduction, have been explored but not completely elucidated. PB alters methylation patterns to a greater extent in liver tumor-prone, as compared to relatively resistant mice, and thus, it has been suggested that DNA methylation plays a role in their differential susceptibilities (reviewed in Goodman and Watson, 2002; Watson and Goodman, 2002). Remarkably, elucidation of PB-elicited methylation changes at early (i.e. 2 and 4 weeks, no lesions evident) and later (23 weeks, precancerous liver and 32 weeks, liver tumors) time points, resulted in 11 identical regions that exhibited methylation changes in both types of susceptible mice. Significantly, 6 genes exhibited RAMs that demonstrated the

same direction of methylation change (Table 6.1), and only 2 of them (*Prickle2* and *Ptpro*) are linked to carcinogenesis. Thus, it is of interest to fully investigate the functions of these 6 genes.

Relationships between gene expression and methylation status at late time points (e.g. in tumors) are often discerned (Esteller, 2001; Esteller, 2007b). My dissertation research provided the extraordinary opportunity to explore the relationship between methylation and expression not only within tumor tissue, but also in liver tissue that lacks frank tumors (i.e. 2, 4, and 23 weeks/precancerous liver). A subset of the genes identified from unique RAMs also exhibited expression changes in the susceptible groups (Table 6.1). These data suggest that in response to PB, DNA methylation might regulate gene expression, specifically within the context of tumorigenesis, since many of the genes play known roles in carcinogenesis-related processes.

The divergent expression patterns of *Bcat2* (repressed at 4 weeks and induced at 23 weeks, precancerous liver) could be the result of an important methylation change that arises early (e.g., new methylation at 4 weeks) but has not yet met a certain threshold which is necessary for increasing expression to levels that are observed at later time points (e.g. 23 weeks, precancerous liver) (Table 6.1). *Tgfbr2* (a main component of TGF-β signaling) is hypomethylated at 4 weeks in livers of B6C3F1 mice (Chapter 1) and induced in liver tumors (Chapter 5). Taken together, these observations lead me to hypothesize that early alterations in methylation changes might not always result in immediate transcriptional consequences. Additional factors must be recruited, such as methyl-binding proteins and other repressive proteins to silence expression at hypermethylated CpG sites, and components of the transcriptional machinery (RNA

polymerase, coactivators, enhancers) to activate transcription from hypomethylated sites. Thus, while methylation changes at 2 or 4 weeks might have been essential for affecting transcription, these might not have instantaneously manifested as expression changes.

There have been limited large-scale PB expression studies (Stahl *et al.*, 2005; Ueda *et al.*, 2002) probing approximately 12,000 and 8,736 transcripts, respectively. In order to better picture how PB might be promoting liver tumor formation, I performed an extensive (i.e. 16,475 transcripts) microarray analysis. Ultimately, unique expression changes were ascertained in susceptible B6C3F1 mice at 2 and 4 weeks, as well as the CAR WT mice at 23 (precancerous liver) and 32 (liver tumors) weeks, as compared to their resistant counterparts. I first focused upon genes that were in common between both types of susceptible mice (e.g., *Gadd45a, Gadd45b, Cxcr7*), as these may be especially important, potentially representing changes which occurred at 2 and/or 4 weeks, conferred a proliferative advantage over neighboring cells, and as a result of clonal expansion, were still altered in precancerous liver and/or liver tumors (Table 6.2).

Disturbance of overall signaling networks is critical for tumor development. For example, in pancreatic cancer and glioblastoma, core signaling pathways are genetically altered, i.e. different tumors of the same type exhibited mutations in various genes involved in the same pathway, and not every tumor harbored all of the mutations (Jones *et al.*, 2008; Parsons *et al.*, 2008). Therefore, I then considered the overarching pathways and processes in which the genes of interest participate. Indeed, in each type of susceptible mice, many of the uniquely active genes (based on microarray analysis), and separately, genes that exhibited unique RAMs (and sometimes, altered expression), play documented roles in cancer-related signaling pathways and processes. Importantly,

however, when both groups of genes are considered together within the context of a particular model system, the crucial pathways and processes that they affect are complementary (Table 6.3). For example, genes whose methylation and/or expression statuses were altered uniquely in B6C3F1 mice participate in the cell cycle, apoptosis, angiogenesis, epithelial-mesenchymal cell transition, invasion, metastasis, and Wnt, Notch, and TGF-β signaling). Similarly, genes whose methylation and/or expression levels were altered uniquely in CAR WT mice participate in the cell cycle, angiogenesis, epithelial-mesenchymal cell transition, and adhesion, plus Wnt, TGF-β, and Hedgehog signaling. Importantly, there are pathways and processes that are in common between both types of susceptible mice (Table 6.3), suggesting that several of these pathways could function at early, as well as late time points, to drive tumor development. Many of these pathways are capable of facilitating the acquisition of the 6 fundamental characteristics of a tumor that control its malignant growth (Hahanhan and Weinberg, 2000)

It is reasonable to propose, based on the aforementioned data, in combination with the observation that the expression of key genes which exhibited unique RAMs was altered (i.e. DNA methylation could be functioning as a regulatory mechanism), that at least some of the aberrant methylation and transcriptional changes observed underlie PB-induced tumorigenesis. Accordingly, I have suggested numerous genes that could be utilized for the development of "fingerprints" of PB exposure (Table 6.1: methylation/expression, and Table 6.2: expression only). These tables contain subsets of the genes proposed in Chapter 5. They were included because they exhibited changes at

both early and later times, and additionally, the methylation status of a particular RAM was unambiguous at the indicated time point.

Biomarker development is an important focal point in cancer biology research. Furthermore, short-term and more cost-effective assays are currently being pursued for the detection of potential nongenotoxic carcinogens, such that compounds which might pose a risk can be identified earlier than 2 years (the length of the standard rodent bioassay). One group, using data from rats treated for 5 days with 1 of a variety of compounds, developed a 37-gene expression signature that was highly predictive of nongenotoxic hepatic tumorigenicity (Fielden *et al.*, 2007). Another group, using rats treated for 24 hours with one of numerous chemicals, elucidated a panel of 6 genes that were successful in identifying nongenotoxic carcinogens (Nie *et al.*, 2006). The approach taken to discern key genes is more appropriate than what is currently in the literature because changes that occurred in the resistant groups were "subtracted out", allowing me to focus on those in the susceptible mice that potentially directly contribute to tumorigenesis. The genes that were discerned, particularly those that were altered at both early and later time points of PB treatment, might be extremely beneficial in the ongoing efforts to classify nongenotoxic hepatocarcinogens.

4) Altered expression of DNA methyltransferase (Dnmt) genes, in addition to genes involved in 1-carbon metabolism, could represent mechanisms by which unique PB-induced RAMs formed in liver-tumor susceptible mice.

The expression of Dnmt genes has been evaluated in the context of tumorigenesis, including human hepatocellular carcinoma (Lin *et al.*, 2001; Robertson *et al.*, 1999),

mainly because of the considerable interest in elucidating mechanisms underlying aberrant methylation changes. A novel facet of my research was the assessment of PB-elicited transcriptional changes of 3 major Dnmt genes (*Dnmt1, 3a,* and *3b*) at very early time points (i.e. 2 and 4 weeks), in addition to precancerous liver and liver tumors, thereby providing their expression statuses across a continuum of treatment. It was remarkable to observe that the expression of all 3 genes was uniquely repressed in susceptible B6C3F1 mice (v. the relatively resistant C57BL/6) at both 2 and 4 weeks, while 2 of them were uniquely induced in precancerous liver (*Dnmt3a*) and liver tumors (*Dnmt1* and *Dnmt3a*) (v. liver tissue from CAR KO, PB-treated mice). Based on the divergent expression statuses at early and later time points, it is likely that the specific functions of the DNMTs are different, depending on the stage of PB treatment. Moreover, the expression of 3 genes involved in 1-carbon metabolism (*Cbs, Mtrr, Shmt1*), which can influence methylation levels (Ulrey *et al.*, 2005), was uniquely altered in B6C3F1 mice at 2 or 4 weeks. Interestingly, *Cbs* was repressed uniquely at both 2 weeks and in liver tumors.

Putative CAR response elements (CAREs) were located within all 3 Dnmt genes, thus providing a potential direct link between PB and altered DNA methylation. Overall, PB-elicited transcriptional changes of these genes could, in part, be responsible for the aberrant methylation changes observed uniquely in the liver tumor-susceptible mice.

5) Evidence supports the role of CAR in mediating gene expression changes that occurred in response to PB treatment, at both early and later time points, which might contribute to carcinogenesis.

CAR is essential for PB-induced tumorigenesis (Yamamoto *et al.*, 2004). Prior to my research, a rather limited (i.e. 8,736 genes/ESTs) gene expression study had been performed, using CAR WT and KO mice, which resulted in the identification of both CAR-dependent and -independent changes (Ueda *et al.*, 2002). In order to obtain a more in-depth view of how CAR might facilitate tumor promotion in response to PB treatment, I performed a more comprehensive (16,475 transcripts) microarray analysis that resulted in the elucidation of unique changes in CAR WT mice (precancerous liver and liver tumors). Indeed, hundreds of genes appear to be under CAR-dependent regulation. Additionally, PB altered the expression statuses of multiple genes identified from unique RAMs in precancerous liver and liver tumors, and the expression levels were different as compared to those observed in liver tissue from PB-treated CAR KO mice. These data reinforce the role of CAR in PB-elicited gene expression changes, and also, in a novel fashion, introduce a vast array of genes affected uniquely by PB in tumor-prone mice. Based upon their known functions in cancer, at least some of these genes might be mechanistically critical for tumor formation. Moreover, numerous genes whose methylation and/or expression statuses were altered uniquely in precancerous liver and/or liver tumors contained putative CAREs, providing further support for the concept that their expression is regulated by CAR.

Notably, as early as 2 or 4 weeks, genes known to be induced by CAR were indeed uniquely up-regulated in B6C3F1 mice, indicating the potential for their modulation by the nuclear receptor. Furthermore, CAREs were present within genes identified from unique RAMs in the susceptible B6C3F1 mice, and the expression of a subset was altered, uniquely in some instances, as compared to the relatively resistant

C57BL/6 mice. Thus, CAR might control key transcriptional changes during the initial stages of promotion by PB. Since a subset of the aforementioned genes are known to participate in tumorigenesis-related processes, it is possible that CAR enhances the selective clonal expansion of cells as early as 2 and/or 4 weeks.

As discussed previously, putative CAREs were present in all 3 Dnmt genes, whose expression was altered uniquely in both the B6C3F1 and CAR WT mice, thus providing a potential direct link to PB and the transcription of genes that can impact methylation patterns. Importantly, CAR might contribute to their regulation, thus potentially affecting the DNA methylation statuses of genes that could facilitate tumorigenesis.

Taken together, data from the B6C3F1-C57BL/6 and CAR model systems implicate CAR in the mediation of key PB-elicited gene expression changes at early, in addition to late time points of treatment, in tumor-susceptible mice. Since many of the affected genes play documented roles in carcinogenesis, CAR might enhance the aberrant expansion of cells harboring these changes, ultimately resulting in tumor formation.

Conclusions

The overall goal of these studies was to elucidate progressive changes, in methylation and expression status, of genes which play key roles in liver tumorigenesis induced by PB, with an emphasis on their potential to affect signaling through critical pathways involved in the regulation of cell growth and differentiation. Two distinct model systems, representing early and late times, were each comprised of a group of liver tumor-prone and tumor-resistant mice and were utilized in combination to evaluate PB-elicited alterations that arose uniquely in the susceptible mice.

The observance of early PB-induced DNA methylation changes and concurrent expression changes, of genes which conceivably function in cancer-related processes, support the assertion that aberrant methylation is a mechanism underlying tumorigenesis. Furthermore, a view of the progressive nature of the multistage model of carcinogenesis was provided, as genes whose expression or methylation statuses were disrupted at 2 and/or 4 weeks remained deregulated in precancerous liver tissue and/or liver tumors. Importantly, many of the genes affected in the susceptible mice play documented roles in cancer, indicative of their possible involvement in tumor formation, and also contain CAREs, which link these changes to CAR. Moreover, 3 DNA methyltransferase genes also harbor CAREs, and their expression levels were altered uniquely at early (*Dnmt1, Dnmt3a*, and *Dnmt3b*) and/or late (*Dnmt1* and *Dnmt3a*) time points, suggestive of a potential direct association between PB and altered DNA methylation patterns.

A critical aspect of this research was the analysis of liver tissue at extremely early time points, as well as precancerous liver and individual tumors, to elucidate unique molecular changes in the susceptible groups. This proved to be an effective strategy for

ascertaining critical changes that occurred across a continuum of PB exposure. My dissertation research culminated in the identification of genes (and the signaling pathways and cellular processes in which they participate) that, by virtue of their unique deregulation in tumor-prone, as compared to resistant mice, could contribute to tumorigenesis. Collectively, these data provide novel insight with regard to a detailed picture of DNA methylation and gene expression changes that facilitate PB-induced hepatocarcinogenesis.

REFERENCES FOR INTRODUCTION, SUMMARY, AND DISCUSSION SECTIONS ARE LISTED ON PAGES 373-391.

REFERENCES

Aaronson, S. A. (1991) Science. Growth factors and cancer. *Science* **254**, 1146-1153.

American Cancer Society. (2005) Cancer Facts and FIGS 2005. American Cancer Society [online], http://www.cancer.org/docroot/home/index.asp

Antequera, F. (2003) Structure, function and evolution of CpG island promoters. *Cell. Mol. Life Sci.* **60**, 1647–1658

Antequera, F., and Bird, A. (1993) Number of CpG islands and genes in human and mouse. *Proc. Natl. Acad. Sci. U S A* **90**, 11995-11999.

Anthony, P., Burt, A., Ishak K., MacSween R., Portman B., and Scheuer P., Eds. (2002) Pathology of the Liver. Churchill Livingstone: London, New York, Sydney, Toronto, p. 711-775.

Aoi, T., Yae, K., Nakagawa, M., Ichisaka, T., Okita, K., Takahashi, K., Chiba, T., and Yamanaka, S. (2008) Generation of pluripotent stem cells from adult mouse liver and stomach cells. *Science* **321**, 699-702.

Aydinlik, H., Nguyen, T. D., Moennikes, O., Buchmann, A., and Schwarz, M. (2001). Selective pressure during tumor promotion by phenobarbital leads to clonal outgrowth of β-catenin-mutated mouse liver tumors. *Oncogene* **22**, 7812-7816.

Bachman, A. N., Phillips, J. M., and Goodman, J. I. (2006) Phenobarbital induces progressive patterns of GC-rich and gene-specific altered DNA methylation in the liver of tumor-prone B6C3F1 mice. *Toxicol. Sci.* **91**, 393-405.

Bachman, K. E., Park, B. H., Rhee, I., Rajagopalan, H., Herman, J. G., Baylin, S. B., Kinzler, K. W., and Vogelstein, B. (2003) Histone modifications and silencing prior to DNA methylation of a tumor suppressor gene. *Cancer Cell.* **3**, 89-95.

Bachman, K. E., Rountree, M. R., and Baylin, S. B. (2001) Dnmt3a and Dnmt3b are transcriptional repressors that exhibit unique localization properties to heterochromatin. *J. Biol. Chem.* **276**, 32282–32287

Badal, V., Chuang, L. S., Tan, E. H., Badal, S., Villa, L. L., Wheeler, C. M., Li, B. F., and Bernard, H. U. (2003) CpG methylation of human papillomavirus type 16 DNA in cervical cancer cell lines and in clinical specimens: genomic hypomethylation correlates with carcinogenic progression. *J. Virol.* **77**, 6227-6234.

Baes, M., Gulick, T., Choi, H. S., Martinoli, M. G., Simha, D., and Moore, D. D. (1994) A new orphan member of the nuclear hormone receptor superfamily that interacts with a subset of retinoic acid response elements. *Mol. Cell. Biol.* **14**, 1544-1552.

Banine, F., Bartlett, C., Gunawardena, R., Muchardt, C., Yaniv, M., Knudsen, E. S., Weissman, B. E., and Sherman, L. S. (2005) SWI/SNF chromatin-remodeling factors induce changes in DNA methylation to promote transcriptional activation. *Cancer Res.* **65**, 3542-3547.

Baylin, S. B., Ohm, J. E. (2006) Epigenetic gene silencing in cancer - a mechanism for early oncogenic pathway addiction? *Nat. Rev. Cancer.* **6**, 107-116.

Becker, F. F. (1982). Morphological classification of mouse liver tumors based on biological characteristics. *Cancer Res.* **42**, 3918-3923.

Bell, A. C., and Felsenfeld, G. (2000) Methylation of a CTCF-dependent boundary controls imprinted expression of the Igf2 gene. *Nature* **405**, 482-485.

Bellacosa, A., de Feo, D., Godwin, A. K., Bell, D. W., Cheng, J. Q., Altomare, D. A., Wan, M., Dubeau, L., Scambia, G., Masciullo, V., Ferrandina, G., Benedetti Panici, P., Mancuso, S., Neri, G., and Testa, J. R. (1995) Molecular alterations of the AKT2 oncogene in ovarian and breast carcinomas. *Int. J. Cancer.* **64**, 280-285.

Berasain, C., Castillo, J., Prieto, J., and Avila, M. A. (2007) New molecular targets for hepatocellular carcinoma: the ErbB1 signaling system. *Liver Int.* **27**, 174-185.

Bergers, G., and Benjamin, L. E. (2003) Tumorigenesis and the angiogenic switch. *Nat. Rev. Cancer.* **3**, 401-410.

Bhattacharya, S. K., Ramchandani, S., Cervoni, N., and Szyf, M. (1999) A mammalian protein with specific demethylase activity for mCpG DNA. *Nature* **397**, 579-583.

Bianchi, A., and Shore, D. (2008) How telomerase reaches its end: mechanism of telomerase regulation by the telomeric complex. *Mol. Cell.* **31**, 153-165.

Biniszkiewicz, D., Gribnau, J., Ramsahoye, B., Gaudet, F., Eggan, K., Humpherys, D., Mastrangelo, M. A., Jun, Z, Walter, J., and Jaenisch, R. (2002) *Dnmt1* overexpression causes genomic hypermethylation, loss of imprinting, and embryonic lethality. *Mol. Cell. Biol.* **22**, 2124-2135.

Bjerkvig, R., Tysnes, B. B., Aboody, K.S., Najbauer, J., and Terzis, A. J. (2005) The origin of the cancer stem cell: current controversies and new insights. *Nat. Rev. Cancer.* **5**, 899-904.

Bjornsson, H. T., Brown, L. J., Fallin, M. D., Rongione, M. A., Bibikova, M., Wickham, E., Fan, J. B., Feinberg, A. P. (2007) Epigenetic specificity of loss of imprinting of the IGF2 gene in Wilms tumors. *J. Natl. Cancer Inst.* **99**, 1270-1273.

Bourc'his, D., and Bestor, T. H. (2004) Meiotic catastrophe and retrotransposon reactivation in male germ cells lacking Dnmt3L. *Nature* **431**, 96-99.

Bourc'his, D., Xu, G. L., Lin, C. S., Bollman, B., and Bestor, T. H. (2001) Dnmt3L and the establishment of maternal genomic imprints. *Science* **294**, 2536-2539.

Brown, S. E., Suderman, M. J., Hallett, M., and Szyf, M. (2008) DNA demethylation induced by the methyl-CpG-binding domain protein MBD3. *Gene* **420**, 99-106.

Bryan, T. M., Englezou, A., Gupta, J., Bacchetti, S., and Reddel, R. R. (1995) Telomere elongation in immortal human cells without detectable telomerase activity. *EMBO J.* **14**, 4240-4248.

Bruix, J., Boix, L., Sala, M., and Llovet, J. M. (2004) Focus on hepatocellular carcinoma. *Cancer Cell* **5**, 215-219.

Bruniquel, D., and Schwartz, R. H. (2003) Selective, stable demethylation of the interleukin-2 gene enhances transcription by an active process. *Nat. Immunol.* **4**, 235-240.

Burgers, W. A., Fuks, F., and Kouzarides, T. (2002) DNA methyltransferases get connected to chromatin. *Trends Genet.* **18**, 275-277.

Bursch, W., Chabicovsky, M., Wastl, U., Grasl-Kraupp, B., Bukowska, K., Taper, H., and Schulte-Hermann, R. (2005a) Apoptosis in stages of mouse hepatocarcinogenesis: failure to counterbalance cell proliferation and to account for strain differences in tumor susceptibility. *Toxicol. Sci.* **85**, 515-529.

Bursch, W., Wastl, U., Hufnagl, K., and Schulte-Hermann, R. (2005b) No increase of apoptosis in regressing mouse liver after withdrawal of growth stimuli or food restriction. *Toxicol. Sci.* **85**, 507-514.

Cameron, E. E., Bachman, K. E., Myöhänen, S., Herman, J. G., and Baylin, S. B. (1999) Synergy of demethylation and histone deacetylase inhibition in the re-expression of genes silenced in cancer. *Nat. Genet.* **21**, 103-107.

Cantley, L. C., and Neel, B. G. (1999) New insights into tumor suppression: PTEN suppresses tumor formation by restraining the phosphoinositide 3-kinase/AKT pathway. *Proc. Natl. Acad. Sci. U S A.* **96**, 4240-4245.

Chedin, F., Lieber, M. R., Hsieh, C. L. (2002) The DNA methyltransferase-like protein DNMT3L stimulates *de novo* methylation by Dnmt3a. *Proc. Natl. Acad. Sci. U S A.* **99**, 16916-16921.

Chen, Y., Ferguson, S. S., Negishi, M., and Goldstein, J. A. (2003) Identification of constitutive androstane receptor and glucocorticoid receptor binding sites in the *CYP2C19* promoter. *Mol. Pharmacol.* **64**, 316-324.

Chen, R. Z., Pettersson, U., Beard, C., Jackson-Grusby, L., and Jaenisch, R. (1998) DNA hypomethylation leads to elevated mutation rates. *Nature* **395**, 89-93.

Chen, T., Ueda, Y., Dodge, J. E., Wang, Z., and Li, E. (2003) Establishment and maintenance of genomic methylation patterns in mouse embryonic stem cells by Dnmt3a and Dnmt3b. *Mol. Cell. Biol.* **23**, 5594-5605.

Choi, H. S., Chung, M, Tzameli, I., Simha, D., Lee, Y. K., Seol, W., and Moore, D. D. (1997) Differential transactivation by two isoforms of the orphan nuclear hormone receptor CAR. *J. Biol. Chem.* **272**, 23565-23571.

Clark, S. J., Harrison, J., and Frommer, M. (1995) CpNpG methylation in mammalian cells. *Nat. Genet.* **10**, 20-27.

Collier, L. S., and Largaespada, D. A. (2007) Transposable elements and the dynamic somatic genome. *Genome Biol.* **8** Suppl 1:S5.

Cortázar, D., Kunz, C., Saito, Y., Steinacher, R., and Schär, P. (2007) The enigmatic thymine DNA glycosylase. *DNA Repair (Amst).* **6**, 489-504.

Counts, J. L., McClain, R. M., and Goodman, J. I. (1997) Comparison of effect of tumor promoter treatments on DNA methylation status and gene expression in B6C3F1 and C57BL/6 mouse liver and in B6C3F1 mouse liver tumors. *Mol. Carcinog.* **18**, 97-106.

Counts, J. L., Sarmiento, J. I., Harbison, M. L., Downing, J. C., McClain, R. M., and Goodman, J. I. (1996). Cell proliferation and global methylation status changes in mouse liver after phenobarbital and/or choline-devoid, methionine-deficient diet administration. *Carcinogenesis* **17**, 1251-1257.

Cravo, M., Fidalgo, P., Pereira, A. D., Gouveia-Oliveira, A., Chaves, P., Selhub, J., Mason, J. B., Mira, F. C., Leitao, C. N. (1994) DNA methylation as an intermediate biomarker in colorectal cancer: modulation by folic acid supplementation. *Eur. J. Cancer. Prev.* **3**, 473-479.

Cross, S. H., and Bird, A. P. (1995) CpG islands and genes. *Curr. Opin. in Genet. and Develop.* **5**, 309-314

Cui, H., Cruz-Correa, M., Giardiello, F. M., Hutcheon, D. F, Kafonek, D. R., Brandenburg, S., Wu, Y., He, X., Powe, N. R., and Feinberg, A. P. (2003) Loss of IGF2 imprinting: a potential marker of colorectal cancer risk. *Science* **14**, 1753-1755.

Dabeva, M. D., and Shafritz, D. A. (2003) Hepatic stem cells and liver repopulation. *Semin Liver Dis.* **4**, 349-362.

Dan, Y.Y., Riehle, K. J., Lazaro, C., Teoh, N., Haque, J., Campbell, J. S., and Fausto, N. (2006) Isolation of multipotent progenitor cells from human fetal liver capable of differentiating into liver and mesenchymal lineages. *Proc. Natl. Acad. Sci. U S A.* **103**, 9912-9917.

De La Fuente, R., Baumann, C., Fan, T., Schmidtmann, A., Dobrinski I, and Muegge K. (2006) Lsh is required for meiotic chromosome synapsis and retrotransposon silencing in female germ cells. *Nat. Cell. Biol.* **8**, 1448-1454.

de Vos, D., and van Overveld, W. (2005) Decitabine: a historical review of the development of an epigenetic drug. *Ann. Hematol.* **84**, 3-8.

DeClerck, Y. A., Mercurio, A. M., Stack, M. S., Chapman, H. A., Zutter, M. M., Muschel, R. J., Raz, A., Matrisian, L. M., Sloane, B. F., Noel, A., Hendrix, M. J., Coussens, L., and Padarathsingh, M. (2004) Proteases, extracellular matrix, and cancer: a workshop of the path B study section. *Am. J. Pathol.* **164**, 1131-119.

Dennis, K., Fan, T., Geiman, T., Yan, Q., and Muegge, K. (2001) Lsh, a member of the SNF2 family, is required for genome-wide methylation. *Genes Dev.* **15**, 2940-2944.

Dodge, J. E., Okano, M., Dick, F., Tsujimoto, N., Chen, T., Wang, S., Ueda, Y., Dyson, N., and Li, E. (2005) Inactivation of Dnmt3b in mouse embryonic fibroblasts results in DNA hypomethylation, chromosomal instability, and spontaneous immortalization. *J. Biol. Chem.* **280**, 17986-17991.

Dodge, J. E., Ramsahoye, B. H., Wo, Z. G., Okano, M., and Li, E. (2002) De novo methylation of MMLV provirus in embryonic stem cells: CpG versus non-CpG methylation. *Gene* **289**, 41–48.

Downward, J. (1998) Mechanisms and consequences of activation of protein kinase B/Akt. *Curr. Opin. Cell. Biol.* **10**, 262-267.

Drinkwater, N. R., and Ginsler, J. J. (1986) Genetic control of hepatocarcinogenesis in C57BL/6J and C3H/HeJ inbred mice. *Carcinogenesis* **7**, 1701-1707.

Drinkwater, N. R., Hanigan, M. H., and Kemp, C. J. (1989) Genetic determinants of hepatocarcinogenesis in the B6C3F1 mouse. *Toxicol. Lett.* **49**, 255-265.

Drucker, C., Parzefall, W., Teufelhofer, O., Grusch, M., Ellinger, A., Schulte-Hermann, R., and Grasl-Kraupp, B. (2006) Non-parenchymal liver cells support the growth advantage in the first stages of hepatocarcinogenesis. *Carcinogenesis* **27**, 152-161.

Eden, A., Gaudet, F., Waghmare, A., and Jaenisch, R. (2003) Chromosomal instability and tumors promoted by DNA hypomethylation. *Science* **300**, 455.

Ehrlich, M. (2002) DNA methylation in cancer: too much, but also too little. *Oncogene* **21**, 5400-5413.

Ehrlich, M. (2003) Expression of various genes is controlled by DNA methylation during mammalian development. *J. Cell. Biochem.* **88**, 899-910.

Ehrlich, M., Gama-Sosa, M. A., Huang, L. H., Midgett, R. M., Kuo, K. C., McCune, R. A., and Gehrke, C. (1982) Amount and distribution of 5-methylcytosine in human DNA from different types of tissues of cells. *Nucleic Acids Res.* **10**, 2709-2721.

Esteller, M. (2007a) Cancer epigenomics: DNA methylomes and histone-modification maps. *Nat. Rev. Genet.* **8**, 286-298.

Esteller, M. (2007b) Epigenetic gene silencing in cancer: the DNA hypermethylome. *Hum. Mol. Genet.* 16 Spec No 1, R50-59.

Esteller, M. (2008) Epigenetics in cancer. *N. Engl. J. Med.* **358**, 1148-1159.

Esteller, M., Corn, P. G., Baylin, S. B., and Herman, J. G. (2001) A gene hypermethylation profile of human cancer. *Cancer Res.* **61**, 3225-3229.

Farazi, P. A., and DePinho, R. A. (2006) Hepatocellular carcinoma pathogenesis: from genes to environment. *Nat. Rev. Cancer* **6**, 674-687.

Feinberg, A. P. (2001) Cancer epigenetics takes center stage. *Proc. Natl. Acad. Sci. U S A.* **98**, 392-394.

Feinberg, A. P., Ohlsson, R., and Henikoff, S. (2006). The epigenetic progenitor origin of human cancer. *Nat. Rev. Genet.* **7**, 21-33.

Feinberg, A. P., and Tycko, B. (2004) The history of cancer epigenetics. *Nat. Rev. Cancer.* **4**, 143-153.

Feinberg, A. P., and Vogelstein, B. (1983a) Hypomethylation distinguishes genes of some human cancers from their normal counterparts. *Nature* **301**, 89-92.

Feinberg, A. P., and Vogelstein, B. (1983b) Hypomethylation of *ras* oncogenes in primary human cancers. *Biochem. Biophys. Res. Commun.* **111**, 47-54.

Fielden, M. R., Brennan, R., and Gollub, J. (2007) A gene expression biomarker provides early prediction and mechanistic assessment of hepatic tumor induction by non-genotoxic chemicals. *Toxicol. Sci.* **99**, 90-100.

Filion, G. J., Zhenilo, S., Salozhin, S., Yamada, D., Prokhortchouk, E., and Defossez, P. A. (2006) A family of human zinc finger proteins that bind methylated DNA and repress transcription. *Mol. Cell. Biol.* **26**, 169-81.

Foley, K. P., and Eisenman, R. N. (1999) Two MAD tails: what the recent knockouts of *Mad1* and *Mxi1* tell us about the MYC/MAX/MAD network. *Biochim. Biophys. Acta* **423**, M37-47.

Forman, B. M., Tzameli, I., Choi, H. S., Chen, J., Simha, D., Seol, W., Evans, R. M., and Moore, D. D. (1998) Androstane metabolites bind to and deactivate the nuclear receptor CAR-β. *Nature* **395**, 612-615.

Frigola, J., Song, J., Stirzaker, C., Hinshelwood, R. A., Peinado, M. A., and Clark, S. J. (2006) Epigenetic remodeling in colorectal cancer results in coordinate gene suppression across an entire chromosome band. *Nat. Genet.* **38**, 540-549.

Fuks, F. (2005) DNA methylation and histone modifications: teaming up to silence genes. *Curr. Opin. Genet. Dev.* **15**, 490-495.

Fuks, F., Hurd, P. J., Deplus, R., and Kouzarides, T. (2003) The DNA methyltransferases associate with HP1 and the SUV39H1 histone methyltransferase. *Nucleic Acids Res.* **31**, 2305-2312

Futscher, B. W., Oshiro, M. M., Wozniak, R. J., Holtan, N., Hanigan, C. L., Duan, H., and Domann, F. E. (2002) Role for DNA methylation in the control of cell type specific maspin expression. *Nat. Genet.* **31**, 175-179.

Gama-Sosa, M. A., Slagel, V. A., Trewyn, R. W., Oxenhandler, R., Kuo, K. C., Gehrke, C. W., and Ehrlich, M. (1983) The 5-methylcytosine content of DNA from human tumors. *Nucleic Acids Res.* **11**, 6883-6894.

Gardiner-Garden M., and Frommer, M. (1987) CpG islands in vertebrate genomes. *J. Mol. Biol.* **196**, 261-282.

Gerbal-Chaloin, S., Daujat, M., Pascussi, J. M., Pichard-Garcia, L., Vilarem, M. J., and Maurel, P. (2002) Transcriptional regulation of *CYP2C9* gene. Role of glucocorticoid receptor and constitutive androstane receptor. *J. Biol. Chem.* **277**, 209-217.

Giancotti, F. G., and Ruoslahti, E. (1999) Integrin signaling. *Science* **285**, 1028-1032.

Gjerset, R. A., and Martin, D. W., Jr. (1982) Presence of a DNA demethylating activity in the nucleus of murine erythroleukemic cells. *J. Biol. Chem.* **257**, 8581-8583.

Goelz, S. E., Vogelstein, B., Hamilton, S. R., and Feinberg, A. P. (1985) Hypomethylation of DNA from benign and malignant human colon neoplasms. *Science* **228**, 187-190.

Gonzalo, S., Jaco, I., Fraga, M. F., Chen, T., Li, E., Esteller, M., Blasco, M. A. (2006) DNA methyltransferases control telomere length and telomere recombination in mammalian cells. *Nat. Cell. Biol.* **8**, 416-424.

Goodman, J. I., and Watson, R. E. (2002) Altered DNA methylation: a secondary mechanism involved in carcinogenesis. *Annu. Rev. Pharmacol. Toxicol.* **42**, 501-525.

Goodwin, B., Hodgson, E., D'Costa, D. J., Robertson, G. R., and Liddle, C. (2002) Transcriptional regulation of the human *CYP3A4* gene by the constitutive androstane receptor. *Mol. Pharmacol.* **62**, 359-365.

Goyal, R., Reinhardt, R., and Jeltsch, A. (2006) Accuracy of DNA methylation pattern preservation by the Dnmt1 methyltransferase. *Nucleic Acids Res.* **34**, 1182–1188.

Hanahan, D., Weinberg, R. A. (2000) The hallmarks of cancer. *Cell* 100, 57-70.

Hanigan, M. H., Kemp, C. J., Ginsler, J. J., and Drinkwater, N. R. (1988) Rapid growth of preneoplastic lesions in hepatocarcinogen-sensitive C3H/HeJ male mice relative to C57BL/6J male mice. *Carcinogenesis* **9**, 885-890.

Hata, K., Okano, M., Lei, H., and Li, E. (2002) Dnmt3L cooperates with the Dnmt3 family of de novo DNA methyltransferases to establish maternal imprints in mice. *Development* **129**, 1983-1993.

Hayflick, L. (1997) Mortality and immortality at the cellular level. A review. *Biochemistry (Mosc)* **11**, 1180-1190.

Heard, E. (2004) Recent advances in X-chromosome inactivation. *Curr. Opin. Cell. Biol.* **16**, 247-255.

Hendrich, B., and Bird, A. (1998) Identification and characterization of a family of mammalian methyl-CpG binding proteins. *Mol. Cell. Biol.* **18**, 6538-6547.

Hergersberg, M. (1991). Biological aspects of cytosine methylation in eukaryotic cells. *Experientia* **47**, 1171-1185.

Herzig, M., and Christofori, G. (2002) Recent advances in cancer research: mouse models of tumorigenesis. *Biochim. Biophys. Acta.* **1602**, 97-113.

Honkakoski, P., Zelko, I., Sueyoshi, T., and Negishi, M. (1998) The nuclear orphan receptor CAR-retinoid X receptor heterodimer activates the phenobarbital-responsive enhancer module of the *CYP2B* gene. *Mol. Cell. Biol.* **18**, 5652-5658.

Howlett, S. K., and Reik, W. (1991) Methylation levels of maternal and paternal genomes during preimplantation development. *Development* **113**, 119-127.

Hood, J. D., and Cheresh, D. A. (2002) Role of integrins in cell invasion and migration. *Nat. Rev. Cancer* **2**, 91-100.

Huang, W., Zhang, J., Chua, S. S., Qatanani, M., Han, Y., Granata, R., and Moore, D. D. (2003) Induction of bilirubin clearance by the constitutive androstane receptor (CAR). *Proc. Natl. Acad. Sci. U S A* **100**, 4156-4161.

Huang, W., Zhang, J., Washington, M., Liu, J., Parant, J. M., Lozano, G., Moore, D. D. (2005) Xenobiotic stress induces hepatomegaly and liver tumors via the nuclear receptor constitutive androstane receptor. *Mol. Endocrinol.* **19**, 1646-1653.
Hunter, T. (1997) Oncoprotein networks. *Cell* **88**, 333-346.

Iguchi-Ariga, S. M., and Schaffner, W. (1989) CpG methylation of the cAMP-responsive enhancer/promoter sequence TGACGTCA abolishes specific factor binding as well as transcriptional activation. *Genes Dev.* **3**, 612-619.

Inoue, S., and Oishi, M. (2005) Effects of methylation of non-CpG sequence in the promoter region on the expression of human synaptotagmin XI (*syt11*). *Gene* **348**, 123-134.

Jacinto, F. V., and Esteller. M. (2007) Mutator pathways unleashed by epigenetic silencing in human cancer. *Mutagenesis* **22**, 247-253.

Jähner, D., and Jaenisch, R. (1985) Retrovirus-induced de novo methylation of flanking host sequences correlates with gene inactivity. *Nature* **315**, 594-597.

Jeanes, A., Gottardi, C. J., and Yap, A. S. (2008) Cadherins and cancer: how does cadherin dysfunction promote tumor progression? *Oncogene* **27**, 6920-6929.

Jeltsch, A., Nellen, W., and Lyko, F. (2006) Two substrates are better than one: dual specificities for Dnmt2 methyltransferases. *Trends Biochem Sci.* **31**, 306-308.

Jiang, W. G. (1998) Cell adhesion molecules in the formation of liver metastasis. *J. Hepatobiliary Pancreat. Surg.* **5**, 375-382.

Jones, P. A. (1999) The DNA methylation paradox. *Trends Genet.* **15**, 34-37.

Jones, S., Zhang, X., Parsons, D. W., Lin, J. C., Leary, R. J., Angenendt, P., Mankoo, P., Carter, H., Kamiyama, H., Jimeno, A., Hong, S. M., Fu, B., Lin, M. T., Calhoun, E. S., Kamiyama, M., Walter, K., Nikolskaya, T., Nikolsky, Y., Hartigan, J., Smith, D. R., Hidalgo, M., Leach, S. D., Klein, A. P., Jaffee, E. M., Goggins, M., Maitra, A., Iacobuzio-Donahue, C., Eshleman, J. R., Kern, S. E., Hruban, R. H., Karchin, R., Papadopoulos, N., Parmigiani, G., Vogelstein, B., Velculescu, V. E., and Kinzler, K. W. (2008) Core signaling pathways in human pancreatic cancers revealed by global genomic analyses. *Science* **321**, 1801-1806.

Jost, J. P. (1993) Nuclear extracts of chicken embryos promote an active demethylation of DNA by excision repair of 5-methyldeoxycytidine. *Proc. Natl. Acad. Sci. USA.* **90**, 4684-4688.

Kaneda, M., Okano, M., Hata, K., Sado, T., Tsujimoto, N., Li, E., and Sasaki, H. (2004) Essential role for *de novo* DNA methyltransferase Dnmt3a in paternal and maternal imprinting. *Nature* **429**, 900-903.

Karpf, A. R., and Matsui, S. (2005) Genetic disruption of cytosine DNA methyltransferase enzymes induces chromosomal instability in human cancer cells. *Cancer Res.* **65**, 8635-8639.

Kawamoto, T., Sueyoshi, T., Zelko, I., Moore, R., Washburn, K., and Negishi, M. (1999) Phenobarbital-responsive nuclear translocation of the receptor CAR in induction of the *CYP2B* gene. *Mol. Cell. Biol.* **19**, 6318-6322.

Kaye, F. J. (2002) RB and cyclin dependent kinase pathways: defining a distinction between RB and p16 loss in lung cancer. *Oncogene* **21**, 6908-6914.

Kelleher, F. C., Fennelly, D., and Rafferty, M. (2006) Common critical pathways in embryogenesis and cancer. *Acta. Oncol.* **45**, 375-388.

Kmieć,Z. (2001) Cooperation of liver cells in health and disease. *Adv. Anat. Embryol. Cell Biol.* **161:III-XIII**, 1-151.

Koike, C., Moore, R., and Negishi, M. (2007) Extracellular signal-regulated kinase is an endogenous signal retaining the nuclear constitutive active/androstane receptor (CAR) in the cytoplasm of mouse primary hepatocytes. *Mol. Pharmacol.* **71**, 1217-1221.

Kolaja, K. L., Stevenson, D. E., Johnson, J. T., Walborg, E. F., Jr., and Klaunig, J. E. (1996a) Subchronic effects of dieldrin and phenobarbital on hepatic DNA synthesis in mice and rats. *Fundam. Appl. Toxicol.* **29**, 219-228.

Kolaja, K. L., Stevenson, D. E., Walborg Jr., E. F., and Klaunig J. E. (1996b). Dose dependence of phenobarbital promotion of preneoplastic hepatic lesions in F344 rats and B6C3F1 mice: effects on DNA synthesis and apoptosis. *Carcinogenesis* **17**, 947-954.

Kouzarides, T. (2007) Chromatin modifications and their function. *Cell* **128**, 693-705.

Kurmasheva, R. T., and Houghton, P. J. (2006) IGF-I mediated survival pathways in normal and malignant cells. *Biochim. Biophys. Acta.* **1766**, 1-22.

Lee, G. H., Nomura, K., Kanda, H., Kusakabe, M., Yoshiki, A., Sakakura, T., and Kitagawa, T. (1991) Strain specific sensitivity to diethylnitrosamine-induced carcinogenesis is maintained in hepatocytes of C3H/HeN in equilibrium with C57BL/6N chimeric mice. *Cancer Res.* **51**, 3257-3260.

Lehnertz, B., Ueda, Y., Derijck, A. A., Braunschweig, U., Perez-Burgos, L., Kubicek, S., Chen, T., Li, E., Jenuwein, T., and Peters, A. H. (2003) Suv39h-mediated histone H3 lysine 9 methylation directs DNA methylation to major satellite repeats at pericentric heterochromatin. *Curr. Biol.* **13**, 1192-1200.

Leonhardt, H., Page, A. W., Weier, H. U., and Bestor, T. H. (1992) A targeting sequence directs DNA methyltransferase to sites of DNA replication in mammalian nuclei. *Cell* **71**, 865-873.

Li, E., Beard, C., and Jaenisch, R. (1993) Role for DNA methylation in genomic imprinting. *Nature* **366**, 362-365.

Li, E., Bestor, T. H., Jaenisch, R. (1992) Targeted mutation of the DNA methyltransferase gene results in embryonic lethality. *Cell* **69**, 915-926.

Li, H., Fan, X., and Houghton, J. J. (2007) Tumor microenvironment: the role of the tumor stroma in cancer. *Cell. Biochem.* **101**, 805-815.

Liang, G., Chan, M. F., Tomigahara, Y., Tsai, Y. C., Gonzales, F. A., Li, E., Laird, P. W., and Jones, P. A. (2002) Cooperativity between DNA methyltransferases in the maintenance methylation of repetitive elements. *Mol. Cell. Biol.* **22**, 480-491.

Lin, C. H., Hsieh, S. Y., Sheen, I. S., Lee, W. C., Chen ,T. C., Shyu, W. C., and Liaw, Y. F. (2001) Genome-wide hypomethylation in hepatocellular carcinogenesis. *Cancer Res.* **61**, 4238-4243.

Loeb, L. A., Harris, C. C. (2008) Advances in chemical carcinogenesis: a historical review and prospective. *Cancer Res.* **68**, 6863-6872.

Lokker, N. A., Sullivan, C. M., Hollenbach, S. J., Israel, M. A., and Giese, N. A. (2002) Platelet-derived growth factor (PDGF) autocrine signaling regulates survival and mitogenic pathways in glioblastoma cells: evidence that the novel PDGF-C and PDGF-D ligands may play a role in the development of brain tumors. *Cancer Res.* **62**, 3729-3735.

Lopez-Serra, L., Ballestar, E., Fraga, M. F., Alaminos, M., Setien, F., and Esteller, M. (2006) A profile of methyl-CpG binding domain protein occupancy of hypermethylated promoter CpG islands of tumor suppressor genes in human cancer. *Cancer Res.* **66**, 8342-8346.

Lopez-Serra, L., and Esteller, M. (2008) Proteins that bind methylated DNA and human cancer: reading the wrong words. *Br. J. Cancer.* **98**, 1881-1885.

Loréal, O., Levavasseur, F., Fromaget, C., Gros, D., Guillouzo, A., Clément, B. (1993) Cooperation of Ito cells and hepatocytes in the deposition of an extracellular matrix in vitro. *Am. J. of Pathology* **143**, 538-544.

Luch, A. (2005) Nature and nurture - lessons from chemical carcinogenesis. *Nat. Rev. Cancer* **5**, 113-125.

Lujambio, A., and Esteller, M. (2007) CpG island hypermethylation of tumor suppressor microRNAs in human cancer. *Cell Cycle* **6**, 1455-1459.

Maglich, J. M., Stoltz, C. M., Goodwin, B., Hawkins-Brown, D., Moore, J. T., and Kliewer, S. A. (2002) Nuclear pregnane x receptor and constitutive androstane receptor regulate overlapping but distinct sets of genes involved in xenobiotic detoxification. *Mol. Pharmacol.* **62**, 638-646.

Mandriota, S. J., and Pepper, M. S. (1997) Vascular endothelial growth factor-induced in vitro angiogenesis and plasminogen activator expression are dependent on endogenous basic fibroblast growth factor. *J. Cell. Sci.* **110 (Pt 18)**, 2293-2302.

Manenti, G., Binelli, G., Gariboldi, M., Canzian, F., De Gregorio, L., Falvella, F. S., Dragani, T. A., and Pierotti, M. A. (1994) Multiple loci affect genetic predisposition to hepatocarcinogenesis in mice. *Genomics* **23**, 118-124.

Métivier, R., Gallais, R., Tiffoche, C., Le Péron, C., Jurkowska, R. Z., Carmouche, R. P., Ibberson, D., Barath, P., Demay, F., Reid, G., Benes, V., Jeltsch, A., Gannon, F., and Salbert, G. (2008) Cyclical DNA methylation of a transcriptionally active promoter. *Nature* **452**, 45-50.

Moennikes, O., Buchmann, A., Romualdi, A., Ott, T., Werringloer, J., Willecke, K., and Schwarz, M. (2000). Lack of phenobarbital-mediated promotion of hepatocarcinogenesis in connexin32-null mice. *Cancer Res.* **15**, 5087-5091.

Mortusewicz, O., Schermelleh, L., Walter, J., Cardoso, M. C., and Leonhardt, H. (2005) Recruitment of DNA methyltransferase I to DNA repair sites. *Proc. Natl. Acad. Sci. U S A.* **102**, 8905-8909.

Nakamura, N., and Takenaga, K. (1998) Hypomethylation of the metastasis-associated S100A4 gene correlates with gene activation in human colon adenocarcinoma cell lines. *Clin. Exp. Metastasis* **16**, 471-479.

Naveh-Many, T., and Cedar, H. (1981) Active gene sequences are undermethylated. *Proc. Natl. Acad. Sci. U S A.* **78**, 4246-4250.

Nie, A. Y., McMillian, M., Parker, J. B., Leone, A., Bryant S., Yieh, L., Bittner, A., Nelson, J., Carmen, A., Wan, J., and Lord, P. G. (2006) Predictive toxicogenomics approaches reveal underlying molecular mechanisms of nongenotoxic carcinogenicity. *Mol. Carcinog.* **45**, 914-933.

Nowell, P.C. (1976). The clonal evolution of tumor cell populations. *Science* **194**, 24-28.

Okano, M., Bell, D. W., Haber, D. A., and Li, E. (1999) DNA methyltransferases Dnmt3a and Dnmt3b are essential for de novo methylation and mammalian development. *Cell* **99**, 247-257.

Okano, M., Xie, S., and Li, E. (1998) Cloning and characterization of a family of novel mammalian DNA (cytosine-5) methyltransferases. *Nat. Genet.* **19**, 219-220.

Ooi, S. K., and Bestor, T. H. (2008) The colorful history of active DNA demethylation. *Cell* **133**, 1145-1148.

Oshimo, Y., Nakayama, H., Ito, R., Kitadai, Y., Yoshida, K., Chayama, K., and Yasui, W. (2003) Promoter methylation of cyclin D2 gene in gastric carcinoma. *Int. J. Oncol.* **23**, 1663-1670.

Oswald, J., Engemann, S., Lane, N., Mayer, W., Olek, A., Fundele, R., Dean, W., Reik, W., and Walter, J. (2000) Active demethylation of the paternal genome in the mouse zygote. *Curr. Biol.* **10**, 475-478.

Parikh, S., and Hyman, D. (2007) Hepatocellular cancer: a guide for the internist. *Am. J. Med.* **120**, 194-202.

Panning, B., and Jaenisch, R. (1996) DNA hypomethylation can activate Xist expression and silence X-linked genes. *Genes Dev.* **10**, 1991-2002.

Parsons, D. W., Jones, S., Zhang, X., Lin, J. C., Leary, R. J., Angenendt, P., Mankoo, P., Carter, H., Siu, I. M., Gallia, G. L., Olivi, A., McLendon, R., Rasheed, B. A., Keir, S., Nikolskaya, T., Nikolsky, Y., Busam, D. A., Tekleab, H., Diaz, L. A. Jr., Hartigan, J., Smith, D. R., Strausberg, R. L., Marie, S. K., Shinjo, S. M., Yan, H., Riggins, G. J., Bigner, D. D., Karchin, R., Papadopoulos, N., Parmigiani, G., Vogelstein, B., Velculescu, V. E., and Kinzler, K. W. (2008) An integrated genomic analysis of human glioblastoma multiforme. *Science* **321**, 1807-1812.

Pascussi, J. M., Gerbal-Chaloin, S., Duret, C., Daujat-Chavanieu, M., Vilarem, M. J., and Maurel, P. (2008) The tangle of nuclear receptors that controls xenobiotic metabolism and transport: crosstalk and consequences. *Annu. Rev. Pharmacol. Toxicol.* **48**, 1-32.

Philchenkov, A., Zavelevich, M., Kroczak, T. J., and Los, M. (2004) Caspases and cancer: mechanisms of inactivation and new treatment modalities. *Exp. Oncol.* **26**, 82-97.

Pitot, H.C., and Dragan, Y.P. (1991) Facts and theories concerning the mechanisms of carcinogenesis. *FASEB J* **5**, 2280-2286.

Pitot, H. C., and Dragan, Y. P. (1994) The multistage nature of chemically induced hepatocarcinogenesis in the rat. *Drug Metab. Rev.* **26**, 209-220.

Pitot, H. C., Dragan, Y., Sargent, L., and Xu, Y.-H. (1991) Biochemical markers associated with the stages of promotion and progression during hepatocarcinogenesis in the rat. *Environ. Health Perspect.* **93**, 181-189.

Qatanani, M., Zhang, J., and Moore, D. D. (2005) Role of the constitutive androstane receptor in xenobiotic-induced thyroid hormone metabolism. *Endocrinology* **146**, 995-1002.

Ramsahoye, B. H., Biniszkiewicz, D., Lyko, F., Clark, V., Bird, A. P., and Jaenisch, R. (2000) Non-CpG methylation is prevalent in embryonic stem cells and may be mediated by DNA methyltransferase 3a. *Proc. Natl. Acad. Sci. U S A* **97**, 5237–5242.

Rangarajan, A., and Weinberg, R. A. (2003) Opinion: Comparative biology of mouse versus human cells: modelling human cancer in mice. *Nat. Rev. Cancer* **3**, 952-959.

Ray, J. S., Harbison, M. L., McClain, R. M., and Goodman, J. I. (1994) Alterations in the methylation status and expression of the *raf* oncogene in phenobarbital-induced and spontaneous B6C3F1 mouse liver tumors. *Mol. Carcinog.* **9**, 155-166.

Reik, W., Dean, W., and Walter, J. (2001) Epigenetic reprogramming in mammalian development. *Science* **293**, 1089-1093.

Reik, W., and Murrell, A. (2000) Genomic imprinting. Silence across the border. *Nature* **405**, 408-409.

Reya, T., Morrison, S. J., Clarke, M. F., and Weissman, I. L. (2001) Stem cells, cancer, and cancer stem cells. *Nature* **414**, 105-111.

Rhim, J. A., Sandgren, E. P., Degen, J. L., Palmiter, R. D., and Brinster, R. L. (1994) Replacement of diseased mouse liver by hepatic cell transplantation. *Science* **263**, 1149-1152.

Ribatti, D., Nico, B., Crivellato, E., Roccaro, A. M., and Vacca, A. (2007) The history of the angiogenic switch concept. *Leukemia* **21**, 44-52.

Robertson, K. D. (2005) DNA methylation and human disease. *Nat. Rev. Genet.* **6**, 597-610.

Robertson, K. D., Uzvolgyi, E., Liang, G., Talmadge, C., Sumegi, J., Gonzales, F. A., and Jones, P. A. (1999) The human DNA methyltransferases (DNMTs) 1, 3a and 3b: coordinate mRNA expression in normal tissues and overexpression in tumors. *Nucleic Acids Res.* **27**, 2291-2298.

Roman-Gomez, J., Jimenez-Velasco, A., Agirre, X., Cervantes, F., Sanchez, J., Garate, L., Barrios, M., Castillejo, J. A., Navarro, G., Colomer, D., Prosper, F., Heiniger, A., and Torres, A. (2005) Promoter hypomethylation of the LINE-1 retrotransposable elements activates sense/antisense transcription and marks the progression of chronic myeloid leukemia. *Oncogene* **24**, 7213-7223.

Rougier, N., Bourc'his, D., Gomes, D. M., Niveleau, A., Plachot, M., Pàldi, A., and Viegas-Péquignot, E. (1998) Chromosome methylation patterns during mammalian preimplantation development. *Genes Dev.* **12**, 2108-2113.

Rüegg, C., and Mariotti, A. (2003) Vascular integrins: pleiotropic adhesion and signaling molecules in vascular homeostasis and angiogenesis. *Cell. Mol. Life. Sci.* **60**, 1135-1157.

Sado, T., Okano, M., Li, E., and Sasaki, H. (2004) De novo DNA methylation is dispensable for the initiation and propagation of X chromosome inactivation. *Development* **131**, 975-982.

Saini, S. P., Sonoda, J., Xu, L., Toma, D., Uppal, H., Mu, Y., Ren, S., Moore, D. D., Evans, R. M., and Xie, W. (2004) A novel constitutive androstane receptor-mediated and CYP3A-independent pathway of bile acid detoxification. *Mol. Pharmacol.* **65**, 292-300.

Schermelleh, L., Haemmer, A., Spada, F., Rösing, N., Meilinger, D., Rothbauer, U., Cardoso, M. C., and Leonhardt, H. (2007) Dynamics of Dnmt1 interaction with the replication machinery and its role in postreplicative maintenance of DNA methylation. *Nucleic Acids Res.* **35**, 4301-4312.

Schubbert, S., Shannon, K., and Bollag, G. (2007) Hyperactive Ras in developmental disorders and cancer. *Nat. Rev. Cancer* **7**, 295-308.

Schulz, W. A., Steinhoff, C., and Florl, A. R. (2006) Methylation of endogenous human retroelements in health and disease. *Curr. Top. Microbiol. Immunol.* **310**, 211-250.

Shay, J. W., and Bacchetti, S. (1997) A survey of telomerase activity in human cancer. *Eur. J. Cancer* **33**, 787-791.

Shivapurkar, N., Reddy, J., Chaudhary, P. M., and Gazdar, A. F. (2003) Apoptosis and lung cancer: a review. *J. Cell. Biochem.* **88**, 885-898.

Stahl S, Ittrich C, Marx-Stoelting P, Köhle C, Ott T, Buchmann A, Schwarz M. (2005) Effect of the tumor promoter phenobarbital on the pattern of global gene expression in liver of connexin32-wild-type and connexin32-deficient mice. *Int. J. Cancer.* **115**, 861-869.

Steenman, M. J., Rainier, S., Dobry, C. J., Grundy, P., Horon, I. L., and Feinberg, A. P. (1994) Loss of imprinting of *IGF2* is linked to reduced expression and abnormal methylation of *H19* in Wilms' tumour. *Nat. Genet.* **7**, 433-439.

Steer, C.J. (1995) Liver regeneration. *FASEB J.* **9**, 1396-1400.

Strahl, B. D., and Allis, C. D. (2000) The language of covalent histone modifications. *Nature* **403**, 41-45.

Sueyoshi, T., Kawamoto, T., Zelko, I., Honkakoski, P., and Negishi, M. (1999) The repressed nuclear receptor CAR responds to phenobarbital in activating the human *CYP2B6* gene. *J. Biol. Chem.* **274**, 6043-6046.

Sueyoshi, T., Moore, R., Sugatani, J., Matsumura, Y., and Negishi, M. (2008) PPP1R16A, the membrane subunit of protein phosphatase 1β, signals nuclear translocation of the nuclear receptor constitutive active/androstane receptor. *Mol. Pharmacol.* **73**, 1113-1121.

Sueyoshi, T, and Negishi, M. (2001) Phenobarbital response elements of cytochrome P450 genes and nuclear receptors. *Annu. Rev. Pharmacol. Toxicol.* **41**, 123-143.

Sugatani, J., Kojima, H., Ueda, A., Kakizaki, S., Yoshinari, K., Gong, Q. H., Owens, I. S., Negishi, M., and Sueyoshi, T. (2001) The phenobarbital response enhancer module in the human bilirubin UDP-glucuronosyltransferase *UGT1A1* gene and regulation by the nuclear receptor CAR. *Hepatology* **33**, 1232-1238.

Sullivan, M. J., Taniguchi, T., Jhee, A., Kerr, N., and Reeve, A. E. (1999) Relaxation of *IGF2* imprinting in Wilms tumours associated with specific changes in *IGF2* methylation. *Oncogene* **18**, 7527-7534.

Swales K, Negishi M. (2004) CAR, driving into the future. *Mol. Endocrinol.* **18**, 1589-1598.

Takahashi, K., Tanabe, K., Ohnuki, M., Narita, M., Ichisaka, T., Tomoda, K., and Yamanaka, S. (2007) Induction of pluripotent stem cells from adult human fibroblasts by defined factors. *Cell* **131**, 861-872.

Takai, D., and Jones, P. A. (2002) Comprehensive analysis of CpG islands in human chromosomes 21 and 22. *Proc. Natl. Acad. Sci. U S A.* **99**, 3740-3745.

Tei, K., Kawakami-Kimura, N., Taguchi, O., Kumamoto, K., Higashiyama, S., Taniguchi, N., Toda, K., Kawata, R., Hisa, Y., and Kannagi, R. (2002) Roles of cell adhesion molecules in tumor angiogenesis induced by cotransplantation of cancer and endothelial cells to nude rats. *Cancer Res.* **62**, 6289-6296.

Theise, N. D., Badve, S., Saxena, R., Henegariu, O., Sell, S., Crawford, J. M., Krause, D. S. (2000) Derivation of hepatocytes from bone marrow cells in mice after radiation-induced myeloablation. *Hepatology* **31**, 235-240.

Timsit, Y. E., and Negishi, M. (2007) CAR and PXR: the xenobiotic-sensing receptors. *Steroids*. **72**, 231-246.

Toretsky, J. A., Thakar, M., Eskenazi, A. E., and Frantz, C. N. (1999) Phosphoinositide 3-hydroxide kinase blockade enhances apoptosis in the Ewing's sarcoma family of tumors. *Cancer Res.* **59**, 5745-5750.

Trosko, J. E., and Chang, C. C. (2001) Mechanism of up-regulated gap junctional intercellular communication during chemoprevention and chemotherapy of cancer. *Mutat. Res.* **480-81**, 219-229.

Turker, M. S. (1999) The establishment and maintenance of DNA methylation patterns in mouse somatic cells. *Semin. Cancer Biol.* **9**, 329-337.

Ueda, A., Hamadeh, H. K., Webb, H. K., Yamamoto, Y., Sueyoshi, T., Afshari, C. A., Lehmann, J. M., and Negishi, M. (2002) Diverse roles of the nuclear orphan receptor CAR in regulating hepatic genes in response to phenobarbital. *Mol. Pharmacol.* **61**, 1-6.

Ulrey, C. L., Liu, L., Andrews, L. G., and Tollefsbol, T. O. (2005) The impact of metabolism on DNA methylation. *Hum. Mol. Genet.* **14** Spec No 1:R139-147.

Vogelstein, B., Lane, D., and Levine, A. J. (2000) Surfing the p53 network. *Nature* **408**, 307-310.

Vorce, R. L., and Goodman, J. I. (1991) Hypomethylation of *ras* oncogenes in chemically induced and spontaneous B6C3F1 mouse liver tumors. *Toxicol. Environ. Health.* **34**, 367-384.

Walsh, C. P., and Bestor, T. H. (1999) Cytosine methylation and mammalian development. *Genes Dev.* **13**, 26-34.

Walsh, C. P., Chaillet, J. R., and Bestor, T. H. (1998) Transcription of IAP endogenous retroviruses is constrained by cytosine methylation. *Nat. Genet.* **20**, 116-117.

Chromatin remodeling and cancer, Part II: ATP-dependent chromatin remodeling.

Wang, G. G., Allis, C. D., and Chi, P. (2007) *Trends Mol. Med.* **13**, 373-380.

Wang, X., Foster, M., Al-Dhalimy, M., Lagasse, E., Finegold, M., Grompe, M. (2003) The origin and liver repopulating capacity of murine oval cells. *Proc. Natl. Acad. Sci. U S A* **100**, Suppl. 1:11881-11888.

Warner, K. A., Fernstrom, M. J., Ruch, R. J. (2003) Inhibition of mouse hepatocyte gap junctional intercellular communication by phenobarbital correlates with strain-specific hepatocarcinogenesis. *Toxicol. Sci.* **71**, 190-197.

Watson, R. E., and Goodman, J. I. (2002) Effects of phenobarbital on DNA methylation in GC-rich regions of hepatic DNA from mice that exhibit different levels of susceptibility to liver tumorigenesis. *Toxicol. Sci.* **68**, 51-58.

Watt, F., and Molloy, P. L. (1988) Cytosine methylation prevents binding to DNA of a HeLa cell transcription factor required for optimal expression of the adenovirus major late promoter. *Genes Dev.* **2**, 1136-1143.

Wei, P., Zhang, J., Egan-Hafley, M., Liang, S., and Moore, D. D. (2000). The nuclear receptor CAR mediates specific xenobiotic induction of drug metabolism. *Nature* **407**, 920-923.

Weiss, A., Keshet, I., Razin, A., and Cedar, H. (1996) DNA demethylation in vitro: involvement of RNA. *Cell* **86**, 709-718.

Wernig, M., Meissner, A., Foreman, R., Brambrink, T., Ku, M., Hochedlinger, K., Bernstein, B. E., and Jaenisch, R. (2007) In vitro reprogramming of fibroblasts into a pluripotent ES-cell-like state. *Nature* **448**, 318–324.

Wilson, A. S., Power, B. E., and Molloy, P. L. (2007) DNA hypomethylation and human diseases. *Biochim. Biophys. Acta.* **1775**, 138-162.

Whitelaw, E., and Martin, D. I. (2001) Retrotransposons as epigenetic mediators of phenotypic variation in mammals. *Nat. Genet.* **27**, 361-365.

Whysner, J., Ross, P. M., and Williams, G. M. (1996). Phenobarbital mechanistic data and risk assessment: enzyme induction, enhanced cell proliferation, and tumor promotion. *Pharmacol. Ther.* **71**, 53-91.

Wong, N., Lam, W. C., Lai, P. B., Pang, E., Lau, W. Y., and Johnson, P. J. (2001) Hypomethylation of chromosome 1 heterochromatin DNA correlates with q-arm copy gain in human hepatocellular carcinoma. *Am. J. Pathol.* **159**, 465-471.

Wutz, A., Smrzka, O. W., Schweifer, N., Schellander, K., Wagner, E. F., Barlow, D. P. (1997) Imprinted expression of the *Igf2r* gene depends on an intronic CpG island. *Nature* **389**, 745-749.

Xu, G. L., Bestor, T. H., Bourc'his, D., Hsieh, C. L., Tommerup, N., Bugge, M., Hulten, M., Qu, X., Russo, J. J., and Viegas-Péquignot, E. (1999) Chromosome instability and immunodeficiency syndrome caused by mutations in a DNA methyltransferase gene. *Nature* **402**, 187-191.

Yamamoto, Y., Kawamoto, T., and Negishi, M. (2003) The role of the nuclear receptor CAR as a coordinate regulator of hepatic gene expression in defense against chemical toxicity. *Arch. Biochem. Biophys.* **409**, 207-211.

Yamamoto, Y., Moore, R., Goldsworthy, T. L., Negishi, M., and Maronpot, R. R. (2004) The orphan nuclear receptor constitutive active/androstane receptor is essential for liver tumor promotion by phenobarbital in mice. *Cancer Res.* **64**, 7197-7200.

Yoder, J. A., Walsh, C. P., and Bestor, T. H. (1997) Cytosine methylation and the ecology of intragenomic parasites. *Trends Genet.* **13**, 335-340.

Yoo, C. B., and Jones, P. A. (2006) Epigenetic therapy of cancer: past, present and future. *Nat. Rev. Drug. Discov.* **5**, 37-50.

Yoon, H. G., Chan, D. W., Reynolds, A. B., Qin, J., and Wong, J. (2003) N-CoR mediates DNA methylation-dependent repression through a methyl CpG binding protein Kaiso. *Mol. Cell.* **12**, 723-734.

Yoshinari, K., Kobayashi, K., Moore, R., Kawamoto, T., and Negishi, M. (2003) Identification of the nuclear receptor CAR:HSP90 complex in mouse liver and recruitment of protein phosphatase 2A in response to phenobarbital. *FEBS Lett.* **548**, 17-20.

Zhang, H., Berezov, A., Wang, Q., Zhang, G., Drebin, J., Murali, R., and Greene, M. I. (2007) ErbB receptors: from oncogenes to targeted cancer therapies. *J. Clin. Invest.* **117**, 2051-2058.

Zhu, B., Zheng, Y., Angliker, H., Schwarz, S., Thiry, S., Siegmann, M., and Jost, J. P. (2000) 5-methylcytosine DNA glycosylase activity is also present in the human MBD4 (G/T mismatch glycosylase) and in a related avian sequence. *Nucleic Acids Res.* **28**, 4157-4165.

Zilberman, D., Gehring, M., Tran, R. K., Ballinger, T., and Henikoff, S. (2007) Genome-wide analysis of Arabidopsis thaliana DNA methylation uncovers an interdependence between methylation and transcription. *Nat. Genet.* **39**, 61-69.

MICHIGAN STATE UNIVERSITY LIBRARIES
3 1293 03063 4145